MCEER
EARTHQUAKE ENGINEERING TO EXTREME EVENTS

ISSN 1520-295X

Modeling and Seismic Performance Evaluation of High Voltage Transformers and Bushings

by
Andrei M. Reinhorn, Konstantinos Oikonomou,
Hwasung Roh, Anshel Schiff and Leon Kempner, Jr.

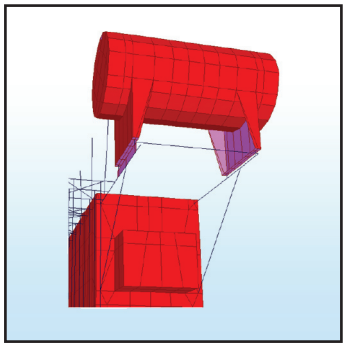

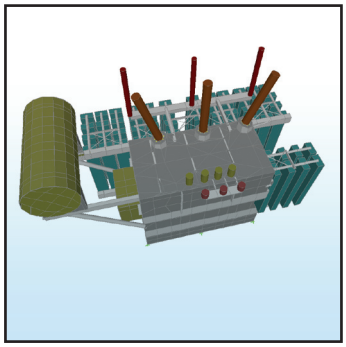


Technical Report MCEER-11-0006

October 3, 2011

This research was conducted at the University at Buffalo, State University of New York. It was sponsored by the Bonnevile Power Administration under Contract Number 00041295 and the California Energy Commission under Contract Number 500-07-037 (Subcontract TRP-08-03).

NOTICE

This report was prepared by the University at Buffalo, State University of New York as a result of research sponsored by the Bonneville Power Administration and the California Energy Commission. Neither MCEER, associates of MCEER, its sponsors, the University at Buffalo, State University of New York, nor any person acting on their behalf:

a. makes any warranty, express or implied, with respect to the use of any information, apparatus, method, or process disclosed in this report or that such use may not infringe upon privately owned rights; or

b. assumes any liabilities of whatsoever kind with respect to the use of, or the damage resulting from the use of, any information, apparatus, method, or process disclosed in this report.

Any opinions, findings, and conclusions or recommendations expressed in this publication are those of the author(s) and do not necessarily reflect the views of MCEER or its sponsors.

Modeling and Seismic Performance Evaluation of High Voltage Transformers and Bushings

by

Andrei M. Reinhorn,[1] Konstantinos Oikonomou,[2] Hwasung Roh,[3]
Anshel Schiff,[4] and Leon Kempner, Jr.[5]

Publication Date: October 3, 2011
Submittal Date: June 15, 2011

Technical Report MCEER-11-0006

Bonneville Power Administration Contract Number 00041295
California Energy Commission Contract Number 500-07-037 (Subcontract TRP-08-03)

1 Clifford C. Furnas Professor of Engineering, Department of Civil, Structural and Environmental Engineering, University at Buffalo, State University of New York
2 Graduate Research Assistant, Department of Civil, Structural and Environmental Engineering, University at Buffalo, State University of New York
3 Research Professor, Department of Civil and Environmental Engineering, Hanyang University, Korea; Former Research Scientist, Department of Civil, Structural and Environmental Engineering, University at Buffalo, State University of New York
4 Consultant, Precision Measurement Instruments
5 Principal Structural Engineer, Bonneville Power Administration

MCEER
University at Buffalo, State University of New York
Red Jacket Quadrangle, Buffalo, NY 14261
Phone: (716) 645-3391; Fax (716) 645-3399
E-mail: *mceer@buffalo.edu*; WWW Site: *http://mceer.buffalo.edu*

Preface

MCEER is a national center of excellence dedicated to the discovery and development of new knowledge, tools and technologies that equip communities to become more disaster resilient in the face of earthquakes and other extreme events. MCEER accomplishes this through a system of multidisciplinary, multi-hazard research, in tandem with complimentary education and outreach initiatives.

Headquartered at the University at Buffalo, The State University of New York, MCEER was originally established by the National Science Foundation in 1986, as the first National Center for Earthquake Engineering Research (NCEER). In 1998, it became known as the Multidisciplinary Center for Earthquake Engineering Research (MCEER), from which the current name, MCEER, evolved.

Comprising a consortium of researchers and industry partners from numerous disciplines and institutions throughout the United States, MCEER's mission has expanded from its original focus on earthquake engineering to one which addresses the technical and socio-economic impacts of a variety of hazards, both natural and man-made, on critical infrastructure, facilities, and society.

The Center derives support from several Federal agencies, including the National Science Foundation, Federal Highway Administration, National Institute of Standards and Technology, Department of Homeland Security/Federal Emergency Management Agency, and the State of New York, other state governments, academic institutions, foreign governments and private industry.

The Bonneville Power Administration (BPA) and the California Energy Commission (CEC) are supporting a series of studies on the resilience of electric power substation equipment that focus on the following topics:

- Reducing Disruption of Power Systems in Earthquakes: Advanced Methods for Protecting Substation Equipment
- Analysis of the Seismic Performance of Transformer Bushings

It is envisioned that these studies will result in the development of cost effective seismic protective solutions for transformer–bushing systems and other electrical substation equipment considering inertial effects and dynamic interaction with conductors. Furthermore, new knowledge discovered about the bushing-transformer seismic interaction will be translated into a proposed revision of the IEEE 693 Standard. A series of MCEER reports will document the results of these studies.

In this study, existing transformers are modeled to explore the effects of modeling variations and structural modifications that could impact the response of bushings mounted on the transformer covers. A model was developed to identify the dynamic characteristics of the transformer and the significant interactions between various components and the high voltage bushings. A number

of structural modifications were introduced to observe the sensitivity of the responses of the bushings when mounted on different transformer models. Each model was investigated using modal and spectral analyses, using random and spectrum compatible (IEEE 693-2005) ground motion. The responses were measured at the top of bushings, the corners of the cover plate and the base of the turrets. Furthermore, the spectra at the corners of the cover plate and at the base of the turrets were obtained and associated with the bushings' response. The transformer was also analyzed for vacuum pressure, to determine the most adverse displacement condition for the interconnected interior cables. Finally, simplified models were explored in which the cover plate, along with its stiffeners and the bushings, was separated from the transformer. Various boundary conditions were examined in an effort to determine the degrees of approximation of bushings' response with respect to the response obtained from the full transformer model. Recommendations for guidelines on modeling transformers and bushings can be derived from this work.

ABSTRACT

Electrical transformers are complex structures, crucial for the operation of a power system, an important infrastructure and lifeline essential for community resilience. Damage sustained in past strong earthquakes rendered many of them unusable, leading to severe economic losses. Of particular interest for the overall performance is the dynamic response of high voltage bushings, the failure of which is closely associated with the loss of functionality of the transformer.

This study deals with the modeling of existing transformers and bushings to evaluate the effects of modeling variations and possible structural modifications that may affect their dynamic characteristics, and the significant interactions between various components and the high voltage bushings. Detailed sensitivity analyses are performed on a finite element model which comprises three identical 196 kV/230 kV bushings mounted on the cover of a 230 kV transformer with variation of properties that simulate different transformers.

Bushings are modeled using properties provided by manufacturers while the transformer's tank cover plate is modeled considering only the important structural features. To determine the behavior of the tank and bushings, the base of the structure is excited alternatively with wide band random motion (white noise) and with the IEEE-693 spectrum compatible ground motions. Transfer functions are calculated to determine the relevant dynamic properties, even when the structure has mild nonlinear behavior.

The interaction between the bushings and several main parts of the transformer is assessed through cross-spectra and coherences. Sensitivity of interaction is determined by modifying properties of interacting critical parts of the transformer, especially the cover, radiators, surge arresters and the core assembly. Moreover, the response quantities of interest (accelerations and displacements) are measured at specific locations related to the bushings, at the corners of the transformer cover and at the base of turrets connecting the bushings to the tank.

Detailed techniques for the modeling of the bushings are presented in this report along with a discussion on the sensitivity of interactions. Additional investigations were conducted to explore feasibility and approximations in analyzing simplified models in which the tank cover and the bushings are separated from the transformer. The report presents the sensitivity study on

modeling various boundary conditions in the simplified model in an effort to match the response of the bushings with the response obtained from the full model.

The report also presents the global amplification effects of the tank construction on the response of the tank cover at base of bushings, and the effects on the apparent dynamic properties of bushings. Recommendations for guidelines on modeling transformers and bushings can be derived from this work.

ACKNOWLEDGEMENTS

This work is part of MCEER Thrust Area 1 (Infrastructure Systems and Public Policy) and is made possible with financial support from the Bonneville Power Administration (Contract No. 00037794) and the California Energy Commission (Contract No. TRP-08-03). Their support is gratefully acknowledged.

TABLE OF CONTENTS

TABLE OF CONTENTS (CONT'D)

LIST OF ILLUSTRATIONS

LIST OF ILLUSTRATIONS (CONT'D)

LIST OF ILLUSTRATIONS (CONT'D)

LIST OF ILLUSTRATIONS (CONT'D)

LIST OF TABLES

LIST OF TABLES (CONT'D)

SECTION 1

INTRODUCTION

1.1 Background on Power Transmission

The transmission of the electrical current from the generating station to the site of distribution is a multi phased procedure. From the moment electricity is produced until it is provided to the consumers, its voltage needs to be modulated many times.

In most cases when the power plant is located a long distance from the load, it is desirable that electricity is transmitted with minimal losses. In electrical engineering terms, for a given power level and conductor diameter higher voltage results in lower current transfer. The power lost is proportional to the square of the current; it is therefore preferable to use a high voltage electric power transmission system.

Figure 1-1 Typical substation (Photo: David Neale)

The load end is most commonly a dedicated plant which is referred to as the substation (Figure 1-1). The substation contains an ensemble of technical equipment serving to step the voltage down and transfer the power to the external distribution system. Among this equipment, the electrical transformer is probably the most crucial component for the operation of the substation.

Electrical transformers (Figure 1-2) are devices used to transform voltage from one level to another. Before the transfer through the high voltage lines is realized, a transformer installed at the production site is used to amplify the voltage of the current produced at the power plant. Accordingly, at the load end, a transformer is used as well to step the voltage down to acceptable levels prior to the distribution through the local transmission lines.

Figure 1-2 Electrical transformer
(Photo: Electrical Technologies Company)

The basic parts of the transformer are: the tank (filled with oil), the bushings, the conservator, the radiators, the core and the coils. The core and coil assembly, through which the transformation of the electrical current is achieved, are located inside the oil filled tank for

insulation purposes and for protection from the elements. The oil serves as a means of cooling for the core, which is heated appreciably during the process of transformation. The oil also provides electrical insulation between the internal components. It is necessary that the oil remains stable at high temperatures for an extended period. To enhance the procedure of cooling through convection, the heated oil is circulated through external radiators, usually attached to the side of the tank. The conservator is an external reservoir tank located above the transformer and connected to the main tank so that the oil in the main tank is free to expand at high temperatures.

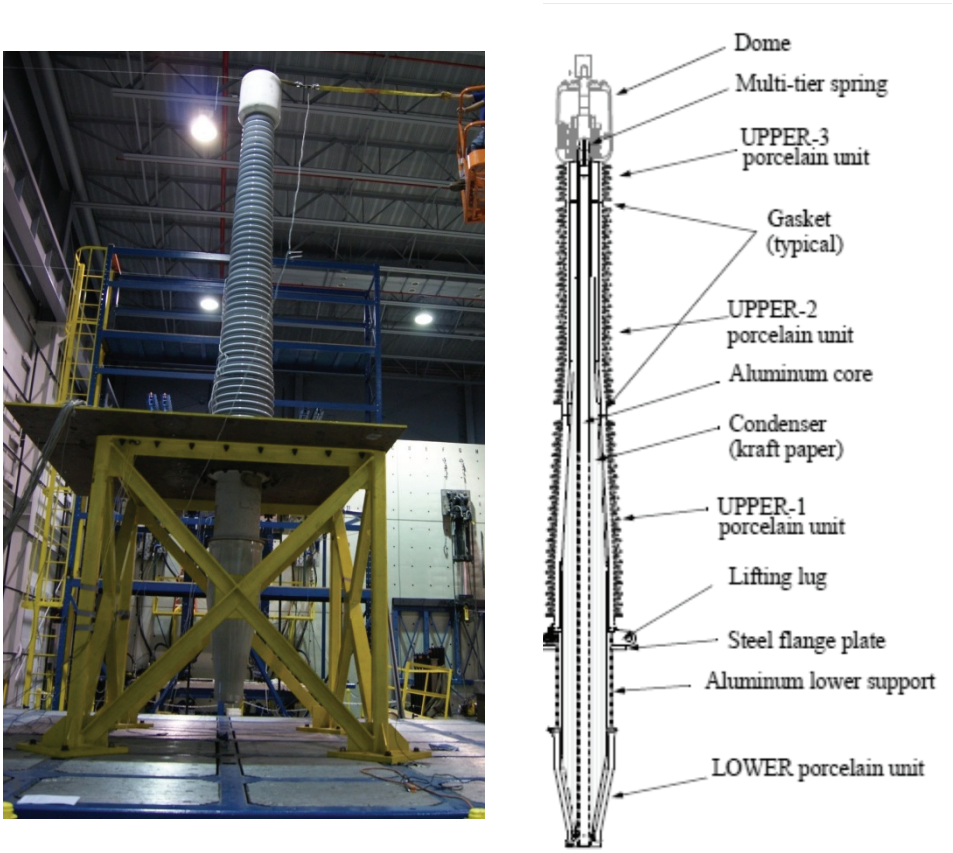

Figure 1-3 A 550 kV high voltage bushing (at SEESL) and its components (courtesy PEER)

The bushings are cantilever-like insulated conductors, mounted directly to the top plate of the transformer tank or on a turret welded to the top of the tank. They serve to connect the high

voltage power lines, while at the same time insulating them from the metallic, conductible walls of the tank. The insulation is typically achieved by placing the conductor inside a case usually made of porcelain. To prevent a flashover the surrounding porcelain is designed to provide a relatively long distance between the power cables and the coils. Therefore, the external part of a bushing is comprised of annular porcelain segments stacked upon one another and held in place (post-tensioned) by the conductor itself. The remaining space between the conductor and the porcelain is filled with kraft paper and oil for more adequate insulation. A representation of a 550 kV bushing and its components is depicted in Figure 1-3(b).

1.2 Performance in Past Earthquakes

During past moderate and severe ground shaking events, the performance of electrical equipment and particularly electrical transformers were shown to be unsatisfactory. Examples of these events are: the 1989 Loma Prieta earthquake, the 1994 Northridge earthquake, the 1995 Kobe earthquake, the 1999 Izmit and Chi-Chi earthquakes (Schiff 1995, 1998, Schiff and Tang 2000, Tang 2000). The immediate estimated cost was in the range of hundreds of millions of dollars for each of these events. Additional costs include: the clearance and replacement expenses of the damaged equipment, the expenses for the restoration of the normal network operation and the daily revenue losses due to the disruption of the network operation because of severe damage to the equipment. Apart from the direct impact on local economy, the restoration of the network operation was also significantly impeded by the loss of power itself, in the case of a blackout.

In consideration of the damage observed in electrical transformers so far, the types of failure could be classified as: global, when the damage inflicted pertains to the stability of the transformer body, and local, when a component of the transformer fails.

Among the global modes of failure, the most commonly encountered are the anchorage failure and the failure of unrestrained transformers. The anchorage is generally achieved by fixing the tank to the foundation with anchor bolts or by welding. There are cases in which the anchorage failed, causing ripping in the tank and oil leakage. There are even cases where the foundation was inadequately designed for the seismic overturning moments and failed, causing the transformer to rock and tilt. Unrestrained transformers, such as rail mounted transformers and transformers simply mounted on top of a foundation pad, experience the most common failures suffering permanent displacements and even overturning when the ground shaking is significant (Figure 1-4).

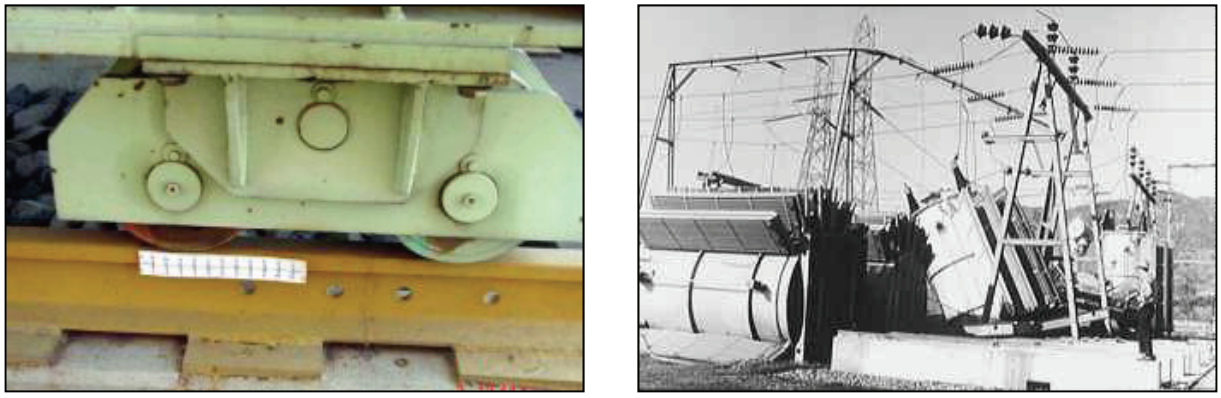

Figure 1-4 Permanent offset (right) and overturning (left) of rail mounted transformers (Photos: Anshel Schiff)

Among the components comprising the transformer, bushings have proven to be the most vulnerable during past earthquakes. Failure in the bushings includes oil leakage due to extrusion of the gasket located at the transformer-bushing interface and fracture of the porcelain (Figure 1-5). This type of damage is closely associated to the nature of their design. Bushings are manufactured relatively long and thus tend to accumulate large moments and stresses close to their base. The problem is aggravated because of the porcelain used externally for insulation,

which is a low strength and inherently brittle material. Therefore, bushings tend to fracture and slip at their base.

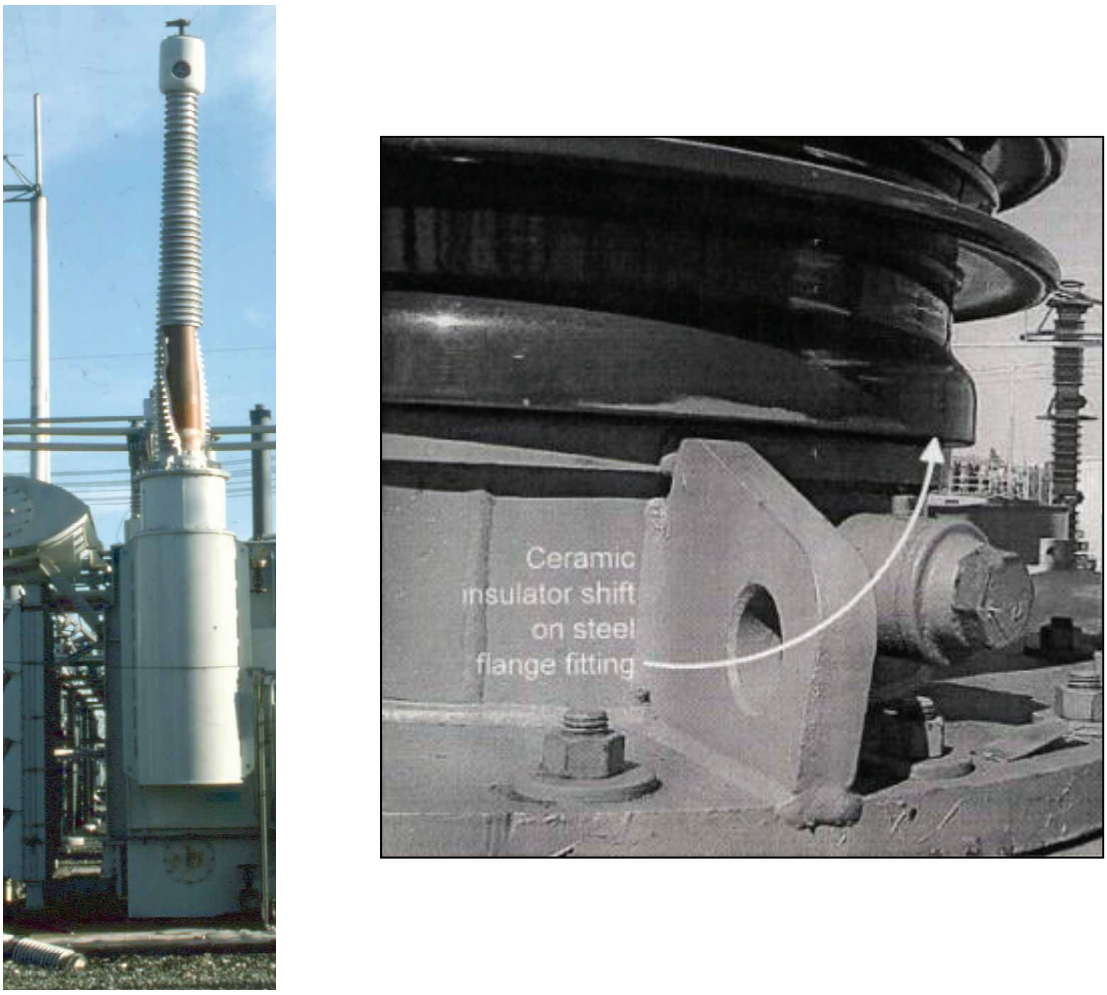

Figure 1-5 Cracked bushing (right) and gasket failure (left) due to slippage (Photos: Anshel Schiff)

Finally, apart from the bushings in which the damage inflicted is usually the most catastrophic for the operation of the transformer, failure has also been observed in various other components such as the radiators, the conservators and the surge arresters.

1.3 Seismic Design Specifications for Electrical Transformers

Past performance has revealed that indispensable components for the functionality of a substation, such as electrical transformers and bushings, are particularly susceptible to damage during a significant earthquake. The seismic design of the equipment which followed much lower seismic standards and adopted prior to the severe events mentioned earlier, is the main cause for the majority of the failures observed. It is thus desirable that the sensitive substation equipment is qualified for high ground excitation levels so that the damage inflicted, and most importantly the disruption of the substation functionality, is minimal.

Towards this end, the Institute of Electrical and Electronic Engineers has developed a national standard entitled "IEEE Recommended Practice for Seismic Design of Substations" (IEEE 693-2005). The standard emphasizes the qualification of the electrical equipment for a range of performance levels and its use is voluntarily.

There are three performance levels (PL) identified in IEEE 693-2005: high, moderate and low. Each PL is represented by a response spectrum that envelopes response spectra from anticipated earthquakes at the location of transformer at his base. The response spectrum for the high-level and the moderate-level qualification corresponds to a peak ground acceleration of 1.0 g and 0.5 g respectively. The low-level performance is permitted when no special consideration is given to seismic performance.

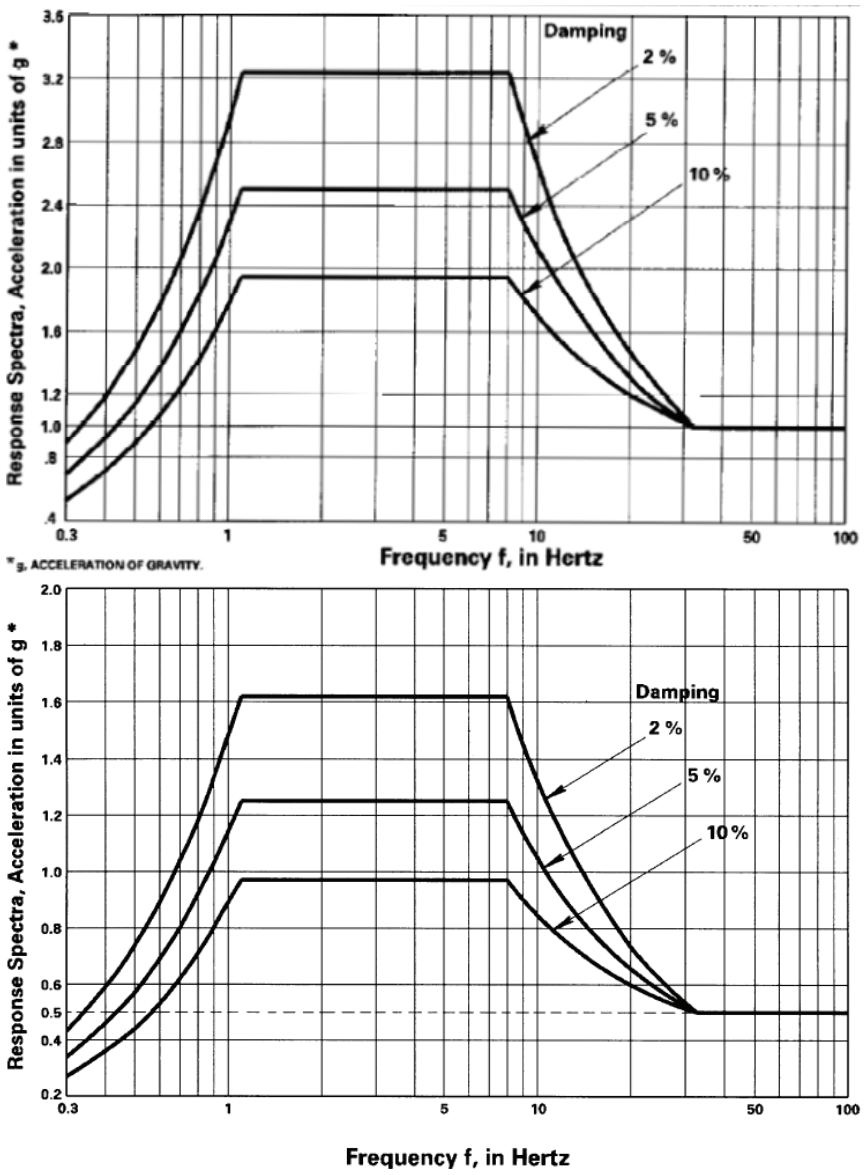

Figure 1-6 High seismic PL (up) and high seismic SQL (down) as per IEEE-693-2005

Procedures for equipment qualification include experimental and more specifically, shake table testing, as well as analytical using engineering computations. IEEE 693-2005 recognizes that it is often impractical or not cost effective to test to the high or moderate PL. On the one hand, it is possible that test laboratories may not be able to attain the required high acceleration levels, and on the other, although yielding of ductile materials is considered acceptable at the PL, some structural components may be damaged and rendered inefficient for further use. Thus, in

the IEEE standard it is suggested that the equipment be tested at one-half of the respective PL accelerations. The reduced level of testing motion is seismic qualification level (SQL). A comparison between the high level PL and the respective SQL spectrum is shown in Figure 1-6.

Equipment tested or analyzed to the SQL is expected to have acceptable performance at the PL. For this purpose the stresses obtained from the analysis at the SQL are measured and compared to the stresses at one-half of the ultimate strength of the porcelain or cast aluminum components. A lower factor of safety against yield is used to account for nonlinear behavior in steel and other ductile components.

IEEE 693-2005 separates the bushings into two categories for their qualification: bushings with voltage capacity less than 161 kV and bushings with voltage capacity equal or greater than 161 kV. Bushings with voltage capacity less than 161 kV can be qualified by a static pull test. In that case, a quasi static load equal to twice the weight of the bushing is applied horizontally at the top of the bushing and held for at least 2 seconds. Bushings with capacity larger than 161 kV need to be qualified through a time history shake table test. The Test Response Spectrum (TRS) obtained from the time history selected, should envelope the Required Response Spectrum (RRS) or its fraction. Since it is impractical to test a bushing attached to a transformer or liquid-filled reactor, the bushing can be mounted on a rigid stand during the test.

IEEE 693-2005 acknowledges that the acceleration which the bushing actually experiences, during the ground excitation, is amplified due to the response of the transformer body and the local flexibility of the area around the bushing. Therefore, it is specified that the bushing, which is mounted in-field on the cover of the transformer, will be tested with an input motion of twice the relative on-the-ground PL or SQL motions to account for this amplification. The testing should be carried out with the bushing installed at no less than its in-service slope

(the slope angle measured from vertical). It is recommended though, that the bushing be tested at 20 degrees measured from vertical, so that it is qualified for use on all transformers with angles varying from vertical to 20 degrees. All bushings at angles greater than 20 degrees will be tested at their in-service angle.

1.4 Background on Behavior of Transformers and Bushings

Several studies have been conducted in the past 15 years for the seismic performance evaluation of porcelain bushings. Most of them involve experimental testing for the qualification of bushings under the recommendations of IEEE 693-2005. Fewer studies were conducted in investigating the detailed finite element modeling of the transformer-bushing assembly performance.

Wilcoski (1997) performed shake table fragility testing of a 500 kV bushing. The fundamental frequency of vibration and the damping ratio were measured in the range of 5.7 to 6.4 Hz and 2.5% to 3% of critical. The bushing experienced oil leakage when the IEEE 693-2005 response spectrum was scaled for a peak ground acceleration (PGA) of 1 g.

Bellorini *et al.* (1997) performed in situ excitation tests on a 230 kV transformer with the objective of determining its dynamic characteristics. The fundamental frequencies of the transformer and the 230 kV bushing attached to it were estimated at 3.5 and 11.0 Hz respectively and the damping ratio was estimated at 2% of critical. A three dimensional finite element model of the full transformer was developed for numerical analyses, from which the modal frequencies obtained approximated the corresponding experimental frequencies. The amplification between the ground and the bushing flange as well as the ground and the bushing center of gravity found from time history analyses were 2.16 and 2.80 respectively. The corresponding values calculated from the IEC 61463 standard (International Electrotechnical Commission “Bushings-Seismic

qualification" Standard) are 1.5 and 4.5. This is considered inadequate in regard to the amplification at the flange but very conservative when the amplification at the bushing center of gravity is concerned.

Seismic shake table testing of 196 kV, 230 kV and 550 kV bushings were carried out by the University of California at Berkeley (Gilani *et al*. 1998, 1999). The main objectives of the studies were to assess the dynamic properties of the bushings and qualify them under the IEEE 693-2005 recommendations. Two 196 kV bushings were mounted on a rigid frame at an angle of 20 degrees and subjected to near-field ground motions that were matched to the IEEE required spectra. The bushing frequencies and damping ratios measured ranged from 14 to 16 Hz and 2% to 4% of critical respectively. Neither bushing 1 or 2 presented evident signs of structural damage or oil leakage and seismically qualified for moderate and high performance level, respectively. Two identical 230 kV bushings were tested under the same configuration on the rigid frame and qualified for high performance level. The frequencies obtained were in the range of 18 to 20 Hz and the damping ratio 2% to 3% of critical. The first bushing was also subjected to static monotonic and cyclic tests. The second bushing was mounted on a flexible plate and subjected to fragility testing. The frequencies obtained in that case were in the range of 6.5 to 7.5 Hz and the damping ratio was 2% to 5% of critical. The last two tests were repeated using two different rings around the gasket as retrofit for the prevention of slip and leakage. Of those, only the ring installed in the second bushing was effective. Finally, three 550 kV bushings were tested. The first bushing was a typical example of a bushing used in practice and the remaining two were modifications of the first with the aim of improving its seismic performance. The assessed frequency and damping ratio was 8 Hz and 4% of critical respectively for all the bushings. The first and second bushings were subjected to fragility testing, while the third

bushing was tested for moderate level qualification. Oil leakage and slip of the upper porcelain unit over the flange was observed for all bushings, which were therefore disqualified.

Villaverde *et al.* (1999) investigated the dynamic properties of two 500 kV and two 230 kV transformers by conducting field tests. The fundamental frequencies ranged from 2.4 to 3.4 Hz for the 500 kV and were close to 4 Hz for the 230 kV transformers. The damping ratios ranged from 1.5% to 3.6% and 1.4% to 4.5% of the critical for the 500 kV and the 230 kV transformers respectively. Moreover, three analytical models were developed for the two 500 kV transformers in order to determine the amplification factor between the ground and the bushing flange. The transformers were represented by flexible beam elements with lumped masses and the numerical frequencies calculated matched closely to experimental ones. Numerical analysis under a wide variety of ground motions revealed that the amplification factor could be twice as large as the factor proposed by IEEE 693-2005.

Ersoy and Saadeghvaziri (2003) developed full finite element models of three different transformers. The three 196 kV bushings mounted on top of each transformer were modeled explicitly so that their properties were captured sufficiently. The transformer frequencies were calculated in the range of 11 to 14 Hz in the weak direction and 18.5 to 22.5 Hz in the strong direction. The as installed bushing frequencies of the bushings were calculated in the range of 10 to 11 Hz. The results from time history analyses revealed that the amplification factor at the flange exceeded the value of 2 and the flexibility of the transformer, especially in the weak direction, affected the seismic response of the bushings.

Filiatrault and Matt (2006) performed time history analyses on finite element models of four different transformers. The objective of the analyses was to assess the amplification factors at the base of the bushings for ground motions that were scaled to the high performance level

spectrum, specified by IEEE 693-2005. The tank fundamental frequencies were in the range of 8 to 14 Hz in the weak direction and 11 to 25 Hz in the strong direction. The as-installed fundamental bushing frequencies were close to 3 Hz for the 500 kV/525 kV bushings and 9 Hz for the 230 kV bushing. It was found that the amplification factor of the bushing frequency can significantly exceed the factor of 2, as proposed by the IEEE 693-2005 standard, especially when the tank frequency is close to the fundamental as installed bushing frequency.

With the exception of 500 kV bushings, the experimental studies have demonstrated excellent seismic performance of this type of electrical equipment. For the bushing qualification, the IEEE 693-2005 standard recommendations were principally followed. The recommendations specify that during the experiments the bushing is mounted on a rigid frame and the ground motions used matched the on-the-ground RRS multiplied by a factor of 2 which is deemed to adequately account for the flexibility of the transformer.

The outcome of the numerical studies carried out on a range of transformer-bushing systems has indicated that the amplification factor at the base of the bushing can exceed the value of 2, as specified by the IEEE 693-2005. More specifically, it has been shown that the cover plate response can be affected by the flexibility of the tank, the flexibility of the cover plate and the response of the individual components comprising the transformer. This could justify the discrepancy between the good experimental results and the actual seismic vulnerability of bushings observed in past earthquakes.

1.5 Objectives of the Research

There are three objectives that constitute the subject of the current research:

(1) The first objective is to appropriately modify and enhance finite element models of actual transformers which are usually modeled according to current practice for static analyses.

These models are then used to identify the dynamic characteristics of the transformers and of the critical components that influence the dynamic response of the high voltage porcelain bushings.

(2) The second objective is to investigate the dynamic response of the high voltage porcelain bushings and assess the amplification that occurs between the base and the top of the tank, at the base of the bushings. From these assessments, a variety of potential structural modifications to improve the model are constructed.

(3) The third objective is to develop a simplified and reduced model, analog to the response of the full transformer model, for the evaluation of the dynamics of the transformer's cover and of the bushings; The reduced model includes a separate cover plate and bushings with various alternative boundary conditions intended to determine the degree of approximation in the dynamic characteristics and the response of the high voltage porcelain bushings.

(4) Finally the current research is intended to suggest some guidelines for modeling transformers and bushings

To aid in the completion of the first objective a finite element model of a commercial transformer model was developed for static analysis and verification of transformers stresses under equivalent (dynamic) loads. However, elaborate re-modeling had to be conducted in order to incorporate the necessary features needed for a reliable dynamic analysis, as desired. The modified model was excited with the random "white-noise" ground motion, from which the dynamic characteristics of the transformer and its components, were determined. These dynamic characteristics were identified through transfer functions in the frequency domain. The interaction between selected transformer components and the high voltage bushings was

investigated, through cross-spectra and coherences in the frequency domain. These methods provide information on the correlation of two individual signals but no information on the real existence of interaction between the components. Therefore, the results were screened also by conducting visual investigation of the modes obtained from modal analysis of the model, at the frequencies of the presumed interaction.

For the second objective, the enhanced finite element model is subjected to a number of modifications that altered the structural properties of the transformer. These modifications dealt with the removal of equipment and various seismic bracing schemes of crucial transformer attachments. The modified models were analyzed for three dimensional base acceleration histories that matched the 2% damped high performance level (HPL) which is 1.0g RRS as specified by the IEEE 693-2005 standard. For each numerical analysis the response at the base of the turrets and the response at the corners of the cover plate were obtained in terms of acceleration. The amplification factors from the ground to the corners of the cover plate and the base of the turrets were assessed and compared with the respective factor of two (x2) suggested by the IEEE 693-2005 Standard

For the final objective, the cover plate is modeled separately from the model of the full transformer's tank and is supported along its perimeter. The components that are usually mounted or directly connected to the cover plate in the full model were excluded from the "separated cover model", except the bushings. In order to determine the conditions for which the as-installed frequencies and response of the bushings approached the respective values obtained when the full transformer model is investigated various boundary conditions are examined. In the full model of the transformer, there are small rotations along the borders of the cover which are the result of the tank's walls flexibilities. Since those are relatively small, those are neglected in

the excitation of the "separated cover model". Moreover these rotations are completely negligible near the corners. Therefore, linear acceleration response at the corners of the cover plate are used to assess the dynamic behavior of the components connected to the "separated cover model" Considering the above, an average of the response at the four corners are used as input motion to the "separated cover model". This average was obtained from the full transformer model subjected to the IEEE 693-2005 compatible ground motion.

1.6 Organization of the Report

The report is organized into nine sections. A general presentation of the transformer investigated and a detailed description of the most significant components of the transformer that are considered in the sensitivity analyses are made in Section 2. The original finite element model of the transformer, provided for static analysis in SAP2000, is presented in Section 3. The modeling variations of critical transformer components in the finite element model and the techniques employed for the assessment of interactions between the high voltage bushings and the critical components modified, are dealt with in Section 4. The analysis results from the dynamic identification of the transformer and the interactions observed are presented in Section 5. The sensitivity of interactions is carefully investigated through various potential structural modifications of the enhanced finite element model and are presented in Section 6. The analyses of the structurally modified models are shown and discussed in Section 7. Special models which comprise the cover plate separated from the transformer and analyzed for various boundary conditions are dealt with in Section 8. A simplified approach for approximating the bushing frequency as installed on the cover in presented in Section 9. Finally, concluding remarks and recommendation for modeling are summarized in section 10.

SECTION 2

DESCRIPTION OF SELECTED MODEL

2.1 Overview

This study deals with the modeling of electrical transformers, the seismic performance identification, and qualification of high voltage bushings. The high voltage bushings are fragile parts of the transformer (usually mounted on the tank cover) and their failure is closely associated with the loss of functionality of the transformer. The behavior of these elements needs to be assessed not only for rigid base conditions, but through interaction with various components of the transformer. These interactions include when the bushings are supported by the cover plate and subsequently, incorporate their as-installed properties. For the purposes of this study, a typical commercial transformer model has been selected. This section deals with the presentation of the transformer components that are expected to affect the dynamic response of the bushings significantly. The properties of the specific components are also described in detail.

2.2 Transformer Construction

The transformer selected for the investigations is a 230 kV Ferranti-Packard model which comprises of three identical 196 kV / 230 kV bushings, mounted on the transformer's cover plate. The first and third bushings are inclined and the central bushing is vertical. This is illustrated in Figure 2-1 where a typical transformer (of a different make) is presented.

Figure 2-1 Typical three phase high voltage transformer

Each bushing is made of three parts: the upper bushing extending over the turret, the lower bushing immersed inside the tank and the bushing flange through which the bushing is connected to the turret cover. The bushing flange has 12 holes for the bushing to be bolted on the turret cover, arranged in a circular array.

The turret is a cylindrical structure welded on the cover plate and has an annular metal cover bolted to the top. At a small distance from the hole there are twelve studs where the holes of the bushing flange are fitted (bolted) and support the bushing. At the bottom of the turret there is an internal annular disk which serves as the support for the two current transformers located at the bottom of the turret.

The main body of the transformer is the tank, which incorporates many essential components for the functionality of the substation, i.e. the core assembly, the conductors and the oil. In addition, the tank in the current model serves as the supporting structure for all of the external parts of the transformer. The most crucial external parts for the dynamic response of the

structure are the bushings, the conservator, the radiators and the high voltage surge arresters. The bushings are vulnerable to dynamic excitation, while the rest are usually massive components that can potentially affect the response of the more sensitive equipment.

Figure 2-2 Transformer tank structure

The tank has a length of $l_t = 190\ in$, a width of $t_t = 100\ in$ and a height of $h_t = 155\ in$. Figure 2-2 depicts the tank as seen from the side where the conservator is intended to be supported. The load tap changer attached to the tank wall and the supporting frame of the conservator can be discerned. Regarding the load tap changer, it is a relatively heavy component with weight of $w_{ltc} = 5500\ lbs$, length $l_{ltc} = 66\ in$, width $t_{ltc} = 32\ in$ and height $h_{ltc} = 54\ in$.

Figure 2-3 Oil conservator and connection to the tank

Figure 2-3 is an illustration of the conservator and its connection to the tank wall. It can be seen that the connection to the tank wall of the beams supporting the conservator are close to the boundaries of the wall. The conservator is in essence a cylindrical oil reservoir used for the surplus oil during its expansion (when heated) in the main tank which is allowed to expand freely without applying pressure to the walls.

The core-coil assembly is a heavy component as specified by the relative drawings. The main part of the core is a frame consisting of three vertical and two horizontal parts. These components run along the top and the bottom of the frame (Figure 2-5) and are made up of thin sheets of magnetic steel. The sheets have different widths that result in an approximate circular

section for the parts of the frame. Around each vertical member, a winding assembly is fitted (Figure 2-4), allowing the coils of the core to be formed. The core and coil assembly is clamped at the top and bottom with two pairs of steel beams running along the longitudinal direction.

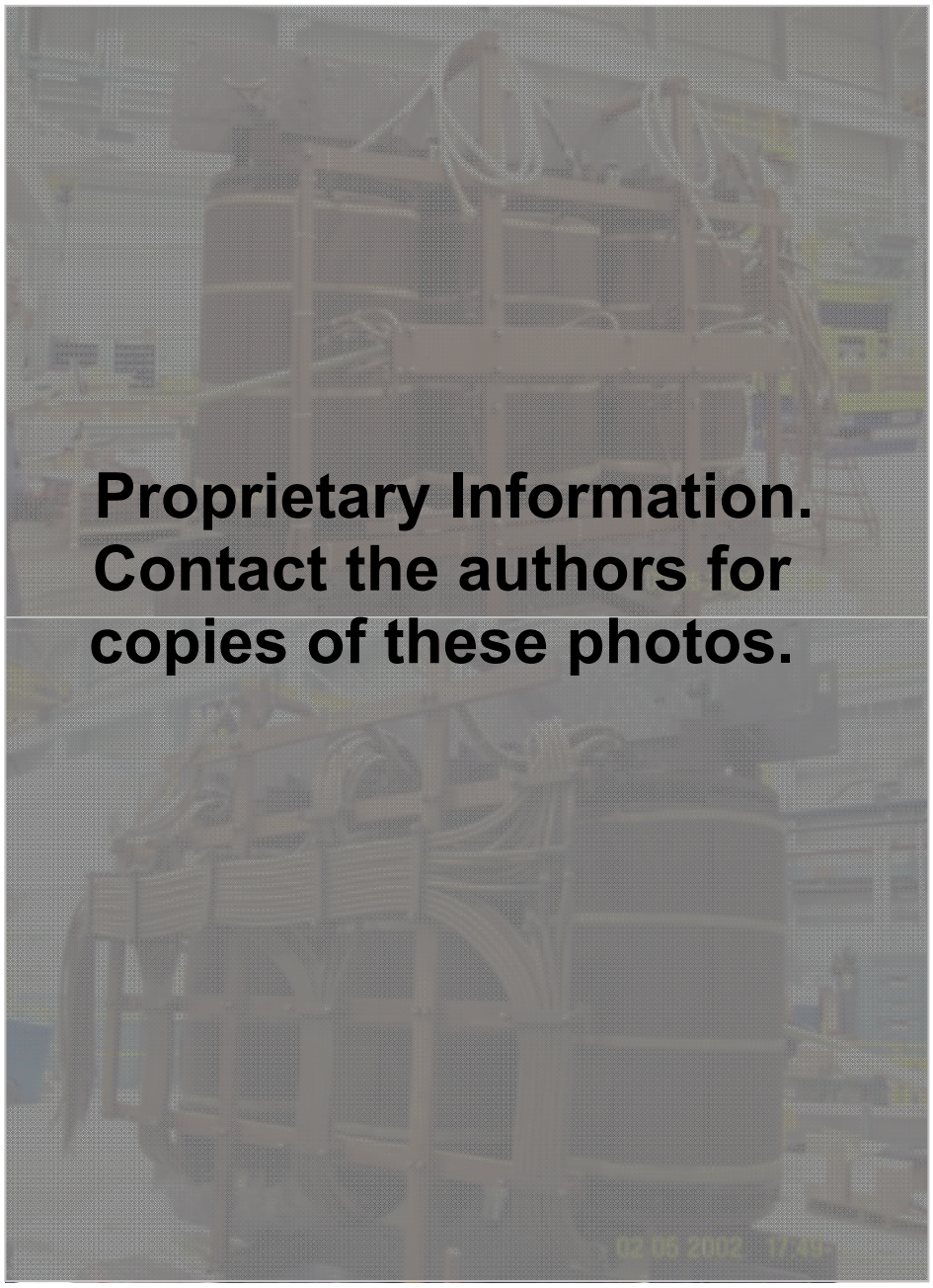

Figure 2-4 Core and coil assembly as seen from the high voltage (up) and the low voltage (down) side

Also shown in Figure 2-4 are the leads connected to the core located at the low voltage side.

The connectivity of the core assembly to the tank is illustrated in Figure 2-5. At the bottom, the core is simply resting on the base plate. More specifically, the notches of the bottom clamps (Figure 2-4) are fitted over the rectangular shaped bars welded on the base plate. The bars act as restrainers in the transverse direction but permit the vertical motion of the clamp.

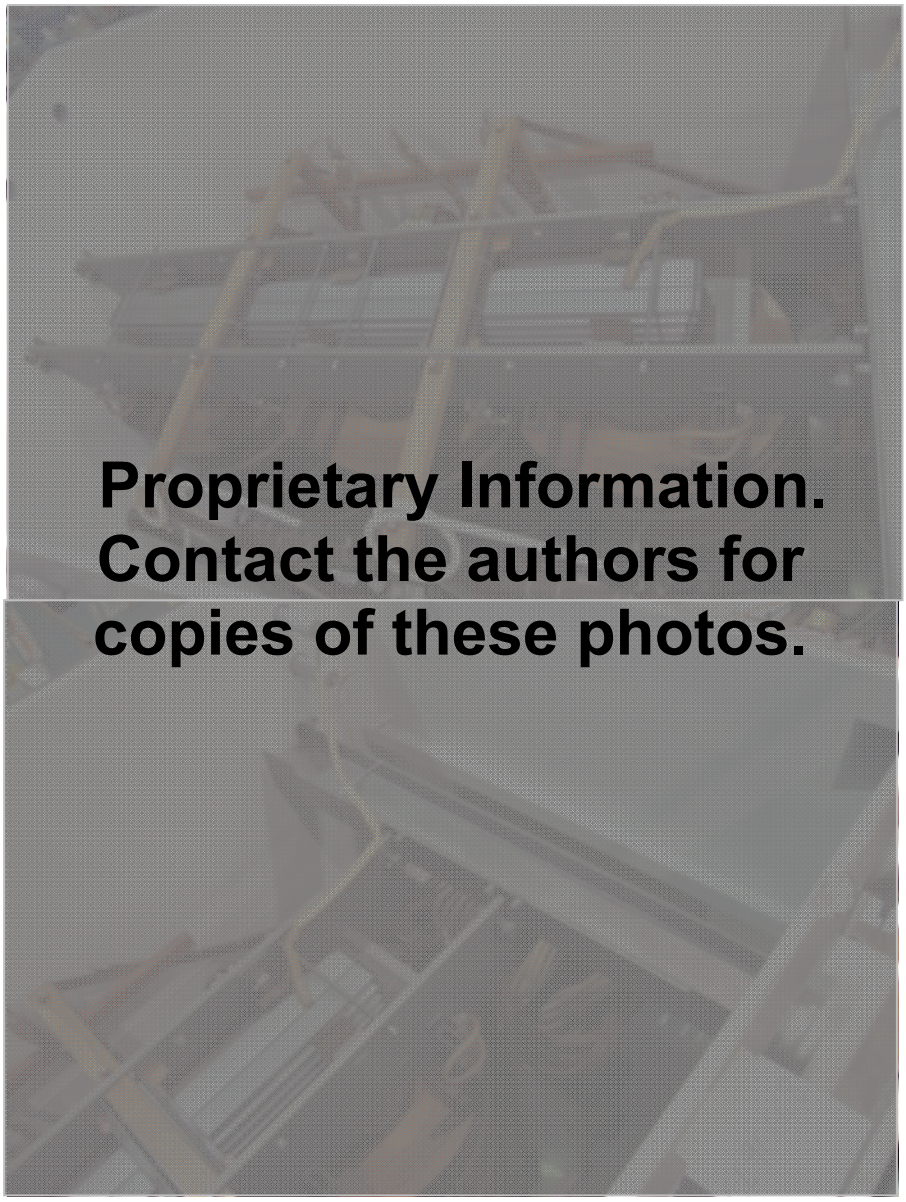

Figure 2-5 Details of core assembly connection to the end walls (up) and to the transverse beam (down)

The top clamps are connected to the end wall on one side and to a transversal beam on the other side. It can be seen from the figures below that the connections are made in such way that some rotation is allowed at these locations.

Apart from the core coil assembly, a small transformer is installed inside the tank, depicted in Figure 2-6 below. This component is bolted on the base plate and also connected to the tank wall.

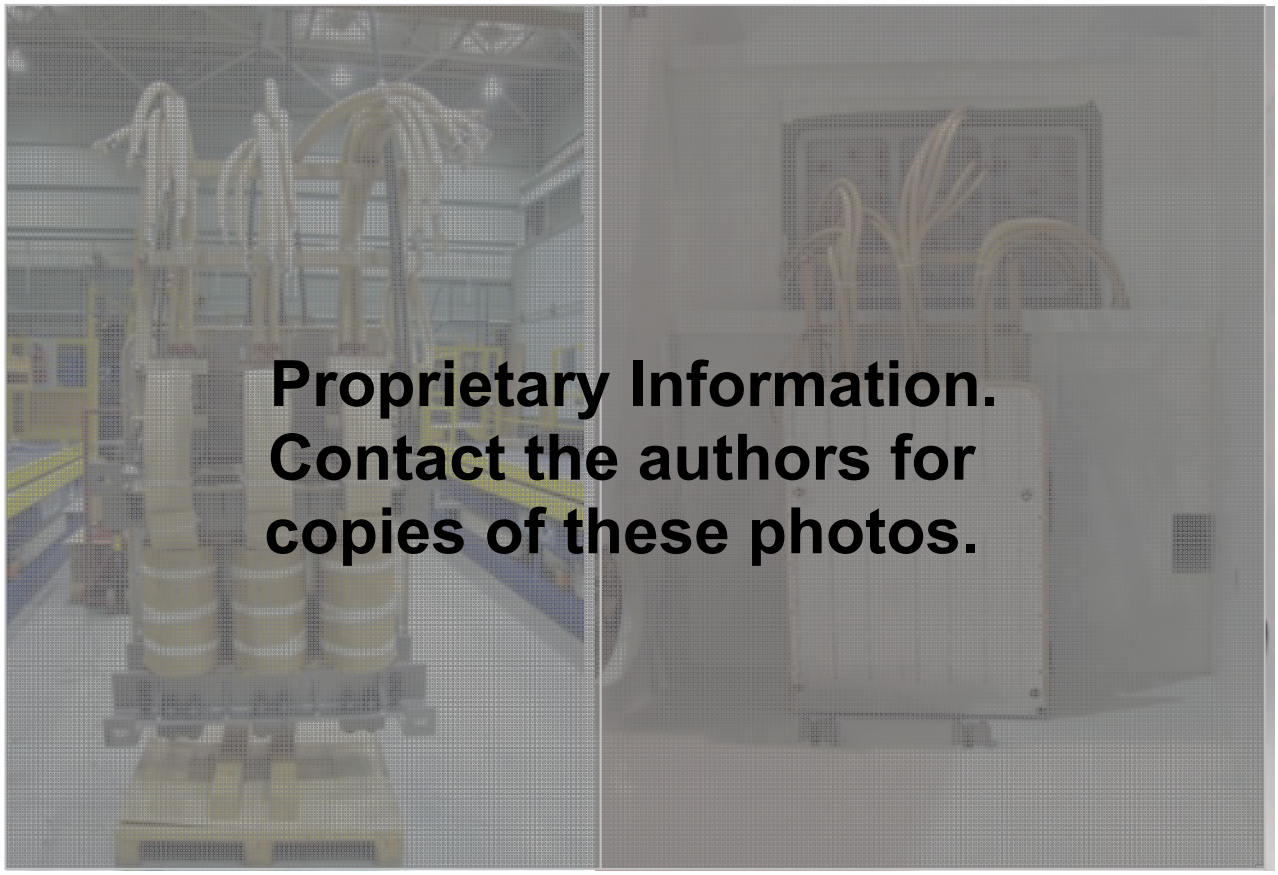

Figure 2-6 Small transformer unit before (left) and after (right) installed in the tank

The transformer comprises a total of fourteen radiators used for cooling the heated oil inside the tank. These radiators are assembled in groups, which are braced by diagonal bars at the top and bottom of each group. The braces connect an L shaped element, which is bolted to the

radiators in the longitudinal direction and used for their support on the tank, with the supporting joints on the tank wall. The connection of each group to the tank is made at distinct locations shown at the top and bottom of the tank wall in Figure 2-7.

Figure 2-7 Side of tank where the radiators are attached. (supporting joints shown)

Finally, the transformer is made of three high voltage surge arresters (not shown in the figures above) connected to the tank cover on the side where the high voltage bushings are located. Note that there are many other components attached to the transformer, such is the reactor. Those parts have relatively small mass to be considered in the dynamic analysis and have shown sufficient performance in past seismic events. Therefore, for reasons of simplicity they have not been referenced in the current section.

SECTION 3

FINITE ELEMENT MODELING OF SELECTED TRANSFORMER

3.1 Overview

A finite element model of the 230kV transformer has been developed with the SAP2000 structural analysis program by W. E. Gundy & Associates, Inc. This model which was prepared for the static analysis was provided for the current research (Figure 3-1)

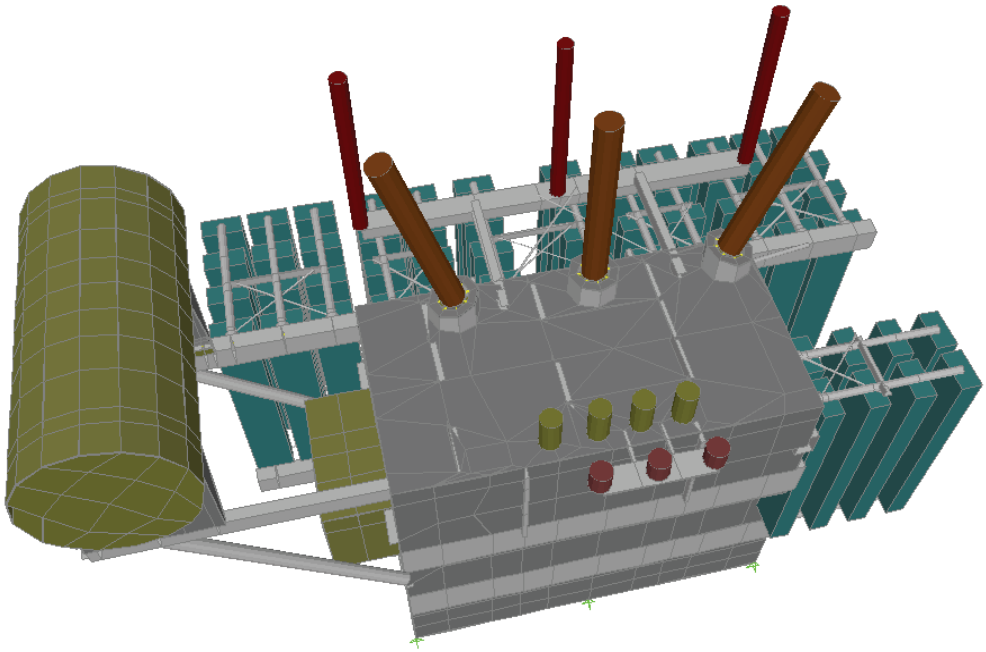

Figure 3-1 Original model in SAP2000

Since the current study deals with the sensitivity of dynamic interactions and special modeling features are needed for some components, proposed modifications on some parts are necessary. .In the following sections, the re-modeling of the most significant parts of the transformer are presented. Also, for sake of simplicity from this point and further, the initial model will be referred as the “original model”.

Additionally, the materials and cross sections used in SAP2000 for the representation of the transformer and its components along with a comprehensive description of the most significant modes of the model are presented in relevant tables.

3.2 Description of Global and Component Modeling

3.2.1 High Voltage Bushings

The high voltage bushings in the current transformer are mounted on the cover plate of the tank as shown in Figure 3-1 and more clearly in Figure 3-2. The central bushing is orientated vertically, the first and third are rotated to the left and to the right respectively, at an angle of 18.5^0. The bushings are coplanar, on a vertical plane in the longitudinal direction of the transformer, as is indicated in the structural drawings provided by the manufacturer.

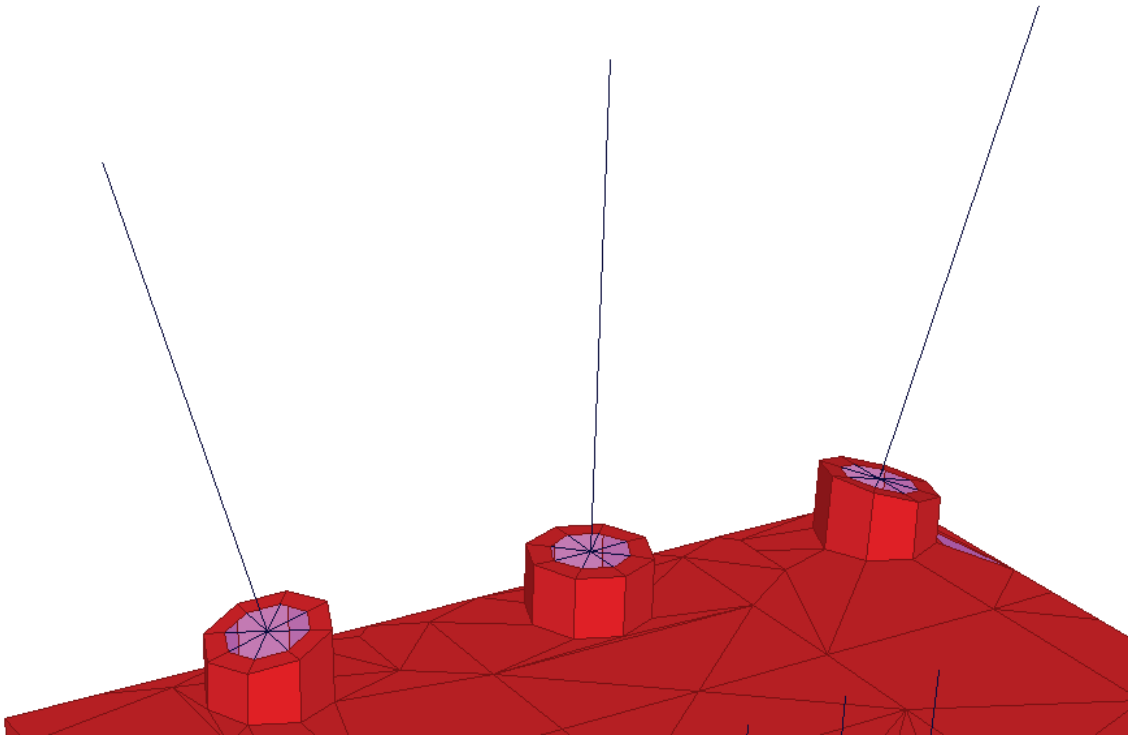

Figure 3-2 High voltage bushings in the original model

Each bushing in the model is an assembly of three parts. The first and upper part represents the actual bushing. It is a beam element with a length of 90 in, distributed mass and weight. The total weight of the bushing is $W_b = 1000\ lbs$ as specified by the manufacturer. The modulus of elasticity of the material used is $E = 6000\ ksi$ and the diameter of the circular cross section used in the beam element is $d = 12\ in$.

The second part is a radial array of rigid elements connected to the turret, which represent the bushing flange. The bushing starts at the center of the flange and is extended upwards using a total of eight elements. Half of the elements have a length of $8\ in$ and the remaining elements have a length of $7.56\ in$.

The lower part in the assembly is the turret. It has a height of $12\ in$ (vertical bushing) and has the shape of a polyhedron with the same number of facets as the number of the radial rigid elements.

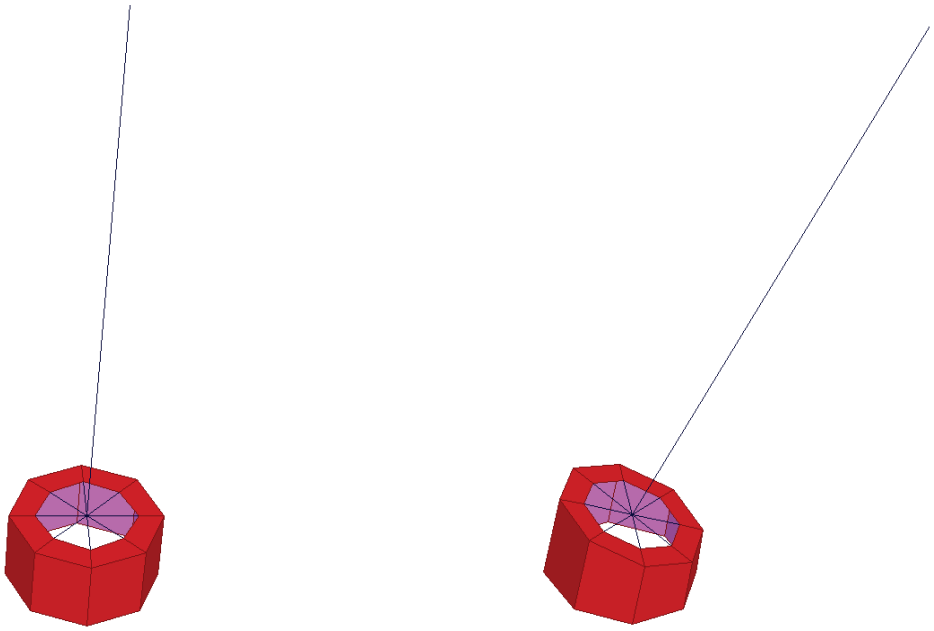

Figure 3-3 Vertical (left) and inclined (right) high voltage bushings in the original model

Removing the bushing along with the flange from the finite element model and fixing the ends of the rigid radial elements, the fixed base frequency obtained is:

$$f = 17.50\ Hz$$

This presents a small discrepancy from the rigid base frequency range provided by the manufacturer (14.1-15.8 Hz). Seeing that the main part of the current study deals with the dynamic identification of the transformer components and the assessment of the interactions between these components, it is important that the existing bushing is modified so that its frequency lies in the range of reference.

In consideration of the fact that SAP2000 automatically calculates the total mass of an element and equally distributes it to the nodes, (using the bushing properties mentioned earlier) the fixed base frequency of the bushing (excluding the flange) can be calculated as:

$$f' = \frac{1}{2\pi}\sqrt{\frac{k}{M}} = \frac{1}{2\pi}\sqrt{\frac{3EI}{h^3}\frac{1}{M}} = \frac{1}{2\pi}\sqrt{\frac{3 * 6000 * 10^3 * \pi * 12^4}{(500/386.22) * 64 * 90^3}} = 22.17\ Hz$$

After comparing the two frequencies, there is a difference which must be attributed to the stiffness of the elements making up the flange, which is a fairly stiff component. For the scope of the current study it is essential that the rigidity of the elements used in the flange is large enough. The reason for this is so the frequency of the bushing, as installed on the turret, matches the fixed base frequency. It is also desired that the interaction between the bushing flange and the turret cover is captured as accurately as possible because this interaction will have an effect on the as installed bushing frequency. In SAP2000, stiffening can be achieved either by using rigid links, or by using elements, the stiffness of which is significantly increased with respect to the stiffness of the remaining elements in the structure. The rigid links should be used carefully because they may produce erroneous results. For the second case increasing the stiffness, of the members that

are intended to be rigid, by an order of 10^6 with respect to the stiffness of the remaining elements in the structure is sufficient.

It is desirable to model the bushing-turret interface as exactly as possible because that may have a significant effect on the as installed frequency of the bushing. Therefore, the number and length of the radial, rigid elements in the flange should be modified appropriately in order to match the data provided by the manufacturer.

Concerning the inclined bushing, the rotation occurs around a transversal axis passing from the center of the flange as it was defined above. Along with the bushing, the flange and the turret cover have been rotated as well. The turret body was not rotated but the wall height was adjusted in order to adapt to the rotation of the turret cover (Figure 3-3).

Finally, the mass of the current transformers needs to be incorporated in the turret for the following dynamic analysis. In the static analysis, for which the original model is intended, the inclusion of these components will not have a significant effect as their weight is relatively small. However, in the current study, in which the as-installed frequency of the bushing-turret assembly plays a major role, the current transformers can potentially affect the analysis results. Following the inclusion of the current transformers, the whole turret body of the vertical bushing assembly could be included in the inclined bushing assembly. However, turret body will be rotated about the transversal axis for the inclined bushings, with a portion of the turret immersed into the tank.

3.2.2 Core-Coil Assembly

The linear and the extruded representation of the core-coil assembly and the base plate in SAP2000 are shown in Figure 3-4. The main parts of the core can be discerned: the top and the bottom clamps, the vertical elements representing the coils, the transverse beam and the rigid

elements at the ends of the top clamps, through which the connection of the core to the side and the end walls respectively is achieved. Also shown aside the core assembly is the small transformer consisting of three vertical coils.

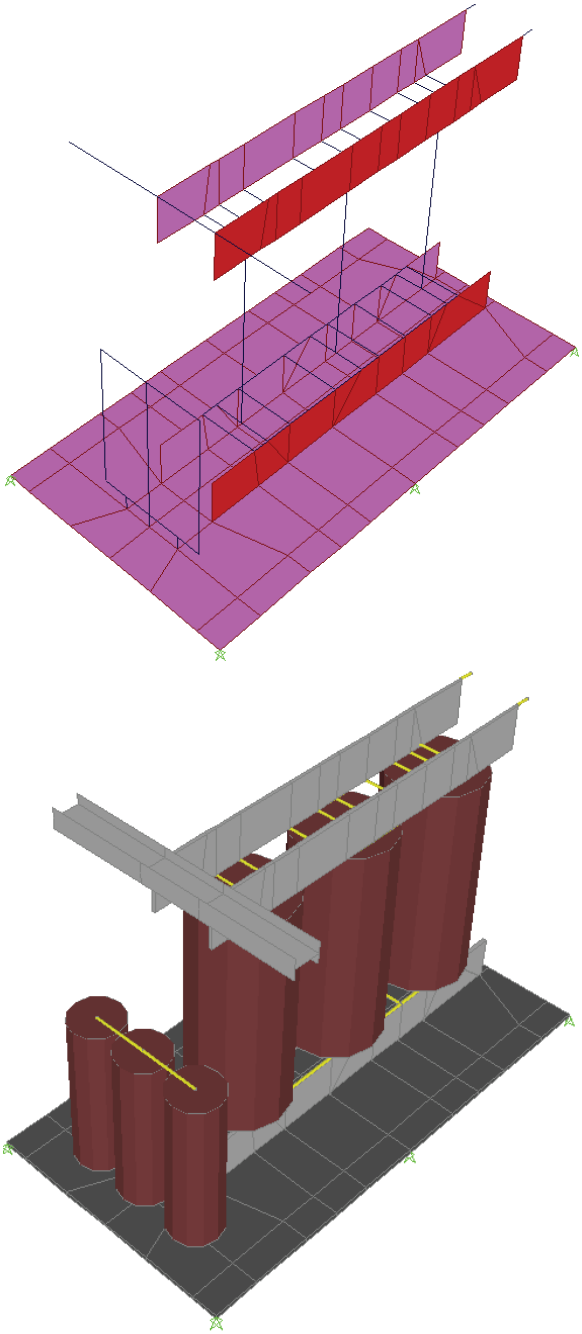

Figure 3-4 Core assembly and base plate linear (up) and extruded (down) representation in the original model

As far as the modeling of the core clamps is concerned, each part of the clamps is a shell with thickness of $t_s = 1.25\ in$, length of $l = 150\ in$ and height of $h = 18.5\ in$ for the clamp located at the bottom and $h = 18\ in$ for the clamp located at the top. The two parts consisting of each clamp are connected with transversal rigid elements of length equal to $24\ in$. This represents the confinement provided to the clamps by the core. The rigid elements are located at the bottom of the top clamp and at the top of the bottom clamp, which are connected at their ends with rigid elements in the longitudinal direction (Figure 3-4). The clamps are connected at a central length, except for an offset of $20\ in$ at their ends, which is not confined by the core and is free to deform. The distance between the top and bottom clamps is equal to the height of the vertical elements, $h = 87\ in$.

In this study the core is considered a crucial component of the transformer, in the sense that it is a massive part (with a total weight of $w_c = 81100\ lbs$) that can affect the dynamic behavior of the whole structure. More importantly the core can affect the dynamic behavior of the bushings, especially in the case that it is braced to the tank wall. Therefore, when the transformer is examined dynamically, the correct modeling of the core assembly is of particular significance. The main part of the core should be modeled as a frame, the vertical parts of which accommodate the coils. This means that the vertical parts of the core should be connected at their ends. Also, the confinement should be applied up to the middle of each clamp because the frame of the core actually extends up to that level. This would have an effect on the deformations of the clamps. Finally, the clamps should be well discretized, especially at their ends, so that their deformations during the dynamic excitation are captured accurately.

3.2.3 Boundary Conditions of the Core-Coil Assembly

On one side the top core clamp is directly connected to the end wall and on the other side it is connected to a transversal beam, which is supported on the side walls (Figure 3-4 and Figure 3-5). The connection at both ends is fixed, and so is the connection of the transversal beam to the side walls. However, as indicated by the manufacturer drawings, this type of connection will allow small displacements and rotations in the clamp. The actual conditions at the ends of the transverse beam also present the same features. The provision for the appropriate modeling of these connections may play an important role in the motion of the core Elaborate dynamic analysis needs to be conducted to determine how the connections play a role in the motion of the core.

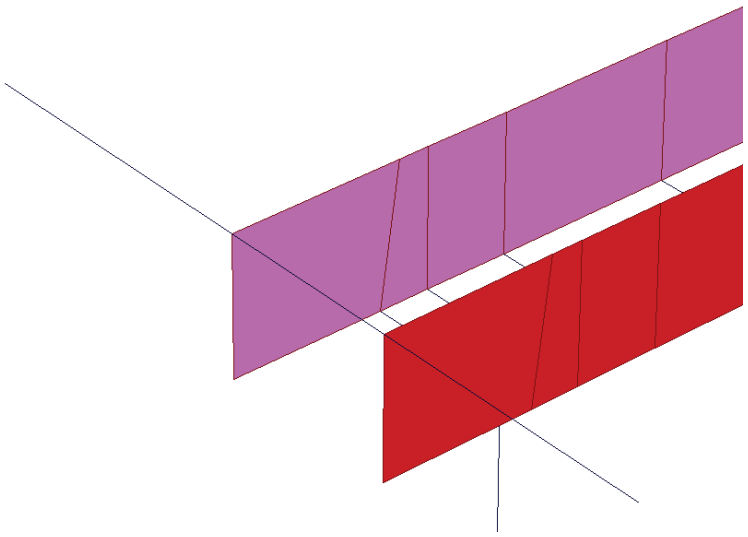

Figure 3-5 Top core clamp and transverse beam connection in the original model

In regards to the connectivity at the bottom of the core assembly, the bottom clamp is connected to the base plate along its whole length in the original model (Figure 3-6). This has a significant impact on the dynamic behavior of the core because in the actual transformer the core

assembly is usually resting on the base plate. More specifically, in the actual model, the bottom clamp is provided with rectangular slots at its bottom at a distance of 5 in from their ends. At the same locations, there are transversal bars welded on the base plate. When the core is placed inside the tank, the slots of the bottom clamp are fitted around the welded bars. The clamp is constrained laterally by restrainers situated at these locations, specifically for that purpose, but not vertically. This should be specifically accounted for in a detailed dynamic analysis.

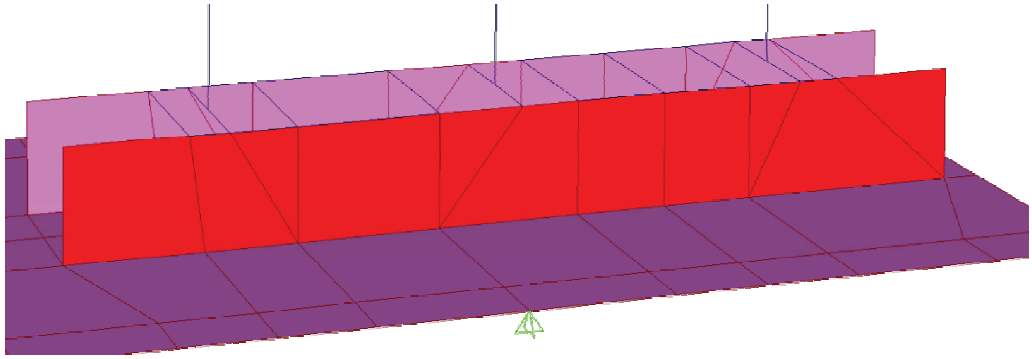

Figure 3-6 Bottom core clamp and base plate connection in the original model

3.2.4 Radiators

The radiators are modeled as depicted in Figure 3-7 and the surge arresters have been removed from the representation for illustrative purposes. The radiators are represented in the original model with vertical elements of rectangular cross section, having a height of $h_r = 118\,in$ and weight of $W_r = 695\,lbs$ each, and are arranged in six groups. Each group composed of diagonally oriented braces on a horizontal plane at the top and the bottom, which extends up to half the length of the group. Also, the radiator groups are directly supported on the tank walls with fixed connections, except for the first and fifth groups away from the conservator. The first and fifth groups are supported on two beams at the top and the bottom, which are fixed to the tank walls. In order to restrain the vertical motion of the first and fifth groups, they are

diagonally braced to the respective tank wall at their bottom and the fifth group is braced additionally at its top.

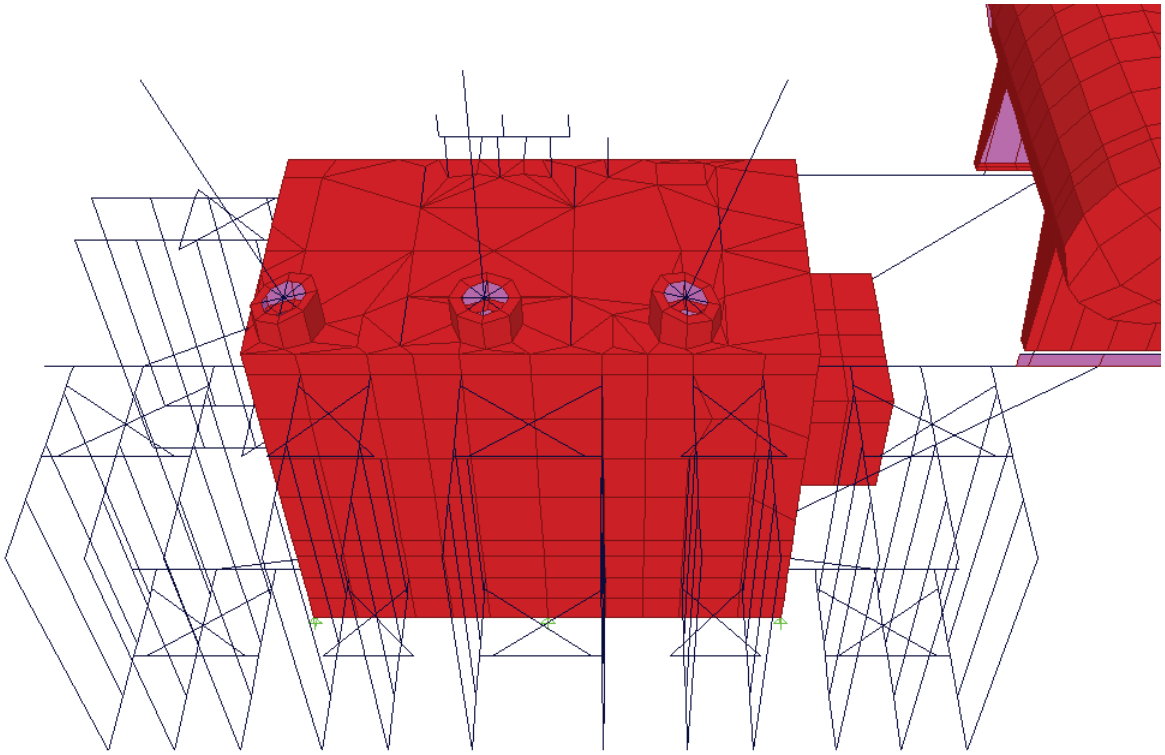

Figure 3-7 Radiators in the original model

3.2.5 Conservator

The conservator is modeled as a cylindrical tank made up of shell elements. The tank is supported by two horizontal and two diagonal beams fixed to the tank wall. It is considered to be full of oil, which has been distributed uniformly on the walls as vertical loading. It is possible that the tank will be half-full of oil at some point, and therefore the effect of the oil sloshing inside the tank, on the dynamic response of the conservator, needs to be investigated in a detailed analysis.

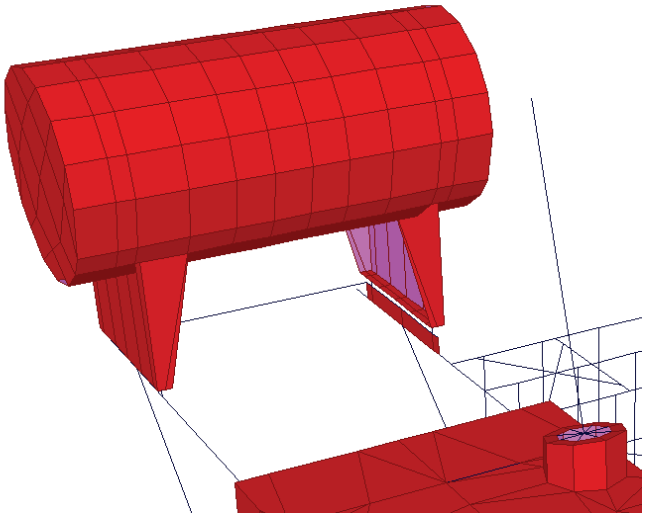

Figure 3-8 Conservator in the original model

3.2.6 Boundary Conditions of the Tank

Naturally, the tank of the transformer rests on a concrete pad which prevents the base plate from deforming downwards. However, in the original model the tank is only being supported at six points on its perimeter (Figure 3-9). That way, not only the base plate can deform, but the vertical displacements will be aggravated by the response of the core-coil assembly. Besides the response being unrealistic, the deformations of the base will certainly affect the response of the walls and subsequently the response of the bushings. It may be desirable that the base plate be supported under the points at which the core assembly is connected to the base plate.

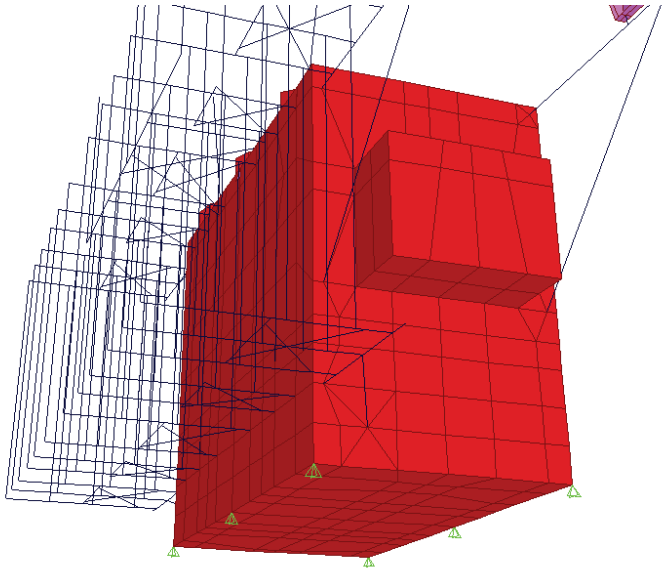

Figure 3-9 Tank supporting system in the original model

3.2.7 High Voltage Surge Arresters

The high voltage surge arresters in the original model are shown in Figure 3-10 in which, for illustrative purposes, the radiators have been removed from the transformer. The arresters are modeled as vertical beams with circular cross section and a height of $h = 90\ in$. Each of the three surge arresters has a weight of $w_{sa} = 154\ lbs$ and is fixed on a longitudinal beam with a length of $l_{lb} = 200\ in$. The longitudinal beam is located at a distance of $d = 50\ in$ from the side wall of the tank. The beam is supported on the tank cover with two transverse beams, which extends at a length of $18\ in$ across the plate from the side wall. In addition to that, two diagonal braces connecting the longitudinal beam and the cover are used in order to reduce the rotation of the assembly.

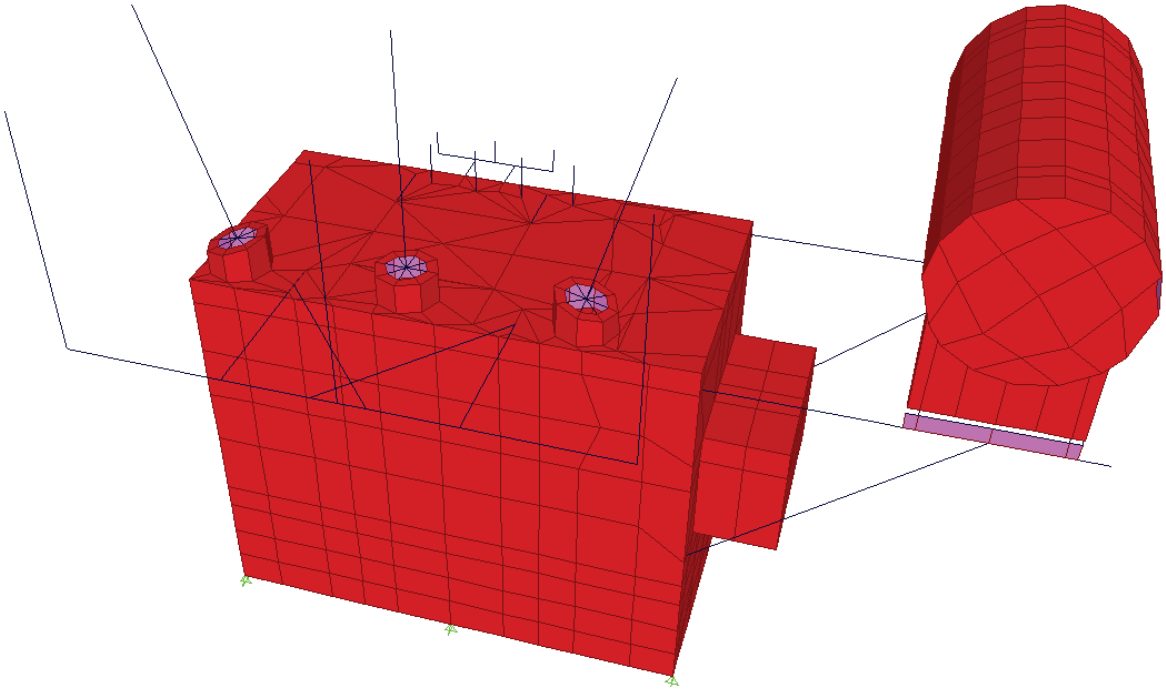

Figure 3-10 High voltage surge arresters in the original model (radiators removed from view)

3.2.8 Modeling of Oil

The tank of the transformer is considered to be full of oil with a total weight of $w_{ot} = 89.35\ kip$. The oil is distributed uniformly on the walls, in the form of vertical forces at the joints of the shell elements comprising the walls. Since the original model is intended for static analysis, the interaction between the oil mass and the core has not been accounted for as the oil mass is completely independent of the core assembly. However, in the current study, that interaction could have some significant effect on the vibration of the core and should be taken into consideration when the dynamic response of the structure is investigated.

The load tap changer tank, supported by the wall located on the conservator side (Figure 3-9), is full of oil with total weight of $w_{oltc} = 2.48\ kip$. This oil is distributed on the walls of the load tap changer in the same way as was explained above.

3.3 Modal Analysis of the Model

An eigenvalue modal analysis was carried out on the original model in a preliminary effort to identify the dynamic characteristics of the transformer and the natural frequencies of the components of interest. The results are presented in Table 3-1. Shown are the periods and frequencies of the first 40 modes of the analysis along with a description of the global as well as of the internal modes of the transformer (core assembly and small transformer)

Table 3-1: Modal analysis results and comments

Mode	Period	Frequency	Mode Description	Internal Modes
	sec	Hz		
1	0.596	1.68	HV Arrester Close to Conservator	None
2	0.595	1.68	HV Arrester Furthest from Conservator	None
3	0.370	2.70	Radiator	None
4	0.368	2.72	Conservator/Radiator	None
5	0.345	2.90	HV Arrester Middle Unit	None
6	0.243	4.12	HV Arrester Support with HV Bushing Movement	None
7	0.233	4.30	Central HV Bushing	None
8	0.192	5.20	Radiator with HV Bushing Movement	None
9	0.186	5.39	Radiator with HV Bushing movement	Top Core Support Bending Movement
10	0.183	5.46	Radiator with HV Bushing Movement	Insignificant Internal Movement
11	0.179	5.59	HV Bushings Outer Units	Insignificant Internal Movement
12	0.170	5.89	Radiator and Conservator With HV Bushing Movement	Slight Movement of Small Transformer
13	0.164	6.09	Radiator and Conservator With HV Bushing Movement	Small Movement of Small Transformer
14	0.159	6.30	HV Bushings Outer Units	Small Transformer Mode
15	0.158	6.31	HV Bushings Outer Units	Small Movement of Small Transformer
16	0.149	6.72	Larger Radiator	Small Movement of Small Transformer
17	0.142	7.05	HV Bushings Large Movement With HV Bushing Next to Conservator	Insignificant Internal Movement

Table 3-1: Modal analysis results and comments (contd)

18	0.139	7.21	Radiators	Insignificant Internal Movement
19	0.131	7.64	Central HV Bushing	Insignificant Internal Movement
20	0.128	7.81	Central HV Bushing	Insignificant Internal Movement
21	0.124	8.08	Radiators	Insignificant Internal Movement
22	0.117	8.56	Radiators	Insignificant Internal Movement
23	0.115	8.72	HV Arrester Support, Vertical Movement	Insignificant Internal Movement
24	0.111	9.01	HV Arrester Support, Vertical Movement	Insignificant Internal Movement
25	0.102	9.79	Radiator	Small Transformer Mode and Vertical Motion of Base Plate
26	0.094	10.68	Radiator	Top Core Support 2nd Bending Movement
27	0.090	11.07	Radiator, Conservator, and LV Arrester Support	Top Core Support 3rd Bending Movement
28	0.087	11.55	Radiator and Conservator	In Plane Core Bending Mode and Small Transformer Mode
29	0.077	12.97	Radiator	Insignificant Internal Movement
30	0.073	13.63	LV Arrester Support	In Plane Bending Mode of the Small Transformer
31	0.069	14.40	Radiator, Conservator, and LV Arrester Support	Rocking Mode of Bottom Core Supports, In Plane Mode of Small Transformer, Top Core Support Higher Mode
32	0.061	16.35	LV Bushings and Arrester Support	Similar to 31 but Bottom Core Support and Small Transformer are out of phase
33	0.056	17.80	LV Bushings and Arrester Support	Insignificant Internal Movement
34	0.049	20.35	Radiator, Conservator, and LV Arrester Support	Insignificant Internal Movement

Table 3-1: Modal analysis results and comments (contd)

35	0.040	25.10	Transformer Tank	Slight Movement of Internal Components
36	0.035	28.35	Transformer Tank, Top Plate Vertical Movement	Small Movement of Internal Components, Higher Modes
37	0.033	29.96	Transformer Tank	In Plane Movement of Bottom Core Leg Supports
38	0.018	54.51	Transformer Tank	Rocking Mode of Bottom Base Plate, Small Transformer and Other Components
39	0.018	55.74	Transformer Tank	Vertical Motion of Base Plate and Other Components
40	0.017	60.39	Transformer Tank, Vertical Movement	Rocking Motion of Base Plate and Other Components

SECTION 4

ADVANCED MODELING, SENSITIVITY AND ASSESSMENT OF INTERACTIONS

4.1 Overview

This section discusses the advanced modeling of specific electrical components incorporated into the 230 kV transformer model (developed in SAP2000), with the intention of using the model for reliable sensitivity analysis. An elaborated description of the modifications on the selected components along with the assumptions is located in this section. Finally, the techniques used for the identification of the dynamic properties of the system and for the assessment of interactions between various components and the bushings are explained in detail.

4.2 Objective of Advanced Modeling

The modeling of the following components of the transformer is considered most essential for the sensitivity analysis:

- High voltage bushing-turret system. The high voltage bushings are the primary components of interest in the transformer and need to be modeled as realistic as possible. They should reflect the same mass distribution, geometric and dynamic properties as the ones provided by the bushing manufacturer. Furthermore, the turret models should be assigned the same mass and geometric characteristics as real turrets used in industry. The current transformers, usually contained inside the turrets, need to be included in the model because their mass can be significant and affect the dynamic response of the bushing. Finally, the interface between the bushing and the turret (including the bolts and the gasket) should be modeled appropriately because it significantly influences the as-installed dynamic properties of the bushing-turret system.

- Cover plate mesh. The shell elements employed, to represent the cover in the finite element model, should be arrayed in a way that allows for all possible deformations of the plate and the bushing-turret assemblies.
- Core-coil assembly. The core is a massive component, the dynamic response of which is likely to have a significant impact on the response of the high voltage bushings. The reason for the significant impact on the high voltage bushings is because it is braced to the transformer walls and must be modeled thoroughly. The main frame of the core, which accommodates the coils, should be considerably stiff. While the mass distribution of the main frame, the weight of the frame, as well as the weight of the windings (coils) should be taken into account. The core clamps located at the top and the bottom part of the core-coil assembly should be confined by the main frame along the length of the frame. While the unconfined overhangs at the ends of the clamps should be properly meshed for the torsional deformations to be unimpeded.
- Core-coil assembly boundary conditions. Since the core is simply resting on the base plate of the transformer, it is imperative that the boundary conditions of the core-coil assembly are modeled accurately so that rocking motion of the core is not prohibited. Moreover, the clamps' connections to the walls should conform to the restrains dictated by the construction drawings. Finally, provisions should be taken for the boundary conditions between the base plate and the ground in the finite element model. Seeing that in most cases the transformer is resting on a concrete pad (preventing the base plate from deforming downwards), a number of supports should be placed between the base plate and the absolute space in the model. All of the supports are needed in the model so the motion of the core will not affect the motion of the base plate.

- Distribution of oil. In the case when the transformer is operating, the tank is full of oil. The dynamic response of the fluid is expected to affect the behavior of the whole tank because its mass is considerable. Thus, a scheme should be considered for the distribution of the oil both on the walls of the tank and the core-coil assembly.

Based on the aforementioned, the original model provided was modified appropriately before the dynamic analyses were carried out. The relevant modifications are presented in the following section explicitly.

4.3 Modifications on the Original Model

4.3.1 High Voltage Bushings

It is essential that the bushing-turret system is modeled as accurately as possible so that the true interactions can be assessed. The bushing included in the original model consists of the turret, the turret flange at the top of the turret, an array of radial rigid elements representing the bushing flange and a bar which is perpendicular to the flange, extending from the center of the flange and above, which represents the high voltage bushing (Figure 4-1). The mass is distributed uniformly over the height of the vertical bar ($m_{HVB} = 9.824 \times 10^{-5}$ kip/in^3) and the flexibility (E = 6000 ksi) is such that the fixed base frequency of the bushing is f = 17.5 Hz.

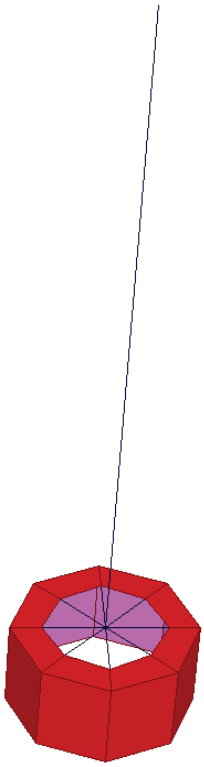

Figure 4-1 Bushing in original model

The bushing used in the transformer examined is the T196W0800AY model, the drawings and the detailed data of which are provided. More specifically, the data of interest are summarized in Table 4-1.

The procedure followed for the modification of the bushing-turret system is described below. The new bushing model is made of three main parts. The top part is a massless beam which represents the upper bushing; its mass is concentrated at the upper bushing center of gravity. The stiffness of the beam is adjusted in such way so that its stiff mounted frequency matches the one provided by the manufacturer. The bottom part represents the lower bushing and is modeled as a rigid beam with its mass concentrated at the lower bushing center of gravity. The lower bushing is composed of a part extending from the bushing flange (mentioned below as interface) and upwards, to the bottom of the upper bushing and a part extending from the bushing

flange and downwards, to the bottom of the bushing (internal connector connection). Finally, the bushing flange is modeled as an assembly of rigid elements in a radial arrangement, the number of which equals the number of the anchor bolts that holds the bushing on the turret.

Table 4-1 High voltage bushing properties

Total Weight (Wt)	lbs	1022.0
Center of Gravity (CG) Location (measured from the top of the bushing flange)	in	13.66
Upper Bushing Center of Gravity (UBCG) Location (measured from the top of the bushing flange)	in	40.4
Upper Bushing Weight (UBWt)	lbs	687.0
Upper Bushing Height (h) (measured from the top of the bushing flange)	in	90.7
Flange-Interface Distance (FID)	in	6.0
Flange to Lower Terminal Distance (FtLT)	in	60.0
Stiff Mounted Bushing Frequency	Hz	14.1-15.6
Diameter of bolt circle	in	21.0

Using the data provided above, the Lower Bushing Weight (LBWt) can easily be calculated as:

$$LBWt = Wt - UBCG = 1022 - 687 = 335\ lbs$$

Also, the Lower Bushing Center of Gravity (LBCG) location is:

$$LBCG = \frac{Wt * \mathrm{CG} - \mathrm{UBWt} * \mathrm{UBCG}}{LBWt} = \frac{1022 * 13.66 - 687 * 40.4}{335} = -41.18\ in$$

Where, the distance calculated is measured from the interface and downwards.

With these data known, a preliminary model was developed (Figure 4-2). This model includes only the first part of the model described above, namely, the upper bushing. It consists of a massless beam fixed at the bottom, with a node at the upper bushing center of gravity where the mass is lumped. The modulus of elasticity of the material assigned to the beam was adjusted so that the stiff mounted frequency of the upper bushing was in the range of frequencies that the manufacturer provided. The modulus of elasticity finally chosen was:

$$E = 350 \text{ ksi}$$

And the stiff mounted frequency achieved was:

$$f = 14.84 \text{ Hz}$$

a value which is in the range provided (14.1 - 15.8 Hz).

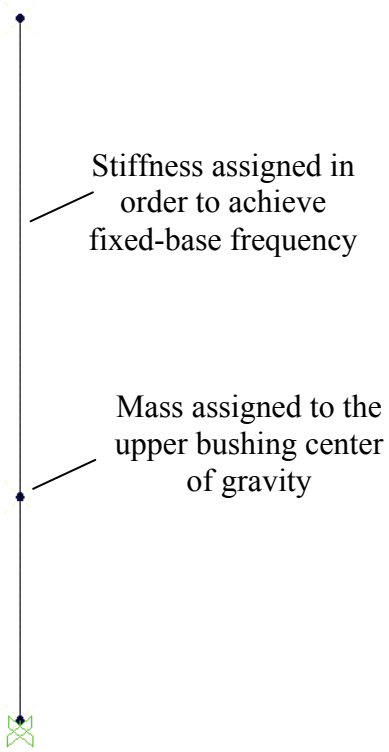

Figure 4-2 Upper bushing model

Next, a transition model was created (Figure 4-3) which serves for the estimation of the turret cover thickness as is demonstrated in the following.

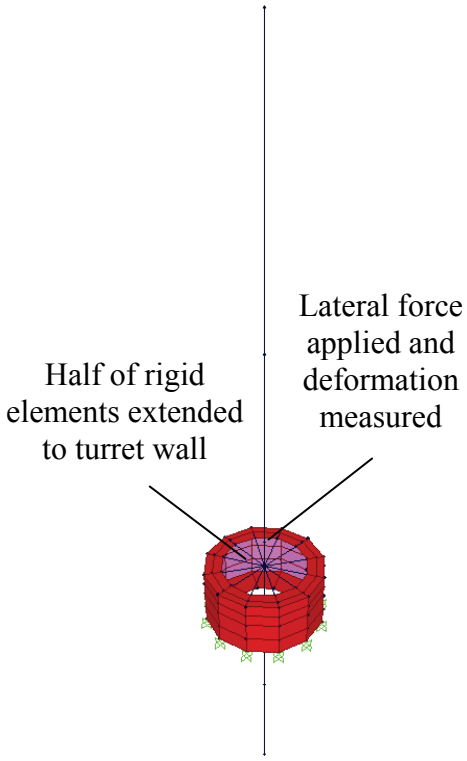

Figure 4-3 Transition model

For this model, certain attributes of the turret were needed, which were given in the drawings provided. Those are presented in Table 4-2:

Table 4-2 Turret properties

Turret outer diameter (OD)	in	23.75
Turret inner diameter (ID)	in	17.25
Turret height	in	12.0
Number of anchor bolts holding the bushing to the turret cover	-	12
Number of Current Transformers (CTs)	-	2
Height of lower CT	in	3.50
Height of upper CT	in	3.75
Weight of lower CT	lbs	184.0
Weight of upper CT	lbs	196.0

The CTs are found inside the turret located at its bottom. The turret wall was divided into four layers, with the heights of the bottom layers being equal to the ones of the CTs. The remaining two layers were assigned heights equal to half of the remaining height of the turret. The material and the thickness of the walls were left intact with regard to the original model. The CTs were accounted for by incorporating their weight into the relative bottom layers. The turret cover was modeled as an annulus with the dimensions provided by the drawings, that is, with OD = 23.75 in and ID = 17.25 in. The annulus was subdivided into two parts with the internal part having an outer diameter equal to the diameter of the bolt circle (21 in).

The bushing flange was represented by twelve rigid elements as discussed above. In the transition model the rigid elements have unequal lengths, more specifically on the left side. Five of these elements extend from the center of the flange to the top of the turret wall, having a length of 12 in. The remaining seven rigid elements extend from the center of the flange to the end of the internal part of the annulus representing the turret cover. Therefore, these elements have a length equal to the radius of the bolt circle, 10.5 in.

The bushing was modeled as discussed above, with the upper bushing having the properties assessed from the upper bushing model initially developed.

Following the modeling of the bushing-turret system, a horizontal force was applied at the top of the lower bushing (bottom of the upper bushing) longitudinally with direction to the left. The magnitude of the force was:

$$F = 1000 \text{ kip}$$

And the horizontal displacement measured at the point of application of the force was:

$$d = 5.14 \times 10^{-2} \text{ in}$$

The transition model was modified and the final bushing-turret assembly model was developed (Figure 4-4). The differences from the previous model are minor. First, the length of the rigid elements representing the bushing flange was modified in order that all of them have the same length. Their length was defined as the average of the radius of the bolt circle and the turret cover radius:

$$L = (11.88+10.5)/2 = 11.19 \text{ in}$$

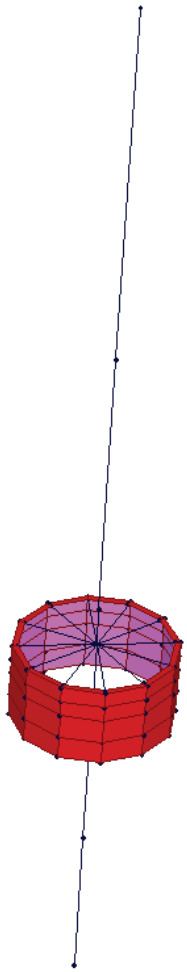

Figure 4-4 Modified bushing model

Afterwards, the turret cover was modified to include an annulus with an outer diameter of 23.75 inches and an inner diameter of 22.38 inches (the equivalent diameter of the bushing flange calculated above). The thickness of the shell elements representing the annulus was

adjusted so that when the same horizontal force is applied at the top of the lower bushing (1000 kip), the same displacement (5.14×10^{-2} in) is found at that point. Finally, the thickness of the cover was determined at:

$$t = 27.25 \times 10^{-2} \text{ in}$$

Since the transformer under examination has two additional identical inclined bushings, the modified bushing was inclined first to the right and then to the left and two more models were created. The angle of inclination was 15^0 as is indicated by the relative drawings. The procedure followed is the same for each of the two models and is described for the bushing inclined to the left only.

In the vertical bushing, a point on the circumference on the left side at the bottom of the turret was chosen. Then the diametrically opposite point to that was found. For convenience, these points were selected to lie on a line parallel to the longitudinal global axis. The distance d of each point at the bottom of the turret from the point chosen on the left side was measured in the longitudinal direction. Then for each point a second point was created at a vertical distance given by:

$$h = d * \sin\theta$$

Where $\theta = 15^0$ is the angle of inclination.

After that, the layers on the turret wall were adjusted in order to incorporate the new points while at the same time retaining their initial properties. Then, the turret was inclined to the left.

The inclined turret is to be partially submerged inside the tank and the connection to the tank cover will be made at the new points created which form an ellipse on the turret wall.

The approach explained above is deemed to approximate the nonlinear behavior of the bushing flange-turret cover interface when the bushing rotates. This would avoid the use of nonlinear elements that would capture the exact response of the bolts and the gasket. To illustrate the concept, the physical representation of the bushing-turret system is considered, a cross section of which is shown in Figure 4-5. In that, the turret, a part of the bushing and the bolts clamping the bushing and turret cover together are shown.

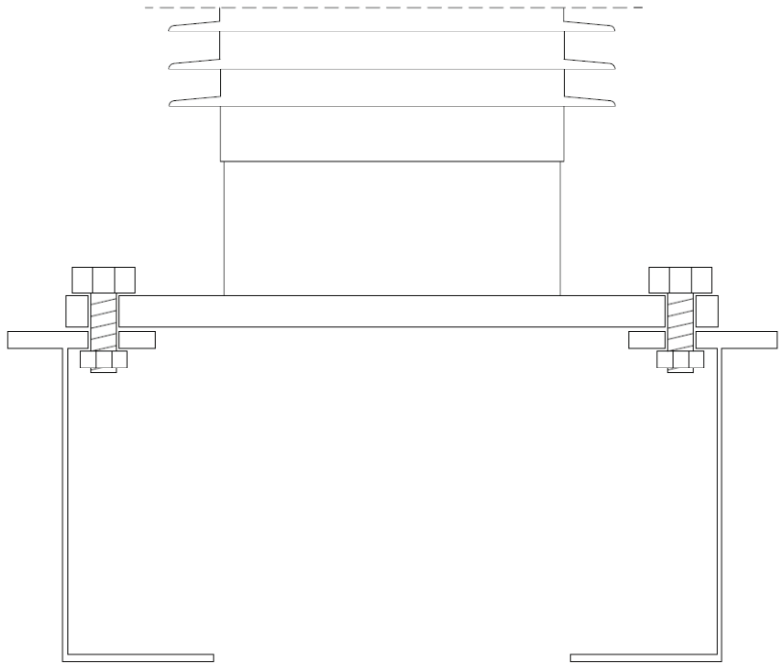

Figure 4-5 Bushing-turret system

Based on the above representation and neglecting the part of the turret cover extending outside the turret walls, a more accurate model for the bushing-turret system is shown in Figure 4-6. The bushing has been simplified to a vertical beam with the same attributes as was done for the upper bushing model explained above. The flange can be represented by an annulus with the same characteristics as the bushing flange and the internal disc defined by the bushing diameter can be modeled as rigid. However, the bushing flange can be considered essentially rigid and has

been represented in Figure 4-6. When the transformer is under dynamic excitation, the bushing flange can rotate and move vertically (upwards). The rotation of the flange is restricted in the sense that when one end of the flange meets the respective end of the turret cover, the flange instantly stops rotating about its centroidal axis. However, the flange will begin rotating about a new pivot point which is the contact point of the flange and the turret cover end. During the dynamic response of the flange, the bolts can be stretched acting as restoring forces for the flange, but cannot be compressed. Therefore, in this model the bolts have been represented with springs and gap elements have been placed between the flange and the turret cover at the locations of contact as shown in Figure 4-6.

The simplified model intended to avoid the use of the gap and spring elements, is shown in Figure 4-7.

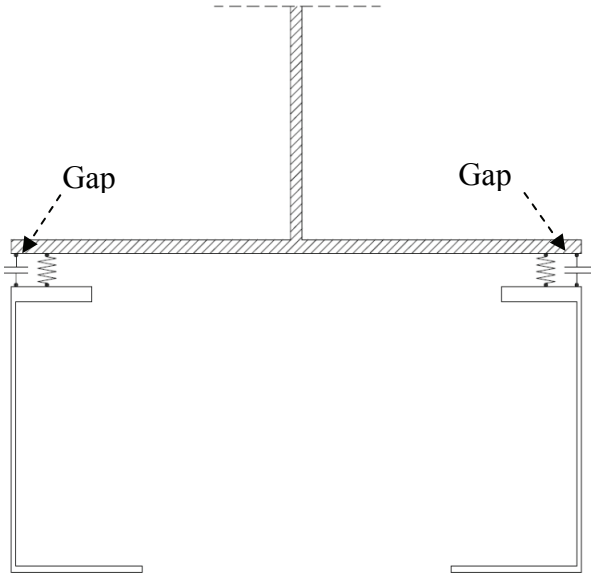

Figure 4-6 Accurate model

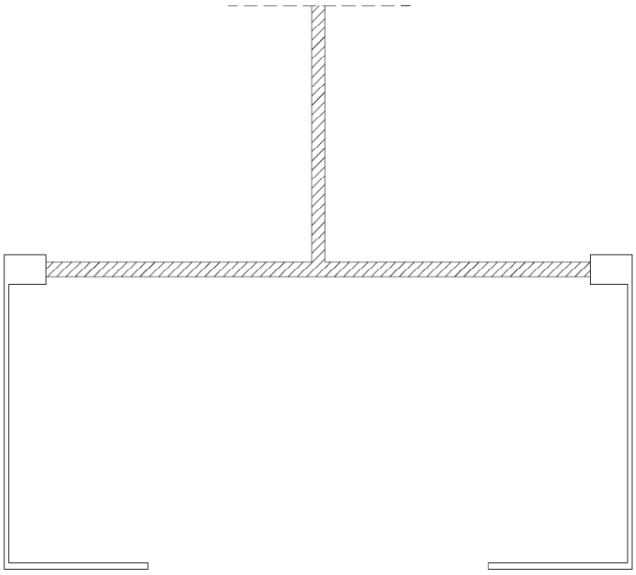

Figure 4-7 Simplified model

When a force is applied on the bushing (a procedure that was followed earlier on the simplified model) the expected deformation of the turret is depicted in Figure 4-8 and Figure 4-9,

for the accurate and the simplified model respectively. It can be deducted that the turret walls deform differently for the two models for the same type of loading.

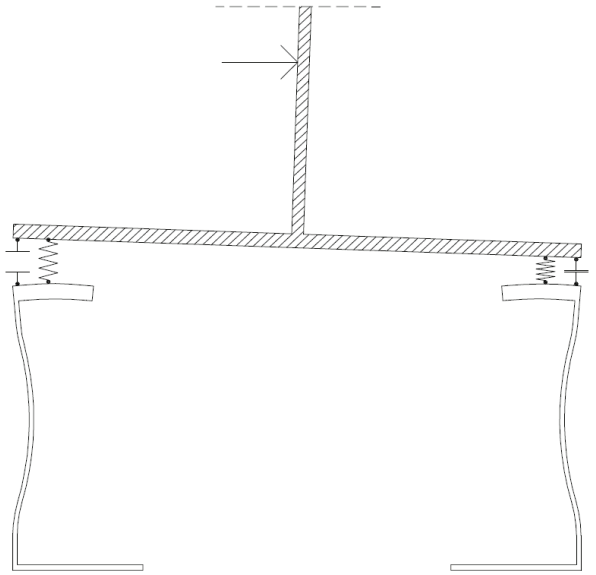

Figure 4-8 Turret deformation in the accurate model

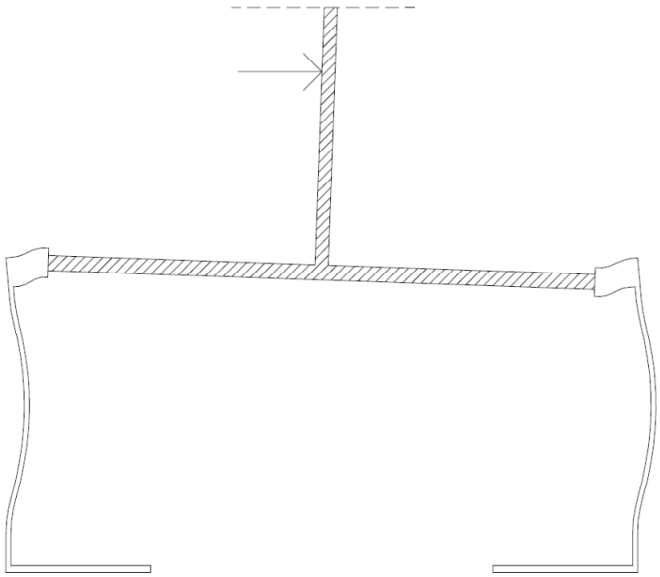

Figure 4-9 Turret deformation in the simplified model

Furthermore, it should be noted that the simplified model includes a turret cover with an equivalent inner diameter (half the sum of the turret and bolt circle diameter) and adjusted thickness so that the behavior of the full turret cover is approximated. This is a rather simplified assumption since a large part of the cover, which would provide resistance to the flange rotation, is neglected. In Figure 4-10 the (excessive) deformation of the turret cover for the accurate model under the loading shown in Figure 4-8 is depicted. It can be seen that the inner part of the annulus is deforming as well, affecting the overall deformation of the cover and consequently of the bushing flange connected to it.

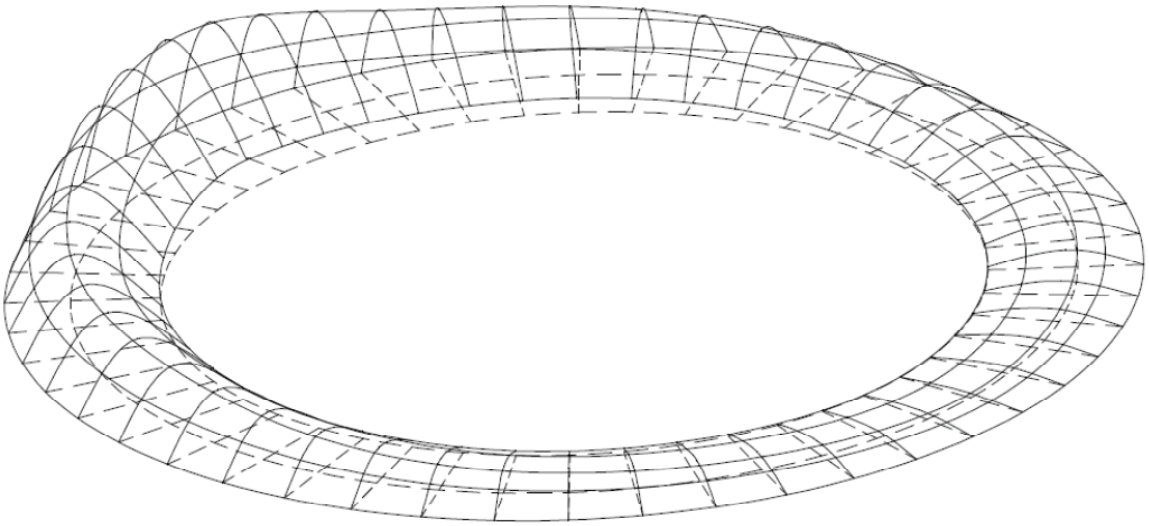

Figure 4-10 Turret cover deformation for lateral loading of the bushing

Bearing all these in mind, it can be considered that the simplified bushing-turret model may present a dynamic response that deviates from the realistic one. However this simplified modeling approach was employed, since the large amount of gap elements in the accurate model would be impractical for the dynamic analysis in SAP2000.

4.3.2 Cover Plate Mesh

The mesh of the cover plate plays a significant role in the assessment of the response of the bushings. It should be adequately fine so that all the important modes of the bushings, as well as of the cover plate, can be captured with sufficient accuracy. The discretization of the cover plate elements in the original model is relatively random and coarse. This results in not all the possible bushing and cover modes appearing during a dynamic analysis.

For this issue to be resolved, the cover plate was initially isolated from the original model and divided into three parts each containing one bushing. By dividing the cover plate in this fashion, three separate models were developed. The border lines for these models are the ends of the cover plate and the stiffeners between the bushings. It is noted that the total width of the

cover plate was chosen to be incorporated into each model since the distance between the stiffeners is larger than half the width of the cover plate.

Initially, for each of the three models the shell elements representing the cover plate were removed and an annular mesh was created around the bushing. The outer diameter of the annular mesh area was chosen such that for the vertical bushing, the width of the annular mesh area, would be 5.5 in. This diameter is equal to the width of the internal ring at the base of the turret, intended to accommodate the CTs. The inclined bushing (as is the case of the bushing farther from the conservator) has the distinctiveness that the boundary between the cover plate and the turret wall is elliptic. In the cover models that incorporate the inclined bushings, the diameter of the annular mesh was kept the same. Since the interface at the connection of the cover to the turret wall is elliptic, the width of the annular mesh varied.

At the natural boundaries of the cover plate (close to where the high voltage bushings are located) a rectangular mesh had to be created with a width of 1 in, while, at the borderlines of the segmental models, defined by the stiffeners, the width of the mesh was larger, 4.5 in. Additionally, a smooth transition mesh was created, connecting the mesh at the borderlines and the edges to the annular mesh located around the turret. The rest of the plate was meshed with rectangular elements except, at the locations where components are connected to the tank (e.g. the surge arresters) or mounted on the cover (e.g. low voltage bushings). At these regions the mesh was made to be as least distorted as possible. Figure 4-11 and Figure 4-12 demonstrate the cover in the original and modified models in SAP2000 and depict the modifications made.

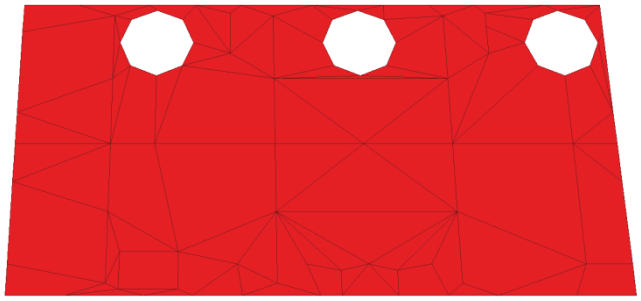

Figure 4-11 Cover in the original model

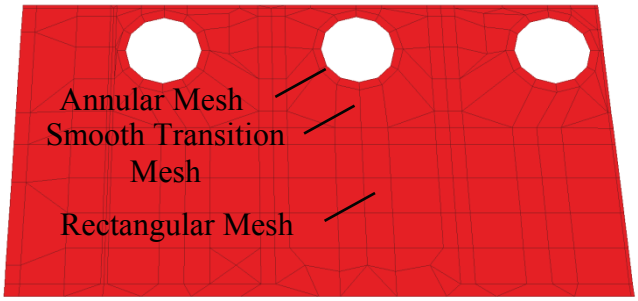

Figure 4-12 Cover in the modified model

In order to determine the adequacy of the cover plate discretization, as far as the dynamic response of the plate and the high voltage bushings is concerned, four additional cases were investigated. For each case, the mesh was coarser or finer with respect to the model of the modified cover, developed through the procedure earlier described. More specifically, the mesh variations considered were:

- Half the mesh of the modified model
- Twice the mesh of the modified model
- Four times the mesh of the modified model
- Four times the mesh of the modified model and the large elements of the cover divided in half

These variations are presented in the figures that follow:

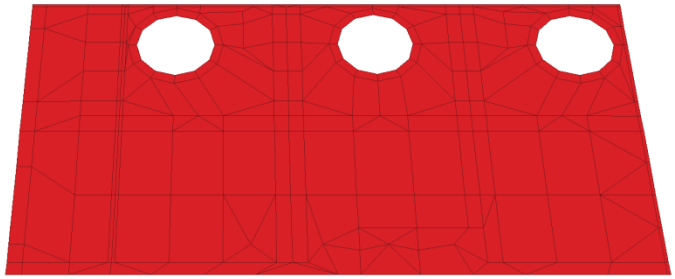

Figure 4-13 Cover with half the mesh

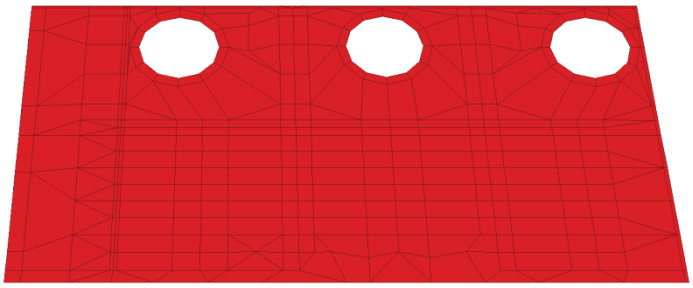

Figure 4-14 Cover with twice the mesh

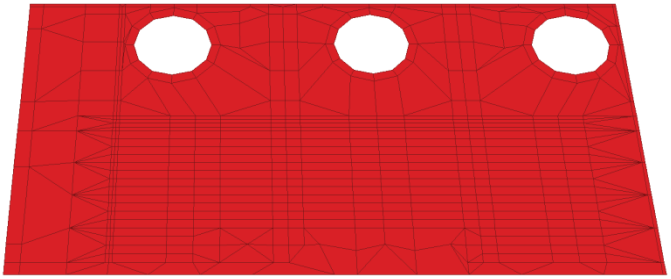

Figure 4-15 Cover with four times the mesh

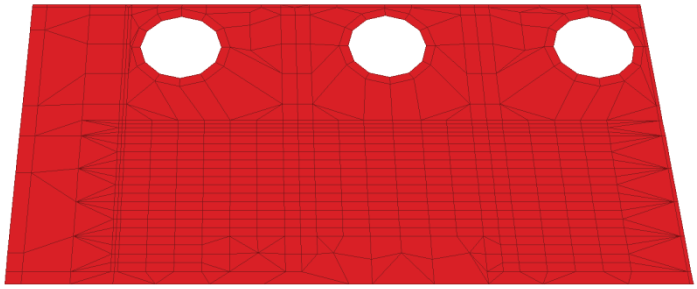

Figure 4-16 Cover with four times the mesh and large elements divided

4.3.3 Core-Coil Assembly Boundary Conditions

In the original model, the bottom clamps of the core were modeled as being fixed to the base plate along their whole length. Furthermore, the top clamps were fixed to a transversal beam on one edge and to the end wall on the other edge. The actual boundary conditions are depicted in Figure 4-17 to Figure 4-19.

Figure 4-17 Core assembly

Figure 4-18 Top clamp-cross beam connection detail

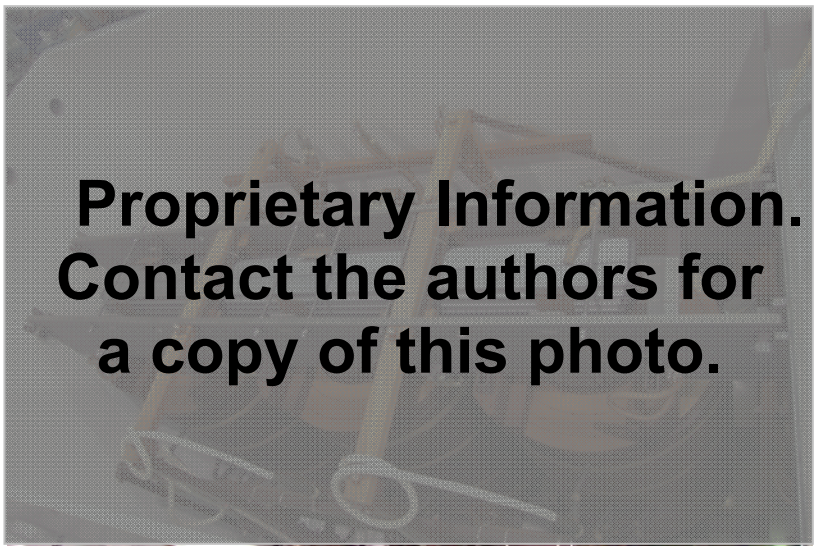

Figure 4-19 Core assembly and connection details

It can be concluded that the core assembly is simply resting on the base plate. At the ends of the bottom clamps there are notches where the core is restricted horizontally but not vertically. Also shown, are the connections of the top clamp with the transversal beam and the end wall. The top clamps are composed of rectangular holes at their ends (Figure 4-17) and the details of the connections can be seen in Figure 4-18 and Figure 4-19. The rectangular bars used for the connection are not fixed by the holes, it is expected that the rotations will not be constrained.

Finally, the transversal beam is shown to be simply supported on the side walls and moment releases can be considered appropriate at these locations.

Accordingly, the following modifications were suggested and made on the original model:

- The core assembly (bottom core clamps) was detached from the base plate. At the points where the notches are actually located, the clamps were pinned to the base plate in the initial models created. While in the final models, gap elements were placed between the bottom clamps and the base plate at the same locations. This would ensure that the vertical motion of the core would be accounted for.
- The original model included supports only in the perimeter of the transformer. Since the transformer is mounted on a concrete foundation, the base plate is not expected to deform in the vertical direction. Thus, the base plate was vertically restricted at the points where the core is supported.
- The top core clamps were released for rotations at their ends. In the final models the transverse beam has also been released at its ends for rotations.

4.3.4 Core-Coil Assembly

As can be deducted from the figures above, the clamps are confined by the core along their length except for a 20 in offset at their ends. When the core is displaced laterally, the clamps are expected to experience torsion at their extremities. This behavior cannot be captured sufficiently with the original model because the mesh of the clamps is rather coarse.

Regarding the main part of the core, three vertical parts (core legs) are connected with a horizontal beam at their top and bottom (Figure 4-19). Over each core leg, a winding assembly is

fitted (Figure 4-17). It is clear from the figures that the core in reality extends up to the middle of each core clamp while in the original model, this is not the case.

The following modifications were applied:

- The main frame of the core was modeled more appropriately. The core legs were extended up to the middle of the core clamps. Horizontal frame elements connecting the core legs at their top and bottom were added in the longitudinal direction. These elements were not added in the middle of the core clamps, but at the bottom of the top clamp and at the top of the bottom clamp levels. That way the representation of the core is expected to be more realistic. Along with these changes, the transverse rigid elements connecting the core clamps in the original model were moved to the middle of the clamps, so that they provide the same confinement as the main frame of the core would do in reality.
- In the original model, elements with material of high modulus of elasticity were used as rigid links for the core. After a series of parametric analyses were carried out, it was found that these elements were not modeled sufficiently rigid. The rigidity of the elements composing of the core was increased accordingly by 10^2 times, since this part of the transformer is essentially stiff. Therefore, the modulus of elasticity of the material used was increased by 10^4 times.
- The mass distribution of the core was modified as well. More specifically, for the main part of the core, the mass of the steel frame was equally distributed over the horizontal elements connecting the core legs and the parts of the core legs located between the top and bottom core clamps ($w_f = 47150\ lbs$). Additionally, the mass of each winding coil was distributed only over part of each core leg located between the top and bottom core clamps ($w_w = 7500\ lbs$). Since the total weight of the core is $w_{tot} = 82700\ lbs$ the

remaining weight ($w_{rem} = 9250\ lbs$) was uniformly distributed over the core legs and the horizontal elements connecting them.

- The mesh of the core clamps was refined. More specifically, the overhangs of the clamps and an additional part of the confined portion of the clamp were meshed more thoroughly than the remaining length. Between these two different mesh arrays, a transitional area of triangular shell elements was created.

Figure 4-20 and Figure 4-21 demonstrates the core in the original and modified models in SAP2000 and summarizes the modifications made.

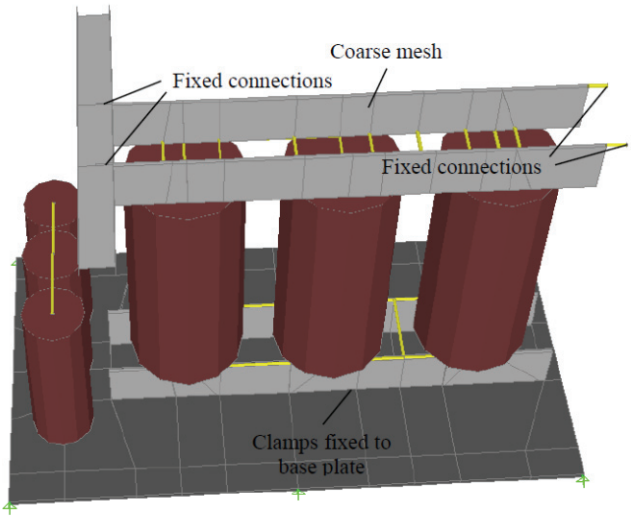

Figure 4-20 Core in the original model

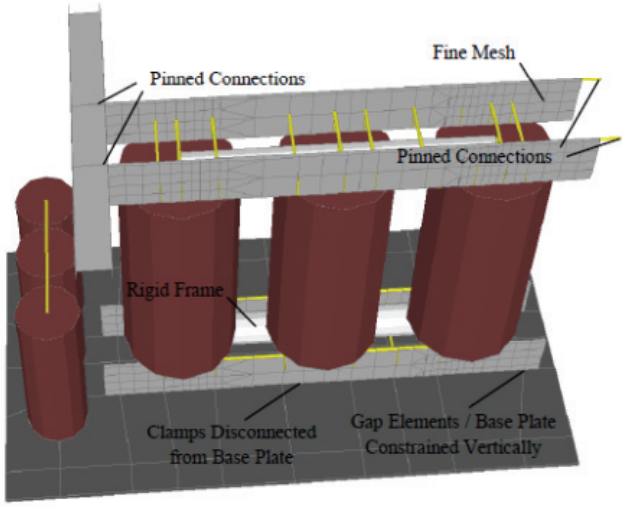

Figure 4-21 Core in the modified model

4.3.5 Distribution of Oil Mass

In the original model, the mass of the oil contained in the tank is treated as distributed on the side walls as nodal masses, acting only in the direction of the gravity. That way, the interaction of the oil with the core, which is likely to have an impact on the core's dynamic response, is not taken into account. This was modified in the latest models as described below.

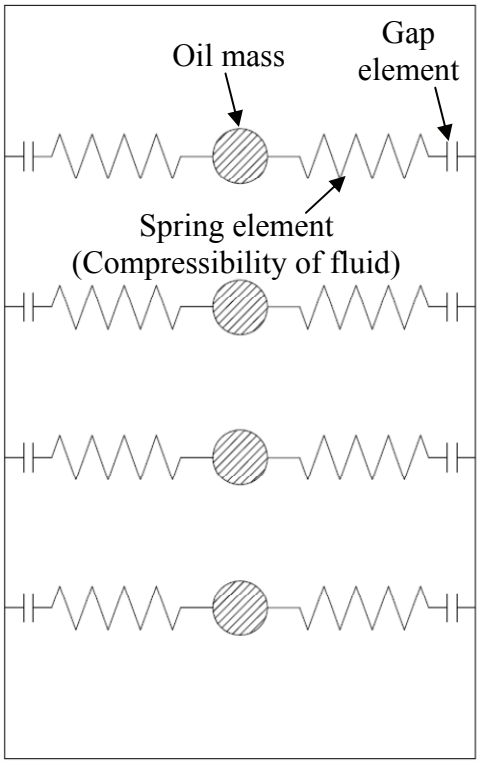

Figure 4-22 Oil distribution between the tank walls

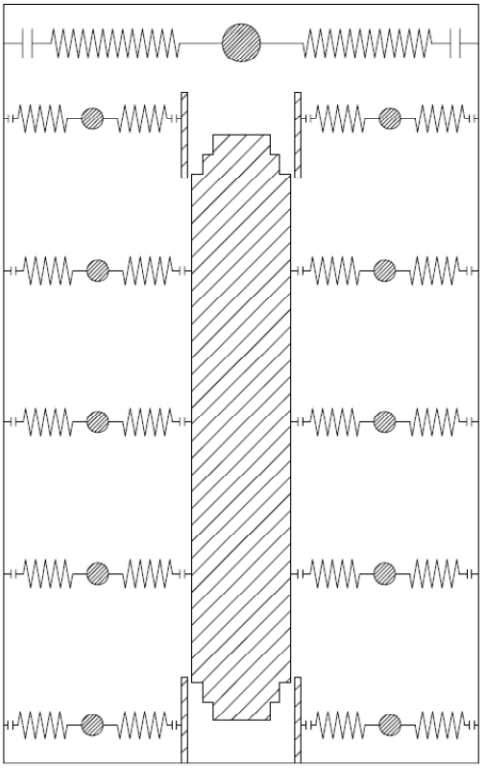

Figure 4-23 Oil distribution between the tank walls and the core

A more realistic approach for the modeling of the oil in SAP2000 is to separate the total mass of the fluid into smaller finite masses, and examine the interaction of these masses with the walls and the core-coil assembly. For explanatory purposes, a unilateral dynamic excitation can be considered, for example along the transversal dimension of the transformer. Due to the cyclic motion of the tank and the behavior of the fluid, a part of the oil mass will affect the core assembly, while another part will affect one of the two side walls for a specific time interval of the cycle and so on. Therefore, the desired approach would be to model each mass using gap elements between the mass and the walls. In addition to these gap elements; there should be gap elements between the mass and the core wherever it is necessary. To account for the

compressibility of the fluid, spring elements with certain stiffness should be placed between the mass and the gap elements. Such a configuration is shown in Figure 4-22 and Figure 4-23.

However, despite the fact that this approach seems quite realistic, its implementation in a structural analysis program is impractical. A hypothetical model incorporating the total amount of the gap elements proposed by this method would be highly nonlinear Due to this nonlinearity there is a possibility that a dynamic time history analysis would have crucial convergence problems. Additional problems arise from the required selection of the gap opening and the spring stiffness, if a dynamic time history analysis is desired to be used. Therefore, a much more simplified approach was used for the modification of the original model. Considering the tank-oil dynamic interaction described above, the mass of the oil was split and attached on the tank and the core using the procedure that is described below.

The concentrated nodal weights on the tank walls were removed and substituted by masses assigned in the longitudinal and the transverse directions. These masses were assumed to account sufficiently for the interaction of the oil with the tank walls in the horizontal direction. Furthermore, a part of the oil weight is considered to affect the motion of the core assembly during the dynamic response of the transformer. Due to this reasoning a part of the total mass was added on the core at specific locations.

A typical value for the oil density used in the electric transformers is:

$$\rho = 0.87\ gr/mL = 3.143 * 10^{-5}\ kip/in^3$$

The dimensions of the tank and the core – coil assembly are shown in Figure 4-24. The dashed area in the middle is the core assembly.

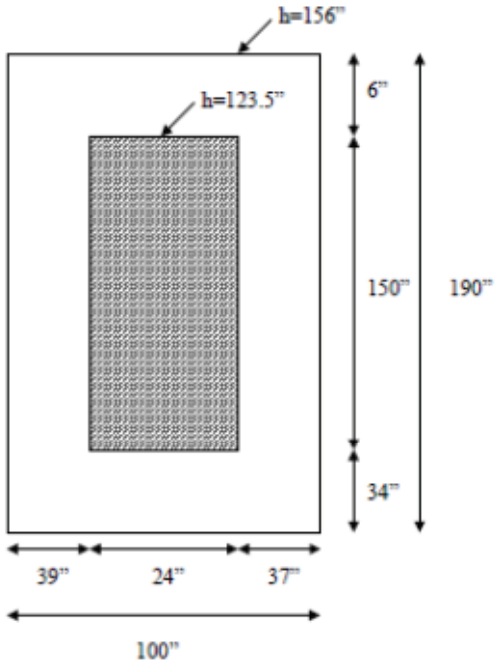

Figure 4-24 Dimensions of tank and core assembly

The tank was considered full and the oil was distributed in two different ways, depending on the location of the oil mass that was to be distributed. More specifically, the fraction of the oil mass over the core assembly was equally divided between the two side walls and the two end walls. Namely, half of the oil mass was assigned to each side wall in the transverse (Y) direction and half of the oil mass was assigned to each end wall in the longitudinal (X) direction. In every case, the mass was distributed equally among the nodes of the wall. The weight of the oil over the core assembly is:

$$W = 3.143 * 10^{-5} * 190 * 100 * 32.5 = 14.033\ kip$$

And the mass assigned to each wall was:

$$m = W/(2g) = 14.033/(2 * 386.22) = 1.817x10^{-2}\ kip * sec^2/in$$

The distribution of the oil is shown schematically in Figure 4-25:

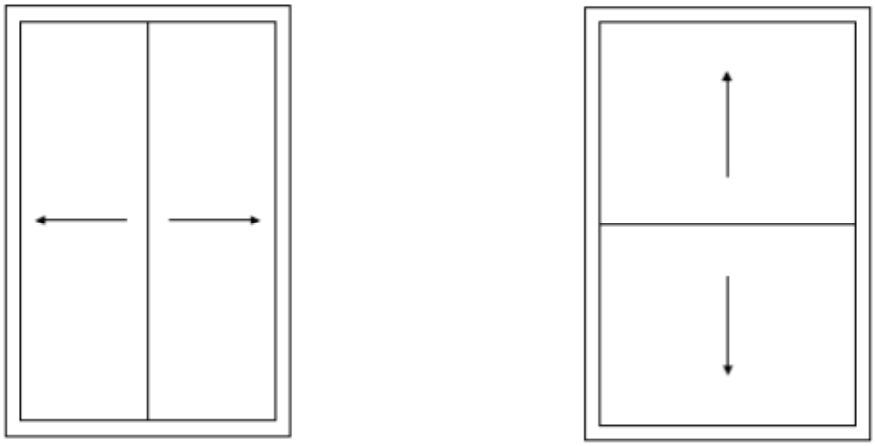

Figure 4-25 Distribution of oil above the top of the core on the side and end walls

The fraction of the oil mass below the top of the core assembly was divided equally between the walls and the core in each direction, shown schematically in Figure 4-26.

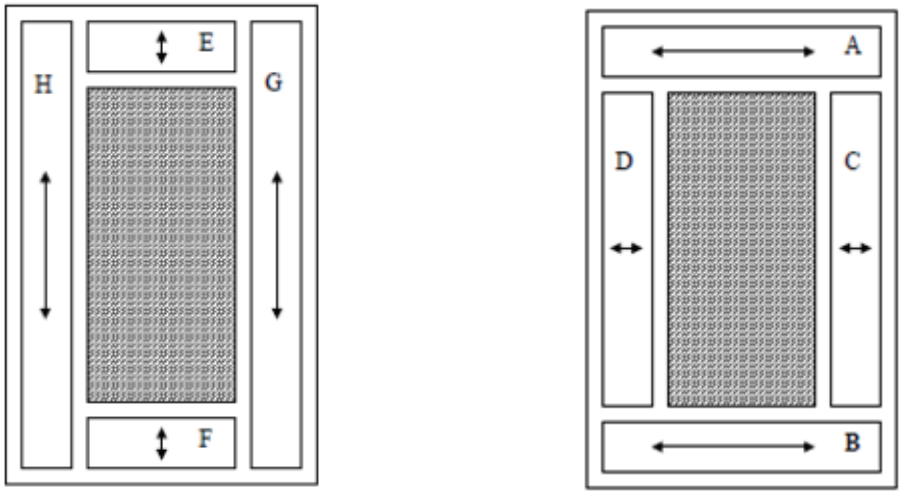

Figure 4-26 Distribution of oil below the top of the core on the side and end walls and the core

The first image refers to the distribution of the oil in the transverse direction and the second image refers to the distribution in the longitudinal direction. The mass assigned to the walls and the core was calculated for every segment (designated with a capital letter) as follows.

In the transverse direction the distribution of the oil mass was:

$m_A = W_A/(2g) = 3.143x10^{-5}x100x123.5x6/(2*386.4) = 3.015x10^{-3}$ kip*sec^2/in

$m_B = W_B/(2g) = 3.143x10^{-5}x100x123.5x34/(2*386.4) = 1.709x10^{-2}$ kip*sec^2/in

$m_C = W_C/(2g) = 3.143x10^{-5}x150x123.5x37/(2*386.4) = 2.789x10^{-2}$ kip*sec^2/in

$m_D = W_D/(2g) = 3.143x10^{-5}x150x123.5x39/(2*386.4) = 2.940x10^{-2}$ kip*sec^2/in

In the longitudinal direction the distribution of the oil mass was:

$m_E = W_E/(2g) = 3.143x10^{-5}x24x123.5x6/(2*386.4) = 7.236x10^{-4}$ kip*sec^2/in

$m_F = W_F/(2g) = 3.143x10^{-5}x24x123.5x34/(2*386.4) = 4.100x10^{-3}$ kip*sec^2/in

$m_G = W_G/(2g) = 3.143x10^{-5}x190x123.5x37/(2*386.4) = 3.533x10^{-2}$ kip*sec^2/in

$m_H = W_H/(2g) = 3.143x10^{-5}x190x123.5x39/(2*386.4) = 3.724x10^{-2}$ kip*sec^2/in

These masses were distributed equally among the nodes of the part of the wall that is located below the top of the core assembly. This wall has a length which is defined by the projection of the core assembly to the wall in the direction of interest. The distribution of the masses on the core had the following pattern: in the transverse direction, the masses were assigned equally to the nodes of the top and bottom core clamp and to the top and bottom nodes of the (three) core legs but only in the side of interest. For example, for the portion of the mass designated as C in Figure 4-26, only the right part of the top and bottom clamps were assigned masses. The top and bottom nodes of the core legs however, were assigned masses for both the C and D portions of oil mass. In the longitudinal direction, the masses were assigned equally, but only at the nodes that were at the ends of the top and bottom clamps and the top and bottom nodes of the core leg in the side of interest. For example, for the portion of mass designated as E, the nodes at the ends of both parts of the top and bottom clamps (20 nodes) and the top and bottom nodes of the core leg closer to the end wall were assigned masses.

An additional model was created in which the distribution of oil followed the same pattern as described above but the whole mass of the oil was only distributed on one side. The oil over the top of the core was fully distributed to the right wall and to the front wall. The oil below the top of the core was distributed as follows: portions H, E and G were fully distributed on the front wall and portion F was fully distributed on the core in the same direction. Respectively, portions A, B and C were fully distributed on the right wall and portion D was fully distributed on the core in the same direction.

Figure 4-27 and Figure 4-28 demonstrate the way the two distributions are represented in SAP2000.

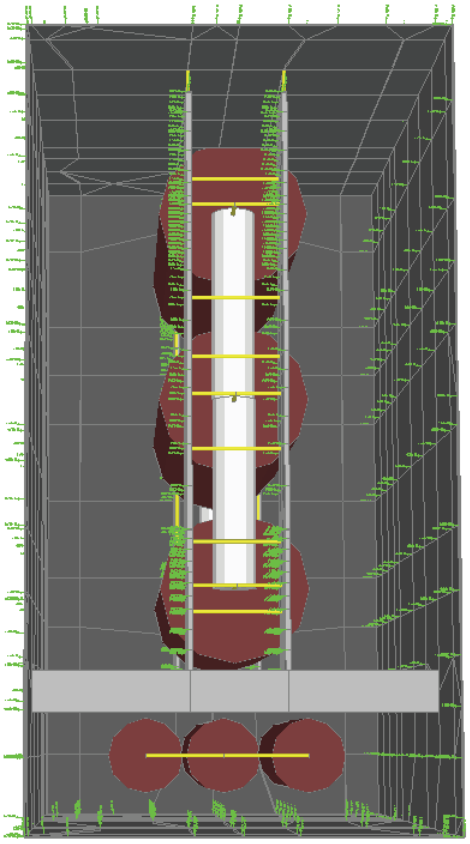

Figure 4-27 Oil distributed on both directions

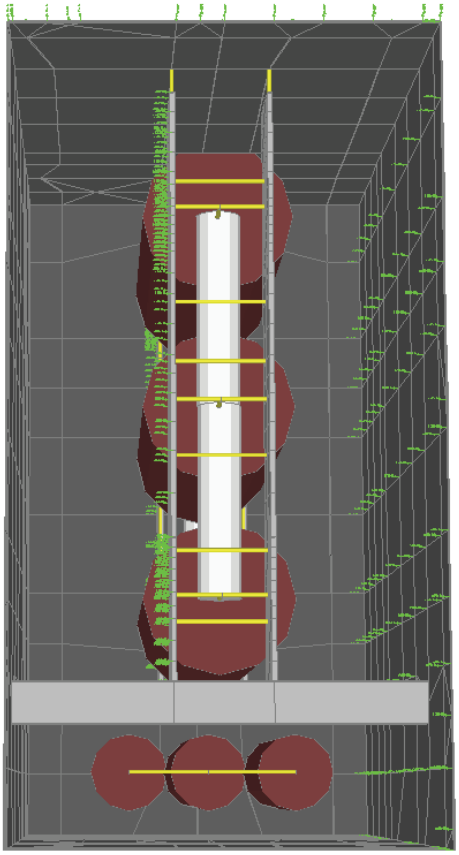

Figure 4-28 Oil distributed on one direction

4.4 Assessment of Interactions

A number of analyses have been carried out using the advanced dynamic models of the transformer. The scope of these analyses was to assess the interaction between several attachments of the transformer and the more vulnerable high voltage bushings.

Since the interactions were initially unknown, a large amount of check points considered critical were selected on the tank, external components of the substation and core assembly. These *critical check points* are shown in the figure that follows:

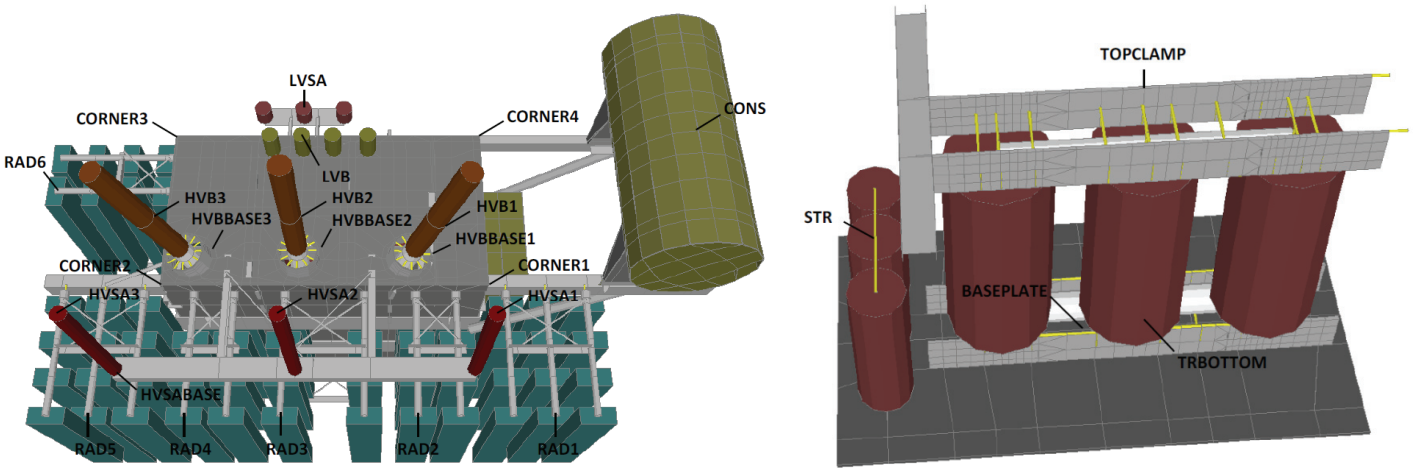

Figure 4-29 Check points selected on the transformer and the core assembly

The abbreviations for the points presented in the figure above, signify the following:

Table 4-3 Nomenclature for check points

HVB	Top of high voltage bushing
HVBBASE	Point on cover at the base of the turret
HVSA	Top of high voltage surge arrester
HVSABASE	Point at the base of the high voltage surge arrester
RAD	Point at the top of the specified radiator group
LVB	Top of low voltage bushing
LVSA	Top of low voltage surge arrester
CONS	Top of conservator
TRTOP	Point at the top of the transformer (core-coil assembly)
TRBOTTOM	Point at the bottom of the transformer (core-coil assembly)
STR	Point at the top of the small transformer
BASEPLATE	Point on the base plate
TOPCLAMP	Point at the top clamp of the transformer
CORNER	Corner of cover plate

Three groups of points are considered to be most important for the investigation of the bushings' response:

- Points at the tops of the high voltage bushings (HVB1, HVB2, HVB3)
- Points on cover, at the base of the turrets (HVBBASE 1, HVBBASE 2, HVBBASE 3)
- Points at corners of the cover plate (CORNER1, CORNER2, CORNER3, CORNER4)

To adequately describe the response of the high voltage bushings there is an expected correlation of the responses at the top of the bushings, the turrets and at the corners of the plate.

The assessment of the interaction is accomplished through a variety of methods:

- Modal analysis of the model with SAP2000. The analysis shows the frequencies at which various components of the transformer respond and can reveal immediate interactions between those and the bushings.

- Wide band random motion (white noise) excitation at the base and generation of transfer functions, cross spectra and coherences (process of the results in the frequency domain).
- Random spectrum-compatible motion (IEEE 693-2005) excitation of the base and process of the results in time domain.

The evaluation of the interactions was performed using several processing techniques; (1) modal analysis; (2) transfer functions analysis; (3) cross-spectrum analysis; (4) coherence analysis; (5) response spectrum analysis.

(1) The modal analysis can provide outstanding information on the response of the transformer and the interactions between various components. It can give a visual representation of the modes such that the modal characteristics can be associated with the components. That way, not only the natural frequencies of the transformer parts can easily be determined but also the interactions. Through the animation of the modes in SAP2000 an engineer can directly observe which components affect the response of the others. However, given that the animation does not provide immediate information for the interactions, a magnitude cannot be assessed.

The force associated with a certain node j on the structure for a specific mode in the modal analysis, can be calculated through the following relationship (Chopra 1995):

$$f_{jn} = \Gamma_n \mathrm{m_j} \varphi_{\mathrm{jn}} \mathrm{A_n}$$

where:

$\Gamma_n = \sum_{\mathrm{j=1}}^{\mathrm{N}} \mathrm{m_j} \varphi_{\mathrm{jn}} / \sum_{\mathrm{j=1}}^{\mathrm{N}} \mathrm{m_j} \varphi_{\mathrm{jn}}^2$ is the modal mass participation factor

$\mathrm{m_j}$ is the nodal mass

φ_{jn} is the jth element of the nth vibration mode

$\mathrm{A_n}$ is the pseudo acceleration of the nth mode single degree of freedom system

It is clear that $\Gamma_n \varphi_{\mathrm{jn}}$ is a dimensionless quantity that describes the modal contribution on the forces applied on the node. If this quantity is presented graphically for all the modes of the structure, one can get an impression of which modes mostly affect the response of the node. If for two separate nodes, i and j, the dimensionless quantities $\Gamma_n \varphi_{\mathrm{in}}$ and $\Gamma_n \varphi_{\mathrm{jn}}$ are multiplied for each mode, the graphical spectrum-like representation of the product can provide an indication of the interaction between those nodes. Especially at the frequencies where the graph presents peaks, interaction between the points could be expected. This can only constitute an indication, since a peak in the graph may signify that the response of the points is governed by the same mode while any interaction between them might not exist. Alternatively, the response of one point could be so large compared to another that the shape of the "composite" graph would not differ from the one with the dominant response alone.

Figure 4-30 is an example of this approach for an initial model which has been slightly modified compared to the original model provided. It shows the composite response for the point at the top of the high voltage surge arrester farthest from the conservator along with the points at the top of the high voltage bushings (normalized to the largest amplification). It reveals some amplification around 6 Hz and 13 Hz, which are close to the frequencies of the bushings, suggesting that the response of the surge arrester might affect the response of the bushings at the specific frequencies. Despite the fact that the graph is referred to as spectrum, it is simply the depiction of discrete points which have been connected with smooth lines, for reasons of illustration, and should not be misidentified for an actual response spectrum.

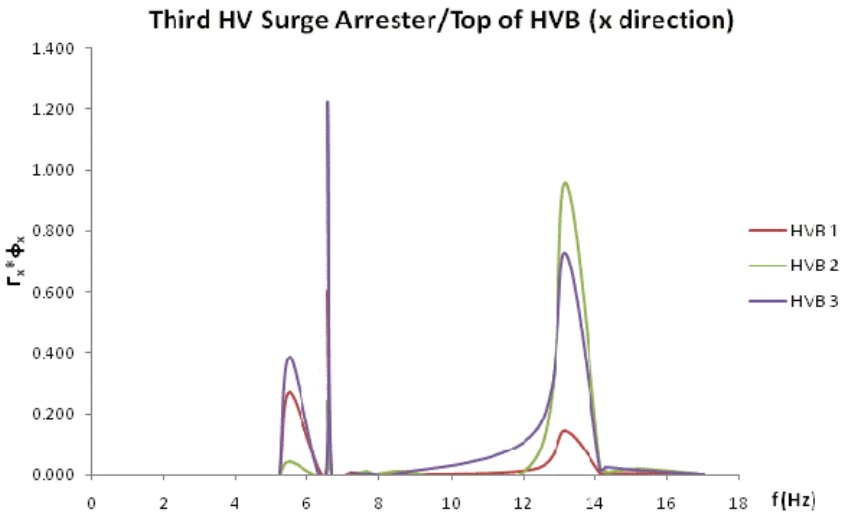

Figure 4-30 Composite response for the top of the third surge arrester and the bushings

(2) The transfer functions give the response at a point with respect to the input at the base and exhibit the significance of the response at certain frequencies. The reason for this significance of the response is because the system is excited with a motion that has the same energy content for all spectral frequencies. The equation:

$$H(\omega) = \frac{Y(\omega)}{X(\omega)} = \frac{F\{y(t)\}}{F\{x(t)\}}$$

relates the transfer function, $H(\omega)$, to the ratio of the output, $Y(\omega)$, (Fourier transform $F\{y(t)\}$ of the response acceleration $y(t)$) to the input $X(\omega)$, (Fourier transform $F\{x(t)\}$ of the input acceleration $x(t)$) in the frequency domain. This means that the transfer function shows the amplification (or diminution) of the input motion at the base of the structure compared to the output at a selected point on the structure for a desirable range of frequencies. That way, estimation can be made on the frequency at which a component of the transformer responds. However, it should be noted that the transfer function incorporates the properties of the structure below the component under examination. The information obtained from the transfer functions

should be cross checked with the modal analysis results before any conclusions are drawn, especially for such a complex system as the transformer.

In Figure 4-31, the transfer functions for the response of the central bushing are presented, after an analysis was carried out on the modified model, which is comprised all of the modifications presented in the previous sections. It is clear that the response of the bushing is mainly at 5.5 Hz, 4.5 Hz and 14 Hz in the longitudinal, transversal and the vertical directions respectively. These are the as-installed frequencies of the bushing and can be verified by the results of the modal analysis. However, the modal analysis alone does not directly reveal the significance of each mode for the response of the bushing, as is the case of the transfer functions.

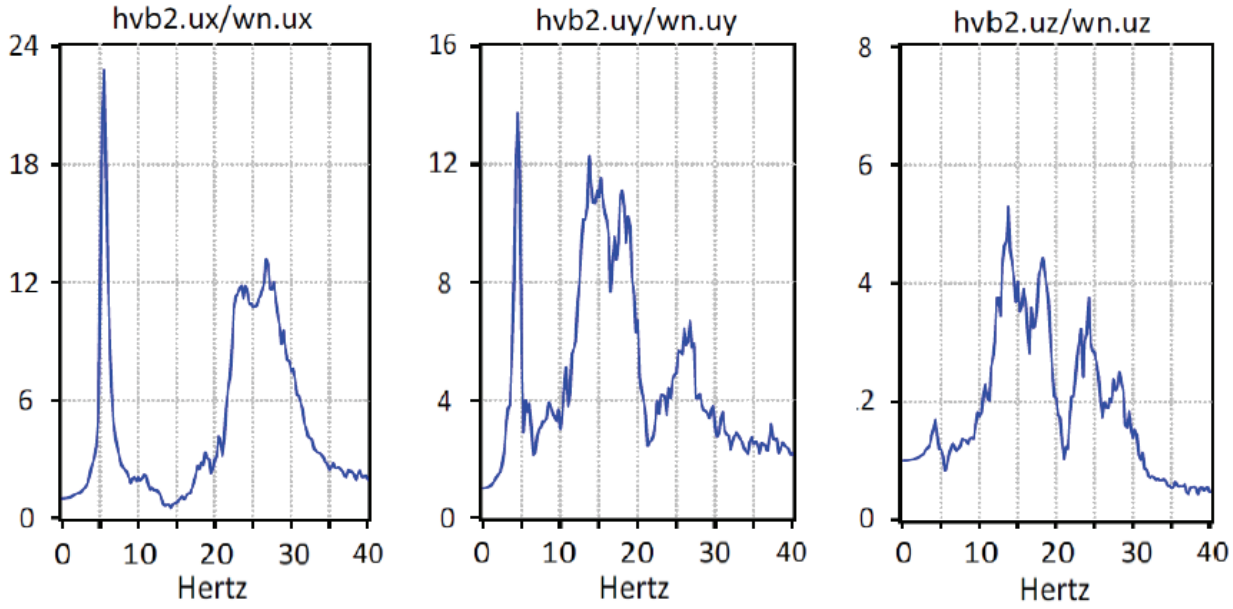

Figure 4-31 Transfer functions of central bushing in the three directions

(3) The cross spectra show the responses of two different points multiplied in the frequency domain and the coherences show the relativity between two waves (phase). Using the cross spectra and coherences in conjunction with the modal analysis results, we can assess the interactions between the bushings and certain components of the transformer.

The cross spectrum, $F_{xy}(f)$, of two signals $f_x(t)$ and $f_y(t)$ is the forward Fourier transform of the cross correlation function, $R_{xy}(t)$. If the individual Fourier spectra $F_x(f)$ and $F_y(f)$ of the signals $f_x(t)$ and $f_y(t)$ are calculated, the cross spectrum is obtained as:

$$F_{xy}(f) = F_x'(f) \cdot F_y(f)$$

where $F_x'(f)$ is the complex conjugate of $F_x(f)$. It should be noted that in signal processing the cross correlation function is a measure of similarity of the two waveforms. By computing the cross spectrum for the responses of the two components on the transformer, one can find an indication that the responses are correlated or not. This correlation will depend on the amplifications (or diminutions) at frequencies of interest on the spectrum.

(4) The coherence is a complex function of frequency that expresses the frequency dependence of correlation. It takes values that vary from zero (waves uncorrelated) to one (waves fully correlated). For the correlations implied by the cross spectra the coherences give an indication of the significance of the correlations.

Figure 4-32 depicts the cross spectra and coherences for the top of the central bushing and the base of the surge arresters. Where magnification, in Figure 4-32, is shown at the as-installed frequencies of the bushing, the coherence is closely unified for the specific frequency in the longitudinal direction. The modal analysis verifies that the motion of the surge arresters' support is affecting the motion of the central bushing. From the modal analyses a conclusion can be drawn that there is interaction between the two parts.

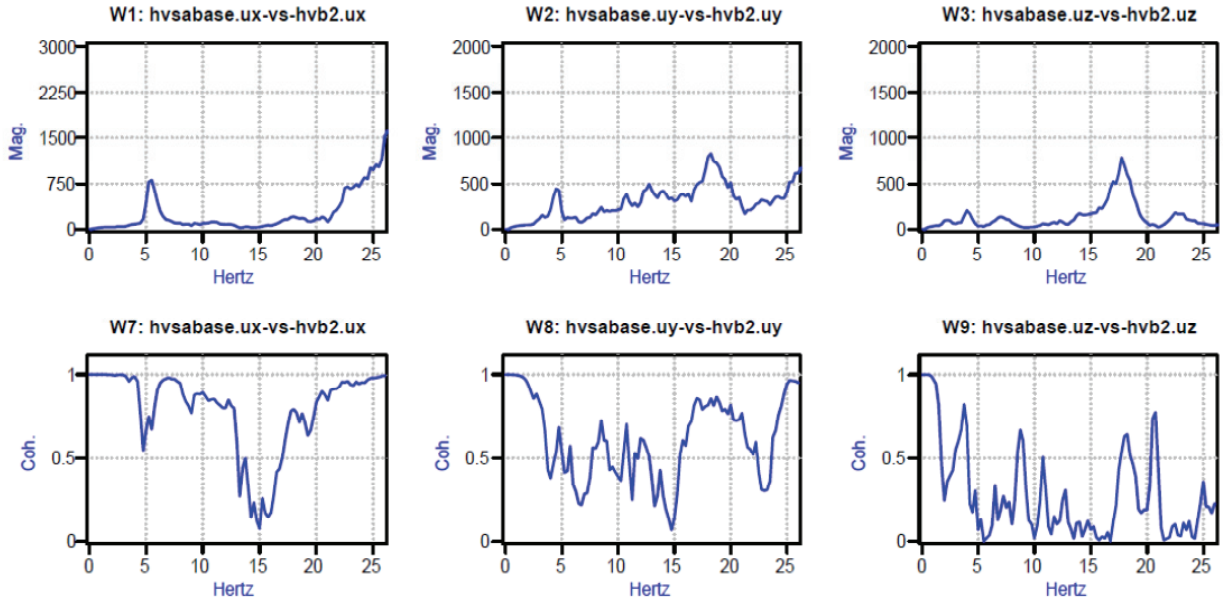

Figure 4-32 Cross spectra and coherences of central bushing and high voltage surge arresters' base in the three linear directions

The transfer functions and the cross spectra can assist in the elimination of some of the check points initially selected. Figure 4-33 shows the transfer functions for a point at the top clamp and for a point at the top of the core assembly. It is clear that their response is essentially the same and therefore one of them can be eliminated.

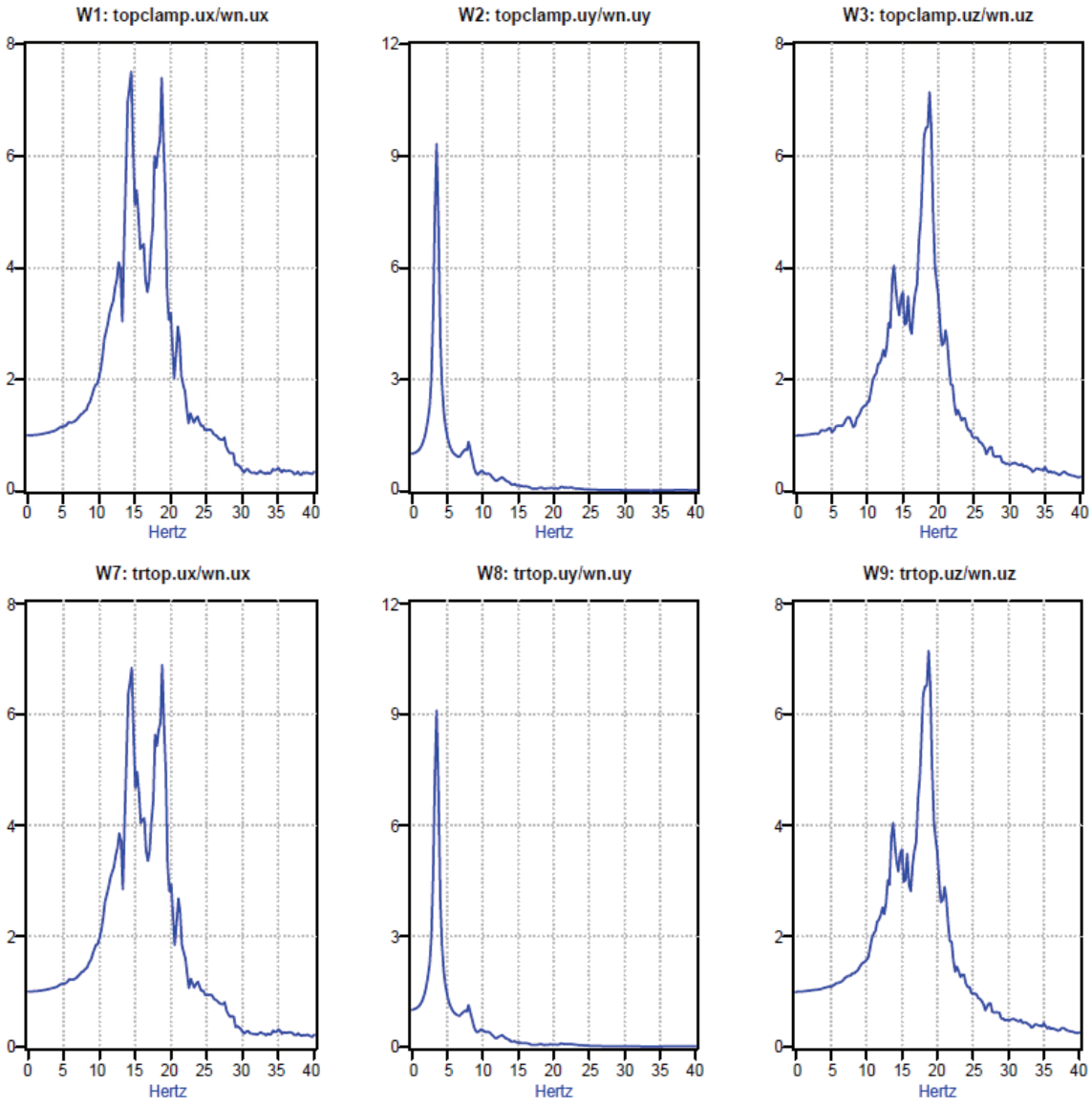

Figure 4-33 Transfer functions of a point at the top clamp and a point at the top of the core assembly in the three linear directions

The acceleration time history of the white noise used in the analyses is plotted and shown in Figure 4-34.

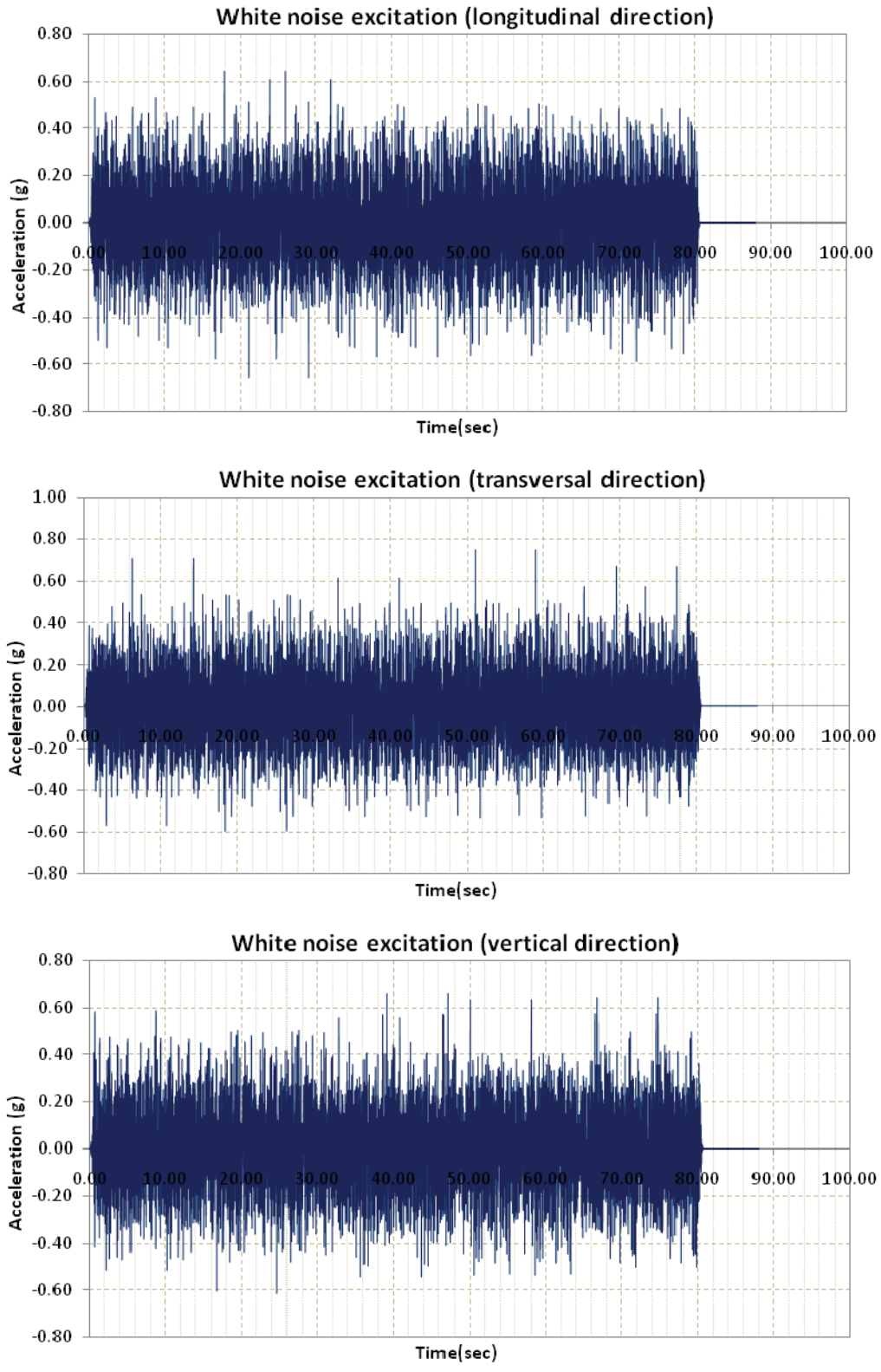

Figure 4-34 White noise acceleration time history in the three linear directions

(5) Response spectrum analysis provides direct information due to random input of seismic type. The excitation of the transformer with the random IEEE 693-2005 spectrum-compatible ground motion (Figure 4-35 to Figure 4-37) can be considered more appropriate for the assessment of the actual dynamic response of the system, than for the interactions between its components. Useful information can be drawn from the response of the system under this type of loading. The main response quantities influenced by the interactions are:

- Accelerations at the center of gravity of the upper high voltage bushings where the mass is concentrated
- Moments at the base of the high voltage bushings
- Displacements at the top of the high voltage bushings
- Displacements at the bottom of the high voltage bushing (part of the bushing immersed inside the tank)
- Accelerations at the corners of the cover plate
- Accelerations at the base of the turrets (points on cover)

Great interest lies within the assessment of the amplifications at the corners of the cover plate and at the top of the turrets, with respect to the ground motion input. The boundary conditions at the corners conduce to considerably large rotational stiffness. Due to this stiffness the linear response of the cover is expected to be sufficiently approximated by the response at the corners. On the other hand, the response at the top of the turrets will incorporate the effect of the attachments of the transformer on the vertical and rotational motion of the cover plate. The comparison of the above spectra with the ones of the IEEE 693-2005 ground motion can reveal amplifications that could potentially affect the high voltage bushings' response. This comparison

can only be made if the natural frequency of the latter lies in the frequency range of the amplifications.

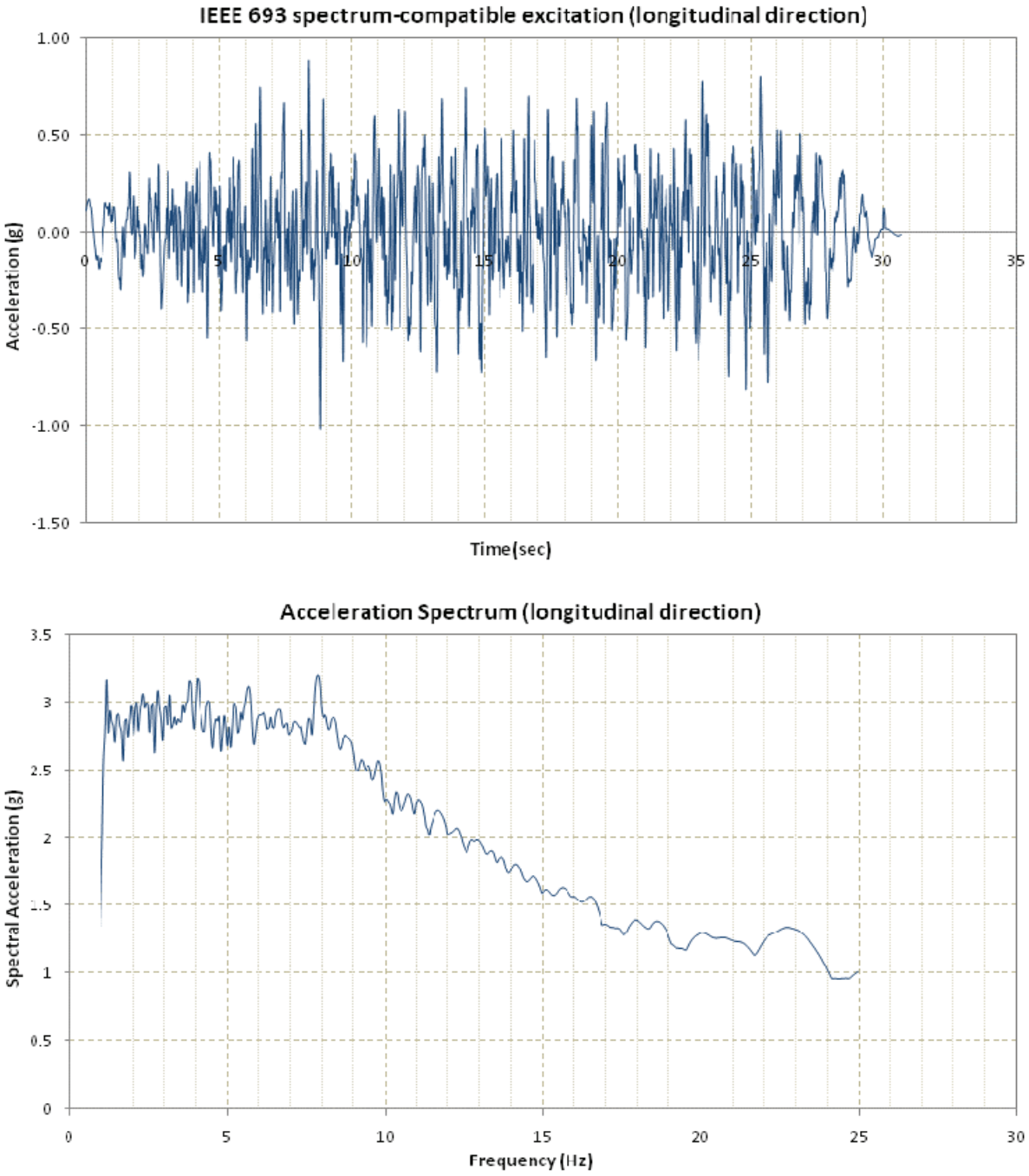

Figure 4-35 IEEE 693 Spectrum-compatible excitation and relative spectrum (longitudinal direction)

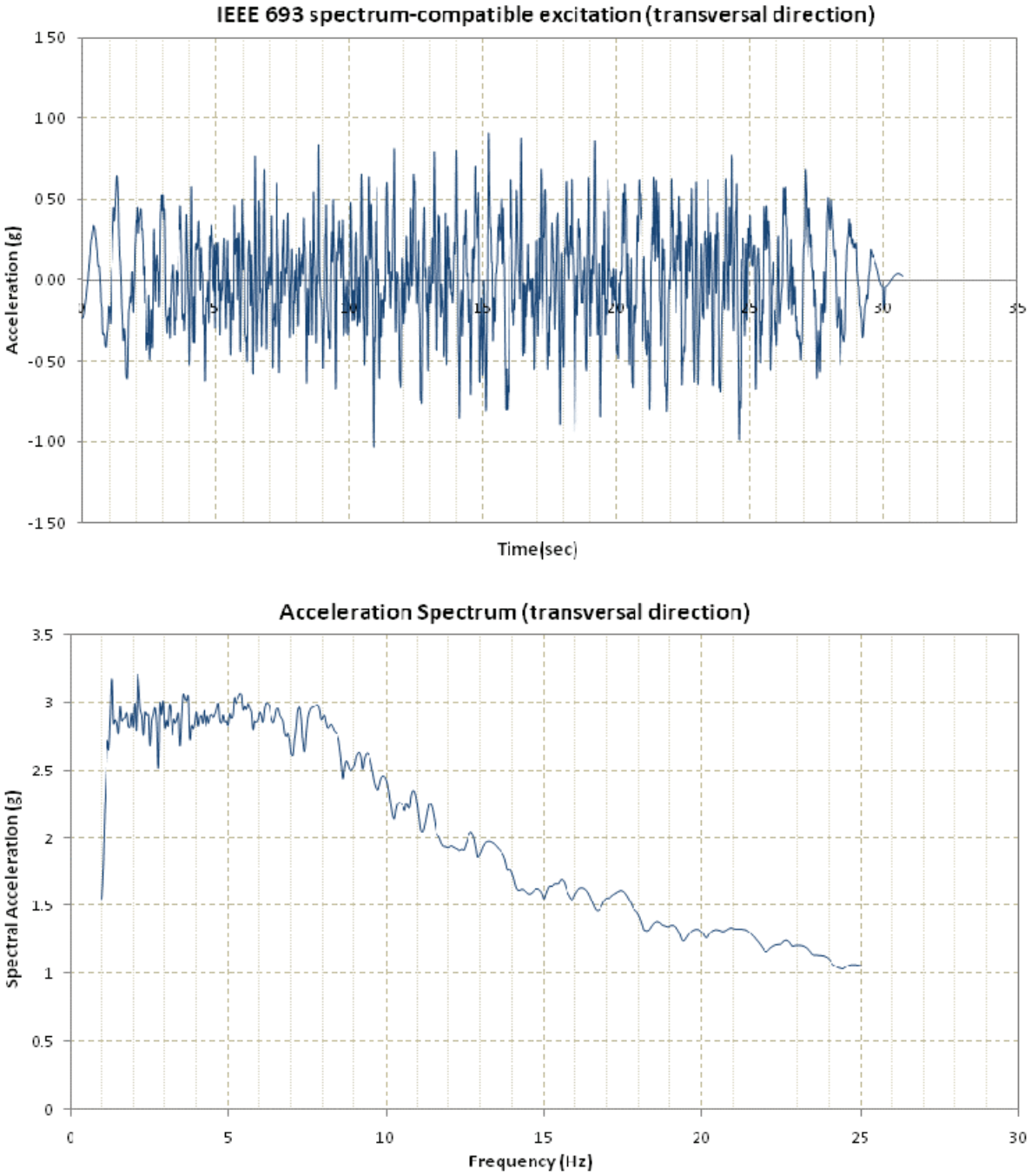

Figure 4-36 IEEE 693 Spectrum-compatible excitation and relative spectrum (transversal direction)

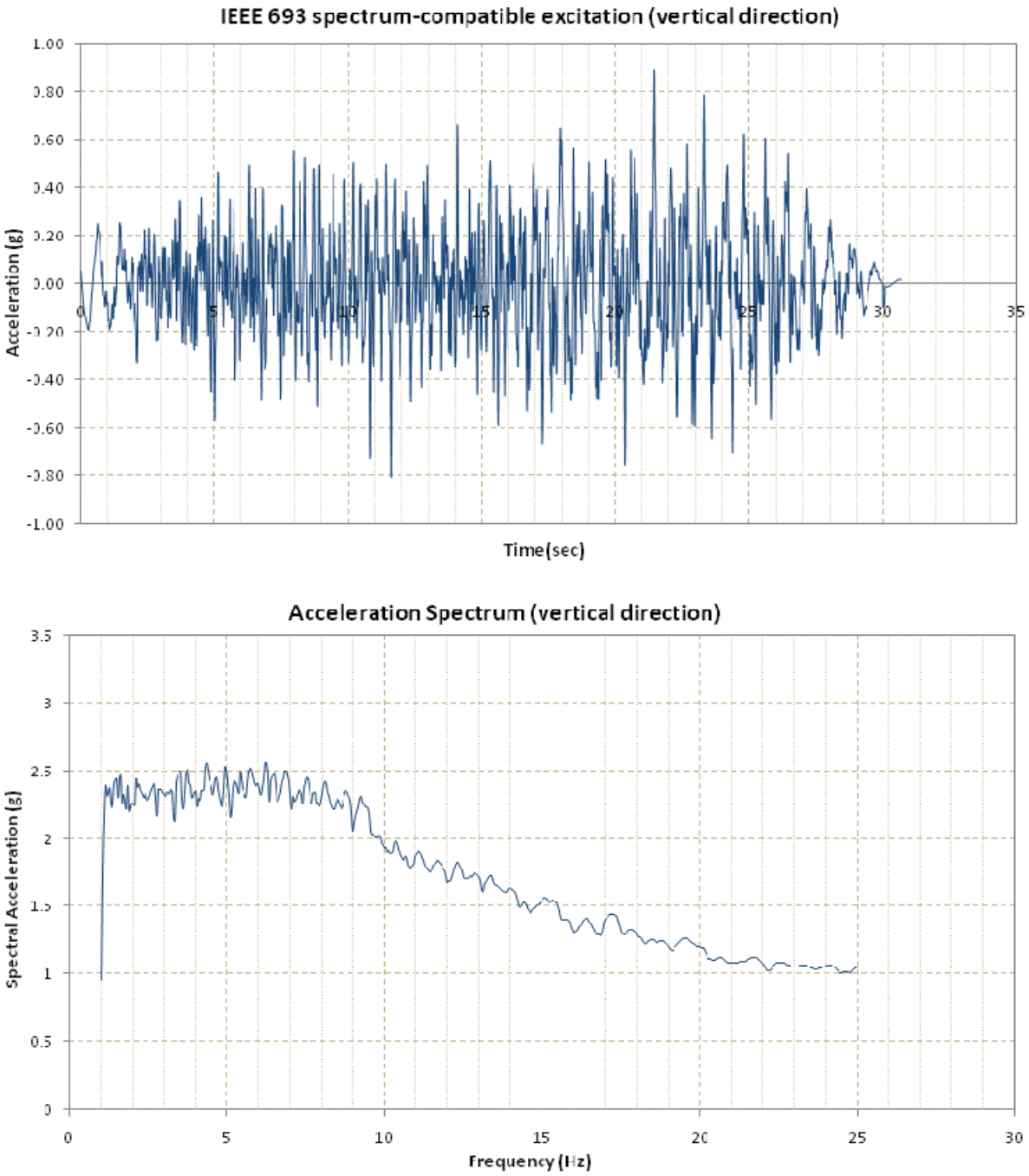

Figure 4-37 IEEE 693 Spectrum-compatible excitation and relative spectrum (vertical direction)

SECTION 5

MODELING SENSITIVITY AND RECOMMENDATIONS

5.1 Overview

The transition from the original model to the latest model, incorporating all of the modifications aforementioned used a series of intermediate models, so that the most realistic dynamic models could be obtained. In this section, the characteristics of the intermediate models are presented, along with the modal analysis results (frequencies) for the components of the transformer mainly modified (the core-coil assembly and the high voltage bushings).

After the identifying of the most adequate (modified) model, the frequency results were determined and are shown in the following sections. The dynamic characteristics were determined using transfer functions. Also, the assessment of interactions between the transformer attachments and the high voltage bushings was done using modal analysis and analysis in the frequency domain. The most critical components that affect the dynamic response of the bushings were identified and discussed.

Finally, a parametric analysis for the effect on the bushing dynamic characteristics due to modeling the cover plate using several mesh variations was carried out by exciting the transformer with the IEEE 693-2005 spectrum-compatible ground motion. The results of these analyses are presented in terms of peak accelerations, moments at the base of bushings and peak displacements.

5.2 Modified Models and Frequencies of Components

The nomenclature used for the modified models is CommercialModif, which signifies that the original model was modified. This nomenclature is accompanied by a version number indicating the various alternative modifications.

For explanatory purposes, it is noted that the longitudinal direction (L) refers to the direction of the longer side of the transformer, the transversal direction (T) refers to the direction of the shorter side of the transformer and the vertical direction (V) is perpendicular to the plane formed by the longitudinal and transverse directions. An illustration is given in Figure 5-1

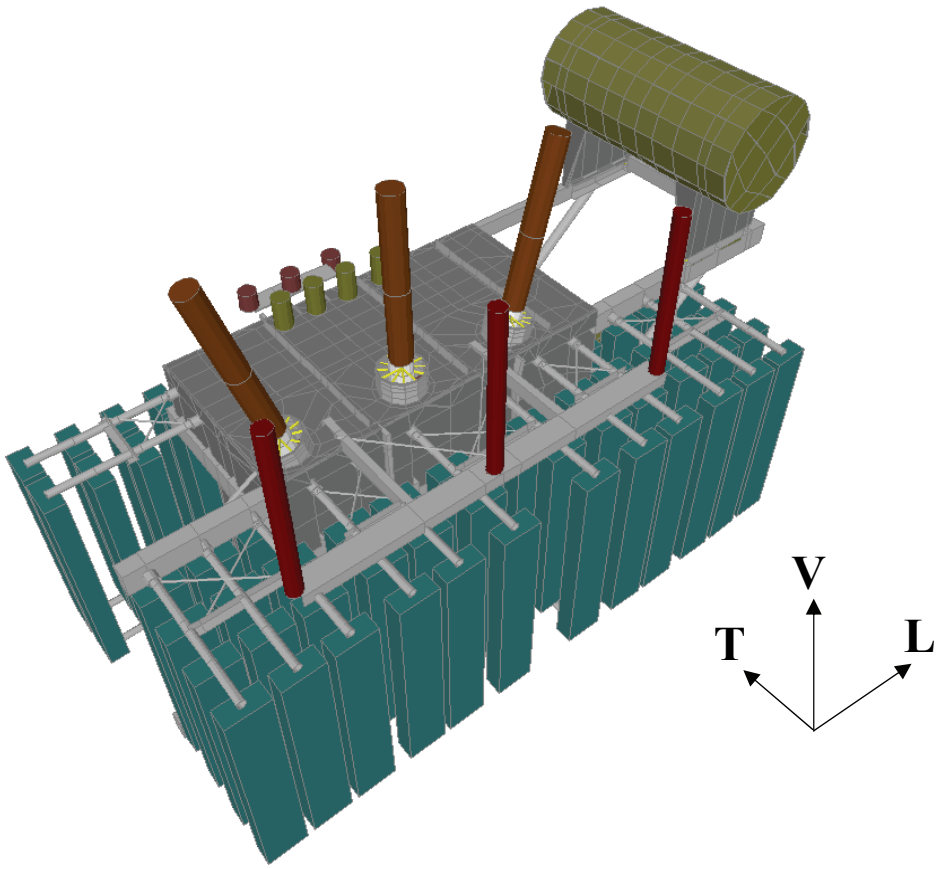

Figure 5-1 Directional vectors used in the analysis results presentation

Summarized in Table 5-1 are the intermediate models developed, along with their most significant characteristics.

Table 5-1 Preliminary modified models for cover and bushing

Variation name	Core								Bushing					
	Bottom Modification	Clamp mesh refined	Top clamp pinned at ends	Vertical members extended	Rigid bars added to clamps	Longer rigid bars added to clamps	Stiffness of rigid bars increased	Mass distribution changed	Detached along with flange	Stiffness and mass center changed	Turret included	Flange modified	Portion of cover included	Finer mesh of cover portion
	m=yes X= variation	m= yes	m= yes	m= yes	m= yes	m= yes	m= yes	m= yes	m= yes	m= yes	m= yes	m= yes	m= yes	m= yes
CommercialModif														
m1	m	m	m											
m2	m	m	m	m	m									
m3	m	m	m	m	m	m								
m4	m	m	m	m	m		m							
m5	m	m	m	m	m		m	m						
m6	m X2	m	m	m	m		m	m						
m7	m X3	m	m	m	m		m	m						
m8	m X4	m	m	m	m		m	m						
m9	m X5	m	m	m	m		m	m						
b1	m	m	m	m	m		m	m	m		m	m		
b2									m		m	m	m	
b3									m		m	m	m	m
Bushing with flange														
v0									m					
m1									m	m				
Bushing and turret														
v0									m		m			
m1									m	m	m	m		

The frequencies of significance for these models are also summarized below:

Table 5-2 Significant frequencies of preliminary modified models (Hz)

Variation name	Core			Bushing	
	Transversal translation	Rotation about the longitudinal axis	Rotation about the vertical axis	Longitudinal translation	Transverse translation
CommercialModif					
m1	3.59	8.05	14.51		
m2	5.02	8.59	16.70		
m3	5.43	9.24	16.82		
m4	5.26	11.01	20.35		
m5	5.19	11.24	20.50		
Sm6	5.43	16.11	-		
m7	5.23	9.96	20.14		
m8	5.38	12.54	-		
m9	5.20	9.52	19.19		
b1				16.60 (fixed)	16.60 (fixed)
b2				3.76	3.64
b3				4.02	3.79
Bushing with flange					
v0				17.50	17.50
m1				14.65	14.65
Bushing and turret					
v0				11.93	11.93
m1				10.56	10.56

For future analyses, the CommercialModif, m5 model was selected as the most suitable base model for future modifications. It sufficiently incorporates the realistic boundary conditions and mass distribution of the core.

Applying the modifications presented in the previous section on the CommercialModif, m5 model, two models were derived, the CommercialModif, m5_CoverModif+Oil_gapelements model and the CommercialModif, m5_CoverModif+Oil_ononedirection model. It is noted that these latest versions comprise detailed modeling of the bushings, refined cover mesh (variations), correct modeling of the core, gap elements between the bottom clamps and the base plate and

two different oil distributions inside the tank respectively. The results from the analysis on those models are presented in the following section.

5.3 Analysis of Modified Models and Results

The main purpose for the analysis of the modified models lies in the assessment of the frequencies of the most significant components of the transformer. These components of the transformer have a dynamic behavior that has an influence on the response of the high voltage bushings. It is this interaction between components that the modified models explore and assess. Additionally, it is desirable to use the modified models with the different oil distributions as well as the versions of the models with the various cover meshes.

In particular, the CommercialModif, m5_CoverModif+Oil_gapelements model and the CommercialModif, m5_CoverModif+Oil_ononedirection model were investigated applying wide band ground motion excitation at the base of the transformer (white noise). In this case, the modal analysis is not an effective approach for the identification of the system's characteristics. Modal analysis is not an effective approach because it is a linear method, while the modified models incorporate nonlinear elements (gap elements). Therefore, the desired information was obtained through processing the output in the frequency domain.

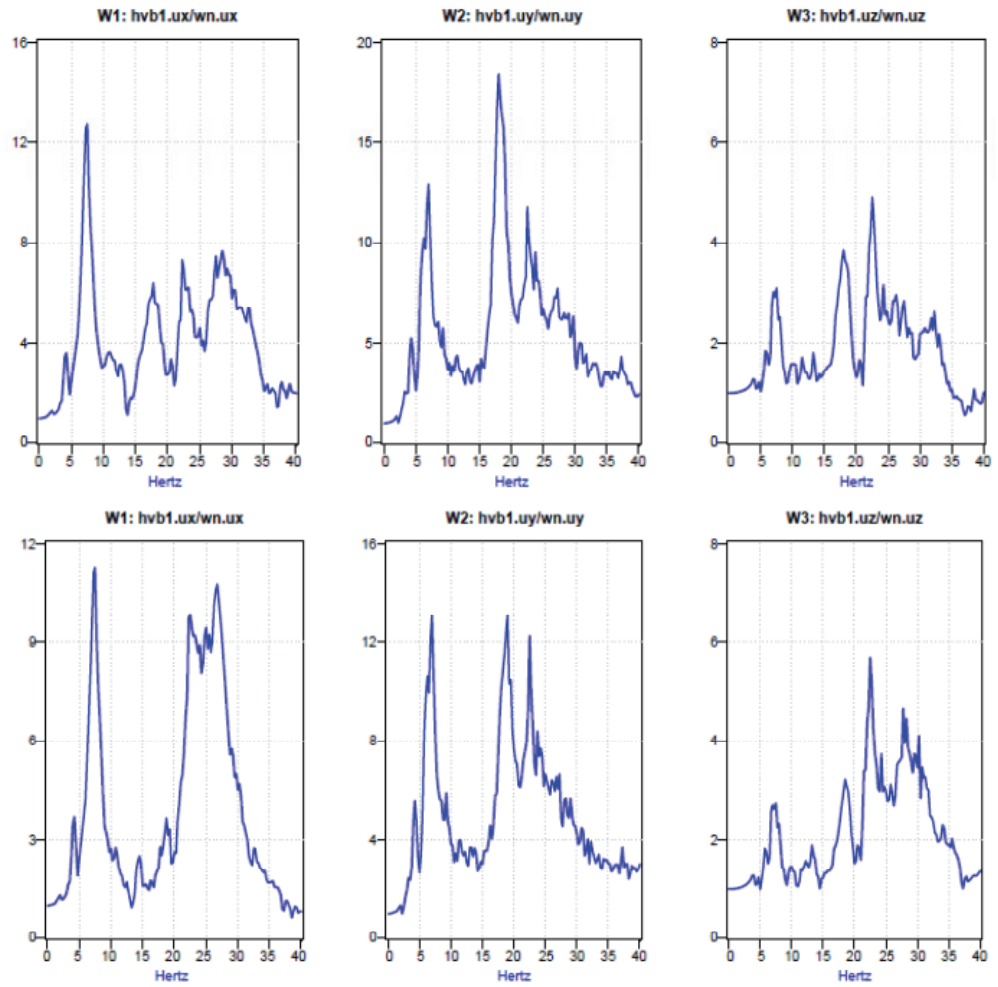

Figure 5-2 Bushing response in the three directions for the model with evenly distributed oil (up) and the model where the oil is distributed on one side (down)

The outcome of the analysis in the frequency domain shows that the response is very similar for the two models. Small differences in the magnitude of the response can be found in the frequency range of 1-20 Hz. This frequency range is where the natural as-installed frequencies of the high voltage bushings are expected, while for higher frequencies, the differences are generally larger. Figure 5-2 and Figure 5-3 show the response of two selected components, namely the bushing closer to the conservator and the core, for the two modified models.

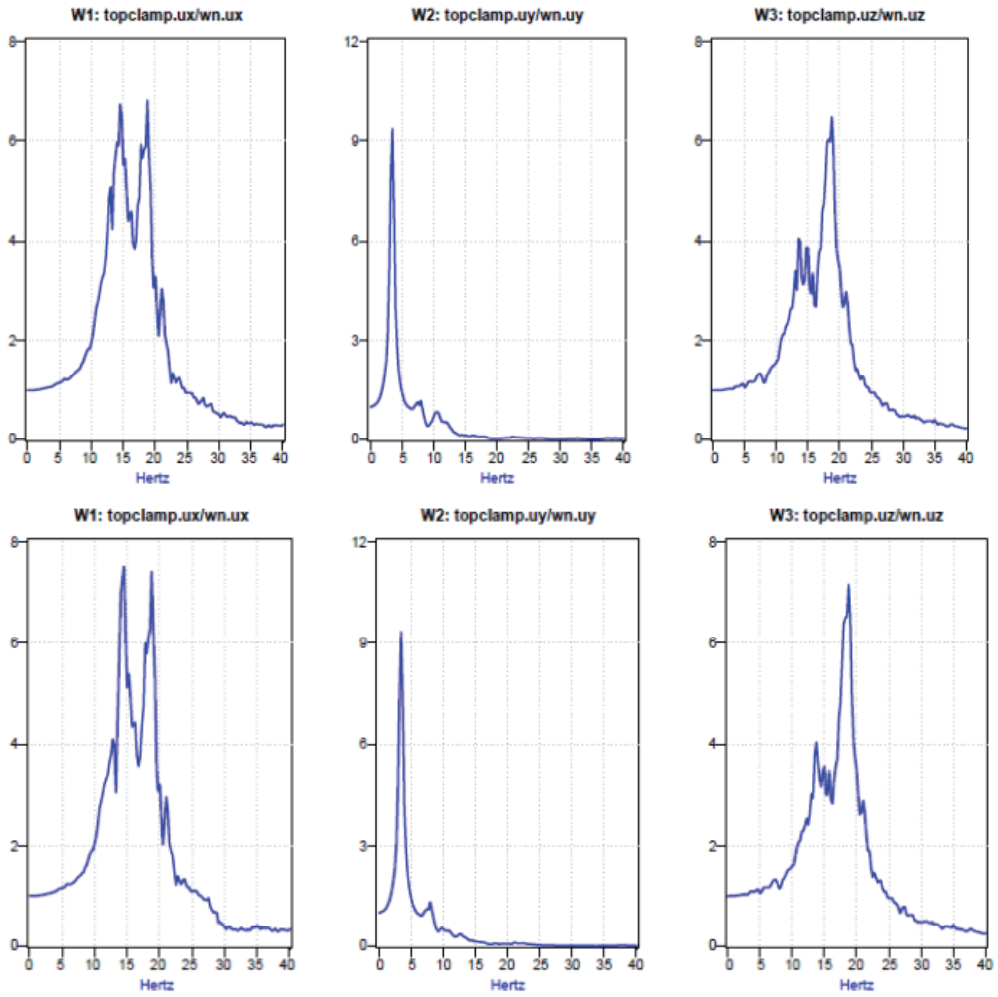

Figure 5-3 Core-assembly response in the three directions for the model with evenly distributed oil (up) and the model where the oil is distributed on one side (down)

From the figures above, it can be understood that some of the components have essentially the same response, even when the same oil mass is differently distributed. Naturally, the response of heavy external components attached to the transformer such as the oil conservator, are not expected to be greatly affected by the variation in the oil distribution (Figure 5-4).

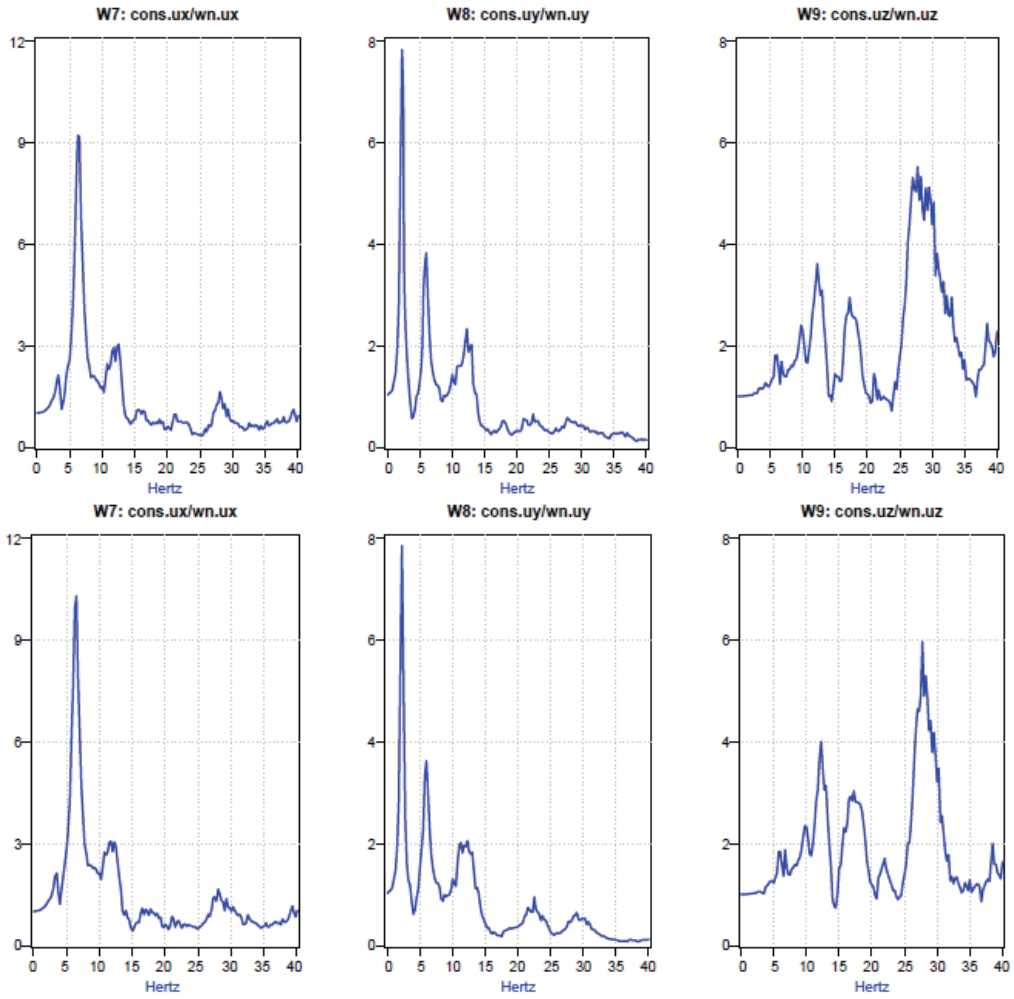

Figure 5-4 Oil conservator response in the three linear directions for the model with evenly distributed oil (up) and the model where the oil is distributed on one side (down)

Despite the differences in the magnitude, it is important that the components of the transformer respond at the same natural frequencies for both models. Therefore, the oil distribution variations applied do not significantly affect the dynamic characteristics of the components. Yet, the dynamic response of the model in which the oil mass is distributed on one side (for both directions) is realistic only for a portion of the cycle of motion. The time for which the model is realistic is when the oil is in contact with one of the two side walls in each direction. Thus, the CommercialModif, m5_CoverModif+Oil_gapelements model was selected as more appropriate for the future analysis of the structure.

Table 5-3 Transformer components' frequencies

Check point	Fundamental Frequencies		
	Longitudinal	Transversal	Vertical
	(Hz)	(Hz)	(Hz)
	(1)	(2)	(3)
hvb1	7.0, 26.5	7.0, 19.0	22.5
hvb2	5.5, 26.5	4.5, 14.0	14.0
hvb3	8.0, 27.0	8.0	8.0, 30.0
hvbbase1	17.5, 27.0	10.5, 23.0	19.0, 27.0
hvbbase2	17.5, 27.0	10.5, 23.0	14.0, 22.0
hvbbase3	17.5, 27.0	10.5, 23.0	15.0, 22.0
hvsa1	8.0, 12.5, 18.0	2.0	4.0, 7.0, 17.0
hvsa2	12.5, 18.0	2.5	4.0, 8.5, 23.0
hvsa3	8.0, 12.5, 18.0	2.0	4.0, 7.0, 17.0
rad1	2.5, 6.0, 13.0	3.0, 12.5, 18.0	10.0, 13.5
rad2	3.5, 16.0	12.5	5.0, 13.0, 22.0
rad3	5.0, 9.0, 19.0	14.0, 29.0	5.0, 14.0, 22.0
rad4	3.5, 13.0, 16.5	10.5, 23.0	5.0, 11.0, 23.5
rad5	2.5, 12.0, 27.0	2.5, 10.5, 27.5	8.0
rad6	13.0	5.0, 13.0, 20.0	9.5, 14.0
hvsabase	16.5, 30.0	10.5, 23.0, 29.5	4.0, 7.0, 17.0
cons	6.5, 11.0	2.0, 6.0, 11.0	12.0, 17.0, 27.5
base plate	-	-	17.5
lvb	27.5	11.0, 12.5, 18.0, 23.5, 25.5	9.0, 13.0, 15.5
lvsa	9.0, 18.0, 27.0	10.0, 17.5, 21.0	11.0, 18.0
str	10.5	15.5	24.0, 32.0
topclamp	15.0, 18.5	3.5	13.5, 19.0
trtop	15.0, 18.5	3.5	13.5, 19.0
trbottom	17.5	3.5	13.5, 19.0
corner1	11.0, 17.0, 27.0	10.5, 22.5, 26.5	-
corner2	11.0, 17.0, 27.0	10.5, 22.5, 26.5	17.0
corner3	11.0, 17.0, 27.0	10.5, 22.5, 26.5	17.0
corner4	11.0, 17.0, 27.0	10.5, 22.5, 26.5	-

Table 5-3 summarizes the most significant frequencies in the three directions, determined from the transfer functions, for the control points selected on the transformer.

From the table above and the comparison between the Transfer Function plots, it is possible to eliminate some of the control points. More specifically, the hvsa1 and hvsa3 points have very similar responses (Figure 5-5) and therefore, point hvsa3 can be eliminated from the set initially selected.

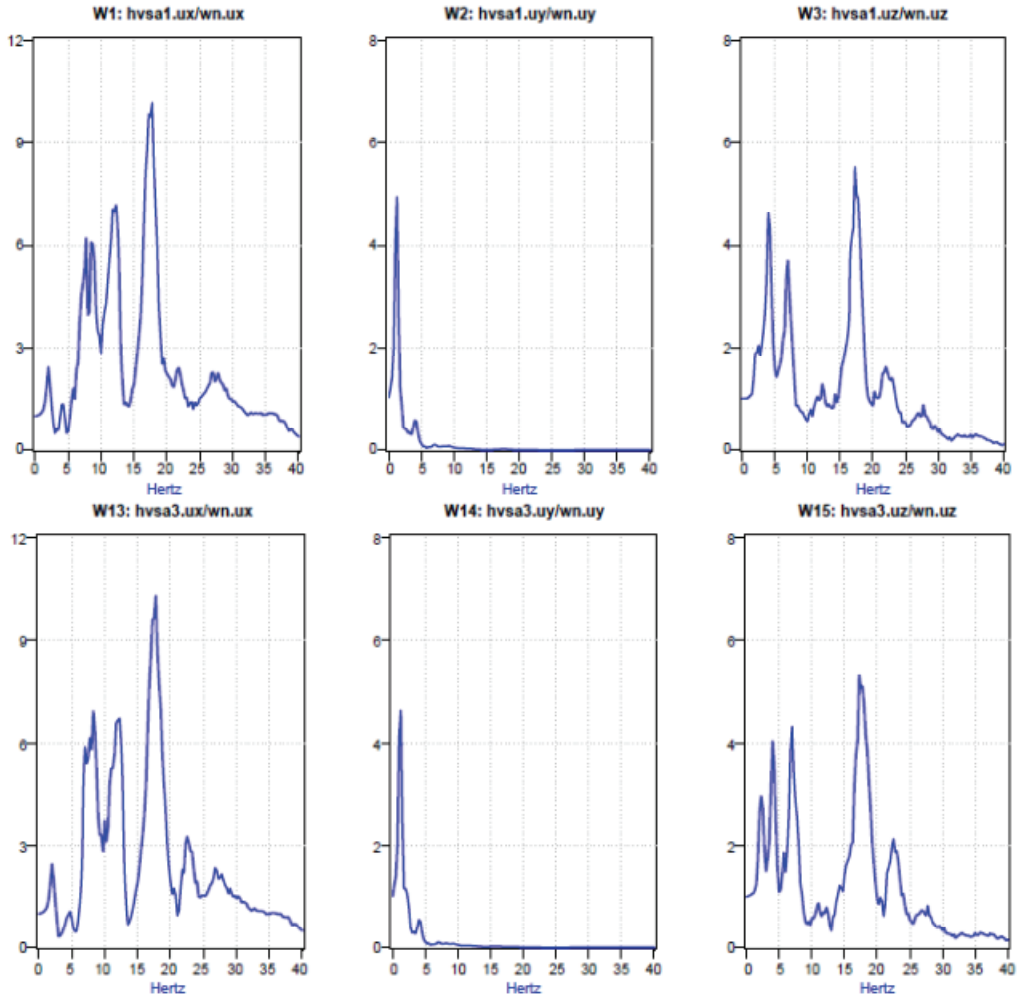

Figure 5-5 Response of high voltage surge arresters 1 and 3 in the three directions

From the points selected to examine the response of the core, the trtop and trbottom points can also be eliminated. The control point at the top clamp (topclamp) has identical response to the point at the top of the middle core leg (trtop). The trbottom point has identical response to the previous two in the vertical and the transverse direction, while in the longitudinal direction the response is almost equal to the ground motion (Figure 5-6).

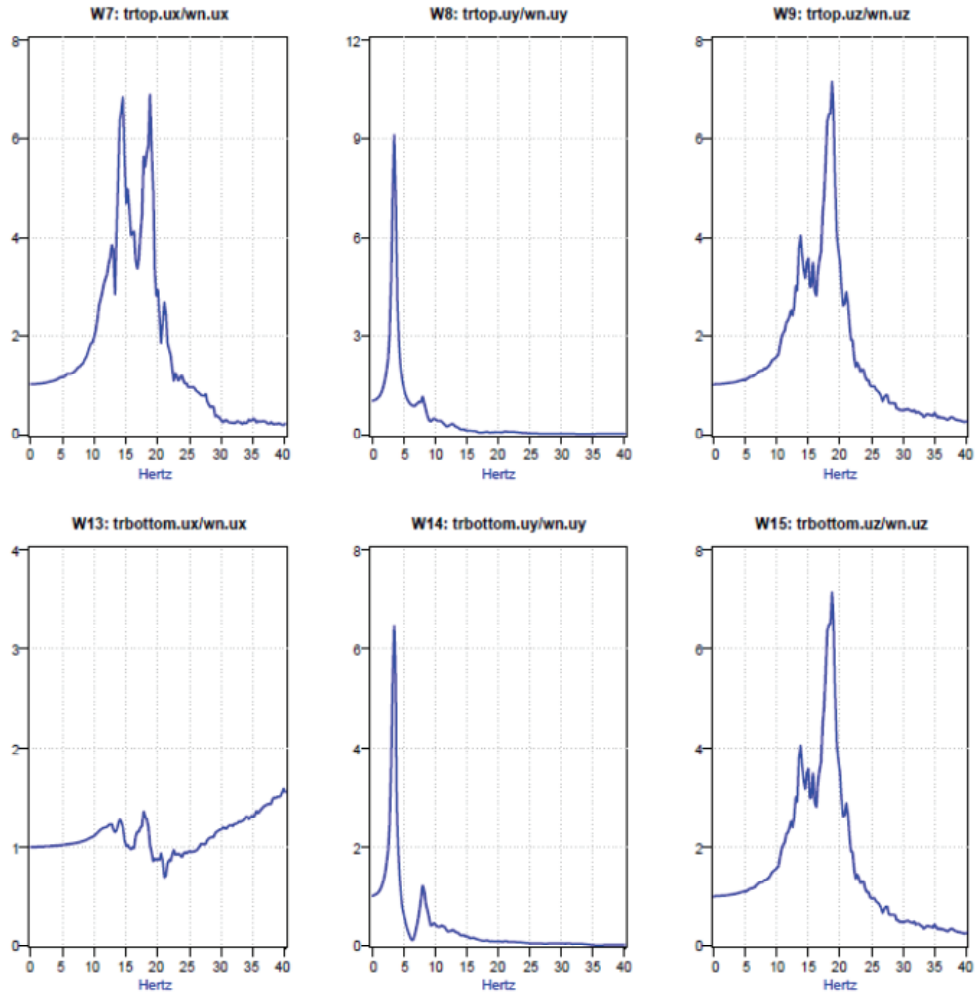

Figure 5-6 Response of top and bottom of the core in the three directions

Finally, the points at the corner of the cover plate have identical responses in the longitudinal and the transverse direction but different responses in the vertical direction. Of

those, the corner2 and corner3 points have very similar transfer functions in the vertical direction and therefore, corner3 can be eliminated (Figure 5-7). For the corner1 and corner4 points the transfer functions in the vertical direction are also very similar and therefore, corner4 can be eliminated.

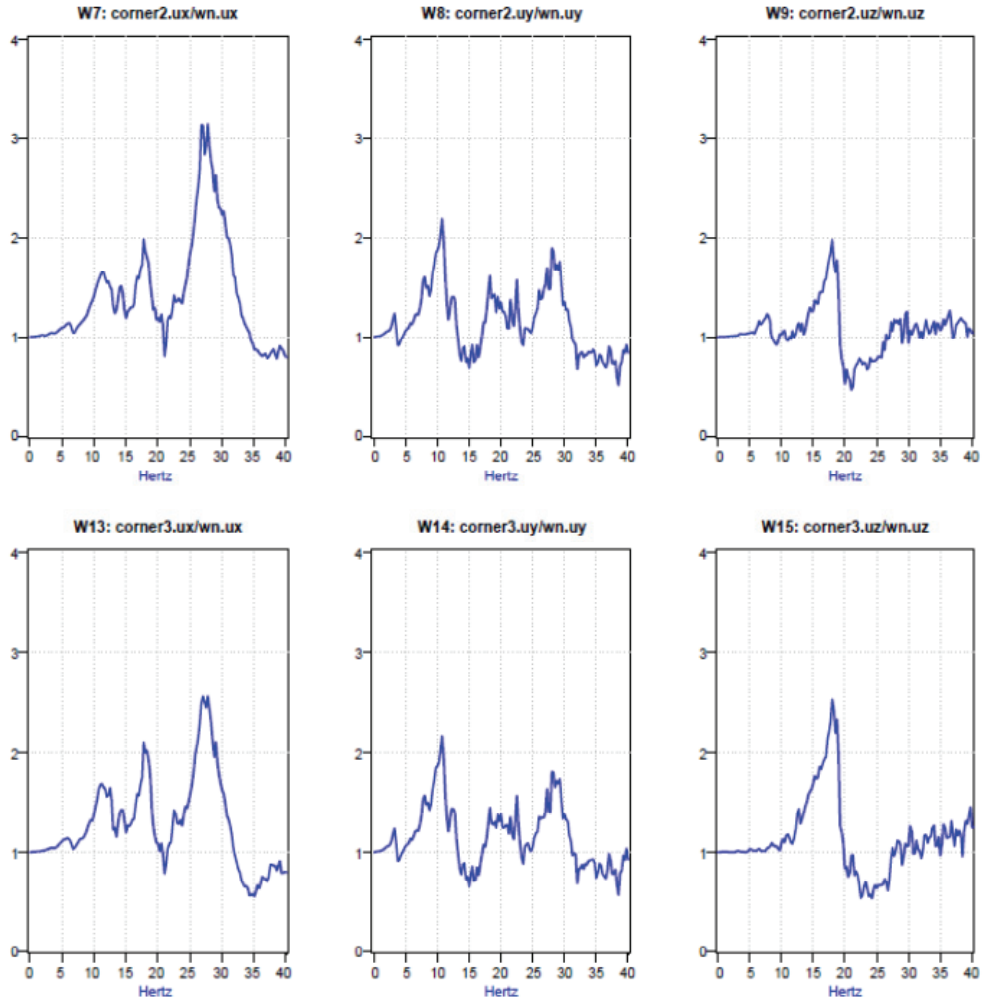

Figure 5-7 Response of corner 3 and 4 of the cover plate in the three directions

5.4 Assessment of Interactions

For the interaction between the control points to be evaluated, the cross spectra and coherences for various pairs of points were determined (three groups of pairs). The control points located below the cover plate were paired with the corners of the cover plate. The points at the base of the high voltage bushings were paired with the corners of the cover plate and the control points located above the cover plate except for the tops of the bushings. Finally, the tops of the bushings were paired with the corners of the cover plate, the points at the base of the bushings and the rest of the points located above the cover plate. This approach helps to identify the interaction between the various elements of the transformer and the bushings, but also associates the response of the bushings to the corner points, the points at the base of the bushings and possibly eliminates some of the control points.

The following tables summarize the interactions as they were assessed after careful inspection of the cross spectra and the coherences obtained from the analysis in the frequency domain.

Table 5-4 presents the interaction for the first group of pairs (corner points and control points below the cover). The control points accounted for were reduced with the technique explained earlier.

Table 5-4 Interaction between control points located below the cover plate and the corners

Check point	Description of interaction	Longitudinal (Hz) (1)	Transverse (Hz) (2)	Vertical (Hz) (3)
rad1	Interaction mainly at radiator frequencies as determined from the transfer functions. The interactions for the corner1 and corner2 are essentially the same for the three principal directions but there are some differences for the rotations about the vertical axis.	2.5, 6.0, 13.0	13.0	10.0, 13.5
rad2		3.5, 6.0, 13.5	13.0	
rad3		5.0	13.0	5.0
rad4		3.8, 16.5	11.0	5, 11
rad5		2.5, 11.5	11.0	8.0
rad6		12.5	5.0, 11.0	9.0, 12.5
topclamp	Interaction mainly at top clamp frequencies. Interactions approximately the same for both corner points.	14.0, 17.0	3.5	18.5
cons	Interaction mainly at conservator frequencies, approximately the same for both corner points	6.5, 12.5	2.5, 12.5	12.5
str	Interaction at small transformer frequencies the same for both corner points	10.5, 12.5	13.0, 15.5	-
base plate	Insignificant interaction in the longitudinal and the transverse direction and interaction at the vertical frequency of the base plate	-	-	17.0

Table 5-5 presents the interaction for the second group of pairs (high voltage bushings' base with control points above the cover and corners of cover). The control points accounted for are reduced compared to the initial ones selected.

Table 5-5 Interaction between the high voltage bushings' base points, the corners and the points above the cover

Check point	Description of interaction	Longitudinal (Hz) (1)	Transverse (Hz) (2)	Vertical (Hz) (3)
hvsa1	Interaction mainly at hvsa1 frequencies in longitudinal and vertical direction and insignificant interaction in transverse direction.	12.5, 17.5	1.5	4.0, 17.5
hvsa2	Interaction mainly at the hvsa2 frequencies in the longitudinal direction and insignificant interaction in the transverse and vertical directions.	12.5, 17.5	2.0	19.0
hvsabase	Insignificant interaction in the longitudinal and the transverse direction. Significant interaction in the vertical direction.	-	-	17.5
lvsa	Interaction mainly at the lvsa frequencies in the transverse and vertical directions.	-	10.0, 12.5, 18.0	18.5
corner1	Interaction mainly in the vertical direction in the frequencies where the base points of the bushings respond.	-	-	19.0
corner2		-	-	17.5, 18.0

Table 5-6 presents the interaction for the third group of pairs (tops of high voltage bushings base with the corners of the cover plate, the points at the base of the bushings and the rest of the points located/connected above the cover plate).

Table 5-6 Interaction between the tops high voltage bushings, the corners, the points at the base of the bushings and the points above the cover

Check point	Description of interaction	Longitudinal (Hz) (1)	Transverse (Hz) (2)	Vertical (Hz) (3)
hvbbase1	Interaction at both the hvb and hvbbase frequencies as determined by the transfer functions. Most significant interaction in the vertical direction.	4.5, 5.5, 7.0, 8.0, 11.0	4.5, 6.5, 8.0, 11.0, 12.5	18.5
hvbbase2		4.5, 5.5, 7.0, 8.0, 11.0	4.5, 6.5, 8.0, 11.0, 12.5	13.5, 17.5, 18.5
hvbbase3		4.5, 5.5, 7.0, 8.0, 11.0	4.5, 6.5, 8.0, 11.0, 12.5	12.5, 14.0, 18.5
hvsa1	Interaction at the bushing frequencies mainly in the longitudinal and vertical directions.	5.5, 7.5, 11.0, 17.5	2.0, 4.0	4.0, 7.0, 17.5
hvsa2	Interaction at the bushing frequencies mainly in the longitudinal and transverse directions.	5.5, 8.0, 17.5	2.0, 4.5	8.0, 17.5,
hvsabase	Interaction with bushings similar to the one of the hvbbase points.	5.5, 7.5 , 8.0, 11.0	4.5, 6.0, 8.0, 11.0, 18.5	7.0, 7.5, 17.5
lvsa	Interaction at the bushing frequencies in all directions.	5.5, 9.0, 18.0, 22.5	9.0, 17.5, 18.0	8.5, 11.0, 14.0, 17.5
corner1	Interaction at the response frequencies of the bushings mainly in the longitudinal and transverse directions.	5.5, 7.5, 8.0, 11.0	4.5, 6.0, 8.0, 11.0, 18.0	-
corner2		5.5, 7.5, 8.0, 11.0	4.5, 6.0, 8.0, 11.0, 18.0	-

The tables above suggest that practically all of the components interact with each other. The significance of the interactions can be assessed by selecting the points for which the most critical interactions (as they were determined from the cross spectra and presented in the tables)

are implied and verifying this assumption with the modal analysis results. As was previously mentioned, the modal analysis is not expected to give accurate results because the model incorporates gap elements between the core and the base plate. However, the animation of the modes may provide very useful information because it will determine if a component is affecting the response of another part through its response.

For example, the low voltage bushing seems to interact with the high voltage bushings especially at its as-installed frequencies (Table 5-6 and Figure 5-8). However, the modal animations do not show interaction for the frequencies of interest, or for the modes related to the motion of the low voltage bushings. It is rather unlikely that there is any interaction between the low voltage bushings and the high voltage bushings.

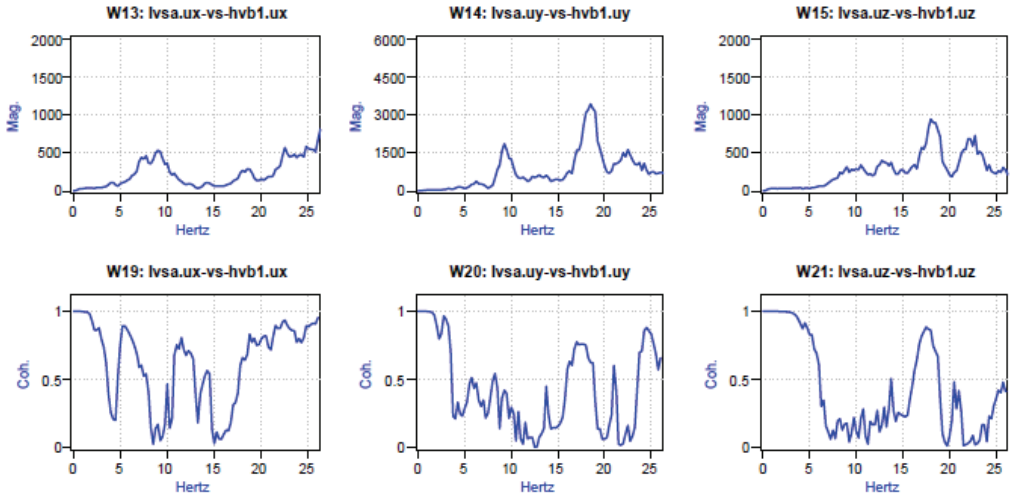

Figure 5-8 Cross spectra and coherences for the low voltage and close to the transformer high voltage bushing response in the three directions

The high voltage surge arresters are also shown to interact with the high voltage bushings especially in the vertical direction (Figure 5-9). In this case, the animation of the surge arresters' modes verifies this assumption. The surge arresters' assembly is connected to the transformer through two horizontal beams which are supported on the cover plate. When the assembly is

rotating or moving in the vertical direction, the horizontal supports force the cover plate to deform out of plane, affecting the response of the high voltage bushings.

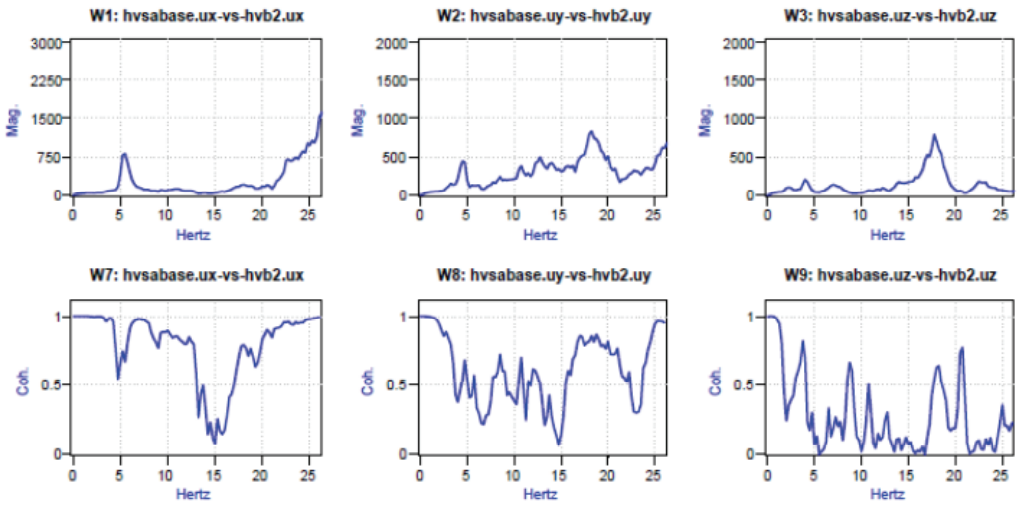

Figure 5-9 Cross spectra and coherences for the surge arresters' base and central high voltage bushing response in the three directions

The analyses results suggest that significant interaction occurs between the high voltage bushings and:

- The high voltage surge arresters assembly
- The radiators

A smaller interaction is observed with:

- The conservator
- The core

It can be inferred that the components having the most considerable effect on the response of the high voltage bushings, *are the ones that mostly affect the cover plate motion*. For instance, the radiators and especially the groups 2-4 directly supported by the side wall can induce appreciable out of plane deformations on the wall. This in turn can influence the cover plate motion and the high voltage bushings.

On that premise, it is expected that the oil conservator will not significantly alter the high voltage bushings' response because its supports are connected very close to the boundaries of the end wall for this particular transformer (Figure 5-10). At these locations the stiffness of the walls is increased and they are hard to deform out of their plane. Therefore, the deformations of the cover will not be affected considerably by the motion of the transformer.

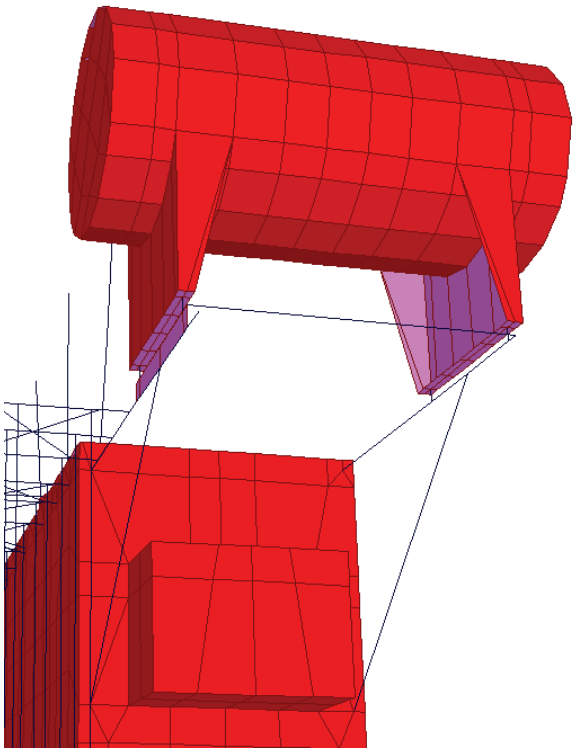

Figure 5-10 Connection of the oil conservator to the end wall

5.5 Cover Plate Mesh Influence

Several variations on the discretization density of the cover elements were examined in order to assess the mesh effect to the bushings' response. The model modified was model MII, a variation of CommercialModif, m5_CoverModif+Oil_gapelements model where the small transformer

Table 5-7 Peak accelerations and moments of the bushing close to the conservator (modified mesh)

No	Model	Peak Acceleration (g)											Moment (kip*in)	
		Corner 1			Bushing 1 Turret Base						Bushing 1		Bushing 1 Base	
		L	T	V	L	T	V	RL	RT	RV	P	T	P	T
Modeling Variations														
1	**MII**	**1.1**	**1.4**	**0.9**	**1.1**	**1.3**	**1.7**	**0.057**	**0.028**	**0.0023**	**4.3**	**2.4**	**120.5**	**66.3**
2	MII-m1	1.1	1.4	0.9	1.1	1.3	1.6	0.059	0.029	0.0022	4.4	2.4	121.9	65.9
3	MII-m2	1.1	1.4	0.9	1.1	1.3	1.7	0.058	0.027	0.0022	4.4	2.4	123.0	65.8
4	MII-m3	1.1	1.4	0.9	1.1	1.3	1.7	0.059	0.028	0.0022	4.5	2.4	124.1	66.3
5	MII-m4	1.1	1.4	0.9	1.1	1.3	1.7	0.058	0.028	0.0022	4.5	2.4	124.1	66.3
No	**Model**	**Corner 1**			**Bushing 2 Turret Base**						**Bushing 2***		**Bushing 2 Base***	
1	**MII**	**1.1**	**1.4**	**0.9**	**1.1**	**1.4**	**2.1**	**0.039**	**0.066**	**0.0019**	**3.6**		**99.3**	
2	MII-m1	1.1	1.4	0.9	1.1	1.4	2.1	0.039	0.066	0.0020	3.6		98.8	
3	MII-m2	1.1	1.4	0.9	1.1	1.4	2.1	0.040	0.066	0.0019	3.6		99.5	
4	MII-m3	1.1	1.4	0.9	1.1	1.4	2.1	0.040	0.067	0.0019	3.6		99.5	
5	MII-m4	1.1	1.4	0.9	1.1	1.4	2.1	0.040	0.069	0.0019	3.6		100.0	
No	**Model**	**Corner 1**			**Bushing 3 Turret Base**						**Bushing 3**		**Bushing 3 Base**	
1	**MII**	**1.1**	**1.4**	**0.9**	**1.1**	**1.3**	**2.1**	**0.047**	**0.044**	**0.0027**	**2.8**	**3.6**	**77.2**	**99.7**
2	MII-m1	1.1	1.4	0.9	1.1	1.3	2.1	0.045	0.046	0.0025	2.8	3.6	78.2	100.6
3	MII-m2	1.1	1.4	0.9	1.1	1.3	2.1	0.045	0.049	0.0029	2.8	3.6	78.4	101.2
4	MII-m3	1.1	1.4	0.9	1.1	1.3	2.1	0.045	0.047	0.0028	2.8	3.7	77.6	102.1
5	MII-m4	1.1	1.4	0.9	1.1	1.3	2.1	0.045	0.047	0.0028	2.8	3.7	77.7	101.9

** The results for Bushing 2 center of gravity and Bushing 2 base are presented in terms of peak instant vector sum of the response measured in the two horizontal directions*

Notation Legend	
L	Lateral
T	Transversal
V	Vertical
P	Perpendicular to bushing axis (CG)
RL	Rotation in the vertical plane (lateral direction)
RT	Rotation in the vertical plane (transversal direction)

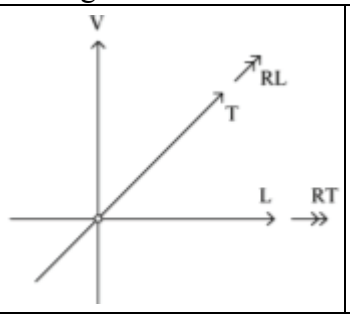

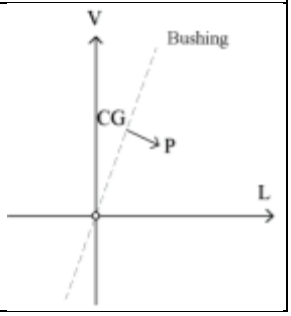

contained in the tank was braced to the end wall. The modified models were subjected to the IEEE693-2005 spectrum compatible ground motion. The response of the bushings, in terms of accelerations and displacements, was obtained at the gravitational center and the top of each bushing respectively.

Table 5-7 shows the comparison for the response acceleration at the gravitational center, the resulting moment at the base of each bushing and the response at the base of each turret for the models examined. The modified models' names are shown in ascending order from the model with the coarser mesh to the model with the finest mesh.

The comparison of the results shows that the bushings present almost identical responses for all of the mesh configurations examined. The same applies for the displacements measured at the top of the bushings. Table 5-8 demonstrates the results in terms of displacements relative to the ground for all bushings:

Table 5-8 Peak displacements of the bushings relative to the ground (modified mesh)

No	Model	Peak Displacement relative to ground (in)												Peak Displacement relative to core (in)		
		Bushing 1 Top			Bushing 2 Top			Bushing 3 Top			Bushing 2 Bottom			Bushing 2 Bottom		
		L	T	V	L	T	V	L	T	V	L	T	V	L	T	V
Modeling Variations																
1	**MII**	**1.66**	**1.17**	**0.42**	**1.96**	**2.80**	**0.29**	**1.27**	**1.33**	**0.29**	**0.70**	**0.97**	**0.29**	**0.69**	**2.80**	**0.28**
2	MII-m1	1.67	1.17	0.42	1.96	2.77	0.29	1.26	1.35	0.30	0.70	0.96	0.29	0.69	2.79	0.28
3	MII-m2	1.69	1.17	0.43	1.96	2.80	0.29	1.25	1.36	0.29	0.70	0.97	0.29	0.69	2.80	0.28
4	MII-m3	1.70	1.18	0.43	1.96	2.79	0.29	1.27	1.37	0.30	0.70	0.97	0.29	0.69	2.80	0.28
5	MII-m4	1.70	1.18	0.43	1.96	2.84	0.30	1.27	1.38	0.30	0.70	0.99	0.30	0.69	2.81	0.29

It can thus be inferred that the regular rectangular mesh of the portion of the cover plate located at some distance from the turret, is not particularly significant for the response of the bushings.

SECTION 6

SENSITIVITY TO STRUCTURAL MODIFICATIONS

6.1 Overview

The modifications presented herein constitute an effort to investigate the dynamic response of the high voltage bushings for a variety of potential structural variations. The procedure is considered necessary, because a generalization of the conclusions is desirable and the transformer used in the current research is only one case of the various types of transformers used in industry.

In the case that a variation is found to appreciably enhance or deteriorate the bushings' response, then the findings could be useful for the development of prospective design recommendations. These findings could be utilized to upgrade the current standards that pertain to the analysis and design of the electrical transformer.

It should be particularly noted that the term "modeling" used in Section 3 signifies the approach followed for the enhancement of the original transformer model and is not related to the term "structural." For the purpose of this section "structural" states that the modifications on the model refer to the design alternatives on the model obtained from the "modeling" procedure.

6.2 Structural Modifications

The base model for a number of structural modifications was the CommercialModif, m5_CoverModif+Oil_gapelements model which is composed of all the corrections defined in the previous sections. For reasons of simplicity, this model is referred to as MI from this point on. The base model for the rest of the modifications was model MII, which was derived from appropriately bracing the core, the radiators and the small transformer in model MI. Therefore

the base models considered in the current analyses were the MI and MII models. The modifications of the components investigated are presented below.

6.2.1 Oil Conservator

In the transformer examined, the conservator is a massive component that lacks seismic bracing. However, there are many transformers that incorporate that feature. In order to assess the response of the high voltage bushings under that condition, the MI model was modified so that the conservator was seismically braced both horizontally and vertically with rigid rods.

On the horizontal plane there are two braces with diagonal orientation forming an X shape, connecting the ends of the horizontal supporting beams of the conservator with the supports. In the vertical direction, there are two braces that again form an X shape and connect the supporting beams with the lower and back part of the conservator tank. The bracing configuration is depicted in Figure 6-1.

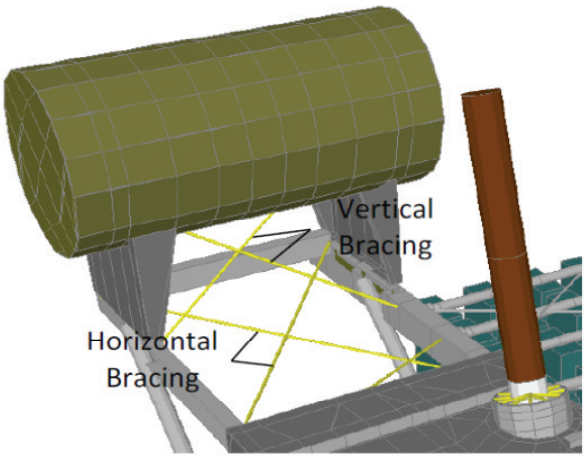

Figure 6-1 Horizontal and vertical bracing of the core in model MI

An additional model was developed from modifying model MII, in which the conservator was completely removed from the transformer (Figure 6-2). This modification is expected to

account for the case in which the conservator is not directly attached to the tank, or is relatively small. If the conservator is considered relatively small, then its influence on the dynamic response of the high voltage bushings is expected to be negligible.

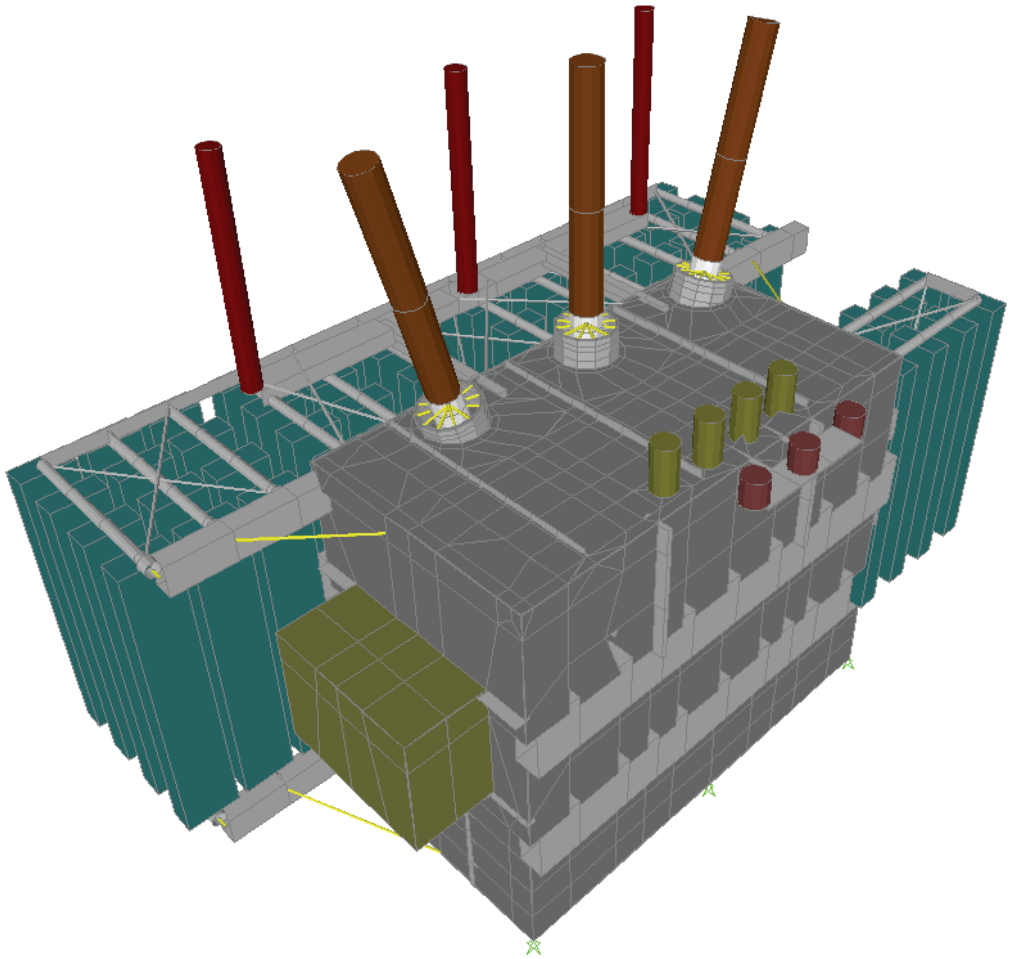

Figure 6-2 Removal of the oil conservator in model MII

6.2.2 Radiators

As deduced from previous analyses of the modified transformer model, the individual response of the radiators significantly affects the high voltage bushings' response. In order to eliminate the individual motion of the radiators and assess the response of the bushings under the new conditions, a modified bracing scheme was considered for the radiator units in model MI.

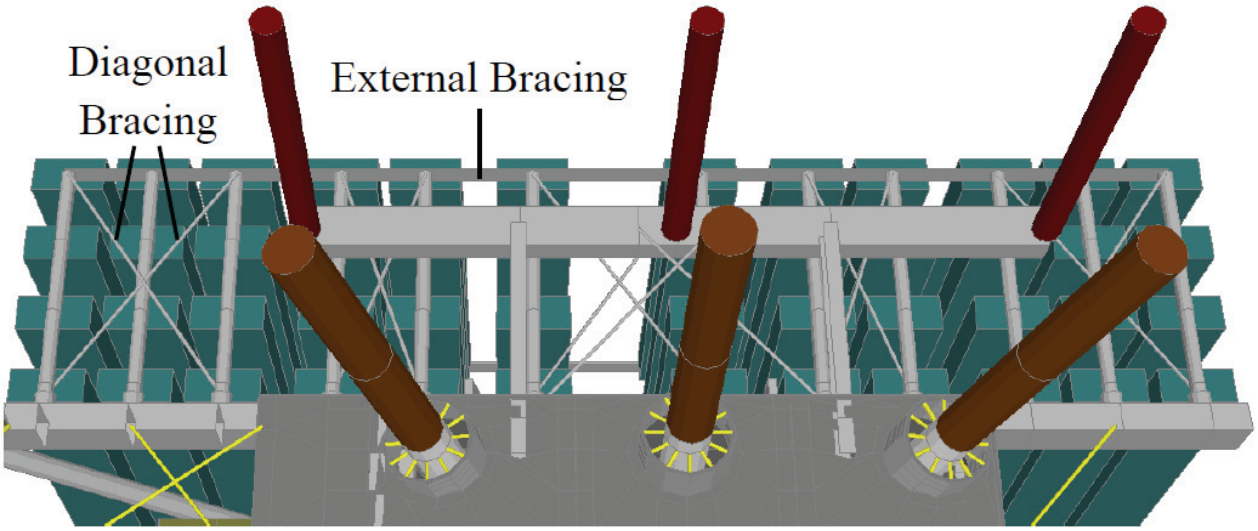

Figure 6-3 Extended X bracing and longitudinal bracing of the radiators in model MI

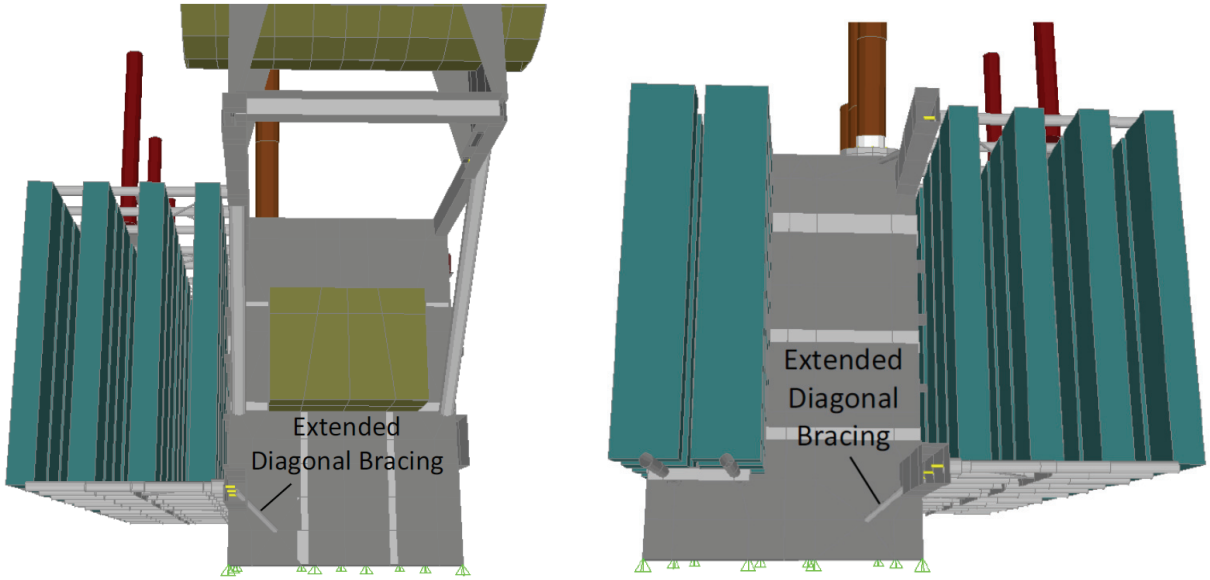

Figure 6-4 Bracing of the radiators on the end walls in model MI

In the finite element model of the transformer initially provided, the radiator groups is composed of diagonal braces in a horizontal plane at their top and bottom supporting beams. These braces, which initially reached up to the middle of the beams, were extended up to the total length. The radiator groups were braced along their ends with L-shaped members, in the longitudinal direction. That way, the individual response of each radiator is expected to be

restrained. Finally, the first and last radiator groups, from the ensemble supported by the longitudinal side wall, were braced along the tank with diagonal elements at their top and bottom. This additional bracing was done so that the radiator group's vertical motion would be further restrained. The modifications are illustrated in Figure 6-3 and Figure 6-4.

It is worth noting that the MII model was developed by bracing both component groups in the MI model with the techniques described above and by bracing the small transformer to the wall of the tank using rigid elements.

6.2.3 High Voltage Surge Arresters

The surge arresters are crucial components of the transformer in terms of interaction with the high voltage bushings. The analyses carried out earlier show that the high voltage surge arresters affect the response of the cover plate directly, through the vertical motion of their supports.

In an effort to resolve this issue, several variations of the supporting conditions for the surge arresters were examined. As a first approach, the MII model was modified so that the surge arresters were supported on the extended cover plate stiffeners. This is depicted in Figure 6-5 in which, for illustrative purposes, only the cover plate of the transformer and the high voltage bushings are shown.

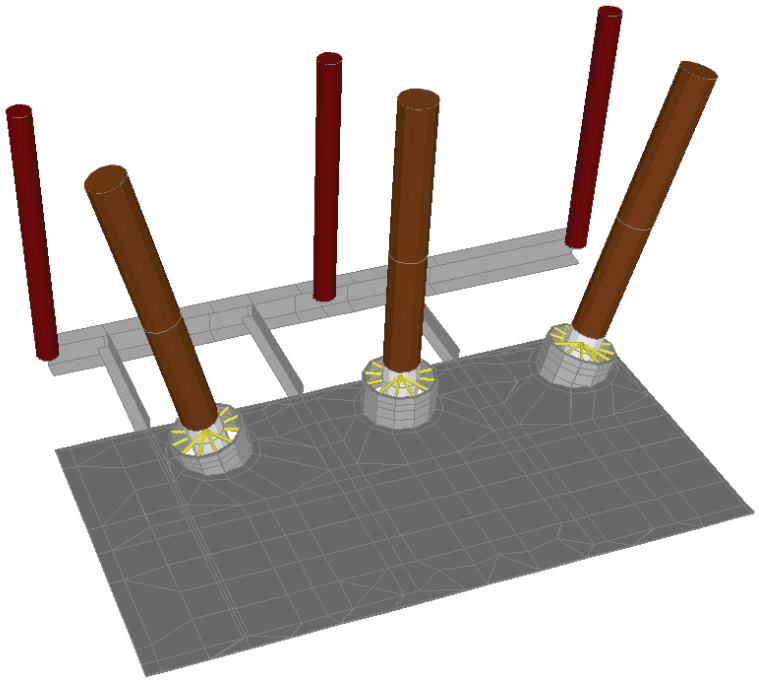

Figure 6-5 High voltage surge arresters supported on cover plate stiffeners in MII model

The model above was further modified by changing the section of the surge arresters' base from channel to a tube with the same dimensions. That way, the torsional stiffness of the surge arresters' base is expected to be increased.

It is desirable to assess the high voltage bushings' response when the surge arresters are made of porcelain instead of a composite material. To achieve this, model MII was slightly modified to incorporate the porcelain bushings. The weight of each composite surge arrester unit in model MII was 154 lbs. In order to incorporate the significantly heavier porcelain surge arresters in the model, the weight of the currently existing surge arresters was simply changed to 672 lbs. This larger weight is the total weight of the porcelain surge arrester unit. No additional changes were applied on the remaining surge arresters' properties, as the frequencies of the units were sufficiently high, which is expected in practice. However, the stiffness of the beams supporting the surge arresters was increased, in a similar fashion as the increase in the weight of the units, so that the units could be efficiently carried.

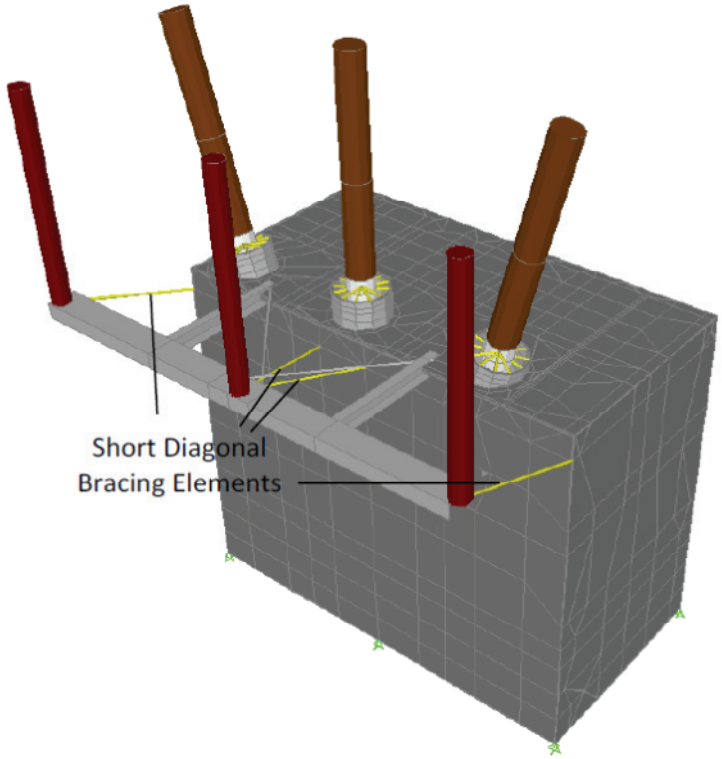

Figure 6-6 Porcelain high voltage surge arresters and short bracing in model MII

In order to eliminate the vertical motion and the rotation of the surge arresters' assembly, the last model was further modified. In particular, diagonal rigid braces were added between the bottom of each porcelain surge arrester and the side wall of the tank. Two braces were used for the middle surge arrester and one brace for the remaining surge arresters. The configuration is shown in Figure 6-6, in which only part of the transformer is depicted for illustrative purposes.

The model was further modified in order to incorporate a more sufficient seismic bracing scheme. On one hand, the angle of the braces in the last model was very small to adequately resist the vertical motion. On the other hand, the braces were connected at a location on the wall where no stiffeners were present. Therefore, the bracing angle and length were increased so that the bracing members were connected to the upper of the two stiffeners on the wall, which were included in the original model. The number of the braces was increased to two for each member (Figure 6-7). Again, only part of the transformer is shown for illustrative purposes.

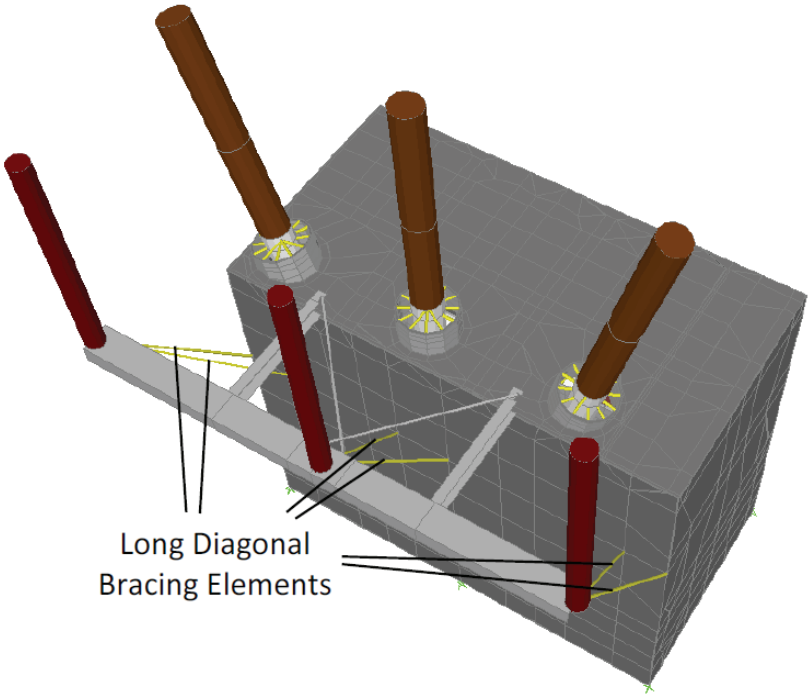

Figure 6-7 Porcelain high voltage surge arresters and long bracing in model MII

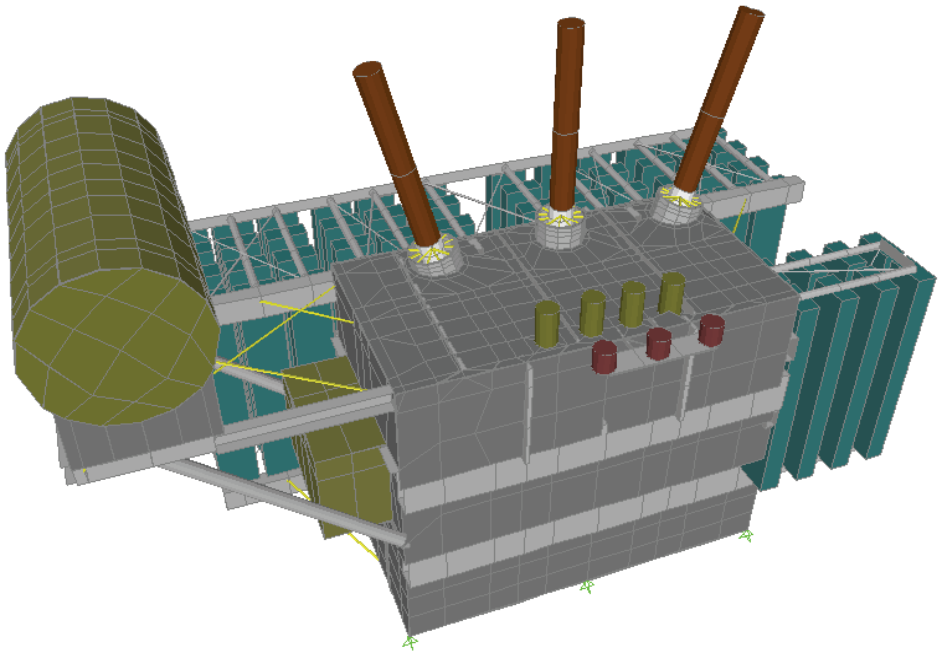

Figure 6-8 Removal of the high voltage surge arresters in model MII

There are transformers in which the surge arresters' assembly is detached from the main tank. In order to be functional in this case, the surge arresters are located close to the transformer,

but stand as an autonomous structure. To account for this scenario, the surge arresters were completely removed from the MII model. The new model created is illustrated in Figure 6-8.

6.2.4 Core-Coil Assembly

As a first design alternative, the core assembly was connected to the corners of the cover plate in model MII. To accomplish this, four of the vertical rigid elements were used as stiffeners for the core assembly; two on each side of the top clamp, were first extended upwards and over the clamp, at a distance half of the clamp's height. After that, rigid bars were employed to connect the top of each extended element to the respective corner (Figure 6-9). The connection at the corners was modeled as pinned.

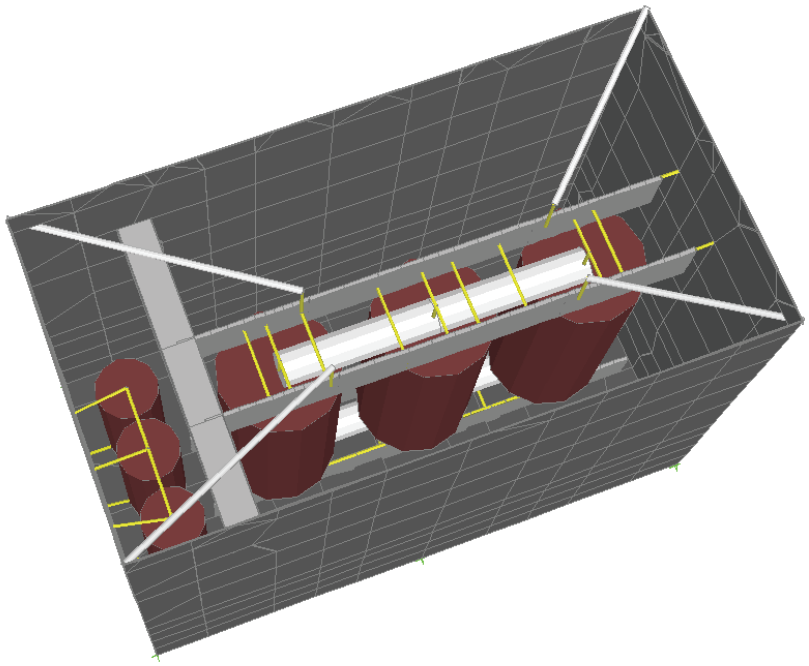

Figure 6-9 Connection of the core to the corners of the cover plate in model MII

The last model was modified so that the connections of the core to the transversal beam and the end wall were eliminated. Figure 6-10 depicts the new model produced and a comparison

to Figure 6-9 can reveal that the transversal beam and the short rigid elements between the core clamps and the end wall have been removed.

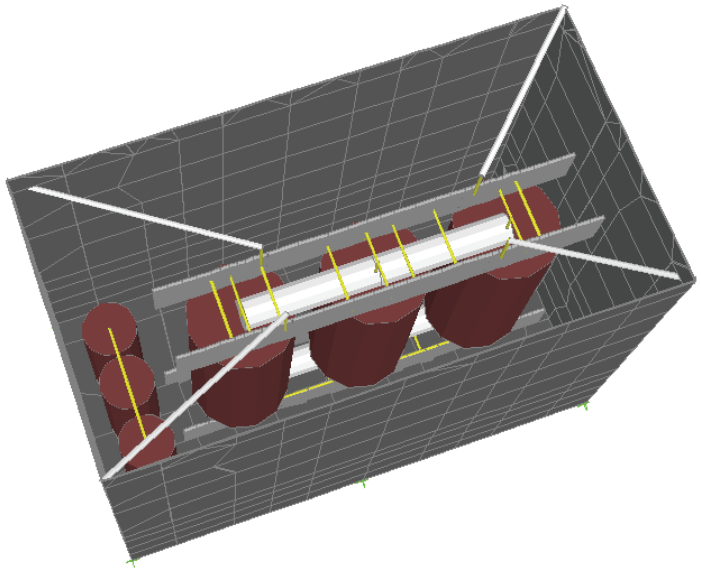

Figure 6-10 Connection of the core to the corners of the cover plate in model MII and detachment from the end wall and the transversal beam

Another potential design variation for the boundary conditions of the core is the direct attachment of the top clamps to the cover plate. This is actually the case for some transformers where the distance between the top of the core and the cover is small enough for the core to be directly connected to the cover. The connection is done through cylindrical pins with one end lying at the top of the core level and the other right above the cover. Here the cylindrical pins are vertically restrained inside cylindrical blocks welded on the cover.

In view of the practical application described above, an appropriate approach was followed in order to achieve the modification. Six of the vertical rigid elements were used as stiffeners for the core assembly; two on each side of the top clamp and two at its center, were extended upwards and over the clamp, at a distance half of the clamp's height. For each pair of the extended elements two rigid diagonal bars were added to the model, starting from the top of

each element and ending at the same node right below the closest node on the cover plate. Finally, for each pair of diagonal elements, the point of their intersection was connected to the node of the cover plate located right above it with a vertical rigid bar. The connection of the rigid bar to the cover plate was modeled as pinned. The result is better depicted in Figure 6-11, in which only the cover, the high voltage bushings and the core have been included for illustrative purposes.

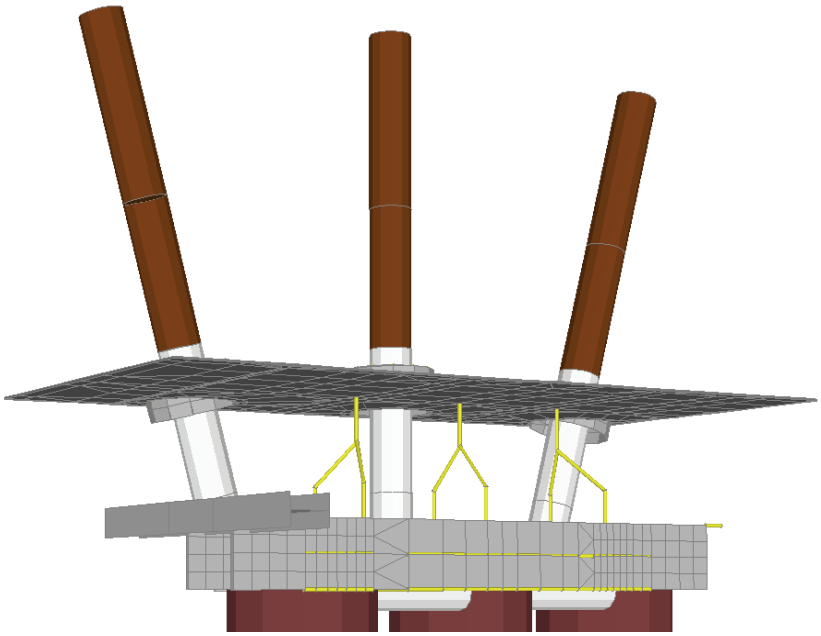

Figure 6-11 Connection of the core directly to the cover plate in model MII

Furthermore, a new model was developed by modifying the last one so that the connections of the core to the transversal beam and the end wall were eliminated. Figure 6-12 shows that the transversal beam and the short rigid elements between the core clamps and the end wall have been removed.

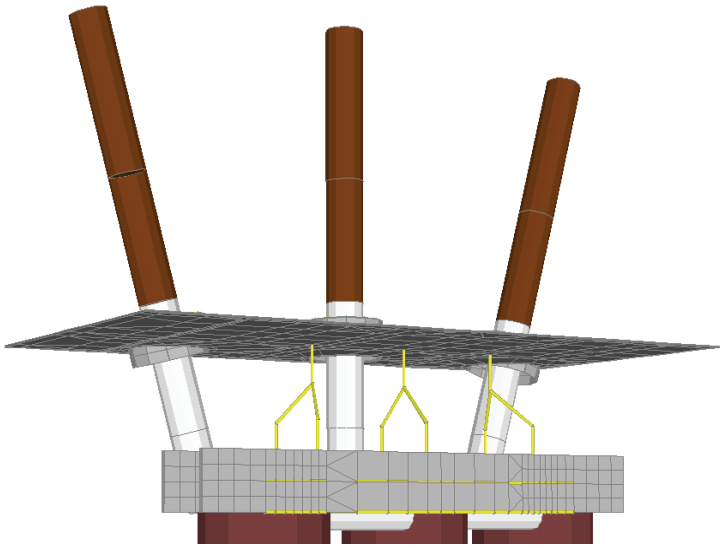

Figure 6-12 Connection of the core directly to the cover plate in model MII and detachment from the end wall and the transversal beam

The last model was further modified with the connections of the vertical rigid elements to the cover plate being changed from pins to clamps.

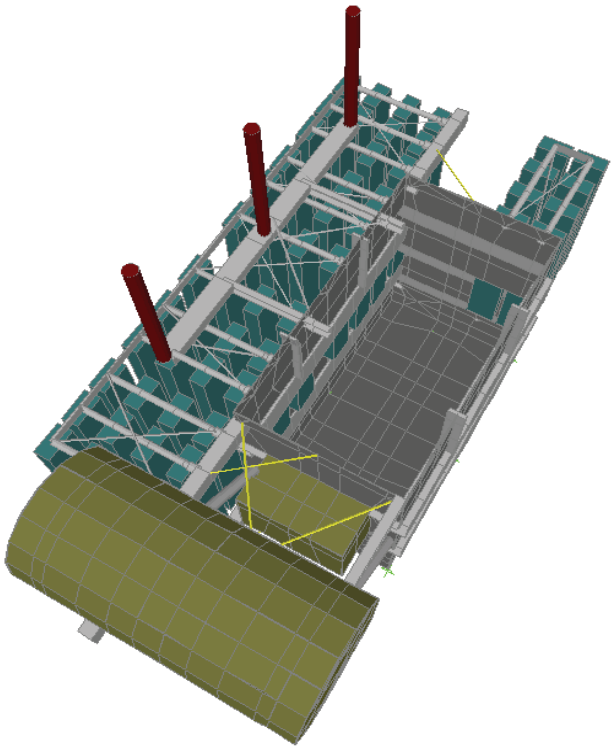

Figure 6-13 Removal of the core in model MII

The transformer model MII was also investigated after the core assembly was completely removed (Figure 6-13). For that model, the oil distribution in model MII was left intact. The approach is representative of a transformer model in which the core assembly is loosely connected to the tank walls. In consideration of the fact that the core is a massive component which is simply resting on the base plate and is not expected to rock significantly during a seismic event. In this type of transformer, the core will not appreciably affect the response of the tank.

6.2.5 High Voltage Bushings

In an effort to investigate the interaction of the bushings due to the individual bushing response, each bushing was in turn removed from the model MII, and three models were developed. That way, by removing a single bushing, the effect on the response of the remaining bushings could be determined.

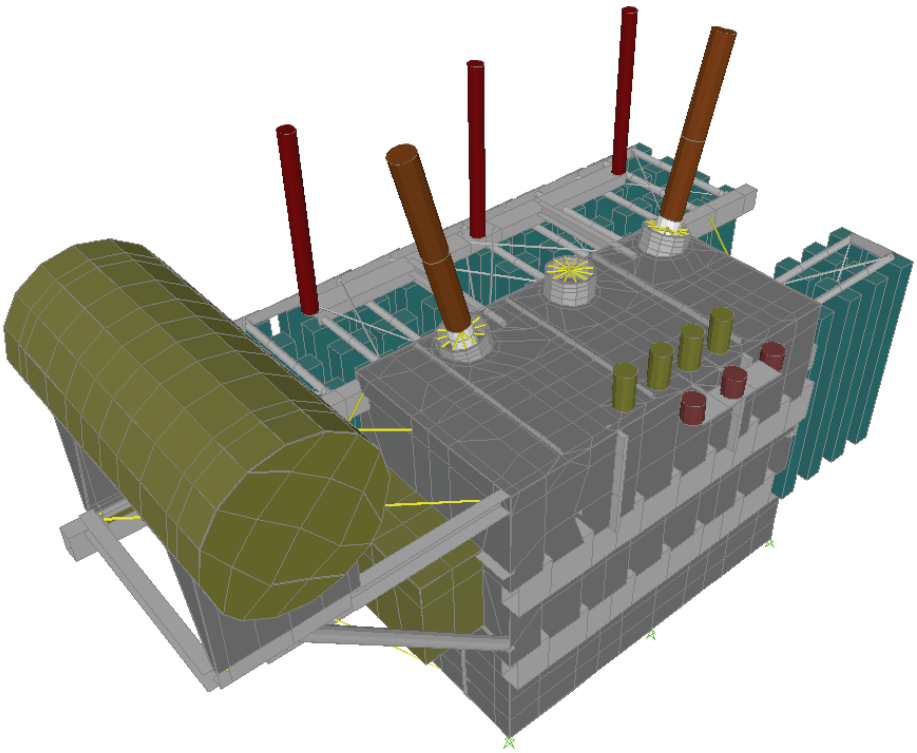

Figure 6-14 Removal of the central bushing in model MII

Finally, a model was developed to determine the response of the bushings for the hypothetical case that the transformer is composed of 230 kV instead of 196 kV bushings. To investigate this case, the material properties and dimensions of the bushings in the MII model were modified appropriately so that they match the attributes provided by the manufacturer. The weight was changed from 1022 lbs (for the 196 kV) to 773 lbs (for the 230 kV) and the properties of the material and the element section for the bushings were assigned in such way so that the fixed base frequency was 20 Hz instead of 15 Hz (for the 196 kV bushings).

6.3 Assessment of the High Voltage Bushings' Response

All of the models, produced from the structural variations presented above, were subjected to the IEEE693-2005 random spectrum compatible ground motion. The most significant components of the response were measured at the base of each bushing and the corners of the cover plate as has already been discussed in Section 3.

The response components of interest are summarized below:

- Accelerations at the gravitational center of the upper high voltage bushings where the mass is concentrated
- Moments at the base of the high voltage bushings
- Displacements at the top of the high voltage bushings
- Displacements at the bottom of the high voltage bushing (part of the bushing immersed inside the tank)
- Accelerations at the corners of the cover plate
- Accelerations at the base of the turrets (points on cover)

The accelerations at the bushings and the moments at the base of the bushings will specify the capacity demand due to the ground motion excitation. The cables connected at the top

as well as at the bottom of each bushing must have a certain amount of slackness for electrical purposes. The displacements at the top of the bushing are measured with respect to the ground and the displacements at the bottom of the bushing are measured with respect to the ground and the top of the core. These data are useful not only for the assessment of the cable's response, but can also provide bounding values in the case when it is desirable that the transformer or the bushing itself is base isolated.

6.4 Effect of Motion Amplifications at Top of Tank

The acceleration spectra at the corners of the cover plate in the three linear directions (longitudinal, transversal and vertical) were produced. In particular, the response history in these directions was obtained from the dynamic analysis of each model and the elastic pseudo acceleration spectra were produced with the use of MATLAB. The response of the transformer is expected to be essentially linear and therefore a small value in the order of 2% was selected for the damping while calculating the spectra.

The pseudo acceleration spectra in the three linear directions were also developed with the use of MATLAB, for the respective response histories obtained at top of each turret. Again a small value of 2% was selected for the critical damping ratio.

When the response spectra at the corners of the cover plate are compared to the respective response spectra computed by the finite element model for the ground motion, the amplifications (or the attenuation) of the response on the cover at certain frequencies are expected. The corners are regions where little or negligible rotational response is expected because the plate and the walls prevent such rotational stiffness. Thus, the horizontal components of the response at the corners are expected to give a very good description of the horizontal motion of the cover plate. The additional in-plane deformations of the cover are expected to be

small due to the high in-plane stiffness of the plate itself. However, the vertical components of the cover response will be much different than the ones measured at the corners. This is due to many other contributions to the vertical motion are not accounted for when one tries to associate the corner response to the cover motion. For example, the rotational input from the side wall response and the vertical motion on the cover due to the high voltage surge arresters' response is not present in the vertical component of the corners.

The IEEE 693-2005 standard recommends that for the dynamic qualification of the bushing in the laboratory, the latter will be mounted on a rigid frame and the input motion will match a required response spectrum (amplified) multiplied by a factor of two. This factor is used to account for the flexibility of the transformer and the cover plate. The corner spectra, obtained from the analysis of the structurally modified models, incorporate the amplifications due to the flexibility of the transformer tank. The response spectra obtained in the finite element analysis at the top of the turrets, incorporate the amplifications due to the combined effect of the transformer flexibility, the plate flexibility and the response of the components attached to the tank. These spectra are important for the expected response of the bushings because they are directly generated from the motion at their base.

The corner spectra are useful when trying to qualify the response of the high voltage bushings as mounted (or as-installed) on the transformer. They are also useful for future design of possible retrofit scheme to remedy undesirable behavior during the high voltage bushings dynamic response: (i) First, if the capacity of the bushing is known from physical testing in laboratory, it can be compared to the expected response from the required response spectra (RRS). From this comparison, it is possible to determine whether the bushing is expected to survive the presumed ground motion or not. This concept is illustrated in Figure 6-15.

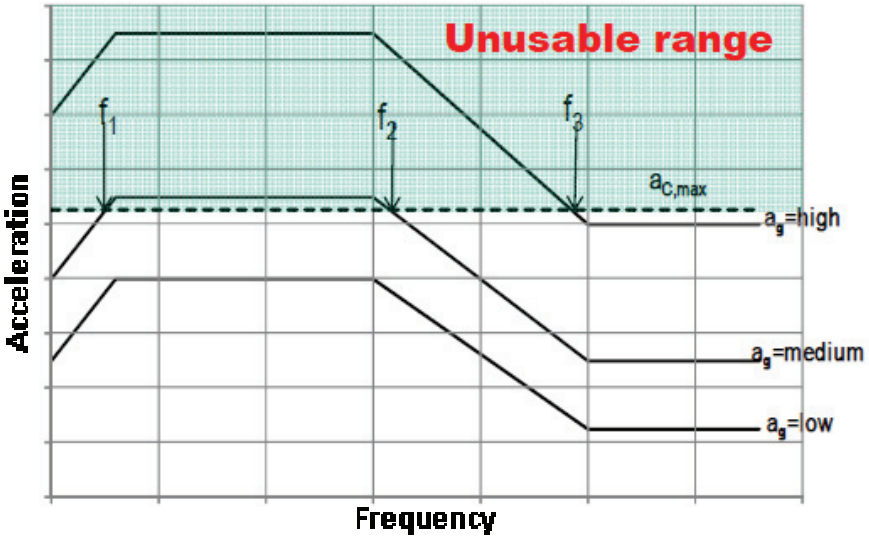

Figure 6-15: Ranges of usability of the bushing (Demand vs Capacity)

Shown in the graph are the amplified required response spectra at top of the tank (cover) for three ground motion intensities (low, medium and high). The dashed line represents the capacity of the bushing provided that it has been specified from experimental testing ($a_{C,max}$). The combination of the required spectra (demand) with the capacity of the bushing, will determine the range of frequencies where the bushing will survive the dynamic excitation. The underlying assumption is that the transformer is represented by a single degree of freedom system with the vertical and rotational effects on the cover neglected.

The required response spectrum for the lowest ground motion intensity in Figure 6-15 shows that the bushing is usable for the whole possible range of as-installed bushing frequencies. The spectrum for the medium ground motion intensity defines a range of frequencies between f_1 and f_2 in which the bushing is expected to suffer damages during the excitation. Finally, for the highest intensity of the ground motion, the bushing is expected to be functional after an earthquake only if its as-installed frequency is greater than f_3. Thus, the shaded area in Figure

6-15 signifies the unusable range of the installed bushing for all the ground motion intensities. It should be noted that the magnitude of bushing capacity and the required spectra in the figure above are hypothetical and presented for explanatory purposes only.

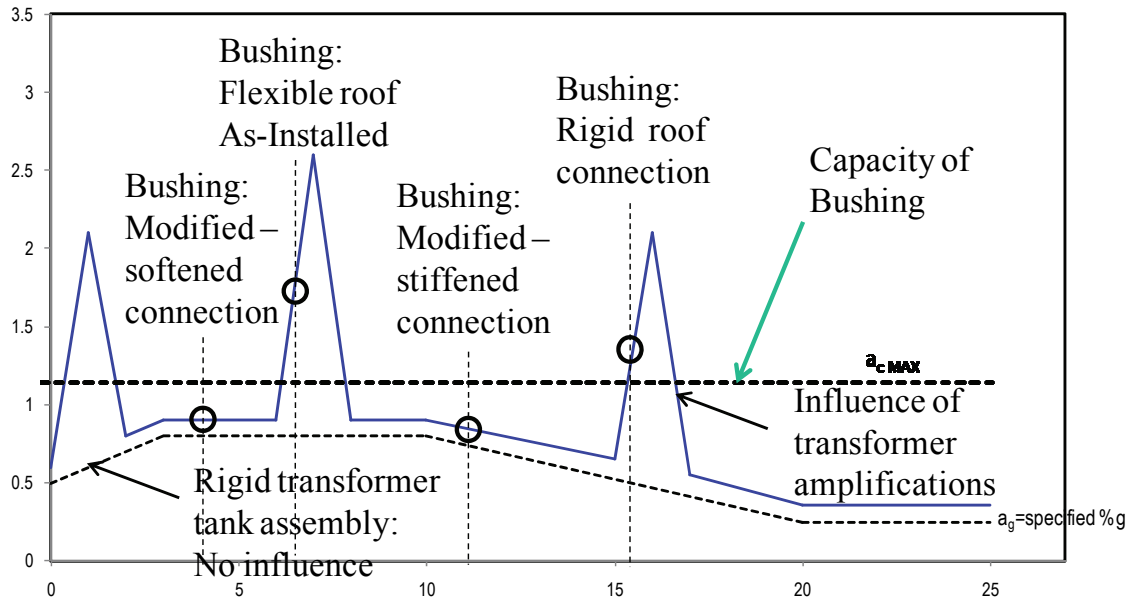

Figure 6-16 Transformer amplifications and as-installed frequencies of bushings

Considering all the amplifications on the cover plate, the required response spectra that represent the cover plate motion will not have the simplified form presented in the Figure 6-15. Instead, they will exhibit peaks at certain frequencies (or ranges of frequencies) that characterize the amplifications on the cover. This is illustrated in Figure 6-16. The dashed line shows the required response spectrum for the transformer, neglecting the amplifications. The continuous line shows the required response spectrum including the amplifications on the cover. It is noted that the presented form, the magnitude and the frequencies at which the amplifications occur are hypothetical, for illustrative purposes only. The bold dashed line shows the capacity of the bushing (with arbitrary magnitude).

It can be inferred that the as-installed frequency of the bushing could be such, that the demand might exceed the capacity of the bushing for the specific frequency due to the influence of the transformer amplification. Such might be the case, if the cover is essentially rigid so that the bushing will respond with its fixed-base frequency.

In order to modify the behavior of the as-installed bushing under these circumstances, without modifying the bushing properties, a solution could be to seismically isolate the transformer, or provide additional damping to the bushings, or a combination of those. Both approaches would lead to a reduction in the acceleration demand for the bushings. Another approach could be to modify the bushing-cover connection either by softening or stiffening techniques depending on the frequency ranges of the amplifications. That way, the as-installed frequency of the bushing could be modified so that the demand would be lower than the actual capacity. For example, Figure 6-16 shows that if the connection is softened properly, for the amplifications shown, the demand is lower than the capacity. An analogous reduction applies if the connection is stiffened appropriately. However, if the connection is stiffened excessively, the as-installed frequency will approach the fixed-base frequency of the bushing. For the current graph, the cover response is amplified and the response will be even more severe than before.

SECTION 7

EFFECTS OF STRUCTURAL MODIFICATIONS ON THE RESPONSE OF BUSHINGS

7.1 Overview

In this section, the results obtained from the analysis of the structurally modified models are reported. First, the nomenclature of the models is summarized for an easier comprehension of the tables presented. Thereafter, the acceleration and displacement responses of the bushings are summarized in relevant tables for the models examined. The section concludes, with the demonstration of the amplification factors obtained for the corners of the cover and the top of the turrets.

7.2 Modified Models Nomenclature

Prior to the presentation of the dynamic analysis results, the modified models discussed earlier are summarized below in Table 7-1. This summarization is done for easy reference of the nomenclature when studying the tables with the results.

Highlighted are the models MI and MII that served as the basis for the structural modifications. For each model developed, the name assigned to it consists of the name of the basis and of a lowercase letter that signifies the type of modification.

For modifications on model **MI**:

- **a** denotes modification of both the conservator and the radiators
- **b** denotes modification of the conservator
- **c** denotes modification of the radiators

For modifications on model **MII**:

- **a** denotes modification of the core

- **b** denotes modification of the bushings
- **c** denotes modification of the surge arresters
- **d** denotes that the 230 kV bushings are incorporated in the model
- **e** denotes modification of the conservator

For the same component, a different number in the model name signifies a different modification. Variations on the same type of modification are denoted with Latin numbering.

7.3 Analysis Results for IEEE-693-2005 Spectrum Compatible Excitation

The response quantities obtained from the dynamic analyses of the modified models for the components of interest are explicitly presented in the following tables. It should be noted that the results in terms of acceleration and moment response are presented differently for each of the bushings. The reasons for the different presentation for each result will be explained shortly.

It can be inferred from the tables that the results for the inclined bushings and the vertical bushing are treated differently. They are treated differently in the sense that for each inclined bushing two accelerations are presented for each analyzed model, while for the vertical bushing only one is shown. For the vertical bushing, both horizontal components are of interest because they are perpendicular to the bushing as by default in SAP2000. Since the vertical bushing is approximately symmetric, the instant vector sum of the horizontal accelerations will describe the resultant acceleration at the center of gravity. The peak value of the instant vector sum is included in the tables prepared for the central bushing.

Table 7-1 Summary of structurally modified models

No	Model	Cover	Core							Bushing			Cons/tor		Rad/s	S. Trans	Surge Arresters						
		Refined Mesh	Bottom Modified	Gap Elements to Base Plate	Braced to Side Walls	Braced to Corners	Braced to Cover Plate	Fixed Braces to Cover	Removed	Original	1=First Removed 2=Center Removed 3=Last Removed	230kV	Braced	Removed	Braced	Braced	On Cover Stiffeners	On Tubular Beam	Porcelain	Support Beams stiffer	Added Stiffeners	Braces to Wall	Removed
		1	2	3	4	5	6	7	8	9	10	11	12	13	14	15	16	17	18	19	20	21	22
1	**MI (Basis)**	■																					
2	MI-a	■											■		■								
3	MI-b	■											■										
4	MI-c	■													■								
5	**MII (Basis)**	■											■		■	■							
6	MII-a1	■				■							■		■	■							
7	MII-a1i	■				■							■		■	■							
8	MII-a2	■					■						■		■	■							
9	MII-a2i	■					■						■		■	■							
10	MII-a2ii	■					■	■					■		■	■							
11	MII-a2iii	■		X 2			■	■					■		■	■							
12	MII-a3	■							■				■		■	■							
13	MII-b1	■									1		■		■	■							
14	MII-b2	■									2		■		■	■							
15	MII-b3	■									3		■		■	■							
16	MII-c1	■											■		■	■	■						
17	MII-c1i	■											■		■	■	■	■					
18	MII-c2	■											■		■	■			■	■			
19	MII-c2i	■											■		■	■			■	■	■		
20	MII-c2ii	■											■		■	■			■	■	■	■	
21	MII-c3	■											■		■	■							■
22	MII-d	■										■	■		■	■							
23	MII-e	■												■	■	■							

For the inclined bushing, the longitudinal component of the response at the center of gravity, as by default in SAP2000, is not perpendicular to the bushing. The same reasoning applies for the vertical component of the response. Rotating these two responses about the transversal axis at the center of gravity of the bushing, one gets a component perpendicular and an axial to the bushing. The axial component is not of particular interest in the current research because the bushing is considered axially rigid. Therefore, only the peak value of the perpendicular component of the inclined bushing component is presented in the tables (in column P).

Illustrated in Figure 7-1, the global axes of the total system are shown at the center of gravity of each bushing and separately. The plane of transformation for the inclined bushing is the one defined by the vertical and longitudinal global axes; as they are presented at the center of gravity of the specific bushing. This is also the plane on which all of the bushings lie, as is indicated in the drawings provided by the manufacturer.

The transverse component of the bushings' response is presented as is, always being perpendicular to the bushing with the vertical component being neglected. However, in the case where large deformation effects are accounted for, the vertical component should be considered.

As far as the response at the base of the bushing is concerned, care should be taken when examining the rotations about the longitudinal and the transversal axes. Mathematically, the rotation of a rigid body about an axis is defined as the motion of a body around the axis of reference. In the current representation, the longitudinal rotation RL is set to signify the rotation about the transversal global axis and the transversal rotation RT, the rotation about the longitudinal local axis. If the bushing-turret system is considered as a rigid body, the peak values of the response components are assumed to coincide temporally and the distance from the center

of gravity to the cover is known. One can directly get an estimate of the expected response at the gravitational center of the bushing, from the maximum response quantities at the turret base, in the desired direction.

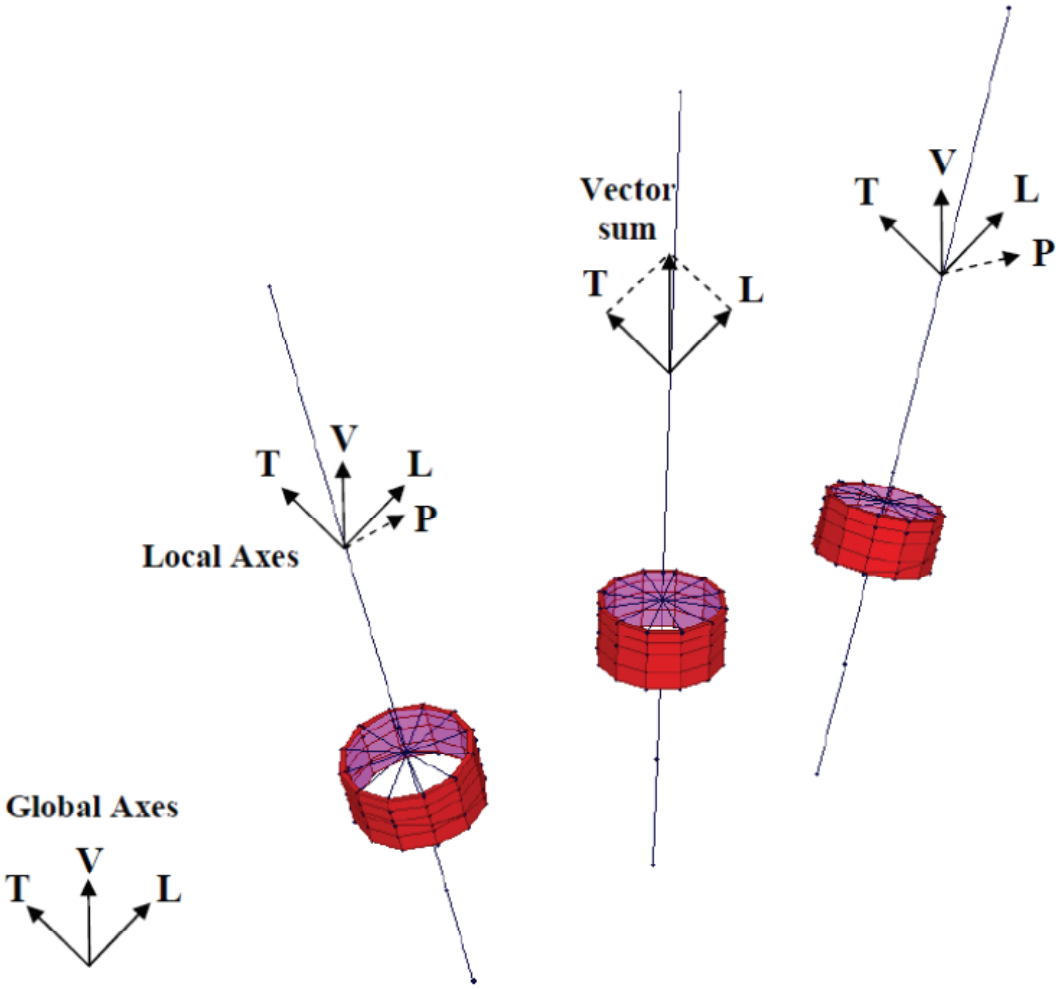

Figure 7-1 Significant components for the bushings' response

Shown in Table 7-2 through Table 7-4 are the peak accelerations at the gravitational center, the moments at the base of each bushing and the accelerations at the turret base and Corner 1 of the corner plate. The models with the most adverse response are highlighted.

Table 7-2 Peak accelerations and moments of the bushing close to the conservator

No	Model	Peak Acceleration (g)											Moment (kip*in)	
		Corner 1			Bushing 1 Turret Base						Bushing 1		Bushing 1 Base	
		L	T	V	L	T	V	RL	RT	RV	P	T	P	T
		(1)	(2)	(3)	(4)	(5)	(6)	(7)	(8)	(9)	(10)	(11)	(12)	(13)
1	**MI (Basis)**	**1.1**	**1.3**	**0.9**	**1.1**	**1.4**	**1.6**	**0.052**	**0.035**	**0.0015**	**4.2**	**2.5**	**115.8**	**68.8**
2	MI-a	1.1	1.3	0.9	1.1	1.4	1.7	0.057	0.028	0.0021	4.4	2.4	122.0	66.1
3	MI-b	1.1	1.4	0.8	1.1	1.4	1.8	0.049	0.032	0.0019	4.4	2.8	123.3	78.8
4	MI-c	1.1	1.5	0.9	1.1	1.5	1.7	0.038	0.026	0.0022	3.2	2.7	89.1	74.8
5	**MII (Basis**	**1.1**	**1.4**	**0.9**	**1.1**	**1.3**	**1.7**	**0.057**	**0.028**	**0.0023**	**4.3**	**2.4**	**120.5**	**66.3**
6	MII-a1	1.1	1.8	0.9	1.0	1.7	1.8	0.058	0.032	0.0033	4.8	3.0	132.3	82.3
7	MII-a1i	1.1	1.8	0.9	1.1	1.7	1.8	0.062	0.033	0.0031	5.1	3.1	141.0	87.2
8	MII-a2	1.0	1.6	0.9	1.1	1.5	2.4	0.063	0.079	0.0040	4.6	3.9	127.0	109.1
9	MII-a2i	1.6	1.6	0.9	1.3	1.7	3.4	0.096	0.201	0.0082	5.4	4.3	149.8	120.5
10	MII-a2ii	1.6	1.6	0.9	1.3	1.7	2.8	0.104	0.209	0.0067	5.7	4.2	157.5	115.9
11	MII-a2iii	2.0	1.9	1.0	1.7	2.8	3.9	0.127	0.328	0.0155	7.6	5.0	210.5	137.7
12	MII-a3	1.1	1.3	0.9	1.1	1.4	1.7	0.061	0.031	0.0022	4.7	2.8	131.7	79.0
13	MII-b1	1.1	1.4	0.9	1.1	1.3	1.7	0.017	0.030	0.0023	-		-	
14	MII-b2	1.1	1.3	0.9	1.1	1.3	1.7	0.056	0.028	0.0022	4.3	2.3	119.6	63.1
15	MII-b3	1.1	1.4	0.9	1.1	1.3	1.9	0.047	0.027	0.0023	3.9	3.5	107.9	98.3
16	MII-c1	1.1	1.4	0.9	1.1	1.3	1.7	0.043	0.029	0.0023	3.6	3.0	101.0	82.5
17	MII-c1i	1.1	1.4	0.9	1.1	1.3	1.7	0.031	0.022	0.0023	2.5	3.2	70.3	87.8
18	MII-c2	1.1	1.4	0.9	1.1	1.3	1.6	0.059	0.028	0.0023	4.6	2.5	126.6	69.0
19	MII-c2i	1.2	1.5	0.9	1.1	1.5	1.9	0.046	0.031	0.0020	3.6	3.9	101.0	107.2
20	MII-c2ii	1.1	1.4	0.9	1.1	1.4	1.7	0.046	0.029	0.0021	3.4	3.3	94.7	90.7
21	MII-c3	1.1	1.4	0.9	1.1	1.3	1.7	0.045	0.033	0.0022	3.3	3.3	92.3	92.2
22	MII-d	1.1	1.4	0.9	1.1	1.3	1.9	0.052	0.030	0.0024	3.9	3.7	75.3	71.2
23	MII-e	1.1	1.5	0.9	1.1	1.5	1.7	0.045	0.028	0.0020	3.8	2.4	106.1	66.8

IEEE Ground Motion (g)		
L	T	V
1.0	1.0	0.9

Table 7-3 Peak accelerations and moments of the central bushing

No	Model	Peak Acceleration (g)										Moment (kip*in)
		Corner 1			Bushing 2 Turret Base						Bushing 2	Bushing 2 Base
		L	T	V	L	T	V	RL	RT	RV	Vector Sum	Vector Sum
		(1)	(2)	(3)	(4)	(5)	(6)	(7)	(8)	(9)	(10)	(11)
1	**MI (Basis)**	**1.1**	**1.3**	**0.9**	**1.1**	**1.4**	**2.4**	**0.038**	**0.057**	**0.0009**	**4.0**	**112.0**
2	MI-a	1.1	1.3	0.9	1.1	1.4	2.0	0.039	0.067	0.0021	3.6	99.5
3	MI-b	1.1	1.4	0.8	1.1	1.4	2.5	0.039	0.053	0.0013	4.1	114.5
4	MI-c	1.1	1.5	0.9	1.1	1.5	2.3	0.035	0.067	0.0014	3.3	92.3
5	**MII (Basis)**	**1.1**	**1.4**	**0.9**	**1.1**	**1.4**	**2.1**	**0.039**	**0.066**	**0.0019**	**3.6**	**99.3**
6	MII-a1	1.1	1.8	0.9	1.0	1.8	3.3	0.039	0.067	0.0029	3.8	105.2
7	MII-a1i	1.1	1.8	0.9	1.1	1.8	3.3	0.039	0.072	0.0029	3.8	105.3
8	MII-a2	1.0	1.6	0.9	1.1	1.6	2.8	0.035	0.128	0.0037	4.8	134.3
9	MII-a2i	1.6	1.6	0.9	1.3	1.7	4.3	0.041	0.443	0.0086	7.7	214.5
10	MII-a2ii	1.6	1.6	0.9	1.3	1.7	4.6	0.042	0.382	0.0076	8.4	233.6
11	MII-a2iii	2.0	1.9	1.0	1.4	2.4	5.4	0.051	0.837	0.0154	10.5	291.1
12	MII-a3	1.1	1.3	0.9	1.1	1.4	2.3	0.040	0.070	0.0019	3.5	96.5
13	MII-b1	1.1	1.4	0.9	1.1	1.4	2.1	0.040	0.064	0.0019	3.7	103.3
14	MII-b2	1.1	1.3	0.9	1.1	1.4	3.8	0.032	0.056	0.0019	-	-
15	MII-b3	1.1	1.4	0.9	1.1	1.4	2.1	0.040	0.067	0.0019	3.9	107.5
16	MII-c1	1.1	1.4	0.9	1.1	1.4	2.0	0.047	0.060	0.0019	4.3	119.8
17	MII-c1i	1.1	1.4	0.9	1.1	1.4	2.1	0.044	0.065	0.0019	4.2	115.6
18	MII-c2	1.1	1.4	0.9	1.1	1.4	2.3	0.040	0.068	0.0020	4.1	114.8
19	MII-c2i	1.2	1.5	0.9	1.1	1.6	2.1	0.042	0.058	0.0021	4.0	110.4
20	MII-c2ii	1.1	1.4	0.9	1.1	1.4	2.1	0.038	0.076	0.0018	3.8	105.6
21	MII-c3	1.1	1.4	0.9	1.1	1.4	2.0	0.041	0.067	0.0019	3.7	103.1
22	MII-d	1.1	1.4	0.9	1.1	1.3	2.4	0.042	0.072	0.0019	4.2	81.2
23	MII-e	1.1	1.5	0.9	1.1	1.5	2.4	0.038	0.068	0.0014	3.6	99.2

IEEE Ground Motion (g)		
L	T	V
1.0	1.0	0.9

Table 7-4 Peak accelerations and moments of the bushing far from the conservator

No	Model	Peak Acceleration (g)											Moment (kip*in)	
		Corner 1			Bushing 3 Turret Base						Bushing 3		Bushing 3 Base	
		L	T	V	L	T	V	RL	RT	RV	P	T	P	T
		(1)	(2)	(3)	(4)	(5)	(6)	(7)	(8)	(9)	(10)	(11)	(12)	(13)
1	**MI (Basis)**	**1.1**	**1.3**	**0.9**	**1.1**	**1.3**	**1.7**	**0.046**	**0.051**	**0.0023**	**1.9**	**3.5**	**53.8**	**96.5**
2	MI-a	1.1	1.3	0.9	1.1	1.4	2.0	0.048	0.057	0.0029	2.7	3.7	74.0	102.3
3	MI-b	1.1	1.4	0.8	1.1	1.3	1.7	0.039	0.052	0.0021	2.2	4.4	61.1	120.8
4	MI-c	1.1	1.5	0.9	1.1	1.5	1.6	0.044	0.041	0.0022	2.3	3.3	64.3	91.1
5	**MII (Basis)**	**1.1**	**1.4**	**0.9**	**1.1**	**1.3**	**2.1**	**0.047**	**0.044**	**0.0027**	**2.8**	**3.6**	**77.2**	**99.7**
6	MII-a1	1.1	1.8	0.9	1.0	1.7	2.1	0.047	0.045	0.0035	2.8	4.4	76.9	120.9
7	MII-a1i	1.1	1.8	0.9	1.1	1.8	2.1	0.048	0.047	0.0034	2.3	5.1	63.9	141.0
8	MII-a2	1.0	1.6	0.9	1.1	1.6	2.3	0.065	0.091	0.0051	2.7	4.1	76.0	114.6
9	MII-a2i	1.6	1.6	0.9	1.5	1.6	3.1	0.109	0.275	0.0086	3.5	5.1	96.5	142.3
10	MII-a2ii	1.6	1.6	0.9	1.4	1.7	2.8	0.105	0.227	0.0105	2.9	4.9	79.2	134.9
11	MII-a2iii	2.0	1.9	1.0	1.9	2.5	3.6	0.141	0.436	0.0157	5.0	6.4	137.7	176.4
12	MII-a3	1.1	1.3	0.9	1.1	1.3	1.9	0.044	0.036	0.0025	2.7	3.9	74.8	107.4
13	MII-b1	1.1	1.4	0.9	1.1	1.3	1.9	0.055	0.040	0.0031	2.9	3.5	79.7	97.8
14	MII-b2	1.1	1.3	0.9	1.1	1.4	2.1	0.050	0.051	0.0029	2.8	3.5	77.1	97.7
15	MII-b3	1.1	1.4	0.9	1.1	1.3	1.4	0.041	0.040	0.0028	-		-	
16	MII-c1	1.1	1.4	0.9	1.1	1.3	1.9	0.056	0.047	0.0029	3.0	3.9	83.8	109.2
17	MII-c1i	1.1	1.4	0.9	1.1	1.3	2.0	0.049	0.040	0.0032	2.8	3.8	78.2	106.3
18	MII-c2	1.1	1.4	0.9	1.1	1.3	2.1	0.061	0.043	0.0034	2.8	4.4	77.9	123.1
19	MII-c2i	1.2	1.5	0.9	1.1	1.5	1.8	0.054	0.054	0.0033	2.3	4.0	65.1	112.3
20	MII-c2ii	1.1	1.4	0.9	1.1	1.3	2.0	0.067	0.048	0.0028	3.0	4.6	82.1	127.5
21	MII-c3	1.1	1.4	0.9	1.1	1.3	2.0	0.050	0.053	0.0037	3.0	3.8	83.8	104.7
22	MII-d	1.1	1.4	0.9	1.1	1.3	2.7	0.072	0.047	0.0026	2.9	6.2	57.0	120.1
23	MII-e	1.1	1.5	0.9	1.1	1.5	1.7	0.040	0.038	0.0038	2.2	3.7	61.6	102.8

IEEE Ground Motion (g)		
L	T	V
1.0	1.0	0.9

Table 7-5 shows the peak accelerations measured at all corners of the cover plate, for the models investigated.

Table 7-5 Peak accelerations of cover plate corners

No	Model	Peak Acceleration (g)											
		Corner 1			Corner 2			Corner 3			Corner 4		
		L	T	V	L	T	V	L	T	V	L	T	V
		(1)	(2)	(3)	(4)	(5)	(6)	(7)	(8)	(9)	(10)	(11)	(12)
1	**MI (Basis)**	**1.1**	**1.3**	**1.0**	**1.1**	**1.3**	**1.0**	**1.1**	**1.3**	**1.0**	**1.1**	**1.3**	**1.1**
2	MI-a	1.1	1.3	1.0	1.1	1.3	1.1	1.1	1.3	1.0	1.1	1.3	1.2
3	MI-b	1.1	1.4	0.9	1.0	1.3	1.0	1.1	1.3	1.1	1.0	1.4	1.1
4	MI-c	1.1	1.5	1.0	1.1	1.4	1.1	1.1	1.4	1.1	1.1	1.5	1.1
5	**MII (Basis)**	**1.1**	**1.4**	**1.0**	**1.1**	**1.3**	**1.2**	**1.1**	**1.3**	**1.0**	**1.1**	**1.4**	**1.1**
6	MII-a1	1.1	1.8	1.0	1.0	1.7	1.1	1.1	1.7	1.1	1.1	1.8	1.2
7	MII-a1i	1.1	1.8	1.0	1.1	1.8	1.1	1.1	1.8	1.1	1.1	1.8	1.2
8	MII-a2	1.0	1.6	1.0	1.1	1.6	1.1	1.1	1.6	1.1	1.1	1.5	1.1
9	MII-a2i	1.6	1.6	1.0	1.6	1.6	1.1	1.6	1.6	1.2	1.8	1.6	1.1
10	MII-a2ii	1.6	1.6	0.9	1.5	1.7	1.0	1.9	1.6	1.1	1.6	1.5	1.0
11	MII-a2iii	2.0	1.9	1.0	2.0	2.5	1.1	2.1	2.3	1.0	2.1	1.9	1.1
12	MII-a3	1.1	1.3	0.9	1.1	1.3	1.0	1.1	1.3	0.9	1.2	1.3	1.0
13	MII-b1	1.1	1.4	1.0	1.1	1.3	1.2	1.1	1.3	1.0	1.1	1.4	1.1
14	MII-b2	1.1	1.3	1.0	1.1	1.3	1.1	1.1	1.3	1.0	1.1	1.3	1.1
15	MII-b3	1.1	1.4	1.0	1.1	1.3	1.2	1.1	1.3	1.0	1.1	1.3	1.1
16	MII-c1	1.1	1.4	1.0	1.1	1.3	1.2	1.1	1.3	1.0	1.1	1.3	1.1
17	MII-c1i	1.1	1.4	1.0	1.1	1.3	1.2	1.1	1.3	1.0	1.1	1.4	1.1
18	MII-c2	1.1	1.4	1.0	1.1	1.3	1.2	1.1	1.3	1.0	1.1	1.4	1.1
19	MII-c2i	1.2	1.5	1.0	1.2	1.5	1.0	1.1	1.5	1.1	1.0	1.5	1.0
20	MII-c2ii	1.1	1.4	1.0	1.1	1.3	1.1	1.1	1.3	1.1	1.1	1.4	1.1
21	MII-c3	1.1	1.4	0.9	1.1	1.3	1.1	1.1	1.3	0.9	1.1	1.3	1.0
22	MII-d	1.1	1.4	1.0	1.1	1.3	1.2	1.1	1.3	1.0	1.1	1.4	1.1
23	MII-e	1.1	1.5	0.9	1.1	1.4	1.0	1.1	1.4	1.0	1.1	1.5	0.9

IEEE Ground Motion (g)		
L	T	V
1.0	1.0	0.9

Finally, Table 7-6 and Table 7-7 show respectively the peak displacements and vector displacements at the top and bottom of the central bushing relative to the ground.

Table 7-6 Peak displacements of bushings relative to the ground and the core

No	Model	Peak Displacement relative to ground (in)												Peak Displacement relative to core (in)		
		Bushing 1 Top			Bushing 2 Top			Bushing 3 Top			Bushing 2 Bottom			Bushing 2 Bottom		
		L	T	V	L	T	V	L	T	V	L	T	V	L	T	V
		(1)	(2)	(3)	(4)	(5)	(6)	(7)	(8)	(9)	(10)	(11)	(12)	(13)	(14)	(15)
1	**MI (Basis)**	**1.76**	**1.59**	**0.43**	**1.72**	**3.20**	**0.33**	**1.39**	**1.76**	**0.37**	**0.61**	**1.15**	**0.33**	**0.62**	**2.91**	**0.32**
2	MI-a	1.68	1.17	0.42	1.96	2.80	0.29	1.27	1.34	0.29	0.70	0.98	0.29	0.69	2.80	0.29
3	MI-b	1.85	1.76	0.45	1.75	3.28	0.34	1.51	2.07	0.37	0.63	1.13	0.34	0.61	2.96	0.32
4	MI-c	1.27	1.29	0.35	1.67	2.97	0.31	1.38	1.07	0.28	0.62	1.10	0.30	0.59	2.78	0.32
5	**MII (Basis)**	**1.66**	**1.17**	**0.42**	**1.96**	**2.80**	**0.29**	**1.27**	**1.33**	**0.29**	**0.70**	**0.97**	**0.29**	**0.69**	**2.80**	**0.28**
6	MII-a1	1.86	1.40	0.48	1.97	2.75	0.32	1.46	1.63	0.33	0.71	1.07	0.32	0.71	1.05	0.31
7	MII-a1i	1.96	1.46	0.50	1.97	2.75	0.32	1.43	1.67	0.34	0.71	1.07	0.32	0.71	1.05	0.31
8	MII-a2	1.97	2.07	0.43	1.54	3.16	0.32	1.79	1.74	0.37	0.55	1.26	0.31	0.55	1.14	0.31
9	MII-a2i	2.45	2.51	0.53	1.46	3.81	0.35	2.20	1.94	0.47	0.51	1.43	0.35	0.52	1.39	0.56
10	MII-a2ii	2.46	2.37	0.54	1.41	4.56	0.40	2.24	2.28	0.42	0.48	1.68	0.39	0.49	1.56	0.62
11	MII-a2iii	2.39	2.51	0.63	1.50	5.78	0.52	2.83	2.57	0.61	0.53	2.04	0.52	0.53	2.20	0.74
12	MII-a3	1.82	1.37	0.45	1.93	2.61	0.28	1.30	1.41	0.30	0.69	0.94	0.28	0.69	0.94	0.28
13	MII-b1	-			1.97	2.95	0.31	1.56	1.23	0.36	0.70	1.04	0.31	0.70	2.85	0.30
14	MII-b2	1.64	1.22	0.41	-			1.22	1.32	0.29	-			-		
15	MII-b3	1.39	1.65	0.44	2.03	2.90	0.31	-			0.72	1.03	0.31	0.72	2.87	0.30
16	MII-c1	1.27	1.55	0.38	2.42	2.52	0.28	1.37	1.64	0.32	0.86	0.95	0.27	0.87	2.93	0.26
17	MII-c1i	1.03	1.79	0.20	2.15	3.35	0.31	1.31	1.19	0.30	0.76	1.19	0.31	0.77	3.10	0.33
18	MII-c2	2.02	1.88	0.48	2.04	3.29	0.33	2.32	2.09	0.41	0.73	1.13	0.33	0.73	2.97	0.32
19	MII-c2i	1.32	1.73	0.34	2.18	3.04	0.30	1.40	1.51	0.35	0.76	1.11	0.30	0.76	2.95	0.31
20	MII-c2ii	1.20	1.55	0.38	1.93	3.03	0.30	1.55	1.54	0.37	0.68	1.07	0.30	0.68	2.85	0.30
21	MII-c3	1.26	1.80	0.37	2.07	2.76	0.29	1.26	1.38	0.32	0.74	0.97	0.29	0.73	2.85	0.28
22	MII-d	1.21	1.04	0.32	1.25	2.24	0.30	1.64	1.36	0.37	0.52	1.04	0.30	0.54	2.28	0.28
23	MII-e	1.48	1.18	0.37	1.93	2.72	0.29	1.32	1.22	0.31	0.70	1.00	0.29	0.69	2.73	0.30

Table 7-7 Peak vector displacements of bushings relative to the ground and the core

No	Model	Peak Vector Displacement relative to ground (in)				Peak Vector Displacement relative to core (in)
		Bushing 1 Top	Bushing 2 Top	Bushing 3 Top	Bushing 2 Bottom	Bushing 2 Bottom
		(1)	(2)	(3)	(4)	(5)
1	**MI (Basis)**	**1.90**	**3.27**	**1.97**	**1.21**	**2.93**
2	MI-a	1.84	2.90	1.72	1.04	2.83
3	MI-b	1.99	3.35	2.13	1.23	3.02
4	MI-c	1.45	3.03	1.74	1.16	2.80
5	**MII (Basis)**	**1.81**	**2.90**	**1.73**	**1.03**	**2.82**
6	MII-a1	2.03	2.82	1.84	1.12	1.09
7	MII-a1i	2.12	2.81	1.86	1.12	1.09
8	MII-a2	2.38	3.24	2.31	1.32	1.17
9	MII-a2i	2.97	3.82	2.62	1.47	1.42
10	MII-a2ii	3.04	4.64	2.73	1.75	1.67
11	MII-a2iii	2.97	5.87	3.24	2.15	2.23
12	MII-a3	1.96	2.68	1.80	0.99	-
13	MII-b1	-	3.04	1.70	1.12	2.87
14	MII-b2	1.79	-	1.70	-	-
15	MII-b3	1.80	3.01	-	1.11	2.89
16	MII-c1	1.66	2.88	1.71	1.05	2.99
17	MII-c1i	1.90	3.38	1.51	1.23	3.14
18	MII-c2	2.37	3.37	2.54	1.20	2.99
19	MII-c2i	1.78	3.13	1.63	1.16	2.98
20	MII-c2ii	1.59	3.09	1.63	1.11	2.88
21	MII-c3	1.89	2.84	1.49	1.02	2.88
22	MII-d	1.31	2.46	1.68	1.15	2.29
23	MII-e	1.65	2.81	1.73	1.07	2.75

7.4 Amplifications at Corners and Top of Turrets

The differences in the bushings' response, presented above for the various models examined, are expected to be well described by the corner spectra, as indicated in the previous section.

In order to illustrate the concept, the spectra for the transversal component of the response have been selected at the most adversely responding corner of the transformer, models MI and MI-a (conservator and radiators braced). For each model, the graph on the right depicts the response spectrum normalized to the ground motion, where the amplifications can easily be assessed (Figure 7-2).

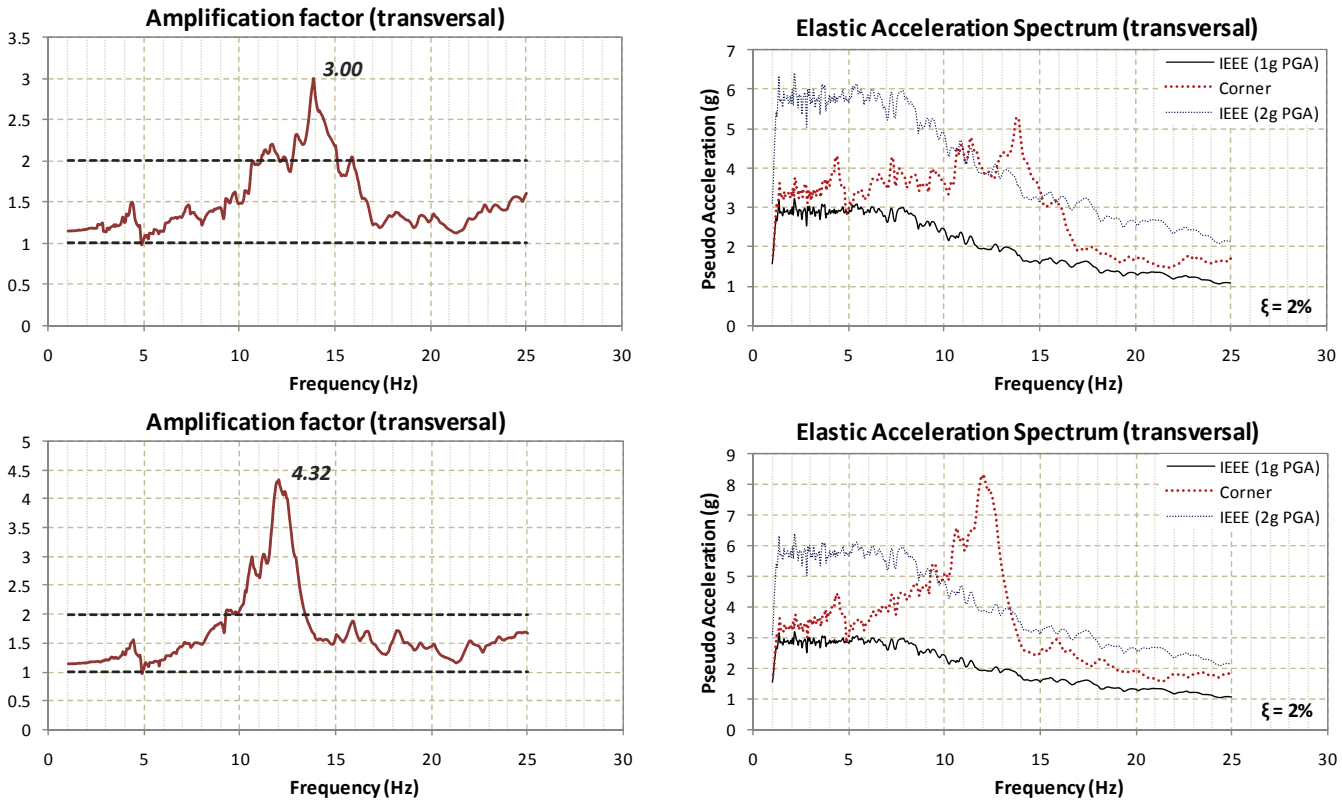

Figure 7-2 Corner response spectra for MI (top) and MI-a (bottom) models (transversal)

It can be recognized that the response spectrum for the MI model already presents some significant amplifications in the range of 11 Hz-16 Hz, with respect to the applied ground motion (1g). In the MI-a model, the maximum amplifications appear in the range of 9 Hz-14 Hz. The

magnitude of the amplification is noticeably large, exceeding the IEEE-693-2005 high performance level spectrum, even when the latter is multiplied by a factor of two. The amplifications occur in a range of frequencies where the as-installed frequency of a bushing could be expected to lie.

It is noted that the response of the bushings is the result of many factors and cannot be described by the corner output alone. The corner spectra reflect the effect of the tank flexibility on the amplification of the ground motion at the cover. They may also give a very good estimate of the expected response of the bushings, given that the cover plate is relatively stiff against out of plane deformation. In consideration of the comparison above, the amplifications are in agreement with the actual response measured at the bushings. As can be inferred from the figure above, in the range of 5Hz to 8 Hz, where the as-installed frequency of the bushings was estimated, the amplifications for the two models are relatively close. These results are similar to ones obtained in past studies (Matt and Filiatrault 2006).

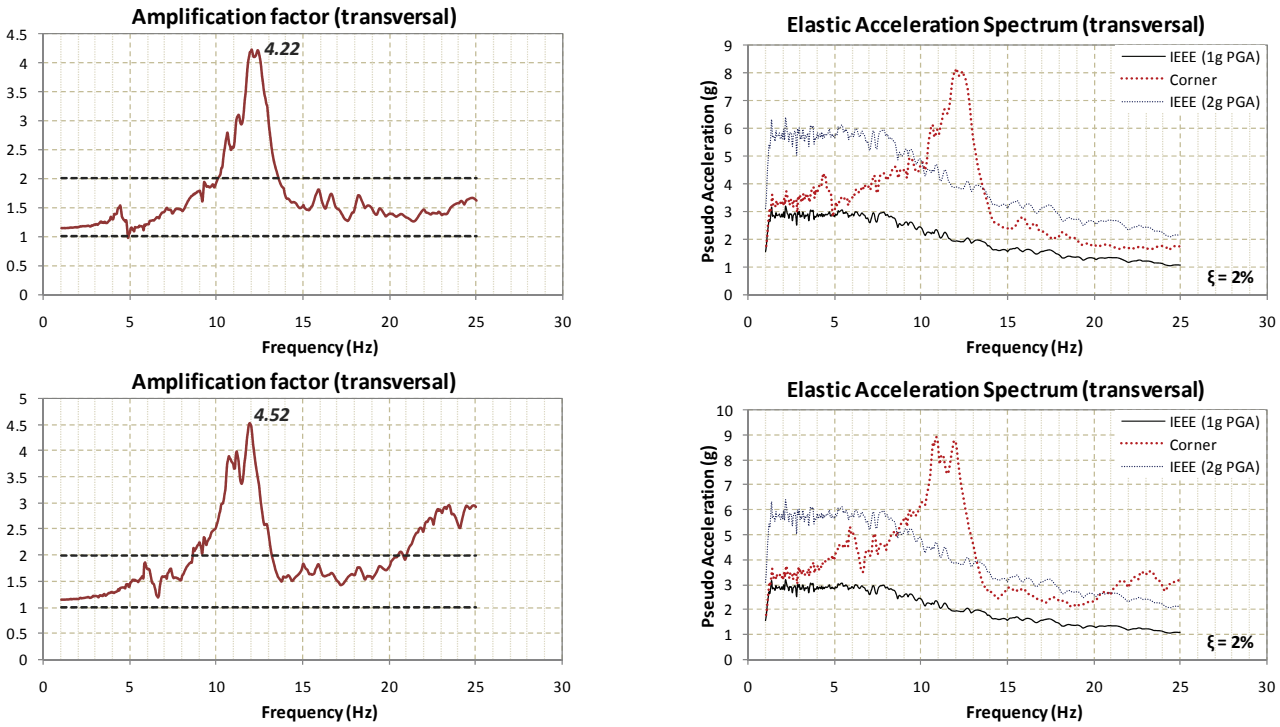

Figure 7-3 Corner response spectra for MII (top) and MII-a2i (bottom) models (transversal)

A more descriptive example is the comparison of the response spectra for the MII and the MII-a2i (core braced to the corners) models. For the MII-a2i it has already been found that the response of the bushings is worsened with respect to the MII model. Figure 7-3 shows that the amplifications are significantly magnified and translated to the left, closer to the as-installed bushing frequencies. In this case, the amplifications for the two models differ noticeably in the range of the as-installed frequencies of the bushings.

The usefulness of the corner spectra lies in the fact that it is a very good method for the identification of the transformer system. If an improvement of the bushing's performance is desired, depending on the structural characteristics of the system, the appropriate structural modifications can be applied. The structural modifications are used on the bushing to avoid the frequency range of amplifications. Moreover, the corner spectra reveal that in the range of 14 to 16 Hz, where the fixed base frequency of the 196 kV bushing usually lies, the maximum amplification observed is close to 2.50. This could be particularly useful if a stiffening technique aiming at increasing the as-installed frequency of the bushing can be implemented. Another technique would be modifying the design features of the transformer so the bushing can be mounted on alternative locations on the cover, where the plate is stiffer.

The acceleration spectra and the amplification factors derived from the normalization of the acceleration spectra, with respect to the IEEE-693-2005 1g PGA and 2g PGA ground motion spectra, were derived at the top of the turrets. The spectra were calculated in the three linear directions from the responses obtained at these points from the analyses of the modified models, excluding the rotational components of the response.

For comparison with Figure 7-3, the response spectra and the amplifications at the top of the turrets in the transversal direction for the MII and the MII-a2i (core braced to the corners)

models are presented below. At first, it can be inferred that the spectra in both figures present amplifications at the same frequencies, in the range of 10 to 15 Hz. However, the spectra at the top of the turrets incorporate peaks at much lower frequencies, close to the as-installed frequencies of the bushings. Considering that the turret is essentially rigid, this indicates that the flexibility of the plate around the turret is affecting the response of the turret-bushing system. On the other hand the amplifications observed at the frequency range of 10 to 15 Hz, express the effect of the tank flexibility which is reflected on the response at the top of the turret. Similar results were obtained in past studies (Matt and Filiatrault 2006).

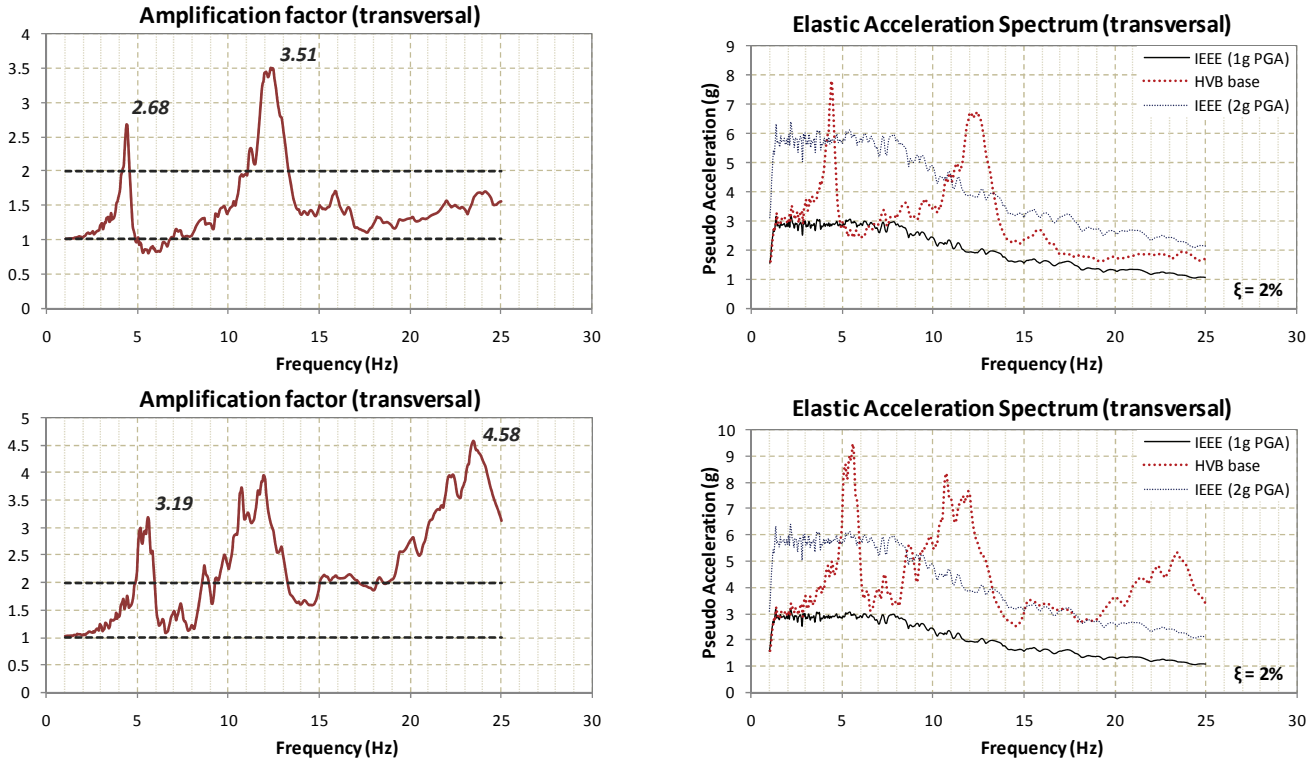

Figure 7-4 HVB base response spectra for MII (top) and MII-a2i (bottom) models (transversal)

When the two approaches are compared for the same frequencies, it can be realized that the spectral accelerations are much larger at the corners of the cover plate than at the top of the turrets. It must be noted that the rotational input on the cover due to the motion of the various components attached to the tank and its contribution to the response of the plate is not accounted

for when examining the motion at the corners of the cover. For instance, it could be possible that the vertical motion of the radiators attached to the side wall may introduce rotational input at the base of the turrets. This would drive the bushings to respond out of phase with respect to their motion due to the horizontal input at the corners of the cover. In any case, observing the remarkable differences in the vertical amplifications between the two approaches, one has to consider that in the current models the bushings are mounted close to the boundary of the cover. This boundary is a region where the vertical and the rotational motion are closely associated. It can be stated that the rotational input from the transformer components and the flexibility of the cover plate are significant for the response of the bushings. Therefore, the rotational input and flexibility cannot be neglected as is done in the case of the corner spectra.

Table 7-8 Amplifications at the cover plate corners

Model	Longitudinal Maximum (1)	Transverse Maximum (2)	Vertical Maximum (3)
MI (Basis)	**2.32**	**3.00**	**1.85**
MI-a	2.54	4.32	2.04
MI-b	2.03	4.17	2.10
MI-c	2.42	3.70	1.99
MII (Basis)	**2.71**	**4.22**	**2.01**
MII-a1	2.19	7.01	2.42
MII-a1i	2.19	7.00	2.52
MII-a2	2.44	4.37	2.14
MII-a2i	2.36	4.52	2.14
MII-a2ii	2.35	4.67	2.24
MII-a2iii	3.54	8.48	3.68
MII-a3	2.00	4.62	2.18
MII-b1	2.70	4.22	2.00
MII-b2	2.69	4.19	1.96
MII-b3	2.69	4.27	2.03
MII-c1	2.61	4.17	2.00
MII-c1i	2.51	4.25	2.02
MII-c2	2.69	4.26	2.03
MII-c2i	2.55	3.71	1.94
MII-c2ii	2.46	3.23	1.89
MII-c3	2.70	4.22	1.99
MII-d	2.67	4.11	1.92
MII-e	2.17	3.69	2.14

Table 7-8 summarizes the maximum amplifications measured at the corners of the cover plate for all the models investigated. While, Table 7-9 summarizes the maximum amplifications measured at the top of the turrets for all the models investigated:

Table 7-9 Amplifications at the top of the turret

Model	Longitudinal		Transverse		Vertical
	Local	Maximum	Local	Maximum	Maximum
	(1)	(2)	(3)	(2)	(3)
MI (Basis)	2.15	2.15	2.83	2.37	10.94
MI-a	2.31	2.31	2.71	3.53	8.53
MI-b	2.11	2.11	2.95	2.95	9.80
MI-c	2.21	2.21	2.79	2.95	8.52
MII (Basis)	2.31	2.31	2.68	3.51	9.26
MII-a1	2.32	2.32	2.34	5.05	8.49
MII-a1i	2.47	2.47	2.33	5.05	8.77
MII-a2	2.11	2.11	2.40	3.68	12.22
MII-a2i	2.67	2.67	3.19	4.58	23.19
MII-a2ii	2.58	2.58	4.24	5.09	23.99
MII-a2iii	3.02	3.80	5.97	9.66	39.66
MII-a3	2.37	2.37	2.19	3.82	7.84
MII-b1	2.36	2.36	2.78	3.53	9.29
MII-b2	2.21	2.21	1.47	3.47	3.98
MII-b3	2.37	2.37	2.77	3.54	9.17
MII-c1	2.79	2.79	2.69	3.47	7.81
MII-c1i	2.40	2.40	2.97	3.50	7.94
MII-c2	2.33	2.33	3.17	3.47	9.29
MII-c2i	2.37	2.37	2.77	2.77	6.65
MII-c2ii	2.60	2.60	2.76	2.76	7.70
MII-c3	2.46	2.46	2.68	3.50	9.07
MII-d	3.42	3.42	3.05	3.41	7.34
MII-e	2.30	2.30	2.65	3.09	7.68

The maximum amplifications are presented in two columns for each of the longitudinal and transversal directions. The first column pertains to the maximum amplification in the frequency range close to the as-installed frequencies of the bushings and the second column pertains to the

overall maximum amplification observed. The vertical maximum amplification is usually of no particular interest for the bushings and therefore is reported in a single column.

It is noted that when studying the tables above, the values presented were chosen to indicate the most adverse corners of the cover or turret top amplification observed in each analysis and therefore, the location of reference may differ from model to model.

SECTION 8

SEPARATED COVER MODELS

8.1 Overview

While the detailed modeling of the transformer produce rich information on all components of the transformer, the dynamic analysis could be too demanding and cost ineffective for practical purposes. In the current section, the feasibility of use of alternative simplified modeling approaches is examined by separating the cover from the tank. For this reason, a series of models have been developed in which the cover plate was separated from the full transformer model. By separating the cover from the transformer careful consideration was given to simulating the boundary support conditions. Two sets of cover models were created in total, one with attachments and one without attachments. The objective of the study is to investigate a variety of supporting conditions for the plate in order to obtain similar response of the cover with the bushings when it is excited with a tri-directional motion, as though if it was installed and the whole transformer subjected to base excitations.

8.2 Separated Cover Models

The cover, along with the high voltage bushings, was removed from the original (MII) model and examined as a separate, autonomous system. The boundary conditions of the separated plate model were comprised of supports assigned to the peripheral nodes of the cover plate. One of the pinned boundary conditions is examined and shown in Figure 8-1, with the pins along the periphery.

Two sets of models were developed and both were comprised of the various boundary conditions, as mentioned above. Concerning the first set, the separated cover models were made as simple as possible, apart from the high voltage bushings, none of the components originally

attached to the cover (such as the high voltage surge arresters) have been included in the modified models.

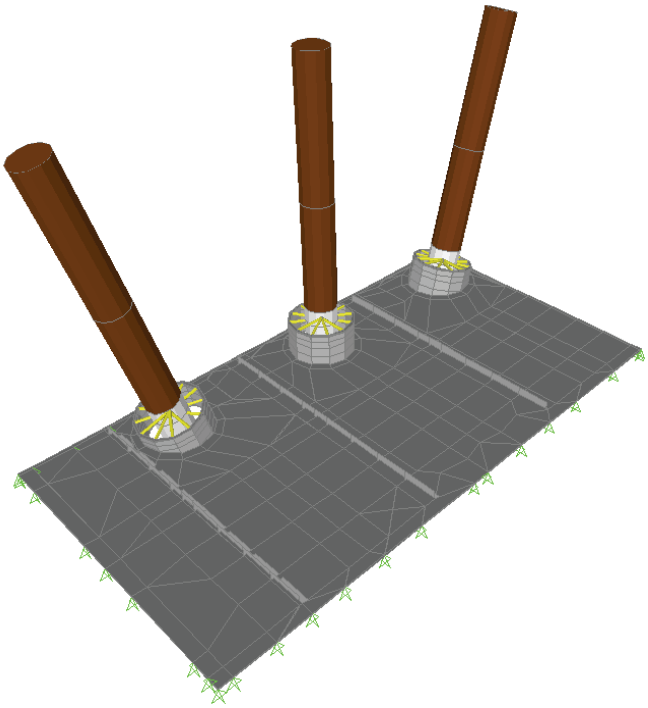

Figure 8-1 Pinned supports on the periphery of the separated cover model

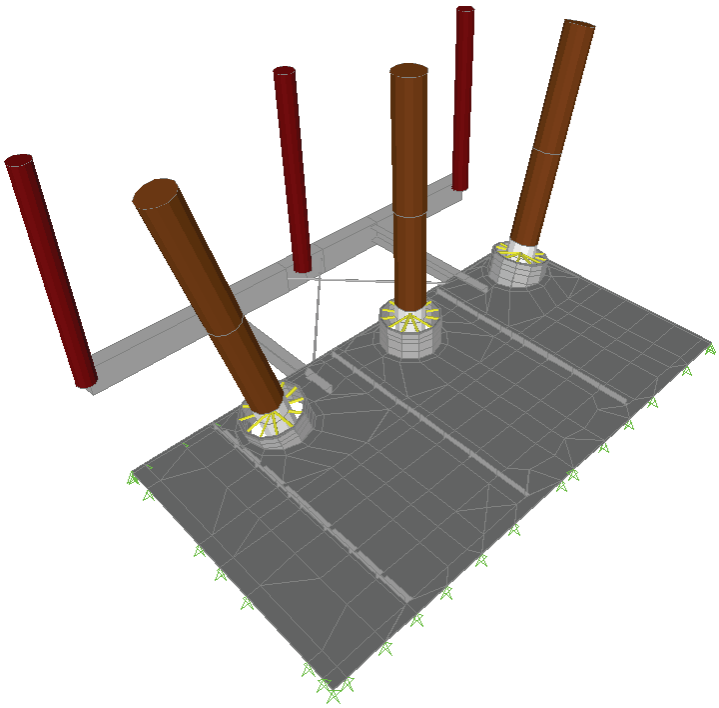

Figure 8-2 Pinned supports on the periphery and inclusion of the high voltage surge arresters in the separated cover model

In the second set, the dynamic effect of some of the attachments was accounted for in the models. More specifically, the models from the first set were appropriately modified so that they incorporated the high voltage surge arresters (Figure 8-2). Other attachments such as the low voltage bushings and the low voltage surge arresters were not included, since their effect was negligible in comparison to the high voltage surge arresters.

The following boundary conditions have been investigated so the actual response could be approached satisfactorily:

- Pinned supports on the periphery (Figure 8-1, Figure 8-2)
- Fixed supports on the periphery
- Combination of pinned and fixed supports on the periphery (four variations)

Table 8-1 Separated cover model nomenclature

Model	Cover		Bushing
	Mesh Modeling	**Connectivity on Boundaries**	**Model**
Original	Coarse	Full	MII
Cover1	Finer	Pinned	MII modified
Cover2	Finer	Fixed	MII modified
Cover3	Finer	Pinned & Fixed (variation 1)	MII modified
Cover4	Finer	Pinned & Fixed (variation 2)	MII modified
Cover5	Finer	Pinned & Fixed (variation 3)	MII modified
Cover6	Finer	Pinned & Fixed (variation 4)	MII modified

The nomenclature for the boundary conditions considered in each set is summarized in Table 8-1. Figure 8-3 also provides an illustration of the boundary conditions considered in the analyses. It is noted that the order of the models corresponds to the order followed in Table 8-1.

It has been earlier discussed that the corners are regions where the cover plate and the side walls are joined. This joining of components contributes to the rotational stiffness in that location and as a result, little rotational response is expected there. It is reasonable to assume that

the response at the corners is mostly influenced by the dynamic motion of the tank. The tank is stiff towards the in-plane deformations of its components and is expected to respond in the horizontal direction and in torsion around the vertical axis.

In view of the above, the full transformer model (MII) was subjected to the spectrum compatible ground motion (IEEE 693-2005). From this ground motion the linear accelerations at the corners of the cover plate were obtained. In order to eliminate the torsional component, the average of the four responses in each direction was calculated.

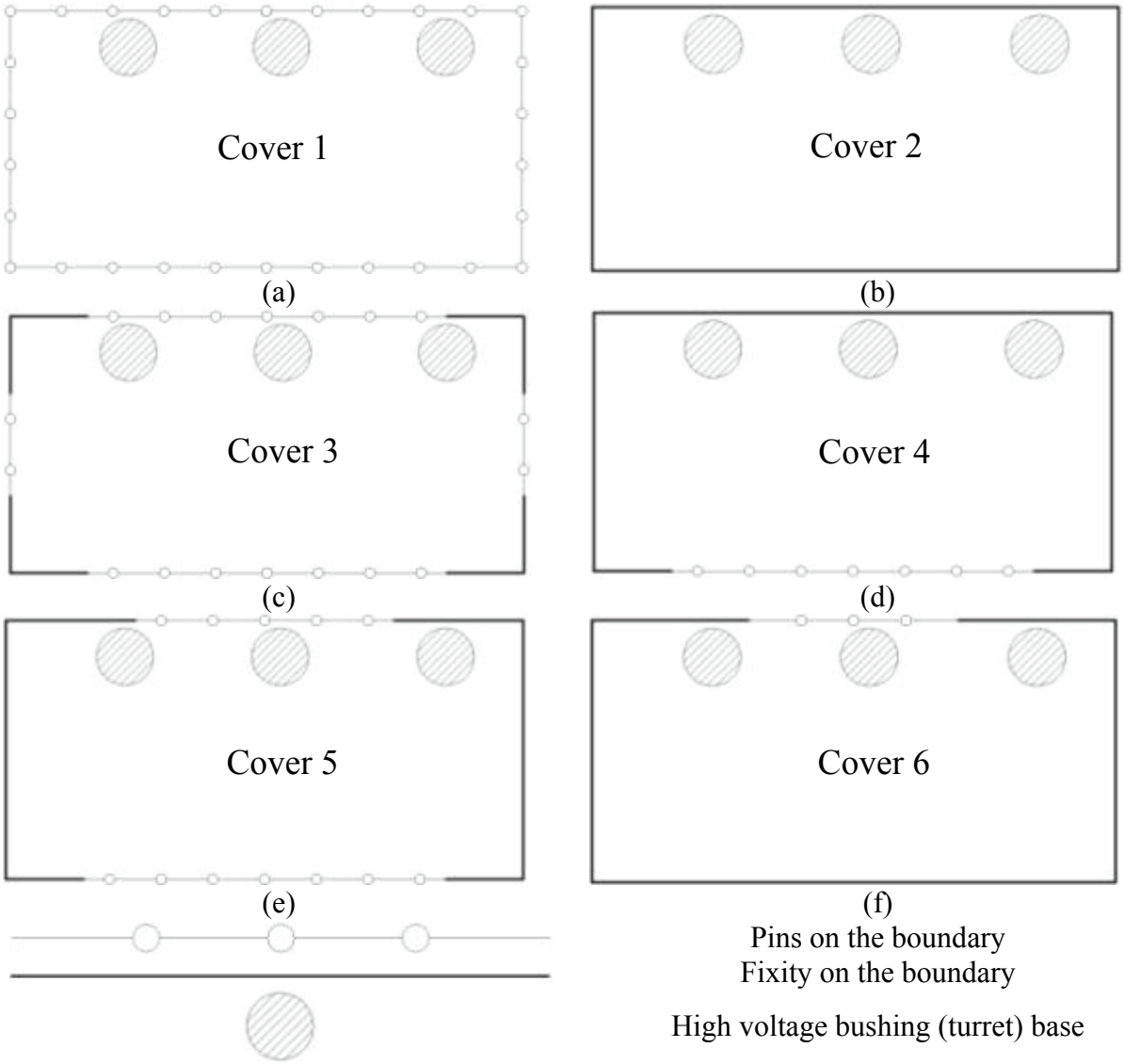

Figure 8-3 Pinned (a), fixed (b) and combination of pinned and fixed boundary conditions (c to f) on the periphery of the cover plate

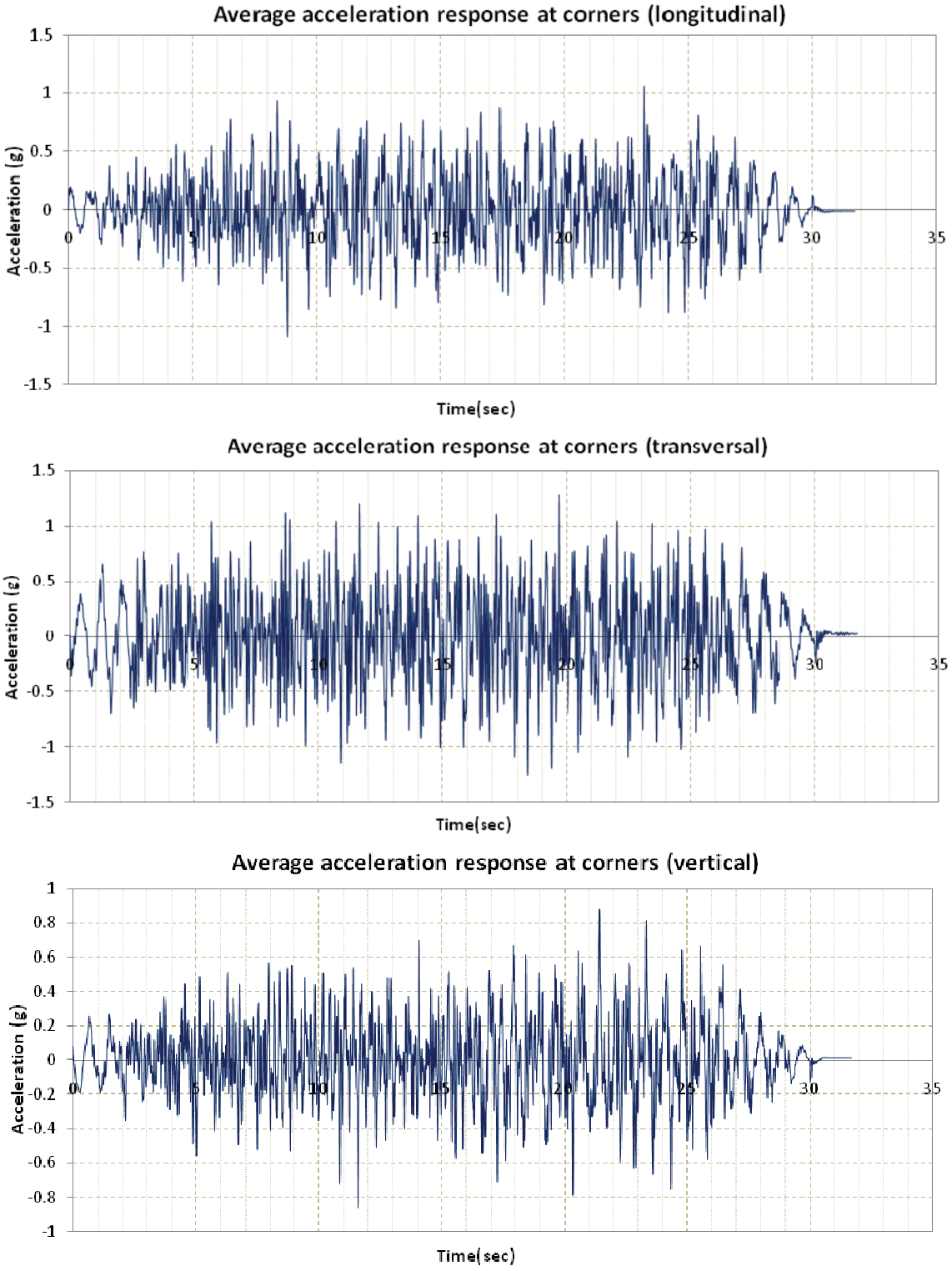

Figure 8-4 Average acceleration response at corners in the three directions, used for the separated cover models excitation

These combined accelerations were employed as the input motion for the analysis of the separated cover models (Figure 8-4).

8.3 Separated Cover Models without Attachments

The results in terms of accelerations for the upper bushing's center of gravity and the accelerations at each bushing's turret base are presented in Table 8-2 through Table 8-4. The MII model results are also presented, in Table 8-2 through Table 8-4, for comparison. Highlighted in the tables are the cover models that are considered to more closely match the behavior obtained from the MII model. The illustration of the nomenclature used in the tables and the differences in the results presentation for each bushing, were discussed in Section 7.

It can be inferred from the tables that the results for the inclined and the vertical bushing are treated differently. For each inclined bushing two accelerations are presented for each analyzed model and for the vertical bushing only one is shown. For the vertical bushing, both horizontal components are of interest because they are perpendicular to the bushing as exported from SAP2000. Since the vertical bushing is approximately symmetric, the instant vector sum of the horizontal accelerations will describe the resultant acceleration at the center of gravity. The peak value of the instant vector sum is included in the tables prepared for the central bushing.

For the inclined bushing, the longitudinal component of the response at the center of gravity, exported from SAP2000, is not perpendicular to the bushing. The same reasoning applies for the vertical component of the response. Rotating these two responses about the transverse axis at the center of gravity of the bushing, one gets a perpendicular and an axial component of the bushing. The peak value of the perpendicular to the inclined bushing component is presented in the tables, in the column P.

The transversal component of the bushings' response is presented as always being perpendicular to the bushing (T) and the axial component is neglected. However, in the case where large deformation effects are accounted for, the axial component should be considered.

Table 8-2 Comparison of response accelerations in separated cover and full transformer models (first bushing)

No	Model	Peak Acceleration (g)						
		Bushing 1 CG		Bushing 1 Turret Base				
		P	T	L	T	V	RL	RT
1	**MII (Basis)**	**4.3**	**2.4**	**1.1**	**1.3**	**1.7**	**0.057**	**0.028**
2	Cover1	3.1	3.5	1.1	1.3	1.9	0.047	0.037
3	Cover2	3.4	3.5	1.1	1.3	1.7	0.045	0.038
4	Cover3	3.5	3.7	1.1	1.3	1.9	0.051	0.032
5	Cover4	3.4	3.5	1.1	1.3	1.8	0.045	0.030
6	Cover5	3.7	3.7	1.1	1.3	1.8	0.047	0.030
7	Cover6	3.7	3.7	1.1	1.3	1.9	0.047	0.035
Relative Difference $(a_{MII} - a_{Cover})/a_{MII}$								
1	Cover1	28%	-46%	0%	0%	-12%	18%	-32%
2	Cover2	21%	-46%	0%	0%	0%	21%	-36%
3	Cover3	19%	-54%	0%	0%	-12%	11%	-14%
4	Cover4	21%	-46%	0%	0%	-6%	21%	-7%
5	Cover5	14%	-54%	0%	0%	-6%	18%	-7%
6	Cover6	14%	-54%	0%	0%	-12%	18%	-25%

Notation Legend			
L	Lateral	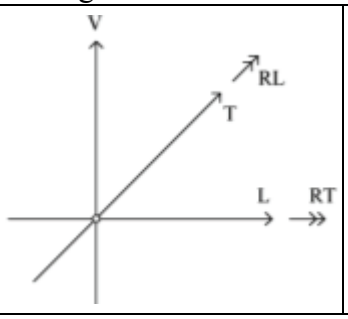	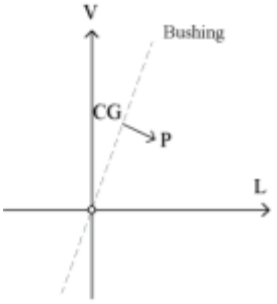
T	Transversal		
V	Vertical		
P	Perpendicular to bushing axis (CG)		
RL	Rotation in the vertical plane (lateral direction)		
RT	Rotation in the vertical plane (transversal direction)		

As far as the response at the base of the bushing is concerned, care should be taken when examining the rotations about the longitudinal and the transverse axes. Mathematically, the rotation of a rigid body about an axis is defined as the motion of a body around the axis of reference. To the contrary, in the current representation, the longitudinal rotation RL is set to signify the rotation about the transversal global axis and the transversal rotation RT, the rotation about the longitudinal local axis.

Despite the fact that Cover2 and Cover4 models are shown to approach the response of the original more closely than the rest of the models, some large discrepancies are observed. These discrepancies in Cover2 and Cover4 are especially true for the peak accelerations in the transversal direction at the bushing's CG. It should be noted that many of the components attached to the cover plate in the full transformer model, as well as the rotational input from the transformer walls, have been discarded in the current approach. It is suggested that the results of Table 8-2 for the first bushing (as well as the results in the rest of the tables for the other bushings) should be compared to the respective results of Table 8-7. The results in Table 8-7 are obtained from the analyses of the separated cover models, in which the surge arresters have been included. The inclusion of the surge arresters will be shown below to provide a closer match to the full model especially, in terms of the response at the bushing's center of gravity.

Table 8-3 Comparison of response accelerations in separated cover and full transformer models (central bushing)

No	Model	Peak Acceleration (g)					
		Bushing 2 CG	Bushing 2 Turret Base				
		Vector Sum	L	T	V	RL	RT
1	**MII (Basis)**	**3.6**	**1.1**	**1.4**	**2.1**	**0.039**	**0.066**
2	Cover1	4.5	1.1	1.3	2.9	0.039	0.028
3	Cover2	3.7	1.1	1.3	1.6	0.039	0.049
4	Cover3	4.8	1.1	1.3	3.0	0.038	0.051
5	Cover4	3.8	1.1	1.3	1.6	0.039	0.059
6	Cover5	4.9	1.1	1.3	2.9	0.039	0.043
7	Cover6	4.4	1.1	1.3	2.6	0.037	0.042
Relative Difference $(a_{MII} - a_{Cover})/a_{MII}$							
1	Cover1	-25%	0%	7%	-38%	0%	58%
2	Cover2	-3%	0%	7%	24%	0%	26%
3	Cover3	-33%	0%	7%	-43%	3%	23%
4	Cover4	-6%	0%	7%	24%	0%	11%
5	Cover5	-36%	0%	7%	-38%	0%	35%
6	Cover6	-22%	0%	7%	-24%	5%	36%

Notation Legend			
L	Lateral	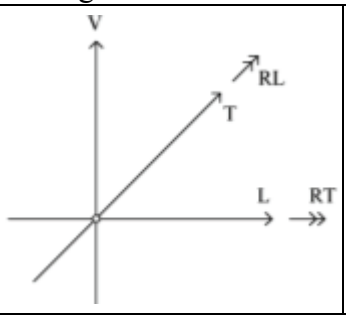	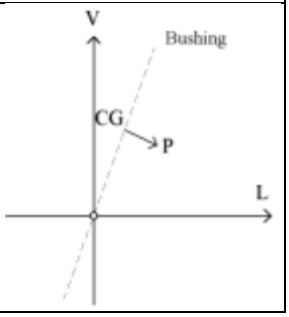
T	Transversal		
V	Vertical		
P	Perpendicular to bushing axis (CG)		
RL	Rotation in the vertical plane (lateral direction)		
RT	Rotation in the vertical plane (transversal direction)		

Table 8-4 Comparison of response accelerations in separated cover and full transformer models (third bushing)

No	Model	Peak Acceleration (g)						
		Bushing 3 CG		Bushing 3 Turret Base				
		P	T	L	T	V	RL	RT
1	**MII (Basis)**	**2.8**	**3.6**	**1.1**	**1.3**	**2.1**	**0.047**	**0.044**
2	Cover1	3.4	4.0	1.1	1.3	2.1	0.051	0.024
3	Cover2	3.0	3.1	1.1	1.3	1.2	0.036	0.029
4	Cover3	3.0	3.2	1.1	1.3	1.1	0.039	0.024
5	Cover4	3.1	3.1	1.1	1.3	1.2	0.039	0.027
6	Cover5	3.0	3.1	1.1	1.3	1.2	0.040	0.027
7	Cover6	3.0	3.1	1.1	1.3	1.2	0.038	0.028
Relative Difference $(a_{MII} - a_{Cover})/a_{MII}$								
1	Cover1	-21%	-11%	0%	0%	0%	-9%	45%
2	Cover2	-7%	14%	0%	0%	43%	23%	34%
3	Cover3	-7%	11%	0%	0%	48%	17%	45%
4	Cover4	-11%	14%	0%	0%	43%	17%	39%
5	Cover5	-7%	14%	0%	0%	43%	15%	39%
6	Cover6	-7%	14%	0%	0%	43%	19%	36%

Notation Legend			
L	Lateral	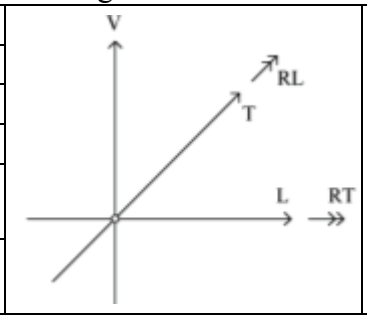	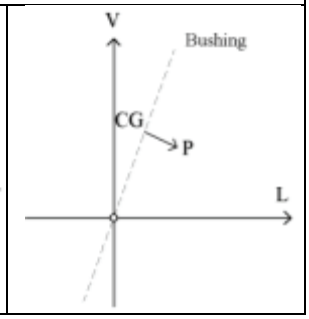
T	Transversal		
V	Vertical		
P	Perpendicular to bushing axis (CG)		
RL	Rotation in the vertical plane (lateral direction)		
RT	Rotation in the vertical plane (transversal direction)		

Table 8-3 and Table 8-4 show that Cover2 and Cover4 models are very efficient at approximating the acceleration response at the bushing's CG for the central and third bushings, with the largest deviation from the full model's response being 14%.

Finally, Table 8-5 shows the peak displacements at the top of the bushings, relative to the ground.

Table 8-5 Comparison of response displacements in separated cover and full transformer models

No	Model	Peak Displacement relative to ground (in)								
		Bushing 1 Top			Bushing 2 Top			Bushing 3 Top		
		L	T	V	L	T	V	L	T	V
1	**MII (Basis)**	**1.66**	**1.17**	**0.42**	**1.96**	**2.80**	**0.29**	**1.27**	**1.33**	**0.29**
2	Cover1	1.82	1.88	0.36	2.51	3.46	0.36	2.06	2.27	0.43
3	Cover2	1.47	1.87	0.30	1.86	2.43	0.21	1.09	0.91	0.24
4	Cover3	2.02	2.22	0.38	2.40	3.80	0.38	1.12	0.92	0.24
5	Cover4	1.50	1.89	0.30	1.86	2.62	0.22	1.09	0.91	0.24
6	Cover5	1.68	2.06	0.33	2.42	3.84	0.37	1.06	0.93	0.24
7	Cover6	1.73	2.03	0.34	2.44	3.51	0.35	1.08	0.91	0.24
Relative Difference $(d_{MII} - d_{Cover})/d_{MII}$										
1	Cover1	-10%	-61%	14%	-28%	-24%	-24%	-62%	-71%	-48%
2	Cover2	11%	-60%	29%	5%	13%	28%	14%	32%	17%
3	Cover3	-22%	-90%	10%	-22%	-36%	-31%	12%	31%	17%
4	Cover4	10%	-62%	29%	5%	6%	24%	14%	32%	17%
5	Cover5	-1%	-76%	21%	-23%	-37%	-28%	17%	30%	17%
6	Cover6	-4%	-74%	19%	-24%	-25%	-21%	15%	32%	17%

Notation Legend			
L	Lateral	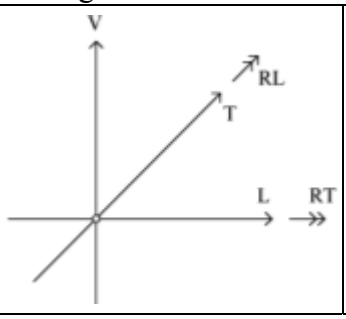	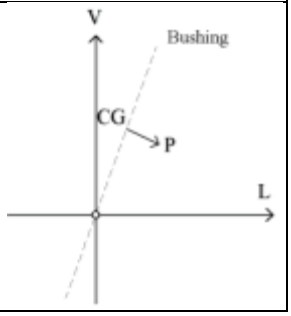
T	Transversal		
V	Vertical		
P	Perpendicular to bushing axis (CG)		
RL	Rotation in the vertical plane (lateral direction)		
RT	Rotation in the vertical plane (transversal direction)		

It can be inferred from the tables above that the models simulating the bushings' response more appropriately in the full model are Cover2 and Cover4. Both models Cover2 and Cover4 provide approximately the same boundary conditions for the three bushings (fixity of the plate). The response acceleration of the second and third bushings is in the range of 15%, compared to the response obtained from the full transformer (model MII). The response of the first bushing is in the range of 20% in the longitudinal direction but in the transversal direction, it deviates from the exact response by approximately 45%.

Regarding the response at the base of the turret, the Cover2 and Cover4 models efficiently approximate the vertical response for the first bushing. For the third and second bushings, no model was successful in achieving a sufficiently good response since discrepancies in the order of 45% were observed.

For the rotations in the longitudinal and the transversal directions, all the models in general deviate appreciably from the exact response for the base of the three turrets. In this case, model Cover4 is the one that matches most closely the rotational response obtained at these points from the analysis of model MII.

In addition to the above, the peak displacements obtained from the analysis of the separated cover models present significant deviations from the exact quantities. Yet overall, the Cover2 and Cover4 models yield much better results than the other models investigated.

These differences are contributed to the neglect of the rotational input from the end and side walls, the cover plate (from the dynamic response of the components directly attached to it) and possibly the insufficiently modeled boundary conditions on the separated cover models. This is supported by the results obtained from the analysis of the models presented in the following section, in which the surge arresters attached to the cover are included.

The time history acceleration responses at the bushing's CG, in Cover 2 and Cover 4 models, have been plotted against the respective responses obtained from full model (MII). Figure 8-5 to Figure 8-10 present the responses in the horizontal directions for the Cover2 and Cover4 models. The differences are in accordance with the tables discussed above. Also compared in each plot is the root mean square (RMS) for the acceleration at the bushing's CG for the full model (MII) and the cover model, which gives a clearer view of the mean acceleration magnitude.

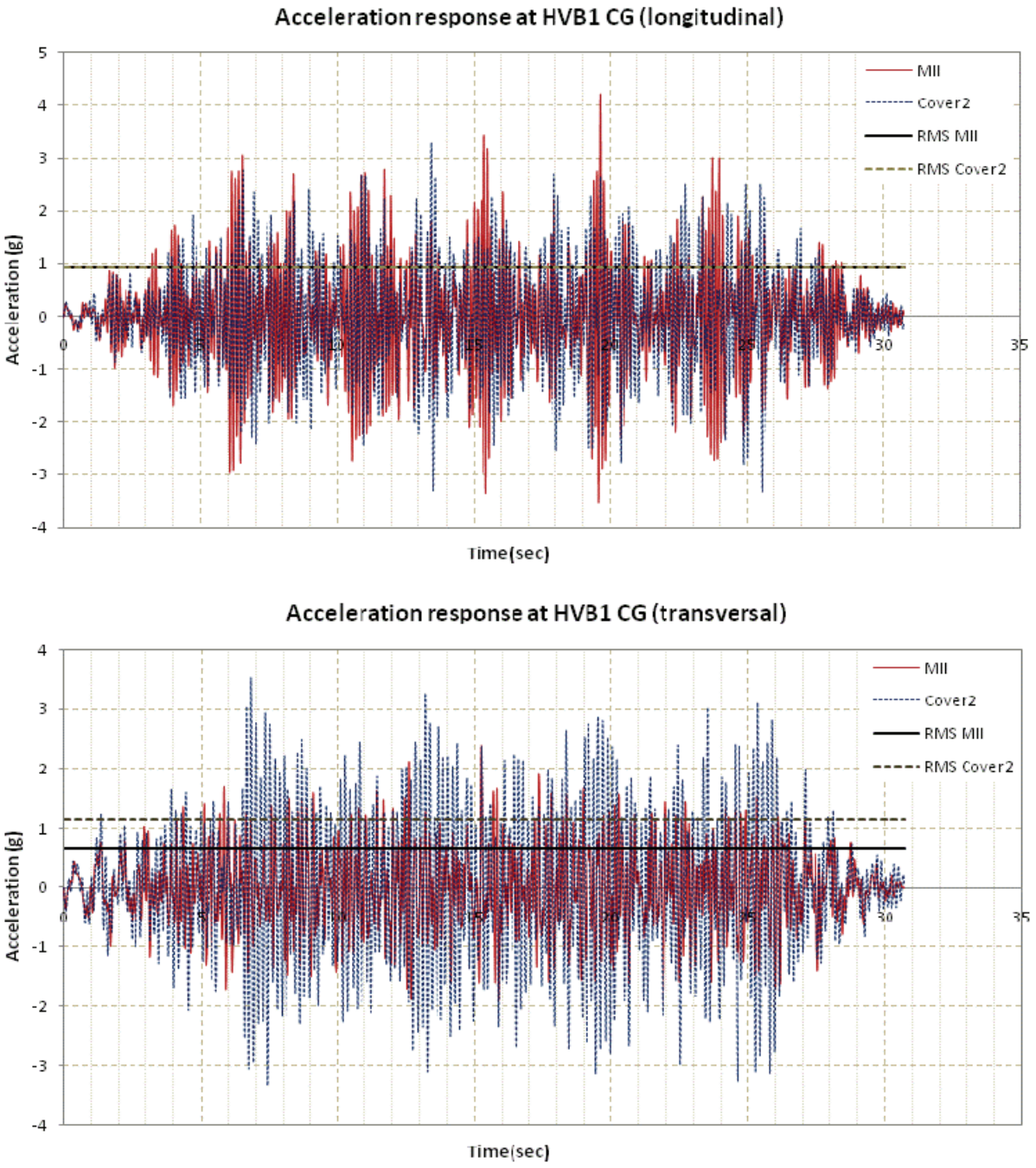

Figure 8-5 Acceleration time history for the Cover2 and MII models (HVB1)

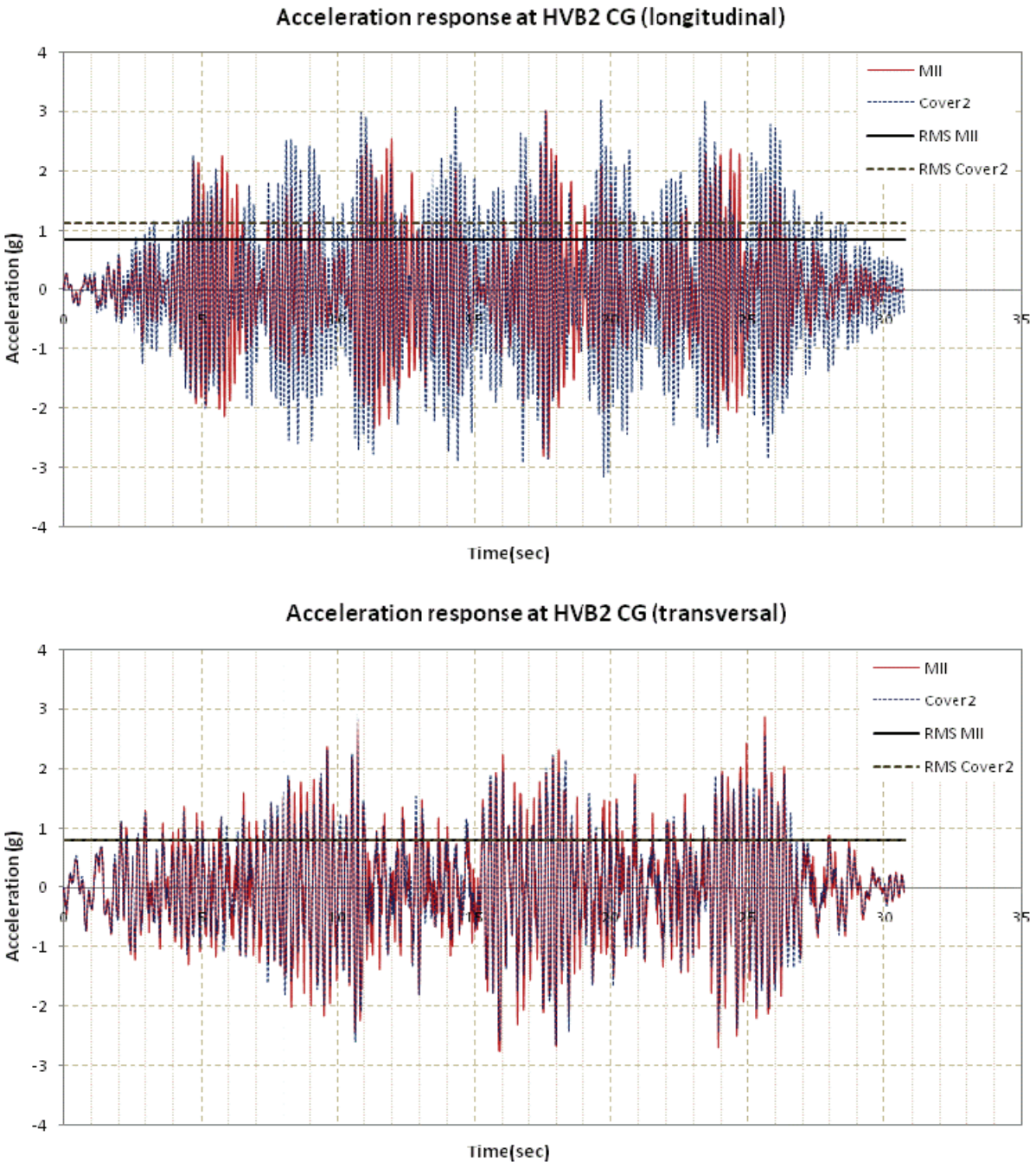

Figure 8-6 Acceleration time history for the Cover2 and MII models (HVB2)

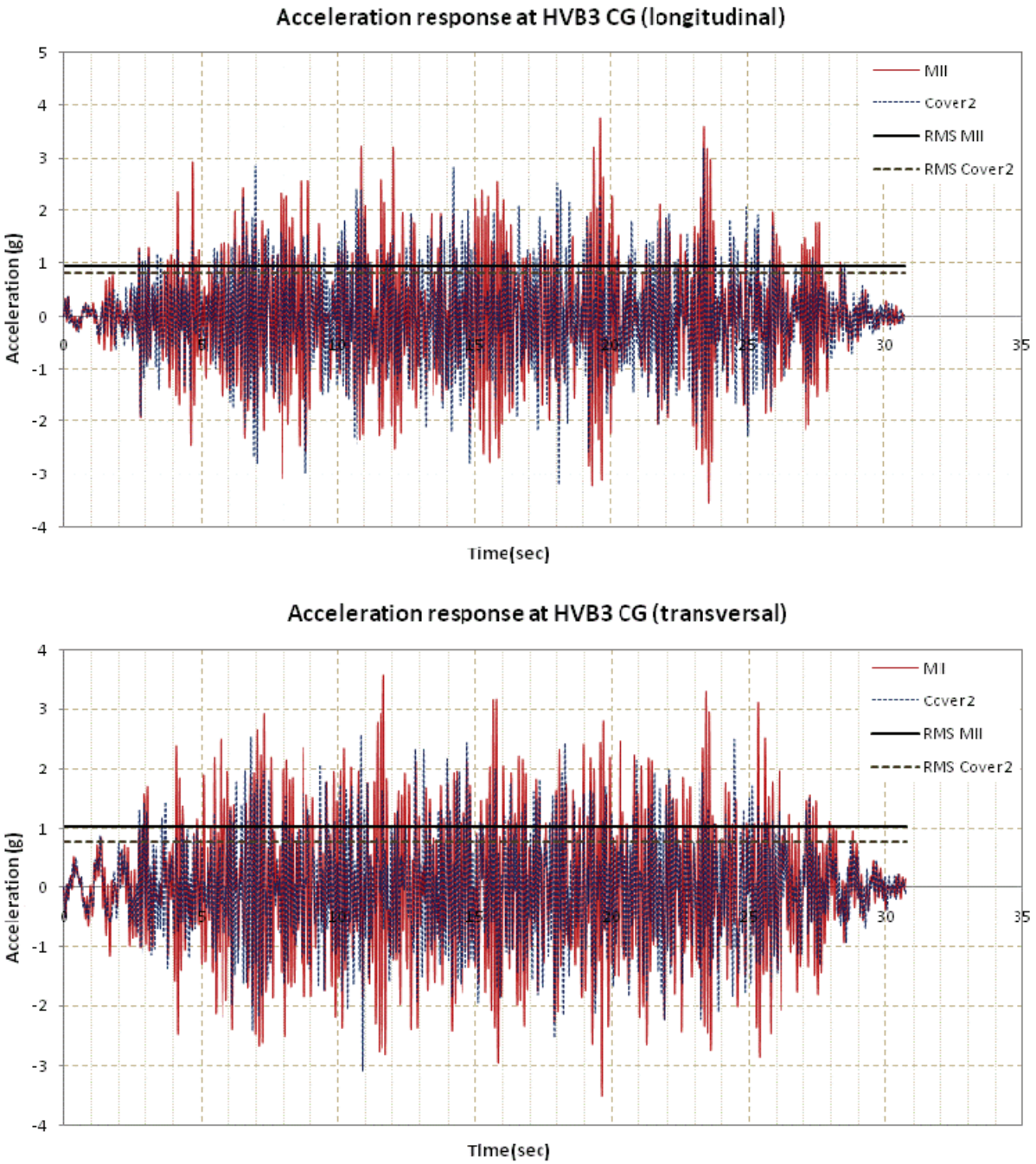

Figure 8-7 Acceleration time history for the Cover2 and MII models (HVB3)

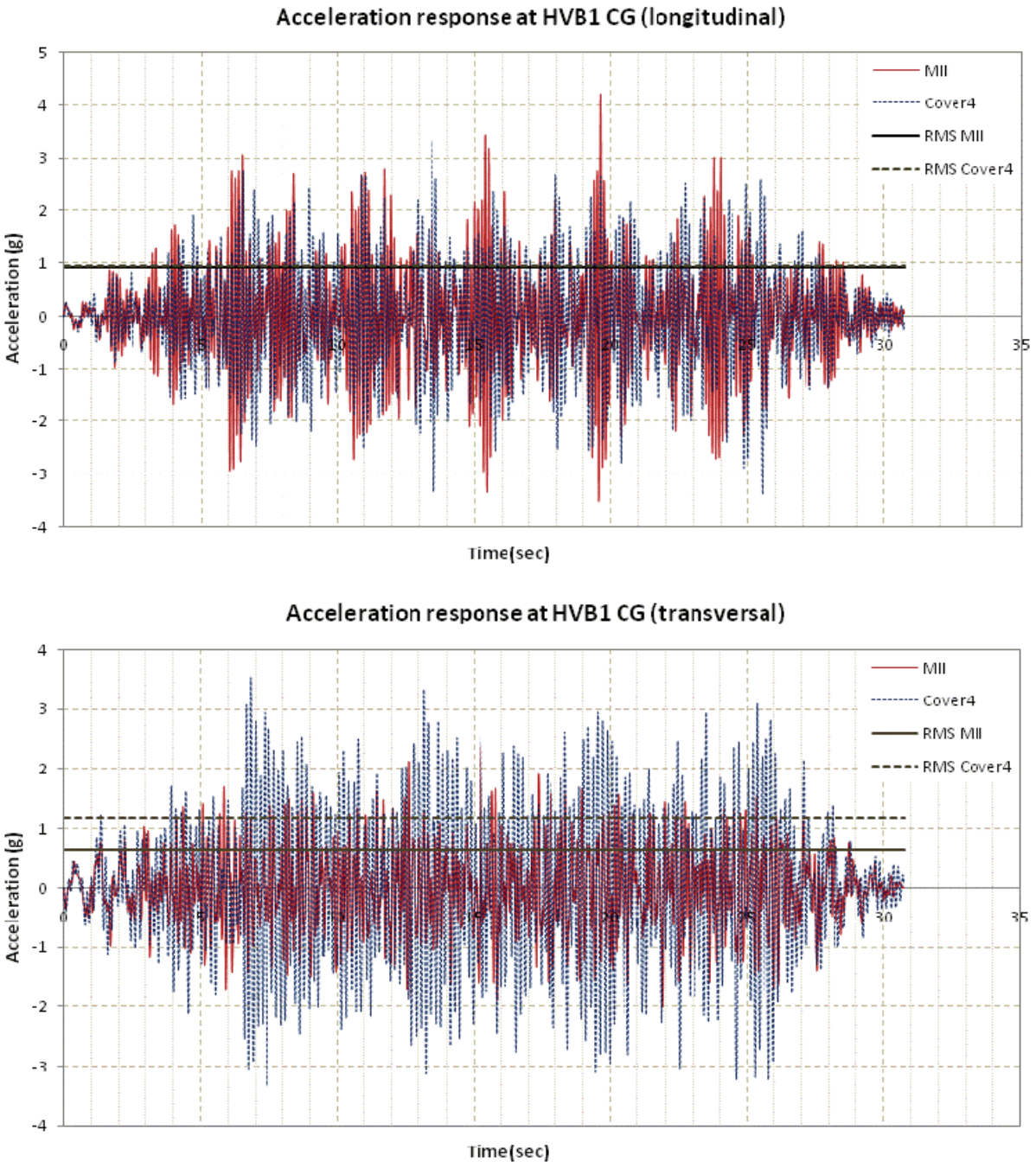

Figure 8-8 Acceleration time history for the Cover4 and MII models (HVB1)

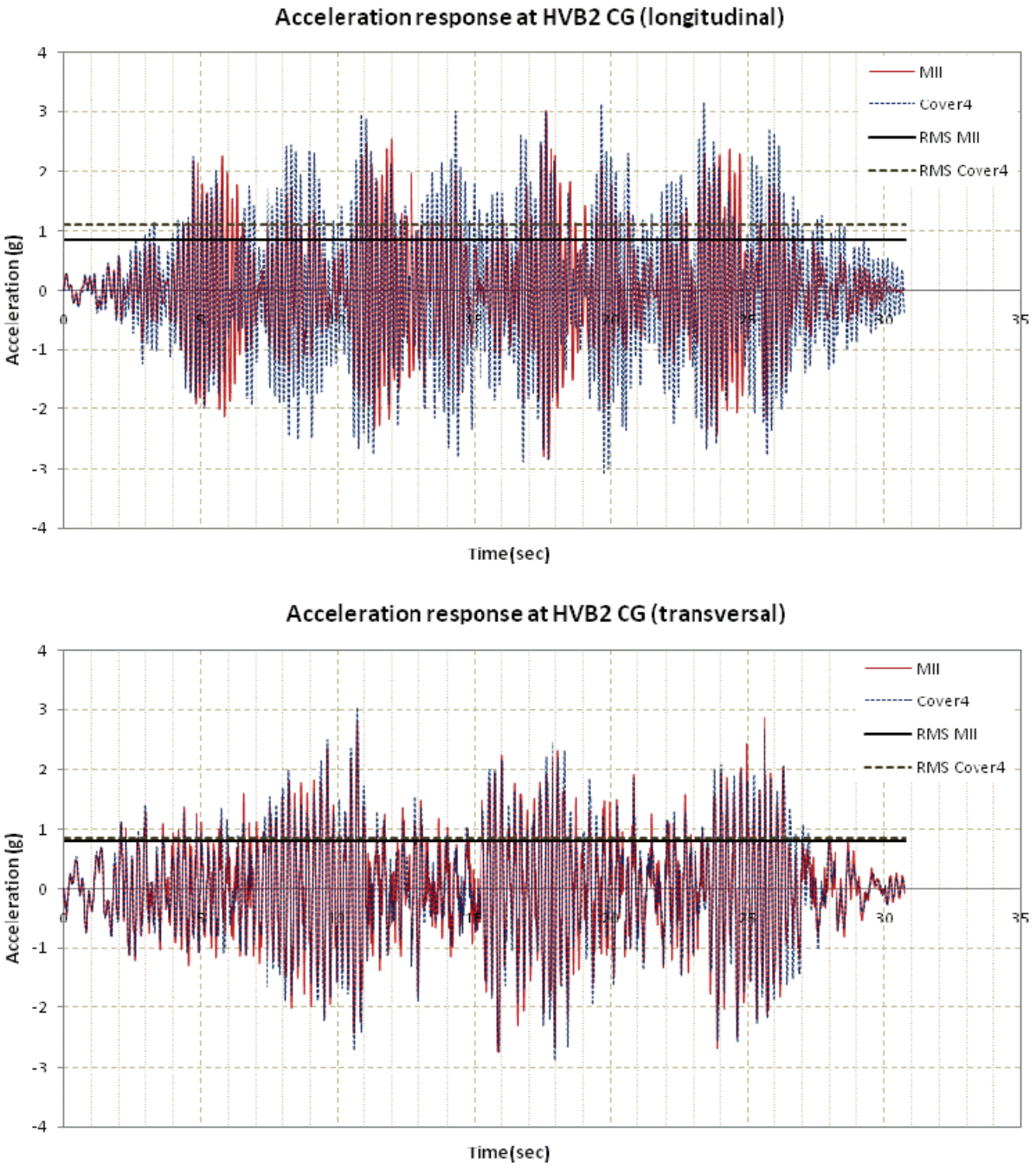

Figure 8-9 Acceleration time history for the Cover4 and MII models (HVB2)

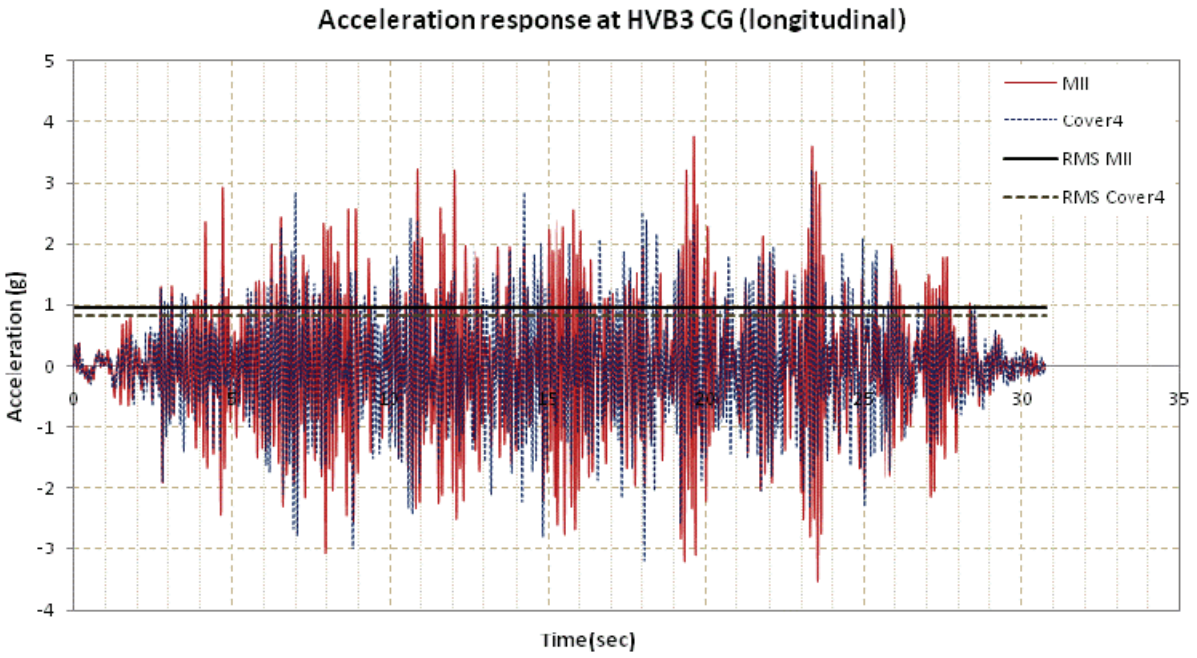

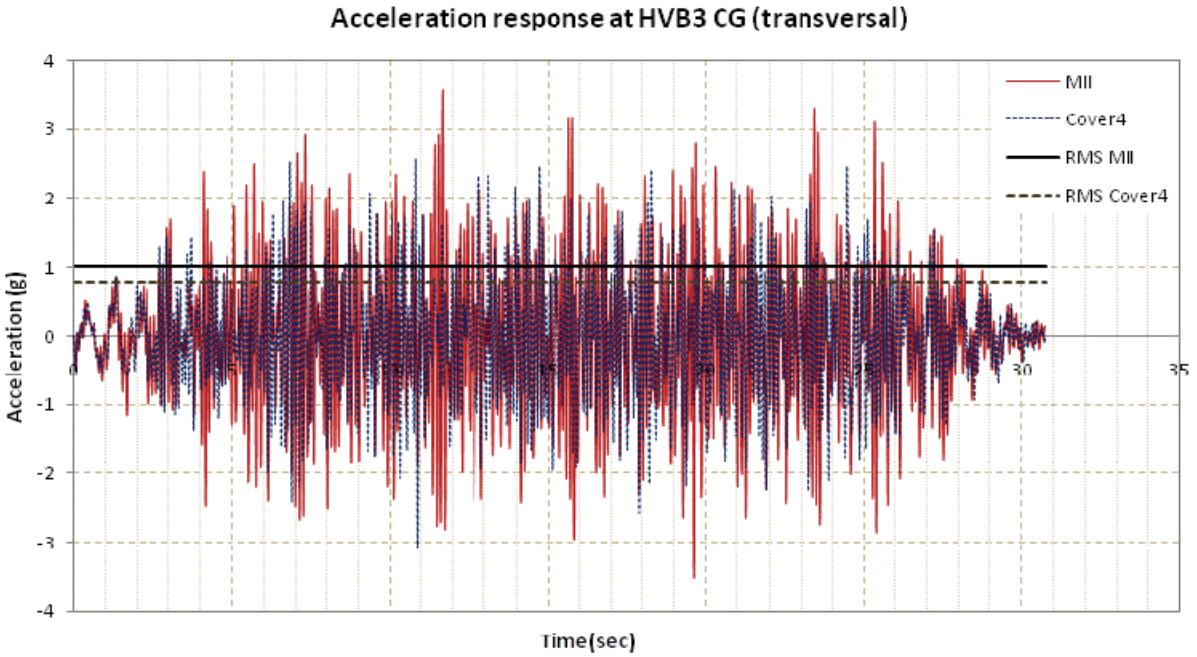

Figure 8-10 Acceleration time history for the Cover4 and MII models (HVB3)

It can be inferred from the comparative plots above, that the acceleration response at the bushings' CG, presents significant differences for the full and the separated cover models. This is naturally expected since the boundary conditions of the plate are modified with respect to the

original model. It should be kept in mind that the input motion for the separated cover models has been taken as the average of the linear responses at the plate corners. These averages were obtained from the full model, while the rotational input as well as the variation of the linear input along the plate boundary has not been accounted for. Inevitably, the excitation at the base of the bushing will be different for the full and for the separated cover models.

The RMS for the bushing's CG acceleration in the full and the separated cover models reveal small differences for the second and third bushings. At the same time the RMS reveals more significant differences for the first bushing's CG acceleration in the transversal direction. Shown in Table 8-6 is the RMS of acceleration at the bushings' CG for all of the separated cover models examined, in comparison with the full model. The results are in agreement with the peak accelerations discussed earlier and shown in the tables above.

Table 8-6 Comparison of RMS of accelerations in separated cover and full transformer models

No	Model	RMS of Acceleration at CG				
		Bushing 1		Bushing 2	Bushing 3	
		P	T	Vector Sum	P	T
1	**MII (Basis)**	**1.0**	**0.6**	**1.2**	**0.9**	**1.0**
2	Cover1	0.8	0.9	1.7	0.9	1.0
3	Cover2	1.0	1.1	1.4	0.7	0.8
4	Cover3	1.0	1.0	1.7	0.8	0.8
5	Cover4	1.0	1.2	1.4	0.8	0.8
6	Cover5	1.0	1.3	1.7	0.8	0.8
7	Cover6	1.0	1.3	1.6	0.8	0.8
Relative Difference $(a_{MII} - a_{Cover})/a_{MII}$						
1	Cover1	19%	-43%	-42%	-10%	4%
2	Cover2	2%	-80%	-17%	13%	23%
3	Cover3	-2%	-64%	-47%	11%	20%
4	Cover4	1%	-85%	-19%	13%	23%
5	Cover5	-2%	-102%	-46%	13%	22%
6	Cover6	-4%	-108%	-33%	13%	23%

8.4 Separated Cover Models Incorporating the High Voltage Surge Arresters

The results for the second set of models are presented in Table 8-7 through Table 8-9 and compared to the MII model results. The results are presented in terms of accelerations at the upper bushing's center of gravity for each bushing and accelerations at each bushing's turret base.

Table 8-7 Comparison of response accelerations in separated cover with SAs and full transformer models (first bushing)

No	Model	Peak Acceleration (g)						
		Bushing 1 CG		Bushing 1 Turret Base				
		P	T	L	T	V	RL	RT
1	**MII (Basis)**	**4.3**	**2.4**	**1.1**	**1.3**	**1.7**	**0.057**	**0.028**
2	Cover1	3.6	3.9	1.1	1.3	2.4	0.039	0.035
3	Cover2	3.8	2.5	1.1	1.3	1.4	0.038	0.045
4	Cover3	3.6	3.0	1.1	1.3	1.7	0.039	0.036
5	Cover4	3.7	2.5	1.1	1.3	1.4	0.038	0.040
6	Cover5	3.0	2.6	1.1	1.3	1.6	0.033	0.039
7	Cover6	3.0	2.6	1.1	1.3	1.5	0.033	0.040
Relative Difference $(a_{MII} - a_{Cover})/a_{MII}$								
1	Cover1	16%	-63%	0%	0%	-41%	32%	-25%
2	Cover2	12%	-4%	0%	0%	18%	33%	-61%
3	Cover3	16%	-25%	0%	0%	0%	32%	-29%
4	Cover4	14%	-4%	0%	0%	18%	33%	-43%
5	Cover5	30%	-8%	0%	0%	6%	42%	-39%
6	Cover6	30%	-8%	0%	0%	12%	42%	-43%

Notation Legend		
L	Lateral	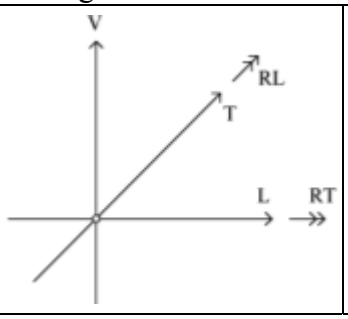
T	Transversal	
V	Vertical	
P	Perpendicular to bushing axis (CG)	
RL	Rotation in the vertical plane (lateral direction)	
RT	Rotation in the vertical plane (transversal direction)	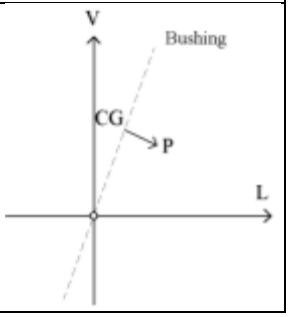

A comparison with the results of Table 8-2 reveals that the response at the CG for the first bushing is better approximated when the components attached to the cover plate in the full model are included in the separated cover models. In particular, the maximum deviation from the exact response is 14% for the separated models with the attachments, while for the models without the attachments the maximum deviation is 46%.

Table 8-8 Comparison of response accelerations in separated cover with SAs and full transformer models (central bushing)

No	Model	Peak Acceleration (g)					
		Bushing 2 CG	Bushing 2 Turret Base				
		Vector Sum	L	T	V	RL	RT
1	**MII (Basis)**	**3.6**	**1.1**	**1.4**	**2.1**	**0.039**	**0.066**
2	Cover1	5.3	1.1	1.3	3.1	0.036	0.034
3	Cover2	3.6	1.1	1.3	1.6	0.035	0.045
4	Cover3	4.9	1.1	1.3	3.0	0.038	0.044
5	Cover4	3.6	1.1	1.3	1.5	0.035	0.061
6	Cover5	4.9	1.1	1.3	2.9	0.038	0.040
7	Cover6	4.5	1.1	1.3	2.6	0.036	0.036
Relative Difference $(a_{MII} - a_{Cover})/a_{MII}$							
1	Cover1	-47%	0%	7%	-48%	8%	48%
2	Cover2	0%	0%	7%	24%	10%	32%
3	Cover3	-36%	0%	7%	-43%	3%	33%
4	Cover4	0%	0%	7%	29%	10%	8%
5	Cover5	-36%	0%	7%	-38%	3%	39%
6	Cover6	-25%	0%	7%	-24%	8%	45%

Notation Legend			
L	Lateral	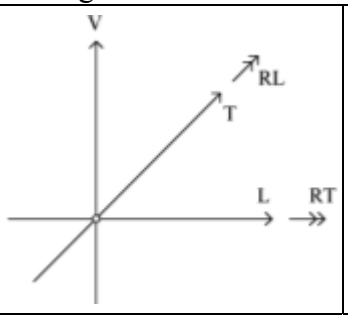	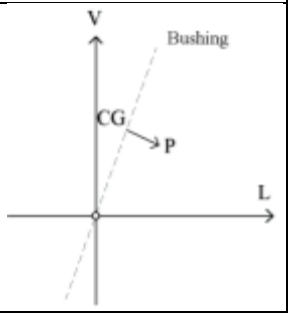
T	Transversal		
V	Vertical		
P	Perpendicular to bushing axis (CG)		
RL	Rotation in the vertical plane (lateral direction)		
RT	Rotation in the vertical plane (transversal direction)		

Table 8-9 Comparison of response accelerations in separated cover with SAs and full transformer models (third bushing)

No	Model	Peak Acceleration (g)						
		Bushing 3 CG		Bushing 3 Turret Base				
		P	T	L	T	V	RL	RT
1	**MII (Basis)**	**2.8**	**3.6**	**1.1**	**1.3**	**2.1**	**0.047**	**0.044**
2	Cover1	3.0	3.2	1.1	1.3	1.7	0.045	0.032
3	Cover2	2.9	3.7	1.1	1.3	1.3	0.034	0.024
4	Cover3	3.1	3.2	1.1	1.3	1.3	0.037	0.025
5	Cover4	2.9	3.7	1.1	1.3	1.3	0.035	0.024
6	Cover5	3.0	2.9	1.1	1.3	1.3	0.038	0.029
7	Cover6	3.1	2.8	1.1	1.3	1.3	0.039	0.027
Relative Difference $(a_{MII} - a_{Cover})/a_{MII}$								
1	Cover1	-7%	11%	0%	0%	19%	4%	27%
2	Cover2	-4%	-3%	0%	0%	38%	28%	45%
3	Cover3	-11%	11%	0%	0%	38%	21%	43%
4	Cover4	-4%	-3%	0%	0%	38%	26%	45%
5	Cover5	-7%	19%	0%	0%	38%	19%	34%
6	Cover6	-11%	22%	0%	0%	38%	17%	39%

Notation Legend			
L	Lateral	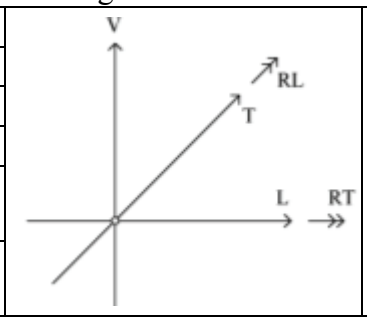	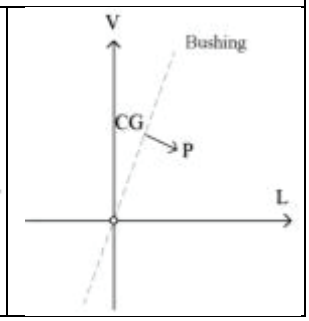
T	Transversal		
V	Vertical		
P	Perpendicular to bushing axis (CG)		
RL	Rotation in the vertical plane (lateral direction)		
RT	Rotation in the vertical plane (transversal direction)		

After including the attachments in the separated cover models, Cover2 and Cover4 models are still the most efficient at approximating the acceleration response at the bushings' CG for the central and third bushings. The largest deviation from the full model response was 4%, compared to the 14% of the models without the attachments.

Table 8-10 presents the peak displacements at the top of the bushings and at the bottom of the central bushing, relative to the ground.

Table 8-10 Comparison of response displacements in separated cover with SAs and full transformer models

No	Model	Peak Displacement relative to ground (in)								
		Bushing 1 Top			Bushing 2 Top			Bushing 3 Top		
		L	T	V	L	T	V	L	T	V
1	**MII (Basis)**	**1.66**	**1.17**	**0.42**	**1.96**	**2.80**	**0.29**	**1.27**	**1.33**	**0.29**
2	Cover1	2.75	2.59	0.52	2.37	4.15	0.45	2.08	2.24	0.35
3	Cover2	1.46	1.48	0.31	1.69	2.67	0.23	1.13	1.25	0.24
4	Cover3	1.79	1.73	0.36	2.39	3.74	0.37	1.40	1.17	0.28
5	Cover4	1.40	1.46	0.30	1.73	2.77	0.24	1.12	1.28	0.24
6	Cover5	1.16	1.35	0.29	2.33	3.70	0.37	1.18	0.95	0.24
7	Cover6	1.17	1.41	0.28	2.33	3.46	0.35	1.17	0.97	0.24
Relative Difference $(d_{MII} - d_{Cover})/d_{MII}$										
1	Cover1	-66%	-121%	-24%	-21%	-48%	-55%	-64%	-68%	-21%
2	Cover2	12%	-26%	26%	14%	5%	21%	11%	6%	17%
3	Cover3	-8%	-48%	14%	-22%	-34%	-28%	-10%	12%	3%
4	Cover4	16%	-25%	29%	12%	1%	17%	12%	4%	17%
5	Cover5	30%	-15%	31%	-19%	-32%	-28%	7%	29%	17%
6	Cover6	30%	-21%	33%	-19%	-24%	-21%	8%	27%	17%

Notation Legend		
L	Lateral	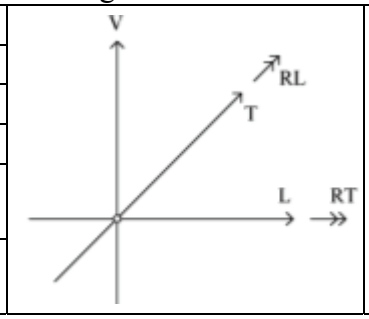 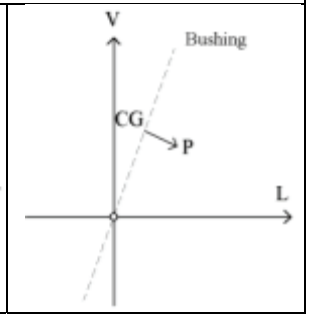
T	Transversal	
V	Vertical	
P	Perpendicular to bushing axis (CG)	
RL	Rotation in the vertical plane (lateral direction)	
RT	Rotation in the vertical plane (transversal direction)	

Similar conclusions can be drawn for the models including the surge arresters respective to the models with no attachments. It can be inferred that the models more appropriately simulating the bushings' response in the full model are Cover2 and Cover4. These two models provide approximately the same boundary conditions for the three bushings (fixity of the plate). The response acceleration of the first bushing is in the range of 14% and the response of the third bushing is in the range of 4%, when compared to the full transformer model (model MII). The response of the second bushing for Cover2 and Cover4 is exact.

Concerning the vertical response at the base of the turret, the Cover2 and Cover4 models deviate from the exact response by approximately 38%. Other cover models more closely simulate this response component such as model Cover3 which, for the turret base of the first bushing yields the exact result. For these models, the matching of the acceleration response at the bushing CG is not as high-quality.

For the rotations in the longitudinal and the transverse directions, all the models in general deviated appreciably from the exact response at the base of the turrets.

The peak displacements obtained from the analysis of the separated cover models present some discrepancy from the exact solution. Yet, the Cover2 and Cover4 models overall yielded much better results in comparison to the other models investigated. The largest deviation using the Cover2 and Cover4 models were in the order of 29%. It is noted that for the models without the attachments, the maximum relative difference was in the order of 60%.

The time history acceleration responses of the bushings, in models Cover 2 and Cover 4, have been plotted against the time histories obtained from the dynamic analysis of model MII. Figures 8-11 through Figure 8-16 present the dynamic analysis of model MII in the horizontal directions. Also compared in each plot is the root mean square (RMS) for the acceleration at the

bushings' CG for the full model (MII) and the cover model, which gives a more clear view of the mean acceleration magnitude.

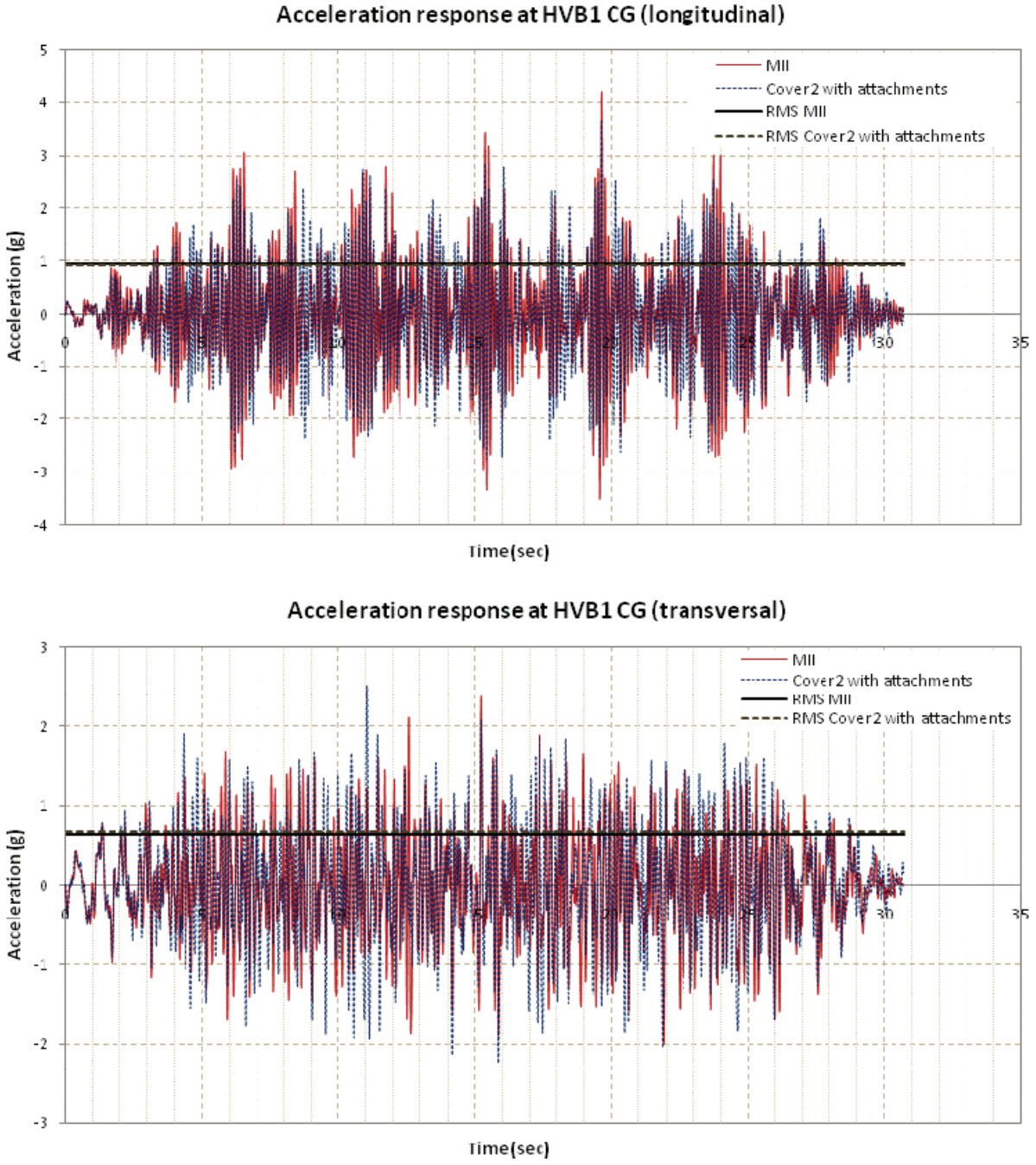

Figure 8-11 Acceleration time history for the Cover2 with SAs and MII models (HVB1)

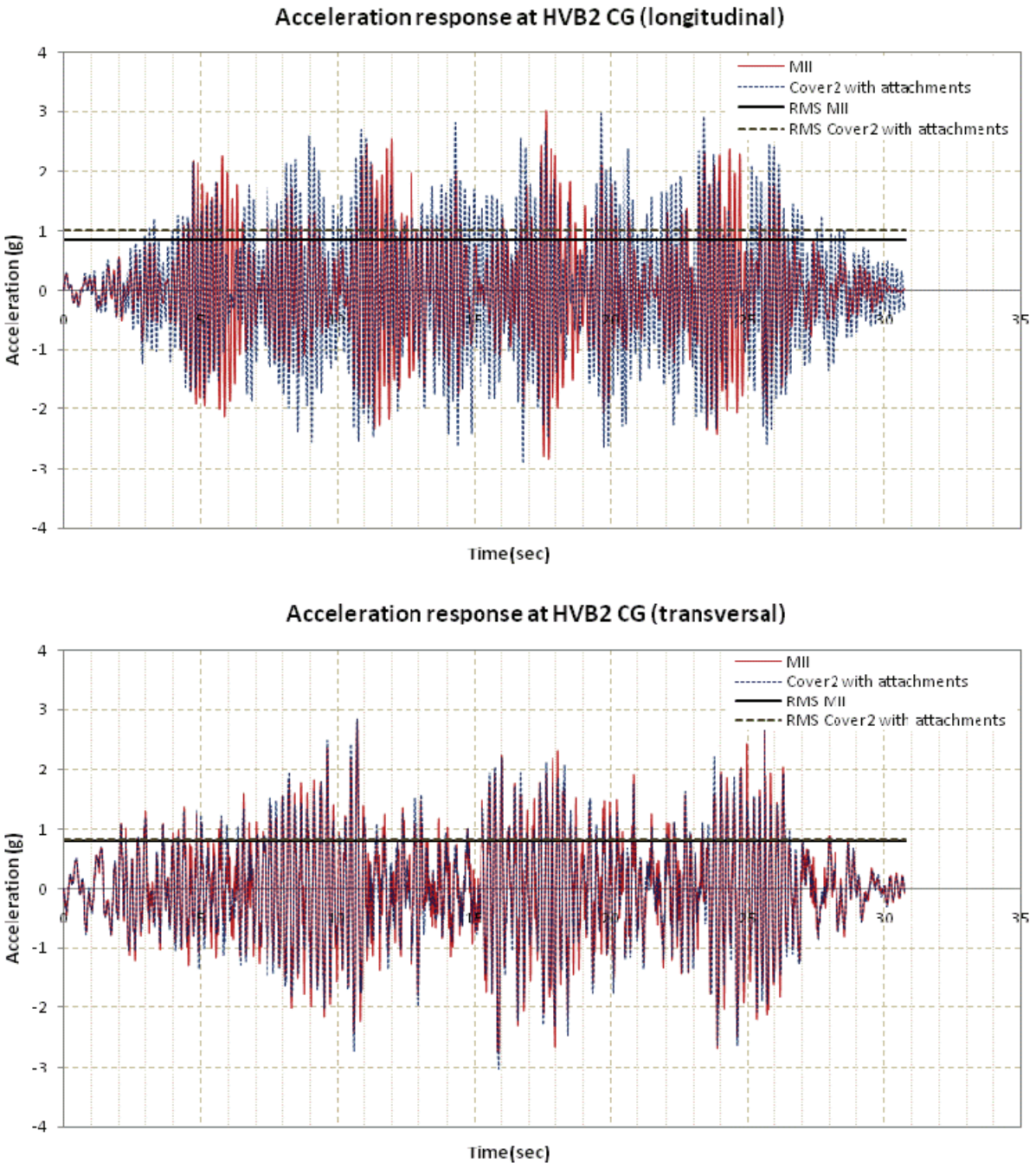

Figure 8-12 Acceleration time history for the Cover2 with SAs and MII models (HVB2)

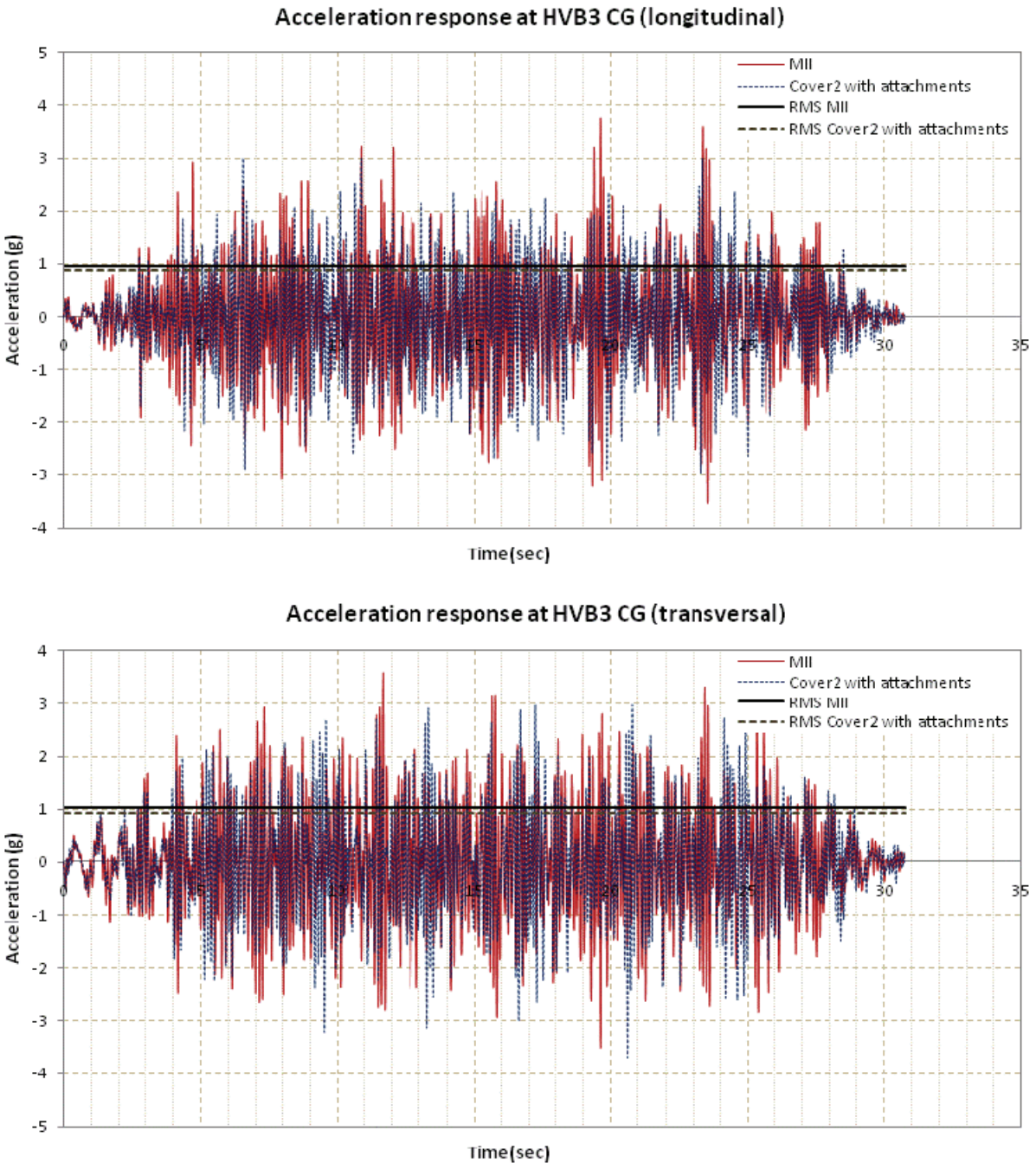

Figure 8-13 Acceleration time history for the Cover2 with SAs and MII models (HVB3)

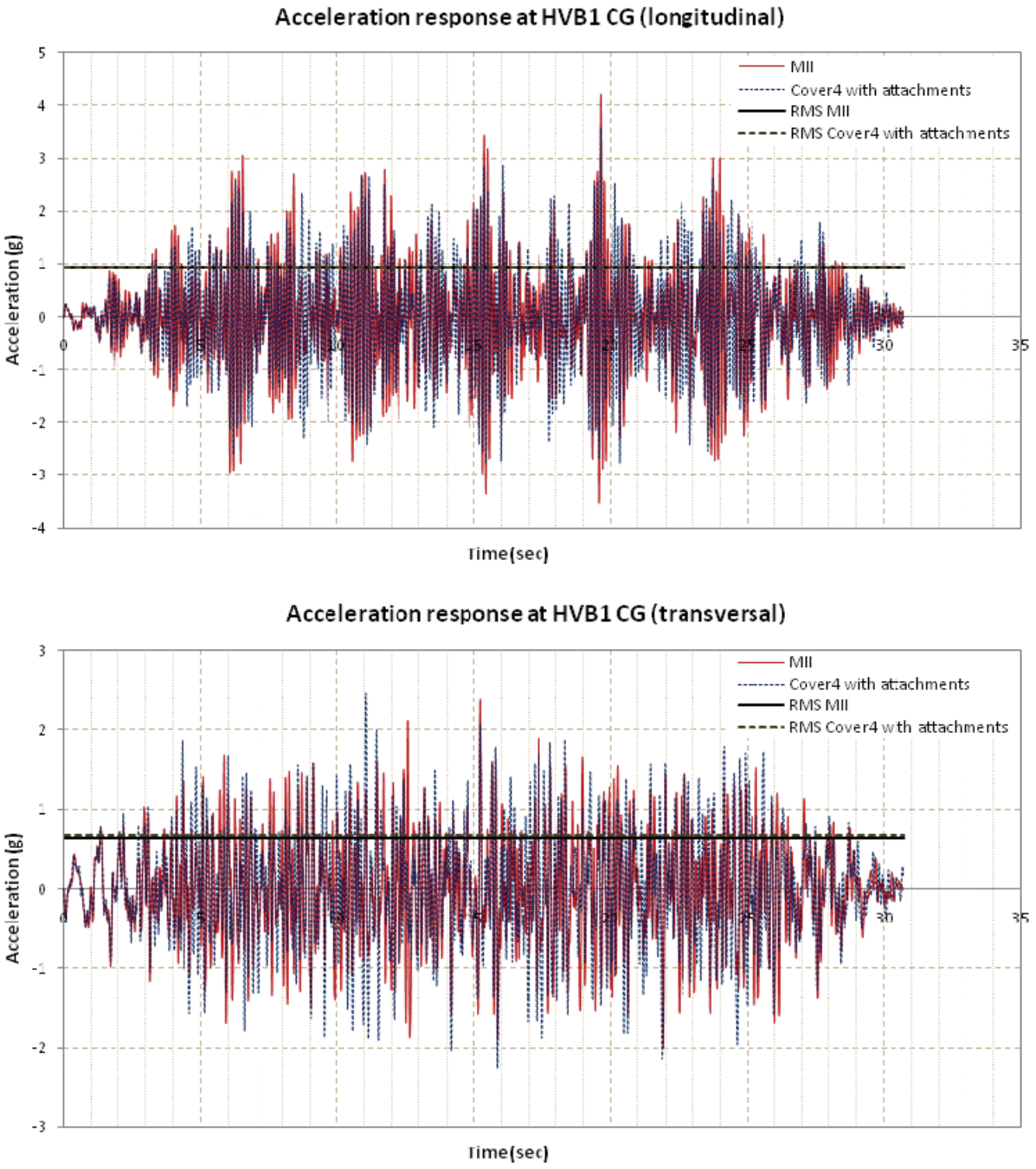

Figure 8-14 Acceleration time history for the Cover4 with SAs and MII models (HVB1)

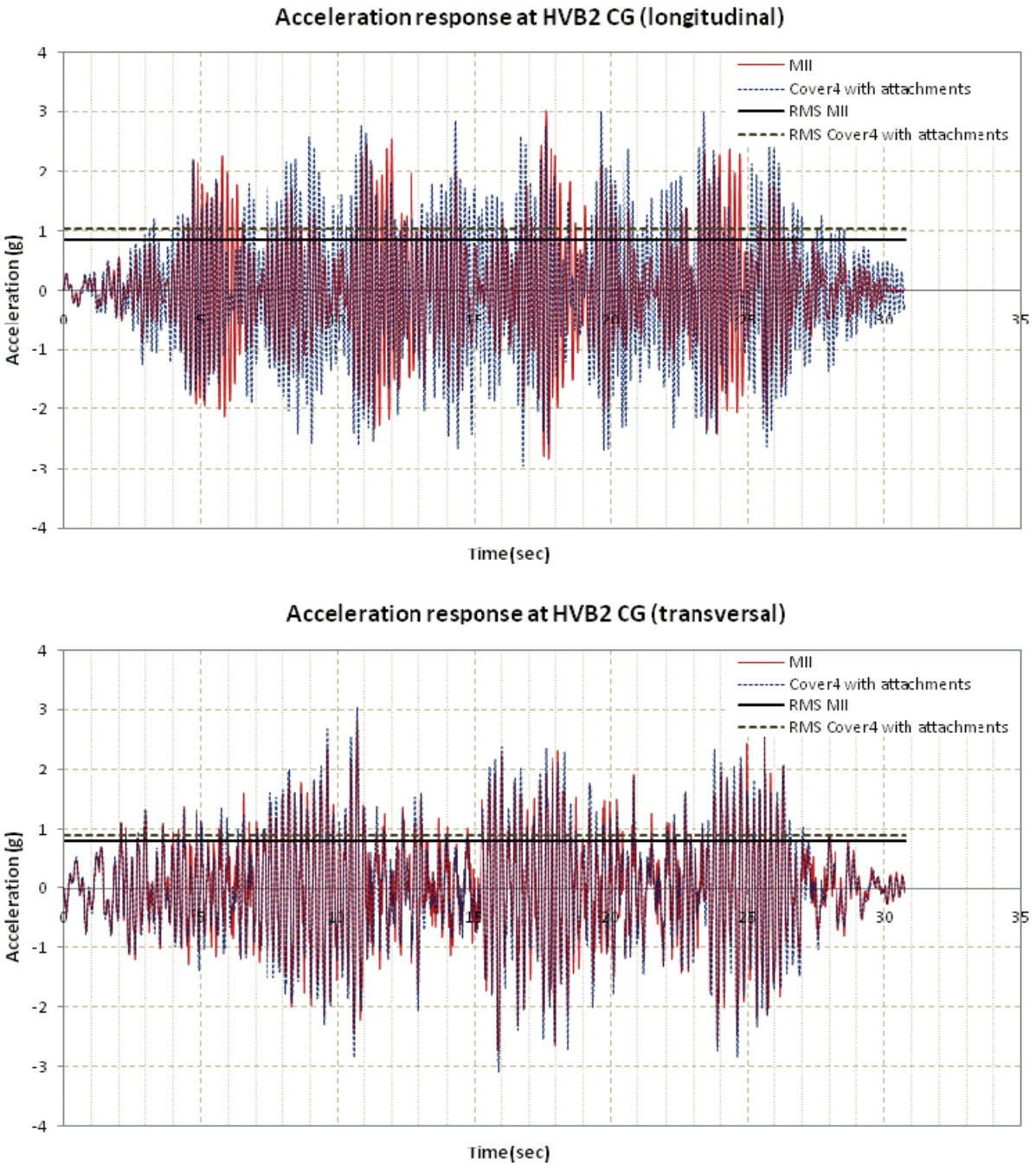

Figure 8-15 Acceleration time history for the Cover4 with SAs and MII models (HVB2)

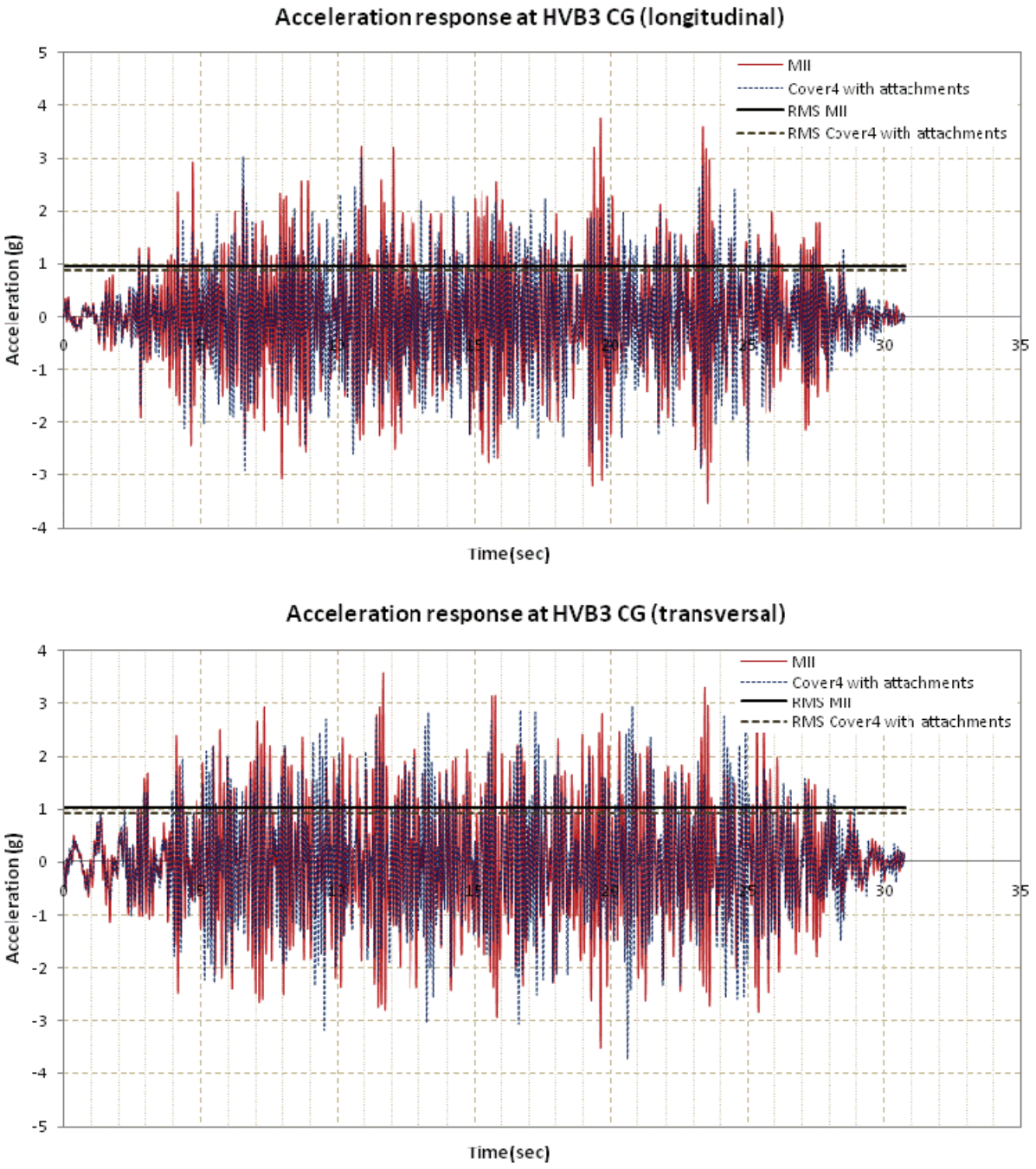

Figure 8-16 Acceleration time history for the Cover4 with SAs and MII models (HVB3)

It can be inferred, from the comparative plots above, that the acceleration response at the bushings' CG present significant differences for the full and the separated cover models. This is naturally expected since the boundary conditions of the plate are modified with respect to the

original model. It should be kept in mind that the input motion for the separated cover models has been taken as the average of the linear responses at the plate corners obtained from the full model. While, the rotational input as well as the variation of the linear input along the plate boundary has not been accounted for. Inevitably, the excitation at the base of the bushing will be different for the full model and separated cover model.

The RMS for the bushing's CG acceleration in the full and the separated cover models, presented in Table 8-11, reveals that the discrepancies from the exact response for the Cover2 and Cover4 models are relatively small, with the maximum relative difference being 16%. For comparison, the maximum relative difference for the respective models without the attachments presented in Table 8-6 was 80%.

Table 8-11 Comparison of RMS of accelerations in separated cover with SAs and full transformer models

No	Model	RMS of Acceleration at CG				
		Bushing 1		Bushing 2	Bushing 3	
		P	T	Vector Sum	P	T
1	**MII (Basis)**	**1.0**	**1.1**	**1.8**	**0.9**	**0.9**
2	Cover1	0.9	0.7	1.3	0.8	0.9
3	Cover2	0.9	0.8	1.7	0.8	0.9
4	Cover3	1.0	0.7	1.4	0.8	0.9
5	Cover4	0.9	0.7	1.7	0.8	0.9
6	Cover5	0.9	0.7	1.6	0.8	0.9
7	Cover6	1.0	1.1	1.8	0.9	0.9
Relative Difference $(a_{MII} - a_{Cover})/a_{MII}$						
1	Cover1	-7%	-80%	-51%	-2%	17%
2	Cover2	2%	-7%	-12%	7%	10%
3	Cover3	4%	-27%	-48%	9%	9%
4	Cover4	1%	-6%	-16%	8%	10%
5	Cover5	4%	-10%	-46%	7%	15%
6	Cover6	4%	-10%	-33%	6%	15%

8.5 Remarks on Simplified Modeling

Based on the results obtained from the analyses performed, it is suggested that the Cover2 and Cover4 models are the ones that match most closely the full transformer model response. In terms of boundary conditions, these are the cover models which are fully fixed across the side of the cover where the bushings are mounted.

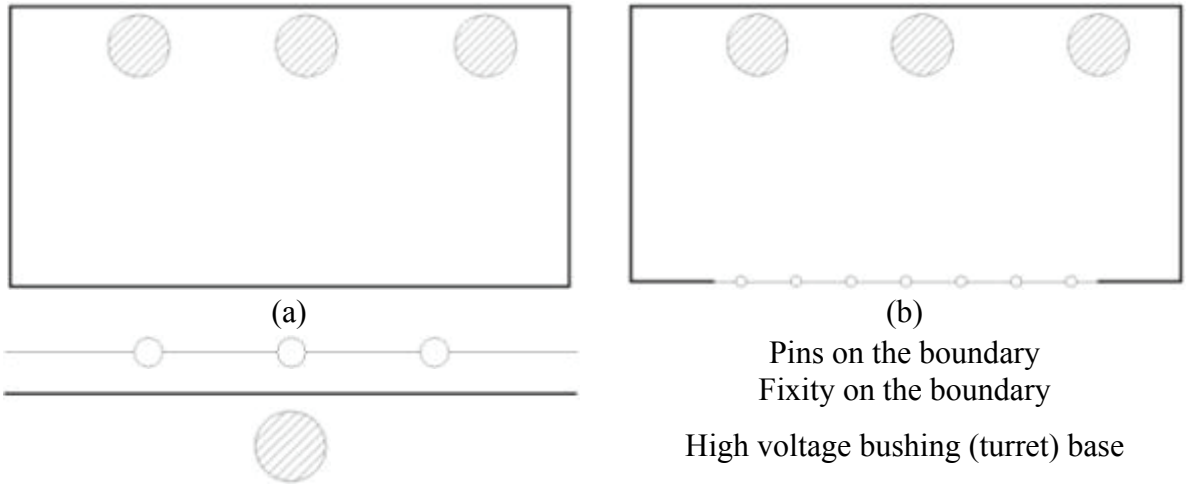

Figure 8-17 Boundary conditions of Cover2 (a) and Cover4 (b) models (repeated from Figure 8-3)

Comparing the Cover2 and Cover4 models, for the case where no attachments were used and the case where the high voltage surge arresters were incorporated in the models, one can infer that the response obtained from the second case was essentially closer to the full model response. This inference can be made as far as the accelerations at the bushing's CG are concerned. The comparison between the best models for the two cases investigated, in terms of accelerations and displacements are presented in Table 8-12 through Table 8-14.

Table 8-12 Comparison of response accelerations between the Cover2 and Cover4 with and without SAs and full transformer models (first bushing)

Model	Peak Acceleration (g)						
	Bushing 1 CG		Bushing 1 Turret Base				
	P	T	L	T	V	RL	RT
MII (Basis)	**4.3**	**2.4**	**1.1**	**1.3**	**1.7**	**0.057**	**0.028**
Cover2 (no SAs)	3.4	3.5	1.1	1.3	1.7	0.045	0.038
Cover4 (no SAs)	3.4	3.5	1.1	1.3	1.8	0.045	0.030
Cover2 (with SAs)	3.8	2.5	1.1	1.3	1.4	0.038	0.045
Cover4 (with SAs)	3.7	2.5	1.1	1.3	1.4	0.038	0.040
Relative Difference $(a_{MII} - a_{Cover})/a_{MII}$							
Cover2 (no SAs)	21%	-46%	0%	0%	0%	21%	-36%
Cover4 (no SAs)	21%	-46%	0%	0%	-6%	21%	-7%
Cover2 (with SAs)	12%	-4%	0%	0%	18%	33%	-61%
Cover4 (with SAs)	14%	-4%	0%	0%	18%	33%	-43%

Notation Legend			
L	Lateral	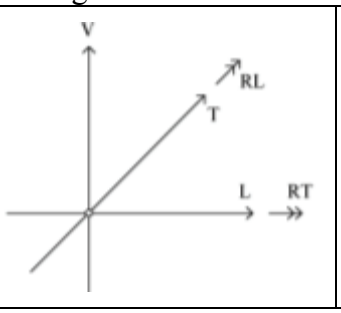	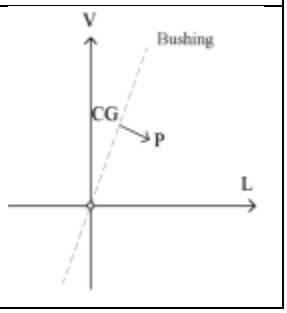
T	Transversal		
V	Vertical		
P	Perpendicular to bushing axis (CG)		
RL	Rotation in the vertical plane (lateral direction)		
RT	Rotation in the vertical plane (transversal direction)		

Table 8-13 Comparison of response accelerations between the Cover2 and Cover4 with and without SAs and full transformer models (central bushing)

Model	Peak Acceleration (g)					
	Bushing 2 CG	Bushing 2 Turret Base				
	Vector Sum	L	T	V	RL	RT
MII (Basis)	**3.6**	**1.1**	**1.4**	**2.1**	**0.039**	**0.066**
Cover2 (no SAs)	3.7	1.1	1.3	1.6	0.039	0.049
Cover4 (no SAs)	3.8	1.1	1.3	1.6	0.039	0.059
Cover2 (with SAs)	3.6	1.1	1.3	1.6	0.035	0.045
Cover4 (with SAs)	3.6	1.1	1.3	1.5	0.035	0.061
Relative Difference $(a_{MII} - a_{Cover})/a_{MII}$						
Cover2 (no SAs)	-3%	0%	7%	24%	0%	26%
Cover4 (no SAs)	-6%	0%	7%	24%	0%	11%
Cover2 (with SAs)	0%	0%	7%	24%	10%	32%
Cover4 (with SAs)	0%	0%	7%	29%	10%	8%

Notation Legend		
L	Lateral	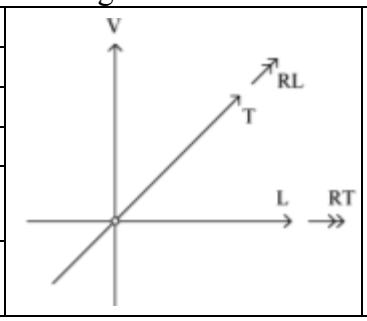
T	Transversal	
V	Vertical	
P	Perpendicular to bushing axis (CG)	
RL	Rotation in the vertical plane (lateral direction)	
RT	Rotation in the vertical plane (transversal direction)	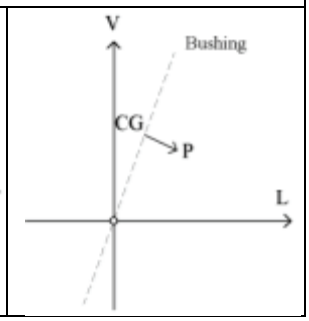

Table 8-14 Comparison of response accelerations between the Cover2 and Cover4 with and without SAs and full transformer models (third bushing)

Model	Peak Acceleration (g)						
	Bushing 3 CG		Bushing 3 Turret Base				
	P	T	L	T	V	RL	RT
MII (Basis)	**2.8**	**3.6**	**1.1**	**1.3**	**2.1**	**0.047**	**0.044**
Cover2 (no SAs)	3.0	3.1	1.1	1.3	1.2	0.036	0.029
Cover4 (no SAs)	3.1	3.1	1.1	1.3	1.2	0.039	0.027
Cover2 (with SAs)	2.9	3.7	1.1	1.3	1.3	0.034	0.024
Cover4 (with SAs)	2.9	3.7	1.1	1.3	1.3	0.035	0.024
Relative Difference $(a_{MII} - a_{Cover})/a_{MII}$							
Cover2 (no SAs)	-7%	14%	0%	0%	43%	23%	34%
Cover4 (no SAs)	-11%	14%	0%	0%	43%	17%	39%
Cover2 (with SAs)	-4%	-3%	0%	0%	38%	28%	45%
Cover4 (with SAs)	-4%	-3%	0%	0%	38%	26%	45%

Notation Legend	
L	Lateral
T	Transversal
V	Vertical
P	Perpendicular to bushing axis (CG)
RL	Rotation in the vertical plane (lateral direction)
RT	Rotation in the vertical plane (transversal direction)

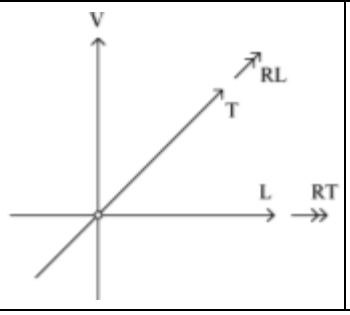

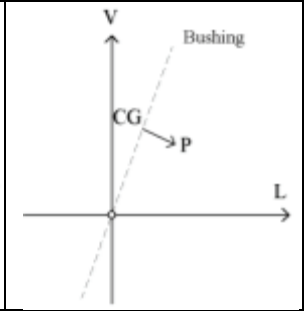

Furthermore, Table 8-15 shows the peak displacements at the top of the bushings and at the bottom of the central bushing, relative to the ground.

Table 8-15 Comparison of response displacements between the Cover2 and Cover4 with and without SAs and full transformer models

Model	Peak Displacement relative to ground (in)								
	Bushing 1 Top			Bushing 2 Top			Bushing 3 Top		
	L	T	V	L	T	V	L	T	V
MII (Basis)	**1.66**	**1.17**	**0.42**	**1.96**	**2.80**	**0.29**	**1.27**	**1.33**	**0.29**
Cover2 (no SAs)	1.47	1.87	0.30	1.86	2.43	0.21	1.09	0.91	0.24
Cover4 (no SAs)	1.50	1.89	0.30	1.86	2.62	0.22	1.09	0.91	0.24
Cover2 (with SAs)	1.46	1.48	0.31	1.69	2.67	0.23	1.13	1.25	0.24
Cover4 (with SAs)	1.40	1.46	0.30	1.73	2.77	0.24	1.12	1.28	0.24
Relative Difference $(d_{MII} - d_{Cover})/d_{MII}$									
Cover2 (no SAs)	11%	-60%	29%	5%	13%	28%	14%	32%	17%
Cover4 (no SAs)	10%	-62%	29%	5%	6%	24%	14%	32%	17%
Cover2 (with SAs)	12%	-26%	26%	14%	5%	21%	11%	6%	17%
Cover4 (with SAs)	16%	-25%	29%	12%	1%	17%	12%	4%	17%

Notation Legend			
L	Lateral	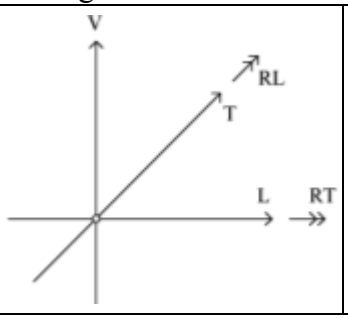	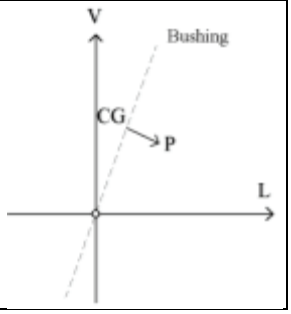
T	Transversal		
V	Vertical		
P	Perpendicular to bushing axis (CG)		
RL	Rotation in the vertical plane (lateral direction)		
RT	Rotation in the vertical plane (transversal direction)		

SECTION 9

CONCLUDING REMARKS

This study deals with the modeling of existing transformers exploring modeling variations and structural modifications that affect the response of bushings mounted on the transformer covers. A model was developed to identify the transformer's dynamic characteristics and the significant interactions between various components and the high voltage bushings. A finite element model originally modeled for static stress analyses was modified to allow dynamic analyses and it was subjected to detailed analyses using dynamic excitations in order to study to the effects of detailed modeling and the interactions of components using time and frequency domain techniques A number of structural modifications were introduced to the transformer model, with the intention of observing the sensitivity of bushing responses and when mounted on different transformer models. Each model was investigated using modal and spectral analyses, using random and spectrum compatible (IEEE 693-2005) ground motion. The response was measured at the bushings, the corners of the cover plate and the base of the turrets for the structurally modified models. Furthermore, the spectra at the corners of the cover plate and at the base of the turrets were obtained and associated with the bushings' response. The transformer was also analyzed for vacuum pressure, to determine the most adverse displacement condition for the interconnected cables. Finally, simplified models were explored in which the cover plate, along with its stiffeners and the bushings, was separated from the transformer. Various boundary conditions were examined in an effort to determine the degrees of approximation of bushings' response in respect to the response obtained from the full transformer model.

Some comments and remarks related to this study are summarized as follows:

(a) Modeling of transformer for dynamic analysis:

1. The modeling of the bushing connection to the turret and to the transformer cover seems to have dominant influence. The fine annular mesh around the turret base and the provision for the transition mesh were found to represent adequately the bushing. This was visible through the modal analysis of the modified model, contrary to the original model in which the coarse mesh did not allow for the turret to move in all possible directions.
2. The mesh size of the cover plate portion, located at a distance from the bushings, showed that the bushings' response was not sensitive to the variations.
3. The as installed frequency of the bushing is strongly influenced by the tank cover and the modeling of the connections. Each high voltage bushing was assigned the properties which yield a fixed base frequency of 15 Hz as provided by the manufacturers so that. When the bushings were incorporated in the numerical model of the whole transformer, their fundamental "as-installed" frequencies were found to be in the range of 5-8 Hz. These "as-installed frequencies are responsible for the actual dynamic response under ground excitations. This shift may explain some of the good experimental behavior of bushings tested in rigid fixtures (such as fixed base) and the problematic seismic response in the field with flexible mountings in "as-installed" conditions..
4. Use of transfer functions allows screening irrelevant interactions. The transfer functions, apart from being used for the identification of the components' dynamic properties, were utilized as the means to eliminate the control points selected in the model for the assessment of interactions with the bushings.
5. Cross spectra and visual animation of modes of vibration can be used in tandem for assessment of interactions. The cross spectra shows the magnitude and the frequencies of

amplifications for the multiplication of two distinct waves, indicating that the relative parts might interact. However, they do not provide any visual proof that the interactions occur. However, the finite element program SAP2000 provides a visual representation of the modes but does not give information about the magnitude of interactions. Therefore, these methods were used in conjunction for the assessment of the interactions.

6. The radiators and the surge arresters, included in the transformer model, were shown to affect significantly the response of the bushings because their dynamic response essentially controls the cover plate and somewhat the out of plane deformation of the side walls. These deformations create rotational and vertical input at the base of the bushings. On the other hand, other large parts that do not add to the motion of the walls or the cover plate, such as the conservator and the core-coil assembly, have little contribution to the bushing's response.

(b) Effect of structural modifications:

7. Bracing of the conservator and the radiators (MI-a model) can alleviate the response of the central bushing but significantly deteriorate the response of the third bushing. Moreover bracing of the conservator only (MI-c model), provides the most favorable modification on the MI model comparatively to the others.
8. If the core is connected directly to the roof cover of the transformer tank (MII model series) influence adversely the behavior of the bushings of all the models examined - specifically, the models MII-a2i, MIIa2ii and MIIa2iii. The response of the first and third bushing was approximately twice the response measured in the MII model and the response of the second bushing is almost three times the respective response.

There are many factors that could lead to this adverse response. First of all, the dynamic properties of the cover plate change due to the significant mass of the core directly attached to it. The vertical motion of the core can directly affect the motion of the cover plate, contrary to the case of the MII model, where the core affects the motion of the cover indirectly by exciting the side walls. However, the results of the dynamic analysis and the animation of the core response, with SAP2000, reveal that the vertical motion of the cover plate is not very significant, on the order of 0.4 in. What is clear though is that the connection of the core to the cover plate changes the boundary conditions of the latter. These changes are done because not only many of the cover plate modes that appeared in the unmodified models are absent in the current model, but the bushing frequencies are increased. The central bushing in particular, which seems to be the most problematic of all three, exhibits modes in the diagonal direction, a case that is typical of a bushing located at the corner of the cover plate. It is possible, that depending on the core-cover connection, corner-like effects may be induced on the bushings.

9. Removing components may attenuate somewhat the bushing response. Among the modified models that involve removal of their components, the MII-c and MII-e models are the ones that alleviate the bushings' response, slightly.
10. The bracing of the internal small transformer to the tank wall in model MII significantly affected the response of the third bushing with respect to model MI, where the small transformer is not connected to the wall due to local effects.
11. The response in terms of displacements, in general, seems to follow the same trend as the accelerations. However, the displacements at the bottom of the central bushing with respect to the core and the ground are reduced for the models in which the core is braced.

(c) Transformer amplifications of tank's roof – cover:

12. In the models investigated, each corner spectrum shows a significant amplification with respect to the base motion when using IEEE 693-2005 spectrum. The spectra at the top of the turrets show an amplification factor of two or more. The corners are essentially stiff regions and therefore the amplification in the corner spectra reflects the effect of the tank flexibility. The top of turret spectra have an amplification associated with the flexibility of the tank and one or more associated with the flexibility of the plate around the bushing-turret assembly.
13. The difference in the magnitude of the amplification factor between the corner and the turret spectra is attributed to neglecting the rotational motion when calculating the first. The largest difference between the two types of spectra is found in the vertical direction. The bushings are located close to the wall, which indicates that the vertical response there is interdependent with the rotation. The fact that the vertical response spectrum at these locations is significantly amplified, suggests that there is rotational input through the boundary of the plate. This rotation input is possibly due to the motion of the surge arresters and the radiators.
14. For most of the variations of the transformer examined, the dynamic amplification factor is much larger than two, a result that corroborates with similar past studies conducted. Therefore, the factor proposed by IEEE693 may not be conservative.

(d) Simplified modeling of bushings and roof cover

15. The analysis of the separated cover plate models show a good approximation to the full transformer model response in certain configuration of simulated boundary conditions, i.e. models with fixed boundaries, especially on the side where the bushings are mounted.

16. The inclusion of the attachments enhances the results both in terms of accelerations at the bushing's CGs and displacements at the top of the bushings, which is the objective of the simplification suggested. Concerning the acceleration at the bushings' CG, which is one of the crucial quantities for the bushing performance, the maximum relative difference from the exact solution, observed after the inclusion of the attachments, is 14%.
17. The differences in the acceleration output at the bushings' CG, between the separated cover and the full transformer models, are attributed to the boundary conditions and the approximated input motion assumed for the modified models. That is, the rotational input due to the flexibility of the side walls, as well as the variation of the linear input along the plate boundary are not accounted for in the analysis of the separated cover models. However in spite of this approximation, the simplified modeling yields reasonable results compared to the response of the full model of transformer.
18. The input motion considered, for the study of the simplified separated cover models, is the average response at the corners of the plate obtained from the full model. For future implementation of the separated cover model approach, reasonable assumptions have to be made in order to obtain the input motion for the simplified model. This input motion will be obtained from the amplification of the ground motion that would be used in case the full transformer was to be modeled.
19. Previous research, as well as the present study, has repeatedly indicated that the response at the cover plate should be magnified by a factor greater than two with respect to the ground motion, (as required by the IEEE 693-2005 specifications). It is essential that the amplification factor from the ground to the cover plate be further studied and associated with various transformer types.

(e) General comments

20. While this study is very detailed, it is not comprehensive and should be viewed in the context of transformers analyzed. However it is clear that the effects determined in this study are general and will appear in most transformers, with different degrees of intensity.

SECTION 10

REFERENCES

Ashrafi, A. (2003). "Issues of seismic response and retrofit for critical substation equipment," *Master Thesis*, New Jersey Institute of Technology, Newark, NJ, August.

Bellorini, S., Salvetti, M., Bettinali, F., and Zafferani, G. (1998). "Seismic qualification of transformer high voltage bushings." *IEEE Transactions on Power Delivery*, 13(4), 1208-1213.

Computers and Structures, Inc. (2003). *SAP2000 Nonlinear V11.0.8*, Berkeley, CA

Ersoy, S. and Saadeghvaziri, M. A. (2004). "Seismic response of transformer-bushing systems." *IEEE Transactions on Power Delivery*, 19(1), 131-137.

Ersoy, S., Saadeghvaziri, M. A., Liu, G.-Y., and Mau, S. T. (2001). "Analytical and experimental seismic studies of transformers isolated with friction pendulum system and design aspects." *Earthquake Spectra*, 17(4), 569-595.

Filiatrault, A. and Matt, H. (2005). "Seismic Response of High-Voltage Transformer-Bushing Systems." *Earthquake Spectra*, 21(4), 1009-1026.

Filiatrault, A. and Matt, H. (2006). "Seismic Response of High Voltage Electrical Transformer–Bushing Systems." *Journal of Structural Engineering*, 132(2), 287-295.

Gilani, A. S., Chavez, J. V., Fenves, G. L., and Whittaker, A. S. (1998). "Seismic Evaluation of 196 kV Porcelain Transformer Bushings." *Report No. PEER-98/02*, Pacific Earthquake Engineering Research Center, San Diego, CA.

Gilani, A. S., Whittaker, A. S., and Fenves, G. L. (1999). "Seismic Evaluation and Retrofit of 230 kV Porcelain Transformer Bushings." *Report No. PEER 1999/14*, Pacific Earthquake Engineering Research Center, San Diego, CA.

Gilani, A. S. J., Whittaker, A. S., and Fenves, G. L. (2001). "Seismic evaluation and retrofit of porcelain transformer bushings." *Earthquake Spectra*, 17 (4), 597–616.

Institute of Electrical and Electronic Engineers (IEEE). (1998). "IEEE Std. 693-1997, Recommended Practices for Seismic Design of Substations." Piscataway, NJ, USA

Institute of Electrical and Electronic Engineers (IEEE). (2006). "IEEE Standard 693-2005, Recommended Practices for Seismic Design of Substations." The Institute of Electrical and Electronics Engineers, Inc.3 Park Avenue, New York, NY 10016-5997, USA

Saadeghvaziri, M. A., Feizi, B., Kempner, L., and Alston, D. (2010). "On Seismic Response of Substation Equipment and Application of Base-Isolation to Transformers." *IEEE Transactions on Power Delivery*, 25(1), 177-186.

Schiff, A. J. (1995). "Northridge Earthquake Lifeline Performance and Post Earthquake Response." *TCLEE-Monograph No. 8*, ASCE

Schiff, A. J. (1998a). "Hyogoken Nabu (Kobe) Earthquake of January 17, 1995 Lifeline Performance." *TCLEE-Monograph No. 14*, ASCE

Schiff, A. J. (1998b). "Guide to improved earthquake performance of electrical power systems." *Rep. No. NIST GCR 98-757*, National Institute for Standards and Testing, Washington, D.C.

Schiff, A. J. and Tang A. K. (2000). "Chi Chi, Taiwan Earthquake of September 21, 1999 Lifeline Performance." *TCLEE- Monograph No. 18*, ASCE

Villaverde, R., Pardoen, G., and Carnalla, S. (2001). "Ground motion amplification at flange level of bushings mounted on electric substation transformers." *Earthquake Engineering and Structural Dynamics*, 30(5), 621-632.

Wilcoski, J. and Smith, S. J. (1997). “Fragility Testing of a Power Transformer Bushing.” *CERL Technical Report 97/57*, US Army Corps of Engineers, Construction Engineering Research Laboratories, Champaign, IL, USA

MCEER Technical Reports

MCEER publishes technical reports on a variety of subjects written by authors funded through MCEER. These reports are available from both MCEER Publications and the National Technical Information Service (NTIS). Requests for reports should be directed to MCEER Publications, MCEER, University at Buffalo, State University of New York, 133A Ketter Hall, Buffalo, New York 14260. Reports can also be requested through NTIS, P.O. Box 1425, Springfield, Virginia 22151. NTIS accession numbers are shown in parenthesis, if available.

NCEER-87-0001 "First-Year Program in Research, Education and Technology Transfer," 3/5/87, (PB88-134275, A04, MF-A01).

NCEER-87-0002 "Experimental Evaluation of Instantaneous Optimal Algorithms for Structural Control," by R.C. Lin, T.T. Soong and A.M. Reinhorn, 4/20/87, (PB88-134341, A04, MF-A01).

NCEER-87-0003 "Experimentation Using the Earthquake Simulation Facilities at University at Buffalo," by A.M. Reinhorn and R.L. Ketter, to be published.

NCEER-87-0004 "The System Characteristics and Performance of a Shaking Table," by J.S. Hwang, K.C. Chang and G.C. Lee, 6/1/87, (PB88-134259, A03, MF-A01). This report is available only through NTIS (see address given above).

NCEER-87-0005 "A Finite Element Formulation for Nonlinear Viscoplastic Material Using a Q Model," by O. Gyebi and G. Dasgupta, 11/2/87, (PB88-213764, A08, MF-A01).

NCEER-87-0006 "Symbolic Manipulation Program (SMP) - Algebraic Codes for Two and Three Dimensional Finite Element Formulations," by X. Lee and G. Dasgupta, 11/9/87, (PB88-218522, A05, MF-A01).

NCEER-87-0007 "Instantaneous Optimal Control Laws for Tall Buildings Under Seismic Excitations," by J.N. Yang, A. Akbarpour and P. Ghaemmaghami, 6/10/87, (PB88-134333, A06, MF-A01). This report is only available through NTIS (see address given above).

NCEER-87-0008 "IDARC: Inelastic Damage Analysis of Reinforced Concrete Frame - Shear-Wall Structures," by Y.J. Park, A.M. Reinhorn and S.K. Kunnath, 7/20/87, (PB88-134325, A09, MF-A01). This report is only available through NTIS (see address given above).

NCEER-87-0009 "Liquefaction Potential for New York State: A Preliminary Report on Sites in Manhattan and Buffalo," by M. Budhu, V. Vijayakumar, R.F. Giese and L. Baumgras, 8/31/87, (PB88-163704, A03, MF-A01). This report is available only through NTIS (see address given above).

NCEER-87-0010 "Vertical and Torsional Vibration of Foundations in Inhomogeneous Media," by A.S. Veletsos and K.W. Dotson, 6/1/87, (PB88-134291, A03, MF-A01). This report is only available through NTIS (see address given above).

NCEER-87-0011 "Seismic Probabilistic Risk Assessment and Seismic Margins Studies for Nuclear Power Plants," by Howard H.M. Hwang, 6/15/87, (PB88-134267, A03, MF-A01). This report is only available through NTIS (see address given above).

NCEER-87-0012 "Parametric Studies of Frequency Response of Secondary Systems Under Ground-Acceleration Excitations," by Y. Yong and Y.K. Lin, 6/10/87, (PB88-134309, A03, MF-A01). This report is only available through NTIS (see address given above).

NCEER-87-0013 "Frequency Response of Secondary Systems Under Seismic Excitation," by J.A. HoLung, J. Cai and Y.K. Lin, 7/31/87, (PB88-134317, A05, MF-A01). This report is only available through NTIS (see address given above).

NCEER-87-0014 "Modelling Earthquake Ground Motions in Seismically Active Regions Using Parametric Time Series Methods," by G.W. Ellis and A.S. Cakmak, 8/25/87, (PB88-134283, A08, MF-A01). This report is only available through NTIS (see address given above).

NCEER-87-0015 "Detection and Assessment of Seismic Structural Damage," by E. DiPasquale and A.S. Cakmak, 8/25/87, (PB88-163712, A05, MF-A01). This report is only available through NTIS (see address given above).

NCEER-87-0016 "Pipeline Experiment at Parkfield, California," by J. Isenberg and E. Richardson, 9/15/87, (PB88-163720, A03, MF-A01). This report is available only through NTIS (see address given above).

NCEER-87-0017 "Digital Simulation of Seismic Ground Motion," by M. Shinozuka, G. Deodatis and T. Harada, 8/31/87, (PB88-155197, A04, MF-A01). This report is available only through NTIS (see address given above).

NCEER-87-0018 "Practical Considerations for Structural Control: System Uncertainty, System Time Delay and Truncation of Small Control Forces," J.N. Yang and A. Akbarpour, 8/10/87, (PB88-163738, A08, MF-A01). This report is only available through NTIS (see address given above).

NCEER-87-0019 "Modal Analysis of Nonclassically Damped Structural Systems Using Canonical Transformation," by J.N. Yang, S. Sarkani and F.X. Long, 9/27/87, (PB88-187851, A04, MF-A01).

NCEER-87-0020 "A Nonstationary Solution in Random Vibration Theory," by J.R. Red-Horse and P.D. Spanos, 11/3/87, (PB88-163746, A03, MF-A01).

NCEER-87-0021 "Horizontal Impedances for Radially Inhomogeneous Viscoelastic Soil Layers," by A.S. Veletsos and K.W. Dotson, 10/15/87, (PB88-150859, A04, MF-A01).

NCEER-87-0022 "Seismic Damage Assessment of Reinforced Concrete Members," by Y.S. Chung, C. Meyer and M. Shinozuka, 10/9/87, (PB88-150867, A05, MF-A01). This report is available only through NTIS (see address given above).

NCEER-87-0023 "Active Structural Control in Civil Engineering," by T.T. Soong, 11/11/87, (PB88-187778, A03, MF-A01).

NCEER-87-0024 "Vertical and Torsional Impedances for Radially Inhomogeneous Viscoelastic Soil Layers," by K.W. Dotson and A.S. Veletsos, 12/87, (PB88-187786, A03, MF-A01).

NCEER-87-0025 "Proceedings from the Symposium on Seismic Hazards, Ground Motions, Soil-Liquefaction and Engineering Practice in Eastern North America," October 20-22, 1987, edited by K.H. Jacob, 12/87, (PB88-188115, A23, MF-A01). This report is available only through NTIS (see address given above).

NCEER-87-0026 "Report on the Whittier-Narrows, California, Earthquake of October 1, 1987," by J. Pantelic and A. Reinhorn, 11/87, (PB88-187752, A03, MF-A01). This report is available only through NTIS (see address given above).

NCEER-87-0027 "Design of a Modular Program for Transient Nonlinear Analysis of Large 3-D Building Structures," by S. Srivastav and J.F. Abel, 12/30/87, (PB88-187950, A05, MF-A01). This report is only available through NTIS (see address given above).

NCEER-87-0028 "Second-Year Program in Research, Education and Technology Transfer," 3/8/88, (PB88-219480, A04, MF-A01).

NCEER-88-0001 "Workshop on Seismic Computer Analysis and Design of Buildings With Interactive Graphics," by W. McGuire, J.F. Abel and C.H. Conley, 1/18/88, (PB88-187760, A03, MF-A01). This report is only available through NTIS (see address given above).

NCEER-88-0002 "Optimal Control of Nonlinear Flexible Structures," by J.N. Yang, F.X. Long and D. Wong, 1/22/88, (PB88-213772, A06, MF-A01).

NCEER-88-0003 "Substructuring Techniques in the Time Domain for Primary-Secondary Structural Systems," by G.D. Manolis and G. Juhn, 2/10/88, (PB88-213780, A04, MF-A01).

NCEER-88-0004 "Iterative Seismic Analysis of Primary-Secondary Systems," by A. Singhal, L.D. Lutes and P.D. Spanos, 2/23/88, (PB88-213798, A04, MF-A01).

NCEER-88-0005 "Stochastic Finite Element Expansion for Random Media," by P.D. Spanos and R. Ghanem, 3/14/88, (PB88-213806, A03, MF-A01).

NCEER-88-0006 "Combining Structural Optimization and Structural Control," by F.Y. Cheng and C.P. Pantelides, 1/10/88, (PB88-213814, A05, MF-A01).

NCEER-88-0007 "Seismic Performance Assessment of Code-Designed Structures," by H.H-M. Hwang, J-W. Jaw and H-J. Shau, 3/20/88, (PB88-219423, A04, MF-A01). This report is only available through NTIS (see address given above).

NCEER-88-0008 "Reliability Analysis of Code-Designed Structures Under Natural Hazards," by H.H-M. Hwang, H. Ushiba and M. Shinozuka, 2/29/88, (PB88-229471, A07, MF-A01). This report is only available through NTIS (see address given above).

NCEER-88-0009 "Seismic Fragility Analysis of Shear Wall Structures," by J-W Jaw and H.H-M. Hwang, 4/30/88, (PB89-102867, A04, MF-A01).

NCEER-88-0010 "Base Isolation of a Multi-Story Building Under a Harmonic Ground Motion - A Comparison of Performances of Various Systems," by F-G Fan, G. Ahmadi and I.G. Tadjbakhsh, 5/18/88, (PB89-122238, A06, MF-A01). This report is only available through NTIS (see address given above).

NCEER-88-0011 "Seismic Floor Response Spectra for a Combined System by Green's Functions," by F.M. Lavelle, L.A. Bergman and P.D. Spanos, 5/1/88, (PB89-102875, A03, MF-A01).

NCEER-88-0012 "A New Solution Technique for Randomly Excited Hysteretic Structures," by G.Q. Cai and Y.K. Lin, 5/16/88, (PB89-102883, A03, MF-A01).

NCEER-88-0013 "A Study of Radiation Damping and Soil-Structure Interaction Effects in the Centrifuge," by K. Weissman, supervised by J.H. Prevost, 5/24/88, (PB89-144703, A06, MF-A01).

NCEER-88-0014 "Parameter Identification and Implementation of a Kinematic Plasticity Model for Frictional Soils," by J.H. Prevost and D.V. Griffiths, to be published.

NCEER-88-0015 "Two- and Three- Dimensional Dynamic Finite Element Analyses of the Long Valley Dam," by D.V. Griffiths and J.H. Prevost, 6/17/88, (PB89-144711, A04, MF-A01).

NCEER-88-0016 "Damage Assessment of Reinforced Concrete Structures in Eastern United States," by A.M. Reinhorn, M.J. Seidel, S.K. Kunnath and Y.J. Park, 6/15/88, (PB89-122220, A04, MF-A01). This report is only available through NTIS (see address given above).

NCEER-88-0017 "Dynamic Compliance of Vertically Loaded Strip Foundations in Multilayered Viscoelastic Soils," by S. Ahmad and A.S.M. Israil, 6/17/88, (PB89-102891, A04, MF-A01).

NCEER-88-0018 "An Experimental Study of Seismic Structural Response With Added Viscoelastic Dampers," by R.C. Lin, Z. Liang, T.T. Soong and R.H. Zhang, 6/30/88, (PB89-122212, A05, MF-A01). This report is available only through NTIS (see address given above).

NCEER-88-0019 "Experimental Investigation of Primary - Secondary System Interaction," by G.D. Manolis, G. Juhn and A.M. Reinhorn, 5/27/88, (PB89-122204, A04, MF-A01).

NCEER-88-0020 "A Response Spectrum Approach For Analysis of Nonclassically Damped Structures," by J.N. Yang, S. Sarkani and F.X. Long, 4/22/88, (PB89-102909, A04, MF-A01).

NCEER-88-0021 "Seismic Interaction of Structures and Soils: Stochastic Approach," by A.S. Veletsos and A.M. Prasad, 7/21/88, (PB89-122196, A04, MF-A01). This report is only available through NTIS (see address given above).

NCEER-88-0022 "Identification of the Serviceability Limit State and Detection of Seismic Structural Damage," by E. DiPasquale and A.S. Cakmak, 6/15/88, (PB89-122188, A05, MF-A01). This report is available only through NTIS (see address given above).

NCEER-88-0023 "Multi-Hazard Risk Analysis: Case of a Simple Offshore Structure," by B.K. Bhartia and E.H. Vanmarcke, 7/21/88, (PB89-145213, A05, MF-A01).

NCEER-88-0024 "Automated Seismic Design of Reinforced Concrete Buildings," by Y.S. Chung, C. Meyer and M. Shinozuka, 7/5/88, (PB89-122170, A06, MF-A01). This report is available only through NTIS (see address given above).

NCEER-88-0025 "Experimental Study of Active Control of MDOF Structures Under Seismic Excitations," by L.L. Chung, R.C. Lin, T.T. Soong and A.M. Reinhorn, 7/10/88, (PB89-122600, A04, MF-A01).

NCEER-88-0026 "Earthquake Simulation Tests of a Low-Rise Metal Structure," by J.S. Hwang, K.C. Chang, G.C. Lee and R.L. Ketter, 8/1/88, (PB89-102917, A04, MF-A01).

NCEER-88-0027 "Systems Study of Urban Response and Reconstruction Due to Catastrophic Earthquakes," by F. Kozin and H.K. Zhou, 9/22/88, (PB90-162348, A04, MF-A01).

NCEER-88-0028 "Seismic Fragility Analysis of Plane Frame Structures," by H.H-M. Hwang and Y.K. Low, 7/31/88, (PB89-131445, A06, MF-A01).

NCEER-88-0029 "Response Analysis of Stochastic Structures," by A. Kardara, C. Bucher and M. Shinozuka, 9/22/88, (PB89-174429, A04, MF-A01).

NCEER-88-0030 "Nonnormal Accelerations Due to Yielding in a Primary Structure," by D.C.K. Chen and L.D. Lutes, 9/19/88, (PB89-131437, A04, MF-A01).

NCEER-88-0031 "Design Approaches for Soil-Structure Interaction," by A.S. Veletsos, A.M. Prasad and Y. Tang, 12/30/88, (PB89-174437, A03, MF-A01). This report is available only through NTIS (see address given above).

NCEER-88-0032 "A Re-evaluation of Design Spectra for Seismic Damage Control," by C.J. Turkstra and A.G. Tallin, 11/7/88, (PB89-145221, A05, MF-A01).

NCEER-88-0033 "The Behavior and Design of Noncontact Lap Splices Subjected to Repeated Inelastic Tensile Loading," by V.E. Sagan, P. Gergely and R.N. White, 12/8/88, (PB89-163737, A08, MF-A01).

NCEER-88-0034 "Seismic Response of Pile Foundations," by S.M. Mamoon, P.K. Banerjee and S. Ahmad, 11/1/88, (PB89-145239, A04, MF-A01).

NCEER-88-0035 "Modeling of R/C Building Structures With Flexible Floor Diaphragms (IDARC2)," by A.M. Reinhorn, S.K. Kunnath and N. Panahshahi, 9/7/88, (PB89-207153, A07, MF-A01).

NCEER-88-0036 "Solution of the Dam-Reservoir Interaction Problem Using a Combination of FEM, BEM with Particular Integrals, Modal Analysis, and Substructuring," by C-S. Tsai, G.C. Lee and R.L. Ketter, 12/31/88, (PB89-207146, A04, MF-A01).

NCEER-88-0037 "Optimal Placement of Actuators for Structural Control," by F.Y. Cheng and C.P. Pantelides, 8/15/88, (PB89-162846, A05, MF-A01).

NCEER-88-0038 "Teflon Bearings in Aseismic Base Isolation: Experimental Studies and Mathematical Modeling," by A. Mokha, M.C. Constantinou and A.M. Reinhorn, 12/5/88, (PB89-218457, A10, MF-A01). This report is available only through NTIS (see address given above).

NCEER-88-0039 "Seismic Behavior of Flat Slab High-Rise Buildings in the New York City Area," by P. Weidlinger and M. Ettouney, 10/15/88, (PB90-145681, A04, MF-A01).

NCEER-88-0040 "Evaluation of the Earthquake Resistance of Existing Buildings in New York City," by P. Weidlinger and M. Ettouney, 10/15/88, to be published.

NCEER-88-0041 "Small-Scale Modeling Techniques for Reinforced Concrete Structures Subjected to Seismic Loads," by W. Kim, A. El-Attar and R.N. White, 11/22/88, (PB89-189625, A05, MF-A01).

NCEER-88-0042 "Modeling Strong Ground Motion from Multiple Event Earthquakes," by G.W. Ellis and A.S. Cakmak, 10/15/88, (PB89-174445, A03, MF-A01).

NCEER-88-0043 "Nonstationary Models of Seismic Ground Acceleration," by M. Grigoriu, S.E. Ruiz and E. Rosenblueth, 7/15/88, (PB89-189617, A04, MF-A01).

NCEER-88-0044 "SARCF User's Guide: Seismic Analysis of Reinforced Concrete Frames," by Y.S. Chung, C. Meyer and M. Shinozuka, 11/9/88, (PB89-174452, A08, MF-A01).

NCEER-88-0045 "First Expert Panel Meeting on Disaster Research and Planning," edited by J. Pantelic and J. Stoyle, 9/15/88, (PB89-174460, A05, MF-A01).

NCEER-88-0046 "Preliminary Studies of the Effect of Degrading Infill Walls on the Nonlinear Seismic Response of Steel Frames," by C.Z. Chrysostomou, P. Gergely and J.F. Abel, 12/19/88, (PB89-208383, A05, MF-A01).

NCEER-88-0047 "Reinforced Concrete Frame Component Testing Facility - Design, Construction, Instrumentation and Operation," by S.P. Pessiki, C. Conley, T. Bond, P. Gergely and R.N. White, 12/16/88, (PB89-174478, A04, MF-A01).

NCEER-89-0001 "Effects of Protective Cushion and Soil Compliancy on the Response of Equipment Within a Seismically Excited Building," by J.A. HoLung, 2/16/89, (PB89-207179, A04, MF-A01).

NCEER-89-0002 "Statistical Evaluation of Response Modification Factors for Reinforced Concrete Structures," by H.H-M. Hwang and J-W. Jaw, 2/17/89, (PB89-207187, A05, MF-A01).

NCEER-89-0003 "Hysteretic Columns Under Random Excitation," by G-Q. Cai and Y.K. Lin, 1/9/89, (PB89-196513, A03, MF-A01).

NCEER-89-0004 "Experimental Study of `Elephant Foot Bulge' Instability of Thin-Walled Metal Tanks," by Z-H. Jia and R.L. Ketter, 2/22/89, (PB89-207195, A03, MF-A01).

NCEER-89-0005 "Experiment on Performance of Buried Pipelines Across San Andreas Fault," by J. Isenberg, E. Richardson and T.D. O'Rourke, 3/10/89, (PB89-218440, A04, MF-A01). This report is available only through NTIS (see address given above).

NCEER-89-0006 "A Knowledge-Based Approach to Structural Design of Earthquake-Resistant Buildings," by M. Subramani, P. Gergely, C.H. Conley, J.F. Abel and A.H. Zaghw, 1/15/89, (PB89-218465, A06, MF-A01).

NCEER-89-0007 "Liquefaction Hazards and Their Effects on Buried Pipelines," by T.D. O'Rourke and P.A. Lane, 2/1/89, (PB89-218481, A09, MF-A01).

NCEER-89-0008 "Fundamentals of System Identification in Structural Dynamics," by H. Imai, C-B. Yun, O. Maruyama and M. Shinozuka, 1/26/89, (PB89-207211, A04, MF-A01).

NCEER-89-0009 "Effects of the 1985 Michoacan Earthquake on Water Systems and Other Buried Lifelines in Mexico," by A.G. Ayala and M.J. O'Rourke, 3/8/89, (PB89-207229, A06, MF-A01).

NCEER-89-R010 "NCEER Bibliography of Earthquake Education Materials," by K.E.K. Ross, Second Revision, 9/1/89, (PB90-125352, A05, MF-A01). This report is replaced by NCEER-92-0018.

NCEER-89-0011 "Inelastic Three-Dimensional Response Analysis of Reinforced Concrete Building Structures (IDARC-3D), Part I - Modeling," by S.K. Kunnath and A.M. Reinhorn, 4/17/89, (PB90-114612, A07, MF-A01). This report is available only through NTIS (see address given above).

NCEER-89-0012 "Recommended Modifications to ATC-14," by C.D. Poland and J.O. Malley, 4/12/89, (PB90-108648, A15, MF-A01).

NCEER-89-0013 "Repair and Strengthening of Beam-to-Column Connections Subjected to Earthquake Loading," by M. Corazao and A.J. Durrani, 2/28/89, (PB90-109885, A06, MF-A01).

NCEER-89-0014 "Program EXKAL2 for Identification of Structural Dynamic Systems," by O. Maruyama, C-B. Yun, M. Hoshiya and M. Shinozuka, 5/19/89, (PB90-109877, A09, MF-A01).

NCEER-89-0015 "Response of Frames With Bolted Semi-Rigid Connections, Part I - Experimental Study and Analytical Predictions," by P.J. DiCorso, A.M. Reinhorn, J.R. Dickerson, J.B. Radziminski and W.L. Harper, 6/1/89, to be published.

NCEER-89-0016 "ARMA Monte Carlo Simulation in Probabilistic Structural Analysis," by P.D. Spanos and M.P. Mignolet, 7/10/89, (PB90-109893, A03, MF-A01).

NCEER-89-P017 "Preliminary Proceedings from the Conference on Disaster Preparedness - The Place of Earthquake Education in Our Schools," Edited by K.E.K. Ross, 6/23/89, (PB90-108606, A03, MF-A01).

NCEER-89-0017 "Proceedings from the Conference on Disaster Preparedness - The Place of Earthquake Education in Our Schools," Edited by K.E.K. Ross, 12/31/89, (PB90-207895, A012, MF-A02). This report is available only through NTIS (see address given above).

NCEER-89-0018 "Multidimensional Models of Hysteretic Material Behavior for Vibration Analysis of Shape Memory Energy Absorbing Devices, by E.J. Graesser and F.A. Cozzarelli, 6/7/89, (PB90-164146, A04, MF-A01).

NCEER-89-0019 "Nonlinear Dynamic Analysis of Three-Dimensional Base Isolated Structures (3D-BASIS)," by S. Nagarajaiah, A.M. Reinhorn and M.C. Constantinou, 8/3/89, (PB90-161936, A06, MF-A01). This report has been replaced by NCEER-93-0011.

NCEER-89-0020 "Structural Control Considering Time-Rate of Control Forces and Control Rate Constraints," by F.Y. Cheng and C.P. Pantelides, 8/3/89, (PB90-120445, A04, MF-A01).

NCEER-89-0021 "Subsurface Conditions of Memphis and Shelby County," by K.W. Ng, T-S. Chang and H-H.M. Hwang, 7/26/89, (PB90-120437, A03, MF-A01).

NCEER-89-0022 "Seismic Wave Propagation Effects on Straight Jointed Buried Pipelines," by K. Elhmadi and M.J. O'Rourke, 8/24/89, (PB90-162322, A10, MF-A02).

NCEER-89-0023 "Workshop on Serviceability Analysis of Water Delivery Systems," edited by M. Grigoriu, 3/6/89, (PB90-127424, A03, MF-A01).

NCEER-89-0024 "Shaking Table Study of a 1/5 Scale Steel Frame Composed of Tapered Members," by K.C. Chang, J.S. Hwang and G.C. Lee, 9/18/89, (PB90-160169, A04, MF-A01).

NCEER-89-0025 "DYNA1D: A Computer Program for Nonlinear Seismic Site Response Analysis - Technical Documentation," by Jean H. Prevost, 9/14/89, (PB90-161944, A07, MF-A01). This report is available only through NTIS (see address given above).

NCEER-89-0026 "1:4 Scale Model Studies of Active Tendon Systems and Active Mass Dampers for Aseismic Protection," by A.M. Reinhorn, T.T. Soong, R.C. Lin, Y.P. Yang, Y. Fukao, H. Abe and M. Nakai, 9/15/89, (PB90-173246, A10, MF-A02). This report is available only through NTIS (see address given above).

NCEER-89-0027 "Scattering of Waves by Inclusions in a Nonhomogeneous Elastic Half Space Solved by Boundary Element Methods," by P.K. Hadley, A. Askar and A.S. Cakmak, 6/15/89, (PB90-145699, A07, MF-A01).

NCEER-89-0028 "Statistical Evaluation of Deflection Amplification Factors for Reinforced Concrete Structures," by H.H.M. Hwang, J-W. Jaw and A.L. Ch'ng, 8/31/89, (PB90-164633, A05, MF-A01).

NCEER-89-0029 "Bedrock Accelerations in Memphis Area Due to Large New Madrid Earthquakes," by H.H.M. Hwang, C.H.S. Chen and G. Yu, 11/7/89, (PB90-162330, A04, MF-A01).

NCEER-89-0030 "Seismic Behavior and Response Sensitivity of Secondary Structural Systems," by Y.Q. Chen and T.T. Soong, 10/23/89, (PB90-164658, A08, MF-A01).

NCEER-89-0031 "Random Vibration and Reliability Analysis of Primary-Secondary Structural Systems," by Y. Ibrahim, M. Grigoriu and T.T. Soong, 11/10/89, (PB90-161951, A04, MF-A01).

NCEER-89-0032 "Proceedings from the Second U.S. - Japan Workshop on Liquefaction, Large Ground Deformation and Their Effects on Lifelines, September 26-29, 1989," Edited by T.D. O'Rourke and M. Hamada, 12/1/89, (PB90-209388, A22, MF-A03).

NCEER-89-0033 "Deterministic Model for Seismic Damage Evaluation of Reinforced Concrete Structures," by J.M. Bracci, A.M. Reinhorn, J.B. Mander and S.K. Kunnath, 9/27/89, (PB91-108803, A06, MF-A01).

NCEER-89-0034 "On the Relation Between Local and Global Damage Indices," by E. DiPasquale and A.S. Cakmak, 8/15/89, (PB90-173865, A05, MF-A01).

NCEER-89-0035 "Cyclic Undrained Behavior of Nonplastic and Low Plasticity Silts," by A.J. Walker and H.E. Stewart, 7/26/89, (PB90-183518, A10, MF-A01).

NCEER-89-0036 "Liquefaction Potential of Surficial Deposits in the City of Buffalo, New York," by M. Budhu, R. Giese and L. Baumgrass, 1/17/89, (PB90-208455, A04, MF-A01).

NCEER-89-0037 "A Deterministic Assessment of Effects of Ground Motion Incoherence," by A.S. Veletsos and Y. Tang, 7/15/89, (PB90-164294, A03, MF-A01).

NCEER-89-0038 "Workshop on Ground Motion Parameters for Seismic Hazard Mapping," July 17-18, 1989, edited by R.V. Whitman, 12/1/89, (PB90-173923, A04, MF-A01).

NCEER-89-0039 "Seismic Effects on Elevated Transit Lines of the New York City Transit Authority," by C.J. Costantino, C.A. Miller and E. Heymsfield, 12/26/89, (PB90-207887, A06, MF-A01).

NCEER-89-0040 "Centrifugal Modeling of Dynamic Soil-Structure Interaction," by K. Weissman, Supervised by J.H. Prevost, 5/10/89, (PB90-207879, A07, MF-A01).

NCEER-89-0041 "Linearized Identification of Buildings With Cores for Seismic Vulnerability Assessment," by I-K. Ho and A.E. Aktan, 11/1/89, (PB90-251943, A07, MF-A01).

NCEER-90-0001 "Geotechnical and Lifeline Aspects of the October 17, 1989 Loma Prieta Earthquake in San Francisco," by T.D. O'Rourke, H.E. Stewart, F.T. Blackburn and T.S. Dickerman, 1/90, (PB90-208596, A05, MF-A01).

NCEER-90-0002 "Nonnormal Secondary Response Due to Yielding in a Primary Structure," by D.C.K. Chen and L.D. Lutes, 2/28/90, (PB90-251976, A07, MF-A01).

NCEER-90-0003 "Earthquake Education Materials for Grades K-12," by K.E.K. Ross, 4/16/90, (PB91-251984, A05, MF-A05). This report has been replaced by NCEER-92-0018.

NCEER-90-0004 "Catalog of Strong Motion Stations in Eastern North America," by R.W. Busby, 4/3/90, (PB90-251984, A05, MF-A01).

NCEER-90-0005 "NCEER Strong-Motion Data Base: A User Manual for the GeoBase Release (Version 1.0 for the Sun3)," by P. Friberg and K. Jacob, 3/31/90 (PB90-258062, A04, MF-A01).

NCEER-90-0006 "Seismic Hazard Along a Crude Oil Pipeline in the Event of an 1811-1812 Type New Madrid Earthquake," by H.H.M. Hwang and C-H.S. Chen, 4/16/90, (PB90-258054, A04, MF-A01).

NCEER-90-0007 "Site-Specific Response Spectra for Memphis Sheahan Pumping Station," by H.H.M. Hwang and C.S. Lee, 5/15/90, (PB91-108811, A05, MF-A01).

NCEER-90-0008 "Pilot Study on Seismic Vulnerability of Crude Oil Transmission Systems," by T. Ariman, R. Dobry, M. Grigoriu, F. Kozin, M. O'Rourke, T. O'Rourke and M. Shinozuka, 5/25/90, (PB91-108837, A06, MF-A01).

NCEER-90-0009 "A Program to Generate Site Dependent Time Histories: EQGEN," by G.W. Ellis, M. Srinivasan and A.S. Cakmak, 1/30/90, (PB91-108829, A04, MF-A01).

NCEER-90-0010 "Active Isolation for Seismic Protection of Operating Rooms," by M.E. Talbott, Supervised by M. Shinozuka, 6/8/9, (PB91-110205, A05, MF-A01).

NCEER-90-0011 "Program LINEARID for Identification of Linear Structural Dynamic Systems," by C-B. Yun and M. Shinozuka, 6/25/90, (PB91-110312, A08, MF-A01).

NCEER-90-0012 "Two-Dimensional Two-Phase Elasto-Plastic Seismic Response of Earth Dams," by A.N. Yiagos, Supervised by J.H. Prevost, 6/20/90, (PB91-110197, A13, MF-A02).

NCEER-90-0013 "Secondary Systems in Base-Isolated Structures: Experimental Investigation, Stochastic Response and Stochastic Sensitivity," by G.D. Manolis, G. Juhn, M.C. Constantinou and A.M. Reinhorn, 7/1/90, (PB91-110320, A08, MF-A01).

NCEER-90-0014 "Seismic Behavior of Lightly-Reinforced Concrete Column and Beam-Column Joint Details," by S.P. Pessiki, C.H. Conley, P. Gergely and R.N. White, 8/22/90, (PB91-108795, A11, MF-A02).

NCEER-90-0015 "Two Hybrid Control Systems for Building Structures Under Strong Earthquakes," by J.N. Yang and A. Danielians, 6/29/90, (PB91-125393, A04, MF-A01).

NCEER-90-0016 "Instantaneous Optimal Control with Acceleration and Velocity Feedback," by J.N. Yang and Z. Li, 6/29/90, (PB91-125401, A03, MF-A01).

NCEER-90-0017 "Reconnaissance Report on the Northern Iran Earthquake of June 21, 1990," by M. Mehrain, 10/4/90, (PB91-125377, A03, MF-A01).

NCEER-90-0018 "Evaluation of Liquefaction Potential in Memphis and Shelby County," by T.S. Chang, P.S. Tang, C.S. Lee and H. Hwang, 8/10/90, (PB91-125427, A09, MF-A01).

NCEER-90-0019 "Experimental and Analytical Study of a Combined Sliding Disc Bearing and Helical Steel Spring Isolation System," by M.C. Constantinou, A.S. Mokha and A.M. Reinhorn, 10/4/90, (PB91-125385, A06, MF-A01). This report is available only through NTIS (see address given above).

NCEER-90-0020 "Experimental Study and Analytical Prediction of Earthquake Response of a Sliding Isolation System with a Spherical Surface," by A.S. Mokha, M.C. Constantinou and A.M. Reinhorn, 10/11/90, (PB91-125419, A05, MF-A01).

NCEER-90-0021 "Dynamic Interaction Factors for Floating Pile Groups," by G. Gazetas, K. Fan, A. Kaynia and E. Kausel, 9/10/90, (PB91-170381, A05, MF-A01).

NCEER-90-0022 "Evaluation of Seismic Damage Indices for Reinforced Concrete Structures," by S. Rodriguez-Gomez and A.S. Cakmak, 9/30/90, PB91-171322, A06, MF-A01).

NCEER-90-0023 "Study of Site Response at a Selected Memphis Site," by H. Desai, S. Ahmad, E.S. Gazetas and M.R. Oh, 10/11/90, (PB91-196857, A03, MF-A01).

NCEER-90-0024 "A User's Guide to Strongmo: Version 1.0 of NCEER's Strong-Motion Data Access Tool for PCs and Terminals," by P.A. Friberg and C.A.T. Susch, 11/15/90, (PB91-171272, A03, MF-A01).

NCEER-90-0025 "A Three-Dimensional Analytical Study of Spatial Variability of Seismic Ground Motions," by L-L. Hong and A.H.-S. Ang, 10/30/90, (PB91-170399, A09, MF-A01).

NCEER-90-0026 "MUMOID User's Guide - A Program for the Identification of Modal Parameters," by S. Rodriguez-Gomez and E. DiPasquale, 9/30/90, (PB91-171298, A04, MF-A01).

NCEER-90-0027 "SARCF-II User's Guide - Seismic Analysis of Reinforced Concrete Frames," by S. Rodriguez-Gomez, Y.S. Chung and C. Meyer, 9/30/90, (PB91-171280, A05, MF-A01).

NCEER-90-0028 "Viscous Dampers: Testing, Modeling and Application in Vibration and Seismic Isolation," by N. Makris and M.C. Constantinou, 12/20/90 (PB91-190561, A06, MF-A01).

NCEER-90-0029 "Soil Effects on Earthquake Ground Motions in the Memphis Area," by H. Hwang, C.S. Lee, K.W. Ng and T.S. Chang, 8/2/90, (PB91-190751, A05, MF-A01).

NCEER-91-0001 "Proceedings from the Third Japan-U.S. Workshop on Earthquake Resistant Design of Lifeline Facilities and Countermeasures for Soil Liquefaction, December 17-19, 1990," edited by T.D. O'Rourke and M. Hamada, 2/1/91, (PB91-179259, A99, MF-A04).

NCEER-91-0002 "Physical Space Solutions of Non-Proportionally Damped Systems," by M. Tong, Z. Liang and G.C. Lee, 1/15/91, (PB91-179242, A04, MF-A01).

NCEER-91-0003 "Seismic Response of Single Piles and Pile Groups," by K. Fan and G. Gazetas, 1/10/91, (PB92-174994, A04, MF-A01).

NCEER-91-0004 "Damping of Structures: Part 1 - Theory of Complex Damping," by Z. Liang and G. Lee, 10/10/91, (PB92-197235, A12, MF-A03).

NCEER-91-0005 "3D-BASIS - Nonlinear Dynamic Analysis of Three Dimensional Base Isolated Structures: Part II," by S. Nagarajaiah, A.M. Reinhorn and M.C. Constantinou, 2/28/91, (PB91-190553, A07, MF-A01). This report has been replaced by NCEER-93-0011.

NCEER-91-0006 "A Multidimensional Hysteretic Model for Plasticity Deforming Metals in Energy Absorbing Devices," by E.J. Graesser and F.A. Cozzarelli, 4/9/91, (PB92-108364, A04, MF-A01).

NCEER-91-0007 "A Framework for Customizable Knowledge-Based Expert Systems with an Application to a KBES for Evaluating the Seismic Resistance of Existing Buildings," by E.G. Ibarra-Anaya and S.J. Fenves, 4/9/91, (PB91-210930, A08, MF-A01).

NCEER-91-0008 "Nonlinear Analysis of Steel Frames with Semi-Rigid Connections Using the Capacity Spectrum Method," by G.G. Deierlein, S-H. Hsieh, Y-J. Shen and J.F. Abel, 7/2/91, (PB92-113828, A05, MF-A01).

NCEER-91-0009 "Earthquake Education Materials for Grades K-12," by K.E.K. Ross, 4/30/91, (PB91-212142, A06, MF-A01). This report has been replaced by NCEER-92-0018.

NCEER-91-0010 "Phase Wave Velocities and Displacement Phase Differences in a Harmonically Oscillating Pile," by N. Makris and G. Gazetas, 7/8/91, (PB92-108356, A04, MF-A01).

NCEER-91-0011 "Dynamic Characteristics of a Full-Size Five-Story Steel Structure and a 2/5 Scale Model," by K.C. Chang, G.C. Yao, G.C. Lee, D.S. Hao and Y.C. Yeh," 7/2/91, (PB93-116648, A06, MF-A02).

NCEER-91-0012 "Seismic Response of a 2/5 Scale Steel Structure with Added Viscoelastic Dampers," by K.C. Chang, T.T. Soong, S-T. Oh and M.L. Lai, 5/17/91, (PB92-110816, A05, MF-A01).

NCEER-91-0013 "Earthquake Response of Retaining Walls; Full-Scale Testing and Computational Modeling," by S. Alampalli and A-W.M. Elgamal, 6/20/91, to be published.

NCEER-91-0014 "3D-BASIS-M: Nonlinear Dynamic Analysis of Multiple Building Base Isolated Structures," by P.C. Tsopelas, S. Nagarajaiah, M.C. Constantinou and A.M. Reinhorn, 5/28/91, (PB92-113885, A09, MF-A02).

NCEER-91-0015 "Evaluation of SEAOC Design Requirements for Sliding Isolated Structures," by D. Theodossiou and M.C. Constantinou, 6/10/91, (PB92-114602, A11, MF-A03).

NCEER-91-0016 "Closed-Loop Modal Testing of a 27-Story Reinforced Concrete Flat Plate-Core Building," by H.R. Somaprasad, T. Toksoy, H. Yoshiyuki and A.E. Aktan, 7/15/91, (PB92-129980, A07, MF-A02).

NCEER-91-0017 "Shake Table Test of a 1/6 Scale Two-Story Lightly Reinforced Concrete Building," by A.G. El-Attar, R.N. White and P. Gergely, 2/28/91, (PB92-222447, A06, MF-A02).

NCEER-91-0018 "Shake Table Test of a 1/8 Scale Three-Story Lightly Reinforced Concrete Building," by A.G. El-Attar, R.N. White and P. Gergely, 2/28/91, (PB93-116630, A08, MF-A02).

NCEER-91-0019 "Transfer Functions for Rigid Rectangular Foundations," by A.S. Veletsos, A.M. Prasad and W.H. Wu, 7/31/91, to be published.

NCEER-91-0020 "Hybrid Control of Seismic-Excited Nonlinear and Inelastic Structural Systems," by J.N. Yang, Z. Li and A. Danielians, 8/1/91, (PB92-143171, A06, MF-A02).

NCEER-91-0021 "The NCEER-91 Earthquake Catalog: Improved Intensity-Based Magnitudes and Recurrence Relations for U.S. Earthquakes East of New Madrid," by L. Seeber and J.G. Armbruster, 8/28/91, (PB92-176742, A06, MF-A02).

NCEER-91-0022 "Proceedings from the Implementation of Earthquake Planning and Education in Schools: The Need for Change - The Roles of the Changemakers," by K.E.K. Ross and F. Winslow, 7/23/91, (PB92-129998, A12, MF-A03).

NCEER-91-0023 "A Study of Reliability-Based Criteria for Seismic Design of Reinforced Concrete Frame Buildings," by H.H.M. Hwang and H-M. Hsu, 8/10/91, (PB92-140235, A09, MF-A02).

NCEER-91-0024 "Experimental Verification of a Number of Structural System Identification Algorithms," by R.G. Ghanem, H. Gavin and M. Shinozuka, 9/18/91, (PB92-176577, A18, MF-A04).

NCEER-91-0025 "Probabilistic Evaluation of Liquefaction Potential," by H.H.M. Hwang and C.S. Lee," 11/25/91, (PB92-143429, A05, MF-A01).

NCEER-91-0026 "Instantaneous Optimal Control for Linear, Nonlinear and Hysteretic Structures - Stable Controllers," by J.N. Yang and Z. Li, 11/15/91, (PB92-163807, A04, MF-A01).

NCEER-91-0027 "Experimental and Theoretical Study of a Sliding Isolation System for Bridges," by M.C. Constantinou, A. Kartoum, A.M. Reinhorn and P. Bradford, 11/15/91, (PB92-176973, A10, MF-A03).

NCEER-92-0001 "Case Studies of Liquefaction and Lifeline Performance During Past Earthquakes, Volume 1: Japanese Case Studies," Edited by M. Hamada and T. O'Rourke, 2/17/92, (PB92-197243, A18, MF-A04).

NCEER-92-0002 "Case Studies of Liquefaction and Lifeline Performance During Past Earthquakes, Volume 2: United States Case Studies," Edited by T. O'Rourke and M. Hamada, 2/17/92, (PB92-197250, A20, MF-A04).

NCEER-92-0003 "Issues in Earthquake Education," Edited by K. Ross, 2/3/92, (PB92-222389, A07, MF-A02).

NCEER-92-0004 "Proceedings from the First U.S. - Japan Workshop on Earthquake Protective Systems for Bridges," Edited by I.G. Buckle, 2/4/92, (PB94-142239, A99, MF-A06).

NCEER-92-0005 "Seismic Ground Motion from a Haskell-Type Source in a Multiple-Layered Half-Space," A.P. Theoharis, G. Deodatis and M. Shinozuka, 1/2/92, to be published.

NCEER-92-0006 "Proceedings from the Site Effects Workshop," Edited by R. Whitman, 2/29/92, (PB92-197201, A04, MF-A01).

NCEER-92-0007 "Engineering Evaluation of Permanent Ground Deformations Due to Seismically-Induced Liquefaction," by M.H. Baziar, R. Dobry and A-W.M. Elgamal, 3/24/92, (PB92-222421, A13, MF-A03).

NCEER-92-0008 "A Procedure for the Seismic Evaluation of Buildings in the Central and Eastern United States," by C.D. Poland and J.O. Malley, 4/2/92, (PB92-222439, A20, MF-A04).

NCEER-92-0009 "Experimental and Analytical Study of a Hybrid Isolation System Using Friction Controllable Sliding Bearings," by M.Q. Feng, S. Fujii and M. Shinozuka, 5/15/92, (PB93-150282, A06, MF-A02).

NCEER-92-0010 "Seismic Resistance of Slab-Column Connections in Existing Non-Ductile Flat-Plate Buildings," by A.J. Durrani and Y. Du, 5/18/92, (PB93-116812, A06, MF-A02).

NCEER-92-0011 "The Hysteretic and Dynamic Behavior of Brick Masonry Walls Upgraded by Ferrocement Coatings Under Cyclic Loading and Strong Simulated Ground Motion," by H. Lee and S.P. Prawel, 5/11/92, to be published.

NCEER-92-0012 "Study of Wire Rope Systems for Seismic Protection of Equipment in Buildings," by G.F. Demetriades, M.C. Constantinou and A.M. Reinhorn, 5/20/92, (PB93-116655, A08, MF-A02).

NCEER-92-0013 "Shape Memory Structural Dampers: Material Properties, Design and Seismic Testing," by P.R. Witting and F.A. Cozzarelli, 5/26/92, (PB93-116663, A05, MF-A01).

NCEER-92-0014 "Longitudinal Permanent Ground Deformation Effects on Buried Continuous Pipelines," by M.J. O'Rourke, and C. Nordberg, 6/15/92, (PB93-116671, A08, MF-A02).

NCEER-92-0015 "A Simulation Method for Stationary Gaussian Random Functions Based on the Sampling Theorem," by M. Grigoriu and S. Balopoulou, 6/11/92, (PB93-127496, A05, MF-A01).

NCEER-92-0016 "Gravity-Load-Designed Reinforced Concrete Buildings: Seismic Evaluation of Existing Construction and Detailing Strategies for Improved Seismic Resistance," by G.W. Hoffmann, S.K. Kunnath, A.M. Reinhorn and J.B. Mander, 7/15/92, (PB94-142007, A08, MF-A02).

NCEER-92-0017 "Observations on Water System and Pipeline Performance in the Limón Area of Costa Rica Due to the April 22, 1991 Earthquake," by M. O'Rourke and D. Ballantyne, 6/30/92, (PB93-126811, A06, MF-A02).

NCEER-92-0018 "Fourth Edition of Earthquake Education Materials for Grades K-12," Edited by K.E.K. Ross, 8/10/92, (PB93-114023, A07, MF-A02).

NCEER-92-0019 "Proceedings from the Fourth Japan-U.S. Workshop on Earthquake Resistant Design of Lifeline Facilities and Countermeasures for Soil Liquefaction," Edited by M. Hamada and T.D. O'Rourke, 8/12/92, (PB93-163939, A99, MF-E11).

NCEER-92-0020 "Active Bracing System: A Full Scale Implementation of Active Control," by A.M. Reinhorn, T.T. Soong, R.C. Lin, M.A. Riley, Y.P. Wang, S. Aizawa and M. Higashino, 8/14/92, (PB93-127512, A06, MF-A02).

NCEER-92-0021 "Empirical Analysis of Horizontal Ground Displacement Generated by Liquefaction-Induced Lateral Spreads," by S.F. Bartlett and T.L. Youd, 8/17/92, (PB93-188241, A06, MF-A02).

NCEER-92-0022 "IDARC Version 3.0: Inelastic Damage Analysis of Reinforced Concrete Structures," by S.K. Kunnath, A.M. Reinhorn and R.F. Lobo, 8/31/92, (PB93-227502, A07, MF-A02).

NCEER-92-0023 "A Semi-Empirical Analysis of Strong-Motion Peaks in Terms of Seismic Source, Propagation Path and Local Site Conditions, by M. Kamiyama, M.J. O'Rourke and R. Flores-Berrones, 9/9/92, (PB93-150266, A08, MF-A02).

NCEER-92-0024 "Seismic Behavior of Reinforced Concrete Frame Structures with Nonductile Details, Part I: Summary of Experimental Findings of Full Scale Beam-Column Joint Tests," by A. Beres, R.N. White and P. Gergely, 9/30/92, (PB93-227783, A05, MF-A01).

NCEER-92-0025 "Experimental Results of Repaired and Retrofitted Beam-Column Joint Tests in Lightly Reinforced Concrete Frame Buildings," by A. Beres, S. El-Borgi, R.N. White and P. Gergely, 10/29/92, (PB93-227791, A05, MF-A01).

NCEER-92-0026 "A Generalization of Optimal Control Theory: Linear and Nonlinear Structures," by J.N. Yang, Z. Li and S. Vongchavalitkul, 11/2/92, (PB93-188621, A05, MF-A01).

NCEER-92-0027 "Seismic Resistance of Reinforced Concrete Frame Structures Designed Only for Gravity Loads: Part I - Design and Properties of a One-Third Scale Model Structure," by J.M. Bracci, A.M. Reinhorn and J.B. Mander, 12/1/92, (PB94-104502, A08, MF-A02).

NCEER-92-0028 "Seismic Resistance of Reinforced Concrete Frame Structures Designed Only for Gravity Loads: Part II - Experimental Performance of Subassemblages," by L.E. Aycardi, J.B. Mander and A.M. Reinhorn, 12/1/92, (PB94-104510, A08, MF-A02).

NCEER-92-0029 "Seismic Resistance of Reinforced Concrete Frame Structures Designed Only for Gravity Loads: Part III - Experimental Performance and Analytical Study of a Structural Model," by J.M. Bracci, A.M. Reinhorn and J.B. Mander, 12/1/92, (PB93-227528, A09, MF-A01).

NCEER-92-0030 "Evaluation of Seismic Retrofit of Reinforced Concrete Frame Structures: Part I - Experimental Performance of Retrofitted Subassemblages," by D. Choudhuri, J.B. Mander and A.M. Reinhorn, 12/8/92, (PB93-198307, A07, MF-A02).

NCEER-92-0031 "Evaluation of Seismic Retrofit of Reinforced Concrete Frame Structures: Part II - Experimental Performance and Analytical Study of a Retrofitted Structural Model," by J.M. Bracci, A.M. Reinhorn and J.B. Mander, 12/8/92, (PB93-198315, A09, MF-A03).

NCEER-92-0032 "Experimental and Analytical Investigation of Seismic Response of Structures with Supplemental Fluid Viscous Dampers," by M.C. Constantinou and M.D. Symans, 12/21/92, (PB93-191435, A10, MF-A03). This report is available only through NTIS (see address given above).

NCEER-92-0033 "Reconnaissance Report on the Cairo, Egypt Earthquake of October 12, 1992," by M. Khater, 12/23/92, (PB93-188621, A03, MF-A01).

NCEER-92-0034 "Low-Level Dynamic Characteristics of Four Tall Flat-Plate Buildings in New York City," by H. Gavin, S. Yuan, J. Grossman, E. Pekelis and K. Jacob, 12/28/92, (PB93-188217, A07, MF-A02).

NCEER-93-0001 "An Experimental Study on the Seismic Performance of Brick-Infilled Steel Frames With and Without Retrofit," by J.B. Mander, B. Nair, K. Wojtkowski and J. Ma, 1/29/93, (PB93-227510, A07, MF-A02).

NCEER-93-0002 "Social Accounting for Disaster Preparedness and Recovery Planning," by S. Cole, E. Pantoja and V. Razak, 2/22/93, (PB94-142114, A12, MF-A03).

NCEER-93-0003 "Assessment of 1991 NEHRP Provisions for Nonstructural Components and Recommended Revisions," by T.T. Soong, G. Chen, Z. Wu, R-H. Zhang and M. Grigoriu, 3/1/93, (PB93-188639, A06, MF-A02).

NCEER-93-0004 "Evaluation of Static and Response Spectrum Analysis Procedures of SEAOC/UBC for Seismic Isolated Structures," by C.W. Winters and M.C. Constantinou, 3/23/93, (PB93-198299, A10, MF-A03).

NCEER-93-0005 "Earthquakes in the Northeast - Are We Ignoring the Hazard? A Workshop on Earthquake Science and Safety for Educators," edited by K.E.K. Ross, 4/2/93, (PB94-103066, A09, MF-A02).

NCEER-93-0006 "Inelastic Response of Reinforced Concrete Structures with Viscoelastic Braces," by R.F. Lobo, J.M. Bracci, K.L. Shen, A.M. Reinhorn and T.T. Soong, 4/5/93, (PB93-227486, A05, MF-A02).

NCEER-93-0007 "Seismic Testing of Installation Methods for Computers and Data Processing Equipment," by K. Kosar, T.T. Soong, K.L. Shen, J.A. HoLung and Y.K. Lin, 4/12/93, (PB93-198299, A07, MF-A02).

NCEER-93-0008 "Retrofit of Reinforced Concrete Frames Using Added Dampers," by A. Reinhorn, M. Constantinou and C. Li, to be published.

NCEER-93-0009 "Seismic Behavior and Design Guidelines for Steel Frame Structures with Added Viscoelastic Dampers," by K.C. Chang, M.L. Lai, T.T. Soong, D.S. Hao and Y.C. Yeh, 5/1/93, (PB94-141959, A07, MF-A02).

NCEER-93-0010 "Seismic Performance of Shear-Critical Reinforced Concrete Bridge Piers," by J.B. Mander, S.M. Waheed, M.T.A. Chaudhary and S.S. Chen, 5/12/93, (PB93-227494, A08, MF-A02).

NCEER-93-0011 "3D-BASIS-TABS: Computer Program for Nonlinear Dynamic Analysis of Three Dimensional Base Isolated Structures," by S. Nagarajaiah, C. Li, A.M. Reinhorn and M.C. Constantinou, 8/2/93, (PB94-141819, A09, MF-A02).

NCEER-93-0012 "Effects of Hydrocarbon Spills from an Oil Pipeline Break on Ground Water," by O.J. Helweg and H.H.M. Hwang, 8/3/93, (PB94-141942, A06, MF-A02).

NCEER-93-0013 "Simplified Procedures for Seismic Design of Nonstructural Components and Assessment of Current Code Provisions," by M.P. Singh, L.E. Suarez, E.E. Matheu and G.O. Maldonado, 8/4/93, (PB94-141827, A09, MF-A02).

NCEER-93-0014 "An Energy Approach to Seismic Analysis and Design of Secondary Systems," by G. Chen and T.T. Soong, 8/6/93, (PB94-142767, A11, MF-A03).

NCEER-93-0015 "Proceedings from School Sites: Becoming Prepared for Earthquakes - Commemorating the Third Anniversary of the Loma Prieta Earthquake," Edited by F.E. Winslow and K.E.K. Ross, 8/16/93, (PB94-154275, A16, MF-A02).

NCEER-93-0016 "Reconnaissance Report of Damage to Historic Monuments in Cairo, Egypt Following the October 12, 1992 Dahshur Earthquake," by D. Sykora, D. Look, G. Croci, E. Karaesmen and E. Karaesmen, 8/19/93, (PB94-142221, A08, MF-A02).

NCEER-93-0017 "The Island of Guam Earthquake of August 8, 1993," by S.W. Swan and S.K. Harris, 9/30/93, (PB94-141843, A04, MF-A01).

NCEER-93-0018 "Engineering Aspects of the October 12, 1992 Egyptian Earthquake," by A.W. Elgamal, M. Amer, K. Adalier and A. Abul-Fadl, 10/7/93, (PB94-141983, A05, MF-A01).

NCEER-93-0019 "Development of an Earthquake Motion Simulator and its Application in Dynamic Centrifuge Testing," by I. Krstelj, Supervised by J.H. Prevost, 10/23/93, (PB94-181773, A-10, MF-A03).

NCEER-93-0020 "NCEER-Taisei Corporation Research Program on Sliding Seismic Isolation Systems for Bridges: Experimental and Analytical Study of a Friction Pendulum System (FPS)," by M.C. Constantinou, P. Tsopelas, Y-S. Kim and S. Okamoto, 11/1/93, (PB94-142775, A08, MF-A02).

NCEER-93-0021 "Finite Element Modeling of Elastomeric Seismic Isolation Bearings," by L.J. Billings, Supervised by R. Shepherd, 11/8/93, to be published.

NCEER-93-0022 "Seismic Vulnerability of Equipment in Critical Facilities: Life-Safety and Operational Consequences," by K. Porter, G.S. Johnson, M.M. Zadeh, C. Scawthorn and S. Eder, 11/24/93, (PB94-181765, A16, MF-A03).

NCEER-93-0023 "Hokkaido Nansei-oki, Japan Earthquake of July 12, 1993, by P.I. Yanev and C.R. Scawthorn, 12/23/93, (PB94-181500, A07, MF-A01).

NCEER-94-0001 "An Evaluation of Seismic Serviceability of Water Supply Networks with Application to the San Francisco Auxiliary Water Supply System," by I. Markov, Supervised by M. Grigoriu and T. O'Rourke, 1/21/94, (PB94-204013, A07, MF-A02).

NCEER-94-0002 "NCEER-Taisei Corporation Research Program on Sliding Seismic Isolation Systems for Bridges: Experimental and Analytical Study of Systems Consisting of Sliding Bearings, Rubber Restoring Force Devices and Fluid Dampers," Volumes I and II, by P. Tsopelas, S. Okamoto, M.C. Constantinou, D. Ozaki and S. Fujii, 2/4/94, (PB94-181740, A09, MF-A02 and PB94-181757, A12, MF-A03).

NCEER-94-0003 "A Markov Model for Local and Global Damage Indices in Seismic Analysis," by S. Rahman and M. Grigoriu, 2/18/94, (PB94-206000, A12, MF-A03).

NCEER-94-0004 "Proceedings from the NCEER Workshop on Seismic Response of Masonry Infills," edited by D.P. Abrams, 3/1/94, (PB94-180783, A07, MF-A02).

NCEER-94-0005 "The Northridge, California Earthquake of January 17, 1994: General Reconnaissance Report," edited by J.D. Goltz, 3/11/94, (PB94-193943, A10, MF-A03).

NCEER-94-0006 "Seismic Energy Based Fatigue Damage Analysis of Bridge Columns: Part I - Evaluation of Seismic Capacity," by G.A. Chang and J.B. Mander, 3/14/94, (PB94-219185, A11, MF-A03).

NCEER-94-0007 "Seismic Isolation of Multi-Story Frame Structures Using Spherical Sliding Isolation Systems," by T.M. Al-Hussaini, V.A. Zayas and M.C. Constantinou, 3/17/94, (PB94-193745, A09, MF-A02).

NCEER-94-0008 "The Northridge, California Earthquake of January 17, 1994: Performance of Highway Bridges," edited by I.G. Buckle, 3/24/94, (PB94-193851, A06, MF-A02).

NCEER-94-0009 "Proceedings of the Third U.S.-Japan Workshop on Earthquake Protective Systems for Bridges," edited by I.G. Buckle and I. Friedland, 3/31/94, (PB94-195815, A99, MF-A06).

NCEER-94-0010 "3D-BASIS-ME: Computer Program for Nonlinear Dynamic Analysis of Seismically Isolated Single and Multiple Structures and Liquid Storage Tanks," by P.C. Tsopelas, M.C. Constantinou and A.M. Reinhorn, 4/12/94, (PB94-204922, A09, MF-A02).

NCEER-94-0011 "The Northridge, California Earthquake of January 17, 1994: Performance of Gas Transmission Pipelines," by T.D. O'Rourke and M.C. Palmer, 5/16/94, (PB94-204989, A05, MF-A01).

NCEER-94-0012 "Feasibility Study of Replacement Procedures and Earthquake Performance Related to Gas Transmission Pipelines," by T.D. O'Rourke and M.C. Palmer, 5/25/94, (PB94-206638, A09, MF-A02).

NCEER-94-0013 "Seismic Energy Based Fatigue Damage Analysis of Bridge Columns: Part II - Evaluation of Seismic Demand," by G.A. Chang and J.B. Mander, 6/1/94, (PB95-18106, A08, MF-A02).

NCEER-94-0014 "NCEER-Taisei Corporation Research Program on Sliding Seismic Isolation Systems for Bridges: Experimental and Analytical Study of a System Consisting of Sliding Bearings and Fluid Restoring Force/Damping Devices," by P. Tsopelas and M.C. Constantinou, 6/13/94, (PB94-219144, A10, MF-A03).

NCEER-94-0015 "Generation of Hazard-Consistent Fragility Curves for Seismic Loss Estimation Studies," by H. Hwang and J-R. Huo, 6/14/94, (PB95-181996, A09, MF-A02).

NCEER-94-0016 "Seismic Study of Building Frames with Added Energy-Absorbing Devices," by W.S. Pong, C.S. Tsai and G.C. Lee, 6/20/94, (PB94-219136, A10, A03).

NCEER-94-0017 "Sliding Mode Control for Seismic-Excited Linear and Nonlinear Civil Engineering Structures," by J. Yang, J. Wu, A. Agrawal and Z. Li, 6/21/94, (PB95-138483, A06, MF-A02).

NCEER-94-0018 "3D-BASIS-TABS Version 2.0: Computer Program for Nonlinear Dynamic Analysis of Three Dimensional Base Isolated Structures," by A.M. Reinhorn, S. Nagarajaiah, M.C. Constantinou, P. Tsopelas and R. Li, 6/22/94, (PB95-182176, A08, MF-A02).

NCEER-94-0019 "Proceedings of the International Workshop on Civil Infrastructure Systems: Application of Intelligent Systems and Advanced Materials on Bridge Systems," Edited by G.C. Lee and K.C. Chang, 7/18/94, (PB95-252474, A20, MF-A04).

NCEER-94-0020 "Study of Seismic Isolation Systems for Computer Floors," by V. Lambrou and M.C. Constantinou, 7/19/94, (PB95-138533, A10, MF-A03).

NCEER-94-0021 "Proceedings of the U.S.-Italian Workshop on Guidelines for Seismic Evaluation and Rehabilitation of Unreinforced Masonry Buildings," Edited by D.P. Abrams and G.M. Calvi, 7/20/94, (PB95-138749, A13, MF-A03).

NCEER-94-0022 "NCEER-Taisei Corporation Research Program on Sliding Seismic Isolation Systems for Bridges: Experimental and Analytical Study of a System Consisting of Lubricated PTFE Sliding Bearings and Mild Steel Dampers," by P. Tsopelas and M.C. Constantinou, 7/22/94, (PB95-182184, A08, MF-A02).

NCEER-94-0023 “Development of Reliability-Based Design Criteria for Buildings Under Seismic Load,” by Y.K. Wen, H. Hwang and M. Shinozuka, 8/1/94, (PB95-211934, A08, MF-A02).

NCEER-94-0024 “Experimental Verification of Acceleration Feedback Control Strategies for an Active Tendon System,” by S.J. Dyke, B.F. Spencer, Jr., P. Quast, M.K. Sain, D.C. Kaspari, Jr. and T.T. Soong, 8/29/94, (PB95-212320, A05, MF-A01).

NCEER-94-0025 “Seismic Retrofitting Manual for Highway Bridges,” Edited by I.G. Buckle and I.F. Friedland, published by the Federal Highway Administration (PB95-212676, A15, MF-A03).

NCEER-94-0026 “Proceedings from the Fifth U.S.-Japan Workshop on Earthquake Resistant Design of Lifeline Facilities and Countermeasures Against Soil Liquefaction,” Edited by T.D. O’Rourke and M. Hamada, 11/7/94, (PB95-220802, A99, MF-E08).

NCEER-95-0001 "Experimental and Analytical Investigation of Seismic Retrofit of Structures with Supplemental Damping: Part 1 - Fluid Viscous Damping Devices," by A.M. Reinhorn, C. Li and M.C. Constantinou, 1/3/95, (PB95-266599, A09, MF-A02).

NCEER-95-0002 "Experimental and Analytical Study of Low-Cycle Fatigue Behavior of Semi-Rigid Top-And-Seat Angle Connections," by G. Pekcan, J.B. Mander and S.S. Chen, 1/5/95, (PB95-220042, A07, MF-A02).

NCEER-95-0003 "NCEER-ATC Joint Study on Fragility of Buildings," by T. Anagnos, C. Rojahn and A.S. Kiremidjian, 1/20/95, (PB95-220026, A06, MF-A02).

NCEER-95-0004 "Nonlinear Control Algorithms for Peak Response Reduction," by Z. Wu, T.T. Soong, V. Gattulli and R.C. Lin, 2/16/95, (PB95-220349, A05, MF-A01).

NCEER-95-0005 "Pipeline Replacement Feasibility Study: A Methodology for Minimizing Seismic and Corrosion Risks to Underground Natural Gas Pipelines," by R.T. Eguchi, H.A. Seligson and D.G. Honegger, 3/2/95, (PB95-252326, A06, MF-A02).

NCEER-95-0006 "Evaluation of Seismic Performance of an 11-Story Frame Building During the 1994 Northridge Earthquake," by F. Naeim, R. DiSulio, K. Benuska, A. Reinhorn and C. Li, to be published.

NCEER-95-0007 "Prioritization of Bridges for Seismic Retrofitting," by N. Basöz and A.S. Kiremidjian, 4/24/95, (PB95-252300, A08, MF-A02).

NCEER-95-0008 "Method for Developing Motion Damage Relationships for Reinforced Concrete Frames," by A. Singhal and A.S. Kiremidjian, 5/11/95, (PB95-266607, A06, MF-A02).

NCEER-95-0009 "Experimental and Analytical Investigation of Seismic Retrofit of Structures with Supplemental Damping: Part II - Friction Devices," by C. Li and A.M. Reinhorn, 7/6/95, (PB96-128087, A11, MF-A03).

NCEER-95-0010 "Experimental Performance and Analytical Study of a Non-Ductile Reinforced Concrete Frame Structure Retrofitted with Elastomeric Spring Dampers," by G. Pekcan, J.B. Mander and S.S. Chen, 7/14/95, (PB96-137161, A08, MF-A02).

NCEER-95-0011 "Development and Experimental Study of Semi-Active Fluid Damping Devices for Seismic Protection of Structures," by M.D. Symans and M.C. Constantinou, 8/3/95, (PB96-136940, A23, MF-A04).

NCEER-95-0012 "Real-Time Structural Parameter Modification (RSPM): Development of Innervated Structures," by Z. Liang, M. Tong and G.C. Lee, 4/11/95, (PB96-137153, A06, MF-A01).

NCEER-95-0013 "Experimental and Analytical Investigation of Seismic Retrofit of Structures with Supplemental Damping: Part III - Viscous Damping Walls," by A.M. Reinhorn and C. Li, 10/1/95, (PB96-176409, A11, MF-A03).

NCEER-95-0014 "Seismic Fragility Analysis of Equipment and Structures in a Memphis Electric Substation," by J-R. Huo and H.H.M. Hwang, 8/10/95, (PB96-128087, A09, MF-A02).

NCEER-95-0015 "The Hanshin-Awaji Earthquake of January 17, 1995: Performance of Lifelines," Edited by M. Shinozuka, 11/3/95, (PB96-176383, A15, MF-A03).

NCEER-95-0016 "Highway Culvert Performance During Earthquakes," by T.L. Youd and C.J. Beckman, available as NCEER-96-0015.

NCEER-95-0017 "The Hanshin-Awaji Earthquake of January 17, 1995: Performance of Highway Bridges," Edited by I.G. Buckle, 12/1/95, to be published.

NCEER-95-0018 "Modeling of Masonry Infill Panels for Structural Analysis," by A.M. Reinhorn, A. Madan, R.E. Valles, Y. Reichmann and J.B. Mander, 12/8/95, (PB97-110886, MF-A01, A06).

NCEER-95-0019 "Optimal Polynomial Control for Linear and Nonlinear Structures," by A.K. Agrawal and J.N. Yang, 12/11/95, (PB96-168737, A07, MF-A02).

NCEER-95-0020 "Retrofit of Non-Ductile Reinforced Concrete Frames Using Friction Dampers," by R.S. Rao, P. Gergely and R.N. White, 12/22/95, (PB97-133508, A10, MF-A02).

NCEER-95-0021 "Parametric Results for Seismic Response of Pile-Supported Bridge Bents," by G. Mylonakis, A. Nikolaou and G. Gazetas, 12/22/95, (PB97-100242, A12, MF-A03).

NCEER-95-0022 "Kinematic Bending Moments in Seismically Stressed Piles," by A. Nikolaou, G. Mylonakis and G. Gazetas, 12/23/95, (PB97-113914, MF-A03, A13).

NCEER-96-0001 "Dynamic Response of Unreinforced Masonry Buildings with Flexible Diaphragms," by A.C. Costley and D.P. Abrams," 10/10/96, (PB97-133573, MF-A03, A15).

NCEER-96-0002 "State of the Art Review: Foundations and Retaining Structures," by I. Po Lam, to be published.

NCEER-96-0003 "Ductility of Rectangular Reinforced Concrete Bridge Columns with Moderate Confinement," by N. Wehbe, M. Saiidi, D. Sanders and B. Douglas, 11/7/96, (PB97-133557, A06, MF-A02).

NCEER-96-0004 "Proceedings of the Long-Span Bridge Seismic Research Workshop," edited by I.G. Buckle and I.M. Friedland, to be published.

NCEER-96-0005 "Establish Representative Pier Types for Comprehensive Study: Eastern United States," by J. Kulicki and Z. Prucz, 5/28/96, (PB98-119217, A07, MF-A02).

NCEER-96-0006 "Establish Representative Pier Types for Comprehensive Study: Western United States," by R. Imbsen, R.A. Schamber and T.A. Osterkamp, 5/28/96, (PB98-118607, A07, MF-A02).

NCEER-96-0007 "Nonlinear Control Techniques for Dynamical Systems with Uncertain Parameters," by R.G. Ghanem and M.I. Bujakov, 5/27/96, (PB97-100259, A17, MF-A03).

NCEER-96-0008 "Seismic Evaluation of a 30-Year Old Non-Ductile Highway Bridge Pier and Its Retrofit," by J.B. Mander, B. Mahmoodzadegan, S. Bhadra and S.S. Chen, 5/31/96, (PB97-110902, MF-A03, A10).

NCEER-96-0009 "Seismic Performance of a Model Reinforced Concrete Bridge Pier Before and After Retrofit," by J.B. Mander, J.H. Kim and C.A. Ligozio, 5/31/96, (PB97-110910, MF-A02, A10).

NCEER-96-0010 "IDARC2D Version 4.0: A Computer Program for the Inelastic Damage Analysis of Buildings," by R.E. Valles, A.M. Reinhorn, S.K. Kunnath, C. Li and A. Madan, 6/3/96, (PB97-100234, A17, MF-A03).

NCEER-96-0011 "Estimation of the Economic Impact of Multiple Lifeline Disruption: Memphis Light, Gas and Water Division Case Study," by S.E. Chang, H.A. Seligson and R.T. Eguchi, 8/16/96, (PB97-133490, A11, MF-A03).

NCEER-96-0012 "Proceedings from the Sixth Japan-U.S. Workshop on Earthquake Resistant Design of Lifeline Facilities and Countermeasures Against Soil Liquefaction, Edited by M. Hamada and T. O'Rourke, 9/11/96, (PB97-133581, A99, MF-A06).

NCEER-96-0013 "Chemical Hazards, Mitigation and Preparedness in Areas of High Seismic Risk: A Methodology for Estimating the Risk of Post-Earthquake Hazardous Materials Release," by H.A. Seligson, R.T. Eguchi, K.J. Tierney and K. Richmond, 11/7/96, (PB97-133565, MF-A02, A08).

NCEER-96-0014 "Response of Steel Bridge Bearings to Reversed Cyclic Loading," by J.B. Mander, D-K. Kim, S.S. Chen and G.J. Premus, 11/13/96, (PB97-140735, A12, MF-A03).

NCEER-96-0015 "Highway Culvert Performance During Past Earthquakes," by T.L. Youd and C.J. Beckman, 11/25/96, (PB97-133532, A06, MF-A01).

NCEER-97-0001 "Evaluation, Prevention and Mitigation of Pounding Effects in Building Structures," by R.E. Valles and A.M. Reinhorn, 2/20/97, (PB97-159552, A14, MF-A03).

NCEER-97-0002 "Seismic Design Criteria for Bridges and Other Highway Structures," by C. Rojahn, R. Mayes, D.G. Anderson, J. Clark, J.H. Hom, R.V. Nutt and M.J. O'Rourke, 4/30/97, (PB97-194658, A06, MF-A03).

NCEER-97-0003 “Proceedings of the U.S.-Italian Workshop on Seismic Evaluation and Retrofit,” Edited by D.P. Abrams and G.M. Calvi, 3/19/97, (PB97-194666, A13, MF-A03).

NCEER-97-0004 "Investigation of Seismic Response of Buildings with Linear and Nonlinear Fluid Viscous Dampers," by A.A. Seleemah and M.C. Constantinou, 5/21/97, (PB98-109002, A15, MF-A03).

NCEER-97-0005 "Proceedings of the Workshop on Earthquake Engineering Frontiers in Transportation Facilities," edited by G.C. Lee and I.M. Friedland, 8/29/97, (PB98-128911, A25, MR-A04).

NCEER-97-0006 "Cumulative Seismic Damage of Reinforced Concrete Bridge Piers," by S.K. Kunnath, A. El-Bahy, A. Taylor and W. Stone, 9/2/97, (PB98-108814, A11, MF-A03).

NCEER-97-0007 "Structural Details to Accommodate Seismic Movements of Highway Bridges and Retaining Walls," by R.A. Imbsen, R.A. Schamber, E. Thorkildsen, A. Kartoum, B.T. Martin, T.N. Rosser and J.M. Kulicki, 9/3/97, (PB98-108996, A09, MF-A02).

NCEER-97-0008 "A Method for Earthquake Motion-Damage Relationships with Application to Reinforced Concrete Frames," by A. Singhal and A.S. Kiremidjian, 9/10/97, (PB98-108988, A13, MF-A03).

NCEER-97-0009 "Seismic Analysis and Design of Bridge Abutments Considering Sliding and Rotation," by K. Fishman and R. Richards, Jr., 9/15/97, (PB98-108897, A06, MF-A02).

NCEER-97-0010 "Proceedings of the FHWA/NCEER Workshop on the National Representation of Seismic Ground Motion for New and Existing Highway Facilities," edited by I.M. Friedland, M.S. Power and R.L. Mayes, 9/22/97, (PB98-128903, A21, MF-A04).

NCEER-97-0011 "Seismic Analysis for Design or Retrofit of Gravity Bridge Abutments," by K.L. Fishman, R. Richards, Jr. and R.C. Divito, 10/2/97, (PB98-128937, A08, MF-A02).

NCEER-97-0012 "Evaluation of Simplified Methods of Analysis for Yielding Structures," by P. Tsopelas, M.C. Constantinou, C.A. Kircher and A.S. Whittaker, 10/31/97, (PB98-128929, A10, MF-A03).

NCEER-97-0013 "Seismic Design of Bridge Columns Based on Control and Repairability of Damage," by C-T. Cheng and J.B. Mander, 12/8/97, (PB98-144249, A11, MF-A03).

NCEER-97-0014 "Seismic Resistance of Bridge Piers Based on Damage Avoidance Design," by J.B. Mander and C-T. Cheng, 12/10/97, (PB98-144223, A09, MF-A02).

NCEER-97-0015 “Seismic Response of Nominally Symmetric Systems with Strength Uncertainty,” by S. Balopoulou and M. Grigoriu, 12/23/97, (PB98-153422, A11, MF-A03).

NCEER-97-0016 “Evaluation of Seismic Retrofit Methods for Reinforced Concrete Bridge Columns,” by T.J. Wipf, F.W. Klaiber and F.M. Russo, 12/28/97, (PB98-144215, A12, MF-A03).

NCEER-97-0017 “Seismic Fragility of Existing Conventional Reinforced Concrete Highway Bridges,” by C.L. Mullen and A.S. Cakmak, 12/30/97, (PB98-153406, A08, MF-A02).

NCEER-97-0018 “Loss Asssessment of Memphis Buildings,” edited by D.P. Abrams and M. Shinozuka, 12/31/97, (PB98-144231, A13, MF-A03).

NCEER-97-0019 “Seismic Evaluation of Frames with Infill Walls Using Quasi-static Experiments,” by K.M. Mosalam, R.N. White and P. Gergely, 12/31/97, (PB98-153455, A07, MF-A02).

NCEER-97-0020 “Seismic Evaluation of Frames with Infill Walls Using Pseudo-dynamic Experiments,” by K.M. Mosalam, R.N. White and P. Gergely, 12/31/97, (PB98-153430, A07, MF-A02).

NCEER-97-0021 “Computational Strategies for Frames with Infill Walls: Discrete and Smeared Crack Analyses and Seismic Fragility,” by K.M. Mosalam, R.N. White and P. Gergely, 12/31/97, (PB98-153414, A10, MF-A02).

NCEER-97-0022 "Proceedings of the NCEER Workshop on Evaluation of Liquefaction Resistance of Soils," edited by T.L. Youd and I.M. Idriss, 12/31/97, (PB98-155617, A15, MF-A03).

MCEER-98-0001 "Extraction of Nonlinear Hysteretic Properties of Seismically Isolated Bridges from Quick-Release Field Tests," by Q. Chen, B.M. Douglas, E.M. Maragakis and I.G. Buckle, 5/26/98, (PB99-118838, A06, MF-A01).

MCEER-98-0002 "Methodologies for Evaluating the Importance of Highway Bridges," by A. Thomas, S. Eshenaur and J. Kulicki, 5/29/98, (PB99-118846, A10, MF-A02).

MCEER-98-0003 "Capacity Design of Bridge Piers and the Analysis of Overstrength," by J.B. Mander, A. Dutta and P. Goel, 6/1/98, (PB99-118853, A09, MF-A02).

MCEER-98-0004 "Evaluation of Bridge Damage Data from the Loma Prieta and Northridge, California Earthquakes," by N. Basoz and A. Kiremidjian, 6/2/98, (PB99-118861, A15, MF-A03).

MCEER-98-0005 "Screening Guide for Rapid Assessment of Liquefaction Hazard at Highway Bridge Sites," by T. L. Youd, 6/16/98, (PB99-118879, A06, not available on microfiche).

MCEER-98-0006 "Structural Steel and Steel/Concrete Interface Details for Bridges," by P. Ritchie, N. Kauhl and J. Kulicki, 7/13/98, (PB99-118945, A06, MF-A01).

MCEER-98-0007 "Capacity Design and Fatigue Analysis of Confined Concrete Columns," by A. Dutta and J.B. Mander, 7/14/98, (PB99-118960, A14, MF-A03).

MCEER-98-0008 "Proceedings of the Workshop on Performance Criteria for Telecommunication Services Under Earthquake Conditions," edited by A.J. Schiff, 7/15/98, (PB99-118952, A08, MF-A02).

MCEER-98-0009 "Fatigue Analysis of Unconfined Concrete Columns," by J.B. Mander, A. Dutta and J.H. Kim, 9/12/98, (PB99-123655, A10, MF-A02).

MCEER-98-0010 "Centrifuge Modeling of Cyclic Lateral Response of Pile-Cap Systems and Seat-Type Abutments in Dry Sands," by A.D. Gadre and R. Dobry, 10/2/98, (PB99-123606, A13, MF-A03).

MCEER-98-0011 "IDARC-BRIDGE: A Computational Platform for Seismic Damage Assessment of Bridge Structures," by A.M. Reinhorn, V. Simeonov, G. Mylonakis and Y. Reichman, 10/2/98, (PB99-162919, A15, MF-A03).

MCEER-98-0012 "Experimental Investigation of the Dynamic Response of Two Bridges Before and After Retrofitting with Elastomeric Bearings," by D.A. Wendichansky, S.S. Chen and J.B. Mander, 10/2/98, (PB99-162927, A15, MF-A03).

MCEER-98-0013 "Design Procedures for Hinge Restrainers and Hinge Sear Width for Multiple-Frame Bridges," by R. Des Roches and G.L. Fenves, 11/3/98, (PB99-140477, A13, MF-A03).

MCEER-98-0014 "Response Modification Factors for Seismically Isolated Bridges," by M.C. Constantinou and J.K. Quarshie, 11/3/98, (PB99-140485, A14, MF-A03).

MCEER-98-0015 "Proceedings of the U.S.-Italy Workshop on Seismic Protective Systems for Bridges," edited by I.M. Friedland and M.C. Constantinou, 11/3/98, (PB2000-101711, A22, MF-A04).

MCEER-98-0016 "Appropriate Seismic Reliability for Critical Equipment Systems: Recommendations Based on Regional Analysis of Financial and Life Loss," by K. Porter, C. Scawthorn, C. Taylor and N. Blais, 11/10/98, (PB99-157265, A08, MF-A02).

MCEER-98-0017 "Proceedings of the U.S. Japan Joint Seminar on Civil Infrastructure Systems Research," edited by M. Shinozuka and A. Rose, 11/12/98, (PB99-156713, A16, MF-A03).

MCEER-98-0018 "Modeling of Pile Footings and Drilled Shafts for Seismic Design," by I. PoLam, M. Kapuskar and D. Chaudhuri, 12/21/98, (PB99-157257, A09, MF-A02).

MCEER-99-0001 "Seismic Evaluation of a Masonry Infilled Reinforced Concrete Frame by Pseudodynamic Testing," by S.G. Buonopane and R.N. White, 2/16/99, (PB99-162851, A09, MF-A02).

MCEER-99-0002 "Response History Analysis of Structures with Seismic Isolation and Energy Dissipation Systems: Verification Examples for Program SAP2000," by J. Scheller and M.C. Constantinou, 2/22/99, (PB99-162869, A08, MF-A02).

MCEER-99-0003 "Experimental Study on the Seismic Design and Retrofit of Bridge Columns Including Axial Load Effects," by A. Dutta, T. Kokorina and J.B. Mander, 2/22/99, (PB99-162877, A09, MF-A02).

MCEER-99-0004 "Experimental Study of Bridge Elastomeric and Other Isolation and Energy Dissipation Systems with Emphasis on Uplift Prevention and High Velocity Near-source Seismic Excitation," by A. Kasalanati and M. C. Constantinou, 2/26/99, (PB99-162885, A12, MF-A03).

MCEER-99-0005 "Truss Modeling of Reinforced Concrete Shear-flexure Behavior," by J.H. Kim and J.B. Mander, 3/8/99, (PB99-163693, A12, MF-A03).

MCEER-99-0006 "Experimental Investigation and Computational Modeling of Seismic Response of a 1:4 Scale Model Steel Structure with a Load Balancing Supplemental Damping System," by G. Pekcan, J.B. Mander and S.S. Chen, 4/2/99, (PB99-162893, A11, MF-A03).

MCEER-99-0007 "Effect of Vertical Ground Motions on the Structural Response of Highway Bridges," by M.R. Button, C.J. Cronin and R.L. Mayes, 4/10/99, (PB2000-101411, A10, MF-A03).

MCEER-99-0008 "Seismic Reliability Assessment of Critical Facilities: A Handbook, Supporting Documentation, and Model Code Provisions," by G.S. Johnson, R.E. Sheppard, M.D. Quilici, S.J. Eder and C.R. Scawthorn, 4/12/99, (PB2000-101701, A18, MF-A04).

MCEER-99-0009 "Impact Assessment of Selected MCEER Highway Project Research on the Seismic Design of Highway Structures," by C. Rojahn, R. Mayes, D.G. Anderson, J.H. Clark, D'Appolonia Engineering, S. Gloyd and R.V. Nutt, 4/14/99, (PB99-162901, A10, MF-A02).

MCEER-99-0010 "Site Factors and Site Categories in Seismic Codes," by R. Dobry, R. Ramos and M.S. Power, 7/19/99, (PB2000-101705, A08, MF-A02).

MCEER-99-0011 "Restrainer Design Procedures for Multi-Span Simply-Supported Bridges," by M.J. Randall, M. Saiidi, E. Maragakis and T. Isakovic, 7/20/99, (PB2000-101702, A10, MF-A02).

MCEER-99-0012 "Property Modification Factors for Seismic Isolation Bearings," by M.C. Constantinou, P. Tsopelas, A. Kasalanati and E. Wolff, 7/20/99, (PB2000-103387, A11, MF-A03).

MCEER-99-0013 "Critical Seismic Issues for Existing Steel Bridges," by P. Ritchie, N. Kauhl and J. Kulicki, 7/20/99, (PB2000-101697, A09, MF-A02).

MCEER-99-0014 "Nonstructural Damage Database," by A. Kao, T.T. Soong and A. Vender, 7/24/99, (PB2000-101407, A06, MF-A01).

MCEER-99-0015 "Guide to Remedial Measures for Liquefaction Mitigation at Existing Highway Bridge Sites," by H.G. Cooke and J. K. Mitchell, 7/26/99, (PB2000-101703, A11, MF-A03).

MCEER-99-0016 "Proceedings of the MCEER Workshop on Ground Motion Methodologies for the Eastern United States," edited by N. Abrahamson and A. Becker, 8/11/99, (PB2000-103385, A07, MF-A02).

MCEER-99-0017 "Quindío, Colombia Earthquake of January 25, 1999: Reconnaissance Report," by A.P. Asfura and P.J. Flores, 10/4/99, (PB2000-106893, A06, MF-A01).

MCEER-99-0018 "Hysteretic Models for Cyclic Behavior of Deteriorating Inelastic Structures," by M.V. Sivaselvan and A.M. Reinhorn, 11/5/99, (PB2000-103386, A08, MF-A02).

MCEER-99-0019 "Proceedings of the 7th U.S.- Japan Workshop on Earthquake Resistant Design of Lifeline Facilities and Countermeasures Against Soil Liquefaction," edited by T.D. O'Rourke, J.P. Bardet and M. Hamada, 11/19/99, (PB2000-103354, A99, MF-A06).

MCEER-99-0020 "Development of Measurement Capability for Micro-Vibration Evaluations with Application to Chip Fabrication Facilities," by G.C. Lee, Z. Liang, J.W. Song, J.D. Shen and W.C. Liu, 12/1/99, (PB2000-105993, A08, MF-A02).

MCEER-99-0021 "Design and Retrofit Methodology for Building Structures with Supplemental Energy Dissipating Systems," by G. Pekcan, J.B. Mander and S.S. Chen, 12/31/99, (PB2000-105994, A11, MF-A03).

MCEER-00-0001 "The Marmara, Turkey Earthquake of August 17, 1999: Reconnaissance Report," edited by C. Scawthorn; with major contributions by M. Bruneau, R. Eguchi, T. Holzer, G. Johnson, J. Mander, J. Mitchell, W. Mitchell, A. Papageorgiou, C. Scaethorn, and G. Webb, 3/23/00, (PB2000-106200, A11, MF-A03).

MCEER-00-0002 "Proceedings of the MCEER Workshop for Seismic Hazard Mitigation of Health Care Facilities," edited by G.C. Lee, M. Ettouney, M. Grigoriu, J. Hauer and J. Nigg, 3/29/00, (PB2000-106892, A08, MF-A02).

MCEER-00-0003 "The Chi-Chi, Taiwan Earthquake of September 21, 1999: Reconnaissance Report," edited by G.C. Lee and C.H. Loh, with major contributions by G.C. Lee, M. Bruneau, I.G. Buckle, S.E. Chang, P.J. Flores, T.D. O'Rourke, M. Shinozuka, T.T. Soong, C-H. Loh, K-C. Chang, Z-J. Chen, J-S. Hwang, M-L. Lin, G-Y. Liu, K-C. Tsai, G.C. Yao and C-L. Yen, 4/30/00, (PB2001-100980, A10, MF-A02).

MCEER-00-0004 "Seismic Retrofit of End-Sway Frames of Steel Deck-Truss Bridges with a Supplemental Tendon System: Experimental and Analytical Investigation," by G. Pekcan, J.B. Mander and S.S. Chen, 7/1/00, (PB2001-100982, A10, MF-A02).

MCEER-00-0005 "Sliding Fragility of Unrestrained Equipment in Critical Facilities," by W.H. Chong and T.T. Soong, 7/5/00, (PB2001-100983, A08, MF-A02).

MCEER-00-0006 "Seismic Response of Reinforced Concrete Bridge Pier Walls in the Weak Direction," by N. Abo-Shadi, M. Saiidi and D. Sanders, 7/17/00, (PB2001-100981, A17, MF-A03).

MCEER-00-0007 "Low-Cycle Fatigue Behavior of Longitudinal Reinforcement in Reinforced Concrete Bridge Columns," by J. Brown and S.K. Kunnath, 7/23/00, (PB2001-104392, A08, MF-A02).

MCEER-00-0008 "Soil Structure Interaction of Bridges for Seismic Analysis," I. PoLam and H. Law, 9/25/00, (PB2001-105397, A08, MF-A02).

MCEER-00-0009 "Proceedings of the First MCEER Workshop on Mitigation of Earthquake Disaster by Advanced Technologies (MEDAT-1), edited by M. Shinozuka, D.J. Inman and T.D. O'Rourke, 11/10/00, (PB2001-105399, A14, MF-A03).

MCEER-00-0010 "Development and Evaluation of Simplified Procedures for Analysis and Design of Buildings with Passive Energy Dissipation Systems, Revision 01," by O.M. Ramirez, M.C. Constantinou, C.A. Kircher, A.S. Whittaker, M.W. Johnson, J.D. Gomez and C. Chrysostomou, 11/16/01, (PB2001-105523, A23, MF-A04).

MCEER-00-0011 "Dynamic Soil-Foundation-Structure Interaction Analyses of Large Caissons," by C-Y. Chang, C-M. Mok, Z-L. Wang, R. Settgast, F. Waggoner, M.A. Ketchum, H.M. Gonnermann and C-C. Chin, 12/30/00, (PB2001-104373, A07, MF-A02).

MCEER-00-0012 "Experimental Evaluation of Seismic Performance of Bridge Restrainers," by A.G. Vlassis, E.M. Maragakis and M. Saiid Saiidi, 12/30/00, (PB2001-104354, A09, MF-A02).

MCEER-00-0013 "Effect of Spatial Variation of Ground Motion on Highway Structures," by M. Shinozuka, V. Saxena and G. Deodatis, 12/31/00, (PB2001-108755, A13, MF-A03).

MCEER-00-0014 "A Risk-Based Methodology for Assessing the Seismic Performance of Highway Systems," by S.D. Werner, C.E. Taylor, J.E. Moore, II, J.S. Walton and S. Cho, 12/31/00, (PB2001-108756, A14, MF-A03).

MCEER-01-0001 "Experimental Investigation of P-Delta Effects to Collapse During Earthquakes," by D. Vian and M. Bruneau, 6/25/01, (PB2002-100534, A17, MF-A03).

MCEER-01-0002 "Proceedings of the Second MCEER Workshop on Mitigation of Earthquake Disaster by Advanced Technologies (MEDAT-2)," edited by M. Bruneau and D.J. Inman, 7/23/01, (PB2002-100434, A16, MF-A03).

MCEER-01-0003 "Sensitivity Analysis of Dynamic Systems Subjected to Seismic Loads," by C. Roth and M. Grigoriu, 9/18/01, (PB2003-100884, A12, MF-A03).

MCEER-01-0004 "Overcoming Obstacles to Implementing Earthquake Hazard Mitigation Policies: Stage 1 Report," by D.J. Alesch and W.J. Petak, 12/17/01, (PB2002-107949, A07, MF-A02).

MCEER-01-0005 "Updating Real-Time Earthquake Loss Estimates: Methods, Problems and Insights," by C.E. Taylor, S.E. Chang and R.T. Eguchi, 12/17/01, (PB2002-107948, A05, MF-A01).

MCEER-01-0006 "Experimental Investigation and Retrofit of Steel Pile Foundations and Pile Bents Under Cyclic Lateral Loadings," by A. Shama, J. Mander, B. Blabac and S. Chen, 12/31/01, (PB2002-107950, A13, MF-A03).

MCEER-02-0001 "Assessment of Performance of Bolu Viaduct in the 1999 Duzce Earthquake in Turkey" by P.C. Roussis, M.C. Constantinou, M. Erdik, E. Durukal and M. Dicleli, 5/8/02, (PB2003-100883, A08, MF-A02).

MCEER-02-0002 "Seismic Behavior of Rail Counterweight Systems of Elevators in Buildings," by M.P. Singh, Rildova and L.E. Suarez, 5/27/02. (PB2003-100882, A11, MF-A03).

MCEER-02-0003 "Development of Analysis and Design Procedures for Spread Footings," by G. Mylonakis, G. Gazetas, S. Nikolaou and A. Chauncey, 10/02/02, (PB2004-101636, A13, MF-A03, CD-A13).

MCEER-02-0004 "Bare-Earth Algorithms for Use with SAR and LIDAR Digital Elevation Models," by C.K. Huyck, R.T. Eguchi and B. Houshmand, 10/16/02, (PB2004-101637, A07, CD-A07).

MCEER-02-0005 "Review of Energy Dissipation of Compression Members in Concentrically Braced Frames," by K.Lee and M. Bruneau, 10/18/02, (PB2004-101638, A10, CD-A10).

MCEER-03-0001 "Experimental Investigation of Light-Gauge Steel Plate Shear Walls for the Seismic Retrofit of Buildings" by J. Berman and M. Bruneau, 5/2/03, (PB2004-101622, A10, MF-A03, CD-A10).

MCEER-03-0002 "Statistical Analysis of Fragility Curves," by M. Shinozuka, M.Q. Feng, H. Kim, T. Uzawa and T. Ueda, 6/16/03, (PB2004-101849, A09, CD-A09).

MCEER-03-0003 "Proceedings of the Eighth U.S.-Japan Workshop on Earthquake Resistant Design f Lifeline Facilities and Countermeasures Against Liquefaction," edited by M. Hamada, J.P. Bardet and T.D. O'Rourke, 6/30/03, (PB2004-104386, A99, CD-A99).

MCEER-03-0004 "Proceedings of the PRC-US Workshop on Seismic Analysis and Design of Special Bridges," edited by L.C. Fan and G.C. Lee, 7/15/03, (PB2004-104387, A14, CD-A14).

MCEER-03-0005 "Urban Disaster Recovery: A Framework and Simulation Model," by S.B. Miles and S.E. Chang, 7/25/03, (PB2004-104388, A07, CD-A07).

MCEER-03-0006 "Behavior of Underground Piping Joints Due to Static and Dynamic Loading," by R.D. Meis, M. Maragakis and R. Siddharthan, 11/17/03, (PB2005-102194, A13, MF-A03, CD-A00).

MCEER-04-0001 "Experimental Study of Seismic Isolation Systems with Emphasis on Secondary System Response and Verification of Accuracy of Dynamic Response History Analysis Methods," by E. Wolff and M. Constantinou, 1/16/04 (PB2005-102195, A99, MF-E08, CD-A00).

MCEER-04-0002 "Tension, Compression and Cyclic Testing of Engineered Cementitious Composite Materials," by K. Kesner and S.L. Billington, 3/1/04, (PB2005-102196, A08, CD-A08).

MCEER-04-0003 "Cyclic Testing of Braces Laterally Restrained by Steel Studs to Enhance Performance During Earthquakes," by O.C. Celik, J.W. Berman and M. Bruneau, 3/16/04, (PB2005-102197, A13, MF-A03, CD-A00).

MCEER-04-0004 "Methodologies for Post Earthquake Building Damage Detection Using SAR and Optical Remote Sensing: Application to the August 17, 1999 Marmara, Turkey Earthquake," by C.K. Huyck, B.J. Adams, S. Cho, R.T. Eguchi, B. Mansouri and B. Houshmand, 6/15/04, (PB2005-104888, A10, CD-A00).

MCEER-04-0005 "Nonlinear Structural Analysis Towards Collapse Simulation: A Dynamical Systems Approach," by M.V. Sivaselvan and A.M. Reinhorn, 6/16/04, (PB2005-104889, A11, MF-A03, CD-A00).

MCEER-04-0006 "Proceedings of the Second PRC-US Workshop on Seismic Analysis and Design of Special Bridges," edited by G.C. Lee and L.C. Fan, 6/25/04, (PB2005-104890, A16, CD-A00).

MCEER-04-0007 "Seismic Vulnerability Evaluation of Axially Loaded Steel Built-up Laced Members," by K. Lee and M. Bruneau, 6/30/04, (PB2005-104891, A16, CD-A00).

MCEER-04-0008 "Evaluation of Accuracy of Simplified Methods of Analysis and Design of Buildings with Damping Systems for Near-Fault and for Soft-Soil Seismic Motions," by E.A. Pavlou and M.C. Constantinou, 8/16/04, (PB2005-104892, A08, MF-A02, CD-A00).

MCEER-04-0009 "Assessment of Geotechnical Issues in Acute Care Facilities in California," by M. Lew, T.D. O'Rourke, R. Dobry and M. Koch, 9/15/04, (PB2005-104893, A08, CD-A00).

MCEER-04-0010 "Scissor-Jack-Damper Energy Dissipation System," by A.N. Sigaher-Boyle and M.C. Constantinou, 12/1/04 (PB2005-108221).

MCEER-04-0011 "Seismic Retrofit of Bridge Steel Truss Piers Using a Controlled Rocking Approach," by M. Pollino and M. Bruneau, 12/20/04 (PB2006-105795).

MCEER-05-0001 "Experimental and Analytical Studies of Structures Seismically Isolated with an Uplift-Restraint Isolation System," by P.C. Roussis and M.C. Constantinou, 1/10/05 (PB2005-108222).

MCEER-05-0002 "A Versatile Experimentation Model for Study of Structures Near Collapse Applied to Seismic Evaluation of Irregular Structures," by D. Kusumastuti, A.M. Reinhorn and A. Rutenberg, 3/31/05 (PB2006-101523).

MCEER-05-0003 "Proceedings of the Third PRC-US Workshop on Seismic Analysis and Design of Special Bridges," edited by L.C. Fan and G.C. Lee, 4/20/05, (PB2006-105796).

MCEER-05-0004 "Approaches for the Seismic Retrofit of Braced Steel Bridge Piers and Proof-of-Concept Testing of an Eccentrically Braced Frame with Tubular Link," by J.W. Berman and M. Bruneau, 4/21/05 (PB2006-101524).

MCEER-05-0005 "Simulation of Strong Ground Motions for Seismic Fragility Evaluation of Nonstructural Components in Hospitals," by A. Wanitkorkul and A. Filiatrault, 5/26/05 (PB2006-500027).

MCEER-05-0006 "Seismic Safety in California Hospitals: Assessing an Attempt to Accelerate the Replacement or Seismic Retrofit of Older Hospital Facilities," by D.J. Alesch, L.A. Arendt and W.J. Petak, 6/6/05 (PB2006-105794).

MCEER-05-0007 "Development of Seismic Strengthening and Retrofit Strategies for Critical Facilities Using Engineered Cementitious Composite Materials," by K. Kesner and S.L. Billington, 8/29/05 (PB2006-111701).

MCEER-05-0008 "Experimental and Analytical Studies of Base Isolation Systems for Seismic Protection of Power Transformers," by N. Murota, M.Q. Feng and G-Y. Liu, 9/30/05 (PB2006-111702).

MCEER-05-0009 "3D-BASIS-ME-MB: Computer Program for Nonlinear Dynamic Analysis of Seismically Isolated Structures," by P.C. Tsopelas, P.C. Roussis, M.C. Constantinou, R. Buchanan and A.M. Reinhorn, 10/3/05 (PB2006-111703).

MCEER-05-0010 "Steel Plate Shear Walls for Seismic Design and Retrofit of Building Structures," by D. Vian and M. Bruneau, 12/15/05 (PB2006-111704).

MCEER-05-0011 "The Performance-Based Design Paradigm," by M.J. Astrella and A. Whittaker, 12/15/05 (PB2006-111705).

MCEER-06-0001 "Seismic Fragility of Suspended Ceiling Systems," H. Badillo-Almaraz, A.S. Whittaker, A.M. Reinhorn and G.P. Cimellaro, 2/4/06 (PB2006-111706).

MCEER-06-0002 "Multi-Dimensional Fragility of Structures," by G.P. Cimellaro, A.M. Reinhorn and M. Bruneau, 3/1/06 (PB2007-106974, A09, MF-A02, CD A00).

MCEER-06-0003 "Built-Up Shear Links as Energy Dissipators for Seismic Protection of Bridges," by P. Dusicka, A.M. Itani and I.G. Buckle, 3/15/06 (PB2006-111708).

MCEER-06-0004 "Analytical Investigation of the Structural Fuse Concept," by R.E. Vargas and M. Bruneau, 3/16/06 (PB2006-111709).

MCEER-06-0005 "Experimental Investigation of the Structural Fuse Concept," by R.E. Vargas and M. Bruneau, 3/17/06 (PB2006-111710).

MCEER-06-0006 "Further Development of Tubular Eccentrically Braced Frame Links for the Seismic Retrofit of Braced Steel Truss Bridge Piers," by J.W. Berman and M. Bruneau, 3/27/06 (PB2007-105147).

MCEER-06-0007 "REDARS Validation Report," by S. Cho, C.K. Huyck, S. Ghosh and R.T. Eguchi, 8/8/06 (PB2007-106983).

MCEER-06-0008 "Review of Current NDE Technologies for Post-Earthquake Assessment of Retrofitted Bridge Columns," by J.W. Song, Z. Liang and G.C. Lee, 8/21/06 (PB2007-106984).

MCEER-06-0009 "Liquefaction Remediation in Silty Soils Using Dynamic Compaction and Stone Columns," by S. Thevanayagam, G.R. Martin, R. Nashed, T. Shenthan, T. Kanagalingam and N. Ecemis, 8/28/06 (PB2007-106985).

MCEER-06-0010 "Conceptual Design and Experimental Investigation of Polymer Matrix Composite Infill Panels for Seismic Retrofitting," by W. Jung, M. Chiewanichakorn and A.J. Aref, 9/21/06 (PB2007-106986).

MCEER-06-0011 "A Study of the Coupled Horizontal-Vertical Behavior of Elastomeric and Lead-Rubber Seismic Isolation Bearings," by G.P. Warn and A.S. Whittaker, 9/22/06 (PB2007-108679).

MCEER-06-0012 "Proceedings of the Fourth PRC-US Workshop on Seismic Analysis and Design of Special Bridges: Advancing Bridge Technologies in Research, Design, Construction and Preservation," Edited by L.C. Fan, G.C. Lee and L. Ziang, 10/12/06 (PB2007-109042).

MCEER-06-0013 "Cyclic Response and Low Cycle Fatigue Characteristics of Plate Steels," by P. Dusicka, A.M. Itani and I.G. Buckle, 11/1/06 06 (PB2007-106987).

MCEER-06-0014 "Proceedings of the Second US-Taiwan Bridge Engineering Workshop," edited by W.P. Yen, J. Shen, J-Y. Chen and M. Wang, 11/15/06 (PB2008-500041).

MCEER-06-0015 "User Manual and Technical Documentation for the REDARS^{TM} Import Wizard," by S. Cho, S. Ghosh, C.K. Huyck and S.D. Werner, 11/30/06 (PB2007-114766).

MCEER-06-0016 "Hazard Mitigation Strategy and Monitoring Technologies for Urban and Infrastructure Public Buildings: Proceedings of the China-US Workshops," edited by X.Y. Zhou, A.L. Zhang, G.C. Lee and M. Tong, 12/12/06 (PB2008-500018).

MCEER-07-0001 "Static and Kinetic Coefficients of Friction for Rigid Blocks," by C. Kafali, S. Fathali, M. Grigoriu and A.S. Whittaker, 3/20/07 (PB2007-114767).

MCEER-07-0002 "Hazard Mitigation Investment Decision Making: Organizational Response to Legislative Mandate," by L.A. Arendt, D.J. Alesch and W.J. Petak, 4/9/07 (PB2007-114768).

MCEER-07-0003 "Seismic Behavior of Bidirectional-Resistant Ductile End Diaphragms with Unbonded Braces in Straight or Skewed Steel Bridges," by O. Celik and M. Bruneau, 4/11/07 (PB2008-105141).

MCEER-07-0004 "Modeling Pile Behavior in Large Pile Groups Under Lateral Loading," by A.M. Dodds and G.R. Martin, 4/16/07(PB2008-105142).

MCEER-07-0005 "Experimental Investigation of Blast Performance of Seismically Resistant Concrete-Filled Steel Tube Bridge Piers," by S. Fujikura, M. Bruneau and D. Lopez-Garcia, 4/20/07 (PB2008-105143).

MCEER-07-0006 "Seismic Analysis of Conventional and Isolated Liquefied Natural Gas Tanks Using Mechanical Analogs," by I.P. Christovasilis and A.S. Whittaker, 5/1/07.

MCEER-07-0007 "Experimental Seismic Performance Evaluation of Isolation/Restraint Systems for Mechanical Equipment – Part 1: Heavy Equipment Study," by S. Fathali and A. Filiatrault, 6/6/07 (PB2008-105144).

MCEER-07-0008 "Seismic Vulnerability of Timber Bridges and Timber Substructures," by A.A. Sharma, J.B. Mander, I.M. Friedland and D.R. Allicock, 6/7/07 (PB2008-105145).

MCEER-07-0009 "Experimental and Analytical Study of the XY-Friction Pendulum (XY-FP) Bearing for Bridge Applications," by C.C. Marin-Artieda, A.S. Whittaker and M.C. Constantinou, 6/7/07 (PB2008-105191).

MCEER-07-0010 "Proceedings of the PRC-US Earthquake Engineering Forum for Young Researchers," Edited by G.C. Lee and X.Z. Qi, 6/8/07 (PB2008-500058).

MCEER-07-0011 "Design Recommendations for Perforated Steel Plate Shear Walls," by R. Purba and M. Bruneau, 6/18/07, (PB2008-105192).

MCEER-07-0012 "Performance of Seismic Isolation Hardware Under Service and Seismic Loading," by M.C. Constantinou, A.S. Whittaker, Y. Kalpakidis, D.M. Fenz and G.P. Warn, 8/27/07, (PB2008-105193).

MCEER-07-0013 "Experimental Evaluation of the Seismic Performance of Hospital Piping Subassemblies," by E.R. Goodwin, E. Maragakis and A.M. Itani, 9/4/07, (PB2008-105194).

MCEER-07-0014 "A Simulation Model of Urban Disaster Recovery and Resilience: Implementation for the 1994 Northridge Earthquake," by S. Miles and S.E. Chang, 9/7/07, (PB2008-106426).

MCEER-07-0015 "Statistical and Mechanistic Fragility Analysis of Concrete Bridges," by M. Shinozuka, S. Banerjee and S-H. Kim, 9/10/07, (PB2008-106427).

MCEER-07-0016 "Three-Dimensional Modeling of Inelastic Buckling in Frame Structures," by M. Schachter and AM. Reinhorn, 9/13/07, (PB2008-108125).

MCEER-07-0017 "Modeling of Seismic Wave Scattering on Pile Groups and Caissons," by I. Po Lam, H. Law and C.T. Yang, 9/17/07 (PB2008-108150).

MCEER-07-0018 "Bridge Foundations: Modeling Large Pile Groups and Caissons for Seismic Design," by I. Po Lam, H. Law and G.R. Martin (Coordinating Author), 12/1/07 (PB2008-111190).

MCEER-07-0019 "Principles and Performance of Roller Seismic Isolation Bearings for Highway Bridges," by G.C. Lee, Y.C. Ou, Z. Liang, T.C. Niu and J. Song, 12/10/07 (PB2009-110466).

MCEER-07-0020 "Centrifuge Modeling of Permeability and Pinning Reinforcement Effects on Pile Response to Lateral Spreading," by L.L Gonzalez-Lagos, T. Abdoun and R. Dobry, 12/10/07 (PB2008-111191).

MCEER-07-0021 "Damage to the Highway System from the Pisco, Perú Earthquake of August 15, 2007," by J.S. O'Connor, L. Mesa and M. Nykamp, 12/10/07, (PB2008-108126).

MCEER-07-0022 "Experimental Seismic Performance Evaluation of Isolation/Restraint Systems for Mechanical Equipment – Part 2: Light Equipment Study," by S. Fathali and A. Filiatrault, 12/13/07 (PB2008-111192).

MCEER-07-0023 "Fragility Considerations in Highway Bridge Design," by M. Shinozuka, S. Banerjee and S.H. Kim, 12/14/07 (PB2008-111193).

MCEER-07-0024 "Performance Estimates for Seismically Isolated Bridges," by G.P. Warn and A.S. Whittaker, 12/30/07 (PB2008-112230).

MCEER-08-0001 "Seismic Performance of Steel Girder Bridge Superstructures with Conventional Cross Frames," by L.P. Carden, A.M. Itani and I.G. Buckle, 1/7/08, (PB2008-112231).

MCEER-08-0002 "Seismic Performance of Steel Girder Bridge Superstructures with Ductile End Cross Frames with Seismic Isolators," by L.P. Carden, A.M. Itani and I.G. Buckle, 1/7/08 (PB2008-112232).

MCEER-08-0003 "Analytical and Experimental Investigation of a Controlled Rocking Approach for Seismic Protection of Bridge Steel Truss Piers," by M. Pollino and M. Bruneau, 1/21/08 (PB2008-112233).

MCEER-08-0004 "Linking Lifeline Infrastructure Performance and Community Disaster Resilience: Models and Multi-Stakeholder Processes," by S.E. Chang, C. Pasion, K. Tatebe and R. Ahmad, 3/3/08 (PB2008-112234).

MCEER-08-0005 "Modal Analysis of Generally Damped Linear Structures Subjected to Seismic Excitations," by J. Song, Y-L. Chu, Z. Liang and G.C. Lee, 3/4/08 (PB2009-102311).

MCEER-08-0006 "System Performance Under Multi-Hazard Environments," by C. Kafali and M. Grigoriu, 3/4/08 (PB2008-112235).

MCEER-08-0007 "Mechanical Behavior of Multi-Spherical Sliding Bearings," by D.M. Fenz and M.C. Constantinou, 3/6/08 (PB2008-112236).

MCEER-08-0008 "Post-Earthquake Restoration of the Los Angeles Water Supply System," by T.H.P. Tabucchi and R.A. Davidson, 3/7/08 (PB2008-112237).

MCEER-08-0009 "Fragility Analysis of Water Supply Systems," by A. Jacobson and M. Grigoriu, 3/10/08 (PB2009-105545).

MCEER-08-0010 "Experimental Investigation of Full-Scale Two-Story Steel Plate Shear Walls with Reduced Beam Section Connections," by B. Qu, M. Bruneau, C-H. Lin and K-C. Tsai, 3/17/08 (PB2009-106368).

MCEER-08-0011 "Seismic Evaluation and Rehabilitation of Critical Components of Electrical Power Systems," S. Ersoy, B. Feizi, A. Ashrafi and M. Ala Saadeghvaziri, 3/17/08 (PB2009-105546).

MCEER-08-0012 "Seismic Behavior and Design of Boundary Frame Members of Steel Plate Shear Walls," by B. Qu and M. Bruneau, 4/26/08 . (PB2009-106744).

MCEER-08-0013 "Development and Appraisal of a Numerical Cyclic Loading Protocol for Quantifying Building System Performance," by A. Filiatrault, A. Wanitkorkul and M. Constantinou, 4/27/08 (PB2009-107906).

MCEER-08-0014 "Structural and Nonstructural Earthquake Design: The Challenge of Integrating Specialty Areas in Designing Complex, Critical Facilities," by W.J. Petak and D.J. Alesch, 4/30/08 (PB2009-107907).

MCEER-08-0015 "Seismic Performance Evaluation of Water Systems," by Y. Wang and T.D. O'Rourke, 5/5/08 (PB2009-107908).

MCEER-08-0016 "Seismic Response Modeling of Water Supply Systems," by P. Shi and T.D. O'Rourke, 5/5/08 (PB2009-107910).

MCEER-08-0017 "Numerical and Experimental Studies of Self-Centering Post-Tensioned Steel Frames," by D. Wang and A. Filiatrault, 5/12/08 (PB2009-110479).

MCEER-08-0018 "Development, Implementation and Verification of Dynamic Analysis Models for Multi-Spherical Sliding Bearings," by D.M. Fenz and M.C. Constantinou, 8/15/08 (PB2009-107911).

MCEER-08-0019 "Performance Assessment of Conventional and Base Isolated Nuclear Power Plants for Earthquake Blast Loadings," by Y.N. Huang, A.S. Whittaker and N. Luco, 10/28/08 (PB2009-107912).

MCEER-08-0020 "Remote Sensing for Resilient Multi-Hazard Disaster Response – Volume I: Introduction to Damage Assessment Methodologies," by B.J. Adams and R.T. Eguchi, 11/17/08 (PB2010-102695).

MCEER-08-0021 "Remote Sensing for Resilient Multi-Hazard Disaster Response – Volume II: Counting the Number of Collapsed Buildings Using an Object-Oriented Analysis: Case Study of the 2003 Bam Earthquake," by L. Gusella, C.K. Huyck and B.J. Adams, 11/17/08 (PB2010-100925).

MCEER-08-0022 "Remote Sensing for Resilient Multi-Hazard Disaster Response – Volume III: Multi-Sensor Image Fusion Techniques for Robust Neighborhood-Scale Urban Damage Assessment," by B.J. Adams and A. McMillan, 11/17/08 (PB2010-100926).

MCEER-08-0023 "Remote Sensing for Resilient Multi-Hazard Disaster Response – Volume IV: A Study of Multi-Temporal and Multi-Resolution SAR Imagery for Post-Katrina Flood Monitoring in New Orleans," by A. McMillan, J.G. Morley, B.J. Adams and S. Chesworth, 11/17/08 (PB2010-100927).

MCEER-08-0024 "Remote Sensing for Resilient Multi-Hazard Disaster Response – Volume V: Integration of Remote Sensing Imagery and VIEWS^{TM} Field Data for Post-Hurricane Charley Building Damage Assessment," by J.A. Womble, K. Mehta and B.J. Adams, 11/17/08 (PB2009-115532).

MCEER-08-0025 "Building Inventory Compilation for Disaster Management: Application of Remote Sensing and Statistical Modeling," by P. Sarabandi, A.S. Kiremidjian, R.T. Eguchi and B. J. Adams, 11/20/08 (PB2009-110484).

MCEER-08-0026 "New Experimental Capabilities and Loading Protocols for Seismic Qualification and Fragility Assessment of Nonstructural Systems," by R. Retamales, G. Mosqueda, A. Filiatrault and A. Reinhorn, 11/24/08 (PB2009-110485).

MCEER-08-0027 "Effects of Heating and Load History on the Behavior of Lead-Rubber Bearings," by I.V. Kalpakidis and M.C. Constantinou, 12/1/08 (PB2009-115533).

MCEER-08-0028 "Experimental and Analytical Investigation of Blast Performance of Seismically Resistant Bridge Piers," by S.Fujikura and M. Bruneau, 12/8/08 (PB2009-115534).

MCEER-08-0029 "Evolutionary Methodology for Aseismic Decision Support," by Y. Hu and G. Dargush, 12/15/08.

MCEER-08-0030 "Development of a Steel Plate Shear Wall Bridge Pier System Conceived from a Multi-Hazard Perspective," by D. Keller and M. Bruneau, 12/19/08 (PB2010-102696).

MCEER-09-0001 "Modal Analysis of Arbitrarily Damped Three-Dimensional Linear Structures Subjected to Seismic Excitations," by Y.L. Chu, J. Song and G.C. Lee, 1/31/09 (PB2010-100922).

MCEER-09-0002 "Air-Blast Effects on Structural Shapes," by G. Ballantyne, A.S. Whittaker, A.J. Aref and G.F. Dargush, 2/2/09 (PB2010-102697).

MCEER-09-0003 "Water Supply Performance During Earthquakes and Extreme Events," by A.L. Bonneau and T.D. O'Rourke, 2/16/09 (PB2010-100923).

MCEER-09-0004 "Generalized Linear (Mixed) Models of Post-Earthquake Ignitions," by R.A. Davidson, 7/20/09 (PB2010-102698).

MCEER-09-0005 "Seismic Testing of a Full-Scale Two-Story Light-Frame Wood Building: NEESWood Benchmark Test," by I.P. Christovasilis, A. Filiatrault and A. Wanitkorkul, 7/22/09.

MCEER-09-0006 "IDARC2D Version 7.0: A Program for the Inelastic Damage Analysis of Structures," by A.M. Reinhorn, H. Roh, M. Sivaselvan, S.K. Kunnath, R.E. Valles, A. Madan, C. Li, R. Lobo and Y.J. Park, 7/28/09 (PB2010-103199).

MCEER-09-0007 "Enhancements to Hospital Resiliency: Improving Emergency Planning for and Response to Hurricanes," by D.B. Hess and L.A. Arendt, 7/30/09 (PB2010-100924).

MCEER-09-0008 "Assessment of Base-Isolated Nuclear Structures for Design and Beyond-Design Basis Earthquake Shaking," by Y.N. Huang, A.S. Whittaker, R.P. Kennedy and R.L. Mayes, 8/20/09 (PB2010-102699).

MCEER-09-0009 "Quantification of Disaster Resilience of Health Care Facilities," by G.P. Cimellaro, C. Fumo, A.M Reinhorn and M. Bruneau, 9/14/09.

MCEER-09-0010 "Performance-Based Assessment and Design of Squat Reinforced Concrete Shear Walls," by C.K. Gulec and A.S. Whittaker, 9/15/09 (PB2010-102700).

MCEER-09-0011 "Proceedings of the Fourth US-Taiwan Bridge Engineering Workshop," edited by W.P. Yen, J.J. Shen, T.M. Lee and R.B. Zheng, 10/27/09 (PB2010-500009).

MCEER-09-0012 "Proceedings of the Special International Workshop on Seismic Connection Details for Segmental Bridge Construction," edited by W. Phillip Yen and George C. Lee, 12/21/09.

MCEER-10-0001 "Direct Displacement Procedure for Performance-Based Seismic Design of Multistory Woodframe Structures," by W. Pang and D. Rosowsky, 4/26/10.

MCEER-10-0002 "Simplified Direct Displacement Design of Six-Story NEESWood Capstone Building and Pre-Test Seismic Performance Assessment," by W. Pang, D. Rosowsky, J. van de Lindt and S. Pei, 5/28/10.

MCEER-10-0003 "Integration of Seismic Protection Systems in Performance-Based Seismic Design of Woodframed Structures," by J.K. Shinde and M.D. Symans, 6/18/10.

MCEER-10-0004 "Modeling and Seismic Evaluation of Nonstructural Components: Testing Frame for Experimental Evaluation of Suspended Ceiling Systems," by A.M. Reinhorn, K.P. Ryu and G. Maddaloni, 6/30/10.

MCEER-10-0005 "Analytical Development and Experimental Validation of a Structural-Fuse Bridge Pier Concept," by S. El-Bahey and M. Bruneau, 10/1/10.

MCEER-10-0006 "A Framework for Defining and Measuring Resilience at the Community Scale: The PEOPLES Resilience Framework," by C.S. Renschler, A.E. Frazier, L.A. Arendt, G.P. Cimellaro, A.M. Reinhorn and M. Bruneau, 10/8/10.

MCEER-10-0007 "Impact of Horizontal Boundary Elements Design on Seismic Behavior of Steel Plate Shear Walls," by R. Purba and M. Bruneau, 11/14/10.

MCEER-10-0008 "Seismic Testing of a Full-Scale Mid-Rise Building: The NEESWood Capstone Test," by S. Pei, J.W. van de Lindt, S.E. Pryor, H. Shimizu, H. Isoda and D.R. Rammer, 12/1/10.

MCEER-10-0009 "Modeling the Effects of Detonations of High Explosives to Inform Blast-Resistant Design," by P. Sherkar, A.S. Whittaker and A.J. Aref, 12/1/10.

MCEER-10-0010 "L'Aquila Earthquake of April 6, 2009 in Italy: Rebuilding a Resilient City to Multiple Hazards," by G.P. Cimellaro, I.P. Christovasilis, A.M. Reinhorn, A. De Stefano and T. Kirova, 12/29/10.

MCEER-11-0001 "Numerical and Experimental Investigation of the Seismic Response of Light-Frame Wood Structures," by I.P. Christovasilis and A. Filiatrault, 8/8/11.

MCEER-11-0002 "Seismic Design and Analysis of Precast Segmental Concrete Bridge Model," by M. Anagnostopoulou, A. Filiatrault and A. Aref, 9/15/11.

MCEER-11-0003 'Proceedings of the Workshop on Improving Earthquake Response of Substation Equipment," Edited by A.M. Reinhorn, 9/19/11.

MCEER-11-0004 "LRFD-Based Analysis and Design Procedures for Bridge Bearings and Seismic Isolators," by M.C. Constantinou, I. Kalpakidis, A. Filiatrault and R.A. Ecker Lay, 9/26/11.

MCEER-11-0005 "Seismic Evaluation, Parameterization and Effect of Light-Frame Steel Studded Gypsum Partition Walls," by R. Davies and A. Filiatrault, 10/12/11.

MCEER-11-0006 "Modeling and Seismic Performance Evaluation of High Voltage Transformers and Bushings," by A.M. Reinhorn, K. Oikonomou, H. Roh, A. Schiff and L. Kempner, Jr., 10/3/11.

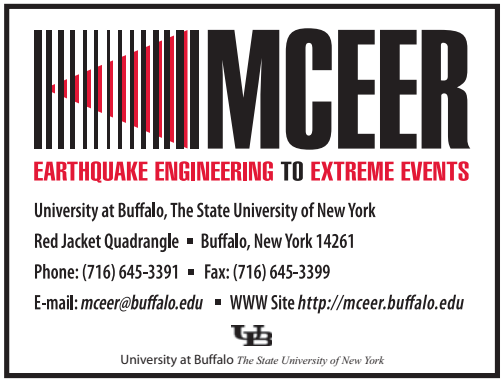

ISSN 1520-295X